Session 3

Models and Assessment

Modèles et évaluation

Modellbildung und Beurteilung

Leere Seite

Blank page

Page vide

Models and Assessment

Modèles et évaluation

Modellbildung und Beurteilung

Alberto PEANO
Director for R & D
ISMES S.p.A
Bergamo,ITALY

Alberto Peano born 1946, is a Dr. Sc. Civ. Eng. from Washington University, St. Louis - Missouri. He was one of the developers of the p-version of the finite element method. Later he applied FEM technology to solve research and application problems in a wide range of engineering fields including the rehabilitation of monumental structures.

SUMMARY

Difficulties to be overcome, conceptual or practical limits to be taken into account, computational strategies to be followed are reviewed. The selection of the most appropriate approach is illustrated, when useful for more clarity, by case histories related to Italian monuments analysed at ISMES.

RÉSUMÉ

On a examiné les difficultés qui doivent être supérées, les limites conceptuelles ou pratiques qui doivent être considérées, les stratégies de calcul qui doivent être suivies. Quand elle est utile pour une plus grande clarté, la sélection de l' approche plus adapte est illustrée par des cas historiques relatifs à des monuments italiens analysés chez ISMES.

ZUSAMMENFASSUNG

In diesem Beitrag werden die Verwicklungen, die präktische un konzeptuelle Begrenzungen, sowie di Rechenverfahrenstrategien, die bzw. zu ueberkommen, zu betrachten und zu befolgen sind, kritisch durchgesehen. Die Auswahl des zweckmässigsten Verfähenswird - wenn für die Klarheit nötig - mit früheren Sächfallen in Beziehung mit einigen von ISMES untermahten italienischen Monumenten erlauedert.

1. INTRODUCTION

Structural analysis of monumental structures faces a number of difficulties unusual in other areas of Civil Engineering: material properties are poorly determined due to limited access to samples for destructive testing and very often also to large property variation within the fabric of the same building; the strength of the connection of the different structural elements is often hard to assess, if at all possible; the original geometric configuration of the building might have been altered by inelastic settlements along the ages and cannot be exactly determined.

Due to the above main difficulties finite element modelling of historical buildings has been widely applied only recently. Surprisingly numerical computations are often motivated by the scarcity of data, which is simultaneously the main source of uncertainty on the quality of numerical results. In fact a very meaningful application of computational models is the interpretation of structural behaviour in order to check the consistency of the scarce data available. For instance this is achieved by calibration of some poorly known parameter of the model until some significant feature (e.g. opening of cracks, frequencies of first few vibration modes, etc.) is correctly reproduced in the numerical results.

This first phase of analysis ("model calibration" phase) is usually a mandatory step in order to assess the reliability or at least the plausibility of the computations aimed at assessing the safety margin of the structure either as it stands or after a strengthening intervention.

The second phase of analysis ("safety assessment phase") requires usually the rational management of at least two main sources of difficulty. The first one is the nonlinear behaviour exhibited by some structures before collapse. Numerical modelling of such behaviour is very difficult and it requires the assumption of additional material properties that usually play no role for model calibration. Unfortunately numerical modeling of nonlinear structural behaviour might be crucial if the linear elastic range is small and does not point out an adequate margin of safety of the structure. The second reason of concern is that the procedure to be followed in order to assess the safety of monumental structures is often not as clearly defined as in other areas of civil engineering, particularly when seismic loads are involved.

The purpose of the paper is to review the difficulties encountered at all stages of numerical modelling of monumental structures, such as: input data gathering and validation, selection of the computational approach, validation and interpretation of numerical results.
The selection of the most appropriate approach in each case will be illustrated, when useful for more clarity, by case hystories related to Italian monuments.

2. NUMERICAL VERSUS PHYSICAL MODELS. VALIDATION OF COMPUTATIONAL APPROACHES

The safety of monumental structures has been investigated also by testing physical models. These tests are usually carried out on reduced scale replicas under static or dynamic loading. A list of monuments investigated at ISMES by physical models is presented in table 1

MONUMENTS	SCALE	LOADING	YEAR
Mole Antonelliana (Torino, Italy) Partial Model	1:4	Static	1956
Duomo di Milano (Milano Cathefral Italy) - Tiburium model	1:15	Static	1967
Duomo di Milano - Models of main columns	1:4.7	Static	1967-81
Colonna Antonina (Rome, Italy) n.3 models	1:26 1:18 1:15	Dynamic	1988
Rotonda di Diana (Baia, Naples,Italy)	1:15	Dynamic	1990

Table 1.: Physical models of some Italian monuments

Of course physical models are often not competitive with numerical models for reasons of costs, time of execution and convenience of use (e.g. it is usually not possible to carry out parametric analyses). Moreover physical models have many drawbacks in common with computational models. Indeed, as mentioned before, when information on materials and geometry of the structure is scarce, it is difficult to define the specifications of any model.

Still there are cases where experimental analysis plays a very important role. Here the example of one static and one dynamic models may be mentioned. The main pillars of the tiburium of the Duomo of Milan deteriorated with ages and have been replaced after extensive investigations [1] Several physical models of one pillar in scale 1:4.7 have been made out of the same Candoglia marble used to build and repair the duomo throughout the centuries. The tests have been carried out under a static load representing the portion of the dead weight of the structure carried by the most stressed pillar.

The aim of the test was to prove that no excess settlement would be caused by the repair strategy adopted. Therefore one sector at a time of the scaled pillar was replaced. The main features of this physical model were:

- the use of the same material. This eliminates possible concerns about the accuracy of numerical modelling of fragile and other nonlinear material behaviours;

- the reproduction of the complete sequence of the operations. Really the only difference with the real intervention was the scale. This eliminates possible concerns about incompleteness of the models (have all possible effects and scenarios taken into account in the specifications of the model?).

Note that the writer, maybe because of his own scientific preferences, believes that appropriate results could have been obtained by numerical models in a cheaper and faster way. Still the uniqueness and importance of the monument, the tremendous consequences in case of a structural failure during strengthening, the need to provide decision makers with evidence robust both from the technical and psychological standpoint well justified the resort to physical modelling.

A second quite different example is the dynamic testing on a shaking table of a number of models of columns built according to different scale. The tests do not appropriately reproduce any specific monument because inertia forces are not correctly reproduced in scaled models made of the same material. Still the tests, carried out for ENEA, provided a set of data that are precious for validation of numerical models. Note that a number of papers have been presented recently on the dynamic behaviour of Greek and Roman temples or of other structures made of superimposed stone blocks.

The assumptions used in the proposed numerical methods are very reasonable, still the complexity of the dynamic behaviour of this kind of structures suggests that a combination of numerical and experimental methods should be used to clarify and validate the range of the computational models.

In conclusion the assessment of monumental structures is more and more carried out by means of numerical models. Under service loading the models are usually validated using monitoring or other experimental data of the real structure, as illustrated in the following section. In case extreme load conditions (such as earthquake) are analysed, the required validation of the methodological approach is difficult, therefore the level of approximation of such analyses should be carefully evaluated.

As data for back analysis of structural failures are scarce, destructive testing of physical models or of ancient buildings of no historical value should be used for validation of computer models.

3.   MODEL CALIBRATION STUDIES

3.1   Aims and Technologies

Extensive numerical computations are usually carried out in combination with the experimental investigation of structural behaviour. As mentioned before, the aim is to check the consistency of the available data as well as of the assumptions that are necessary to build a numerical model.

Moreover the studies may be carried out in order to improve the postprocessing of the experimental tests or in order to derive data that cannot be directly measured (e.g. settlements through ages) [19,15,17,18].

Calibration of poorly known parameters is often based on parameter sensitivity analysis and on heuristic approaches. Nevertheless mathematical optimization techniques are also used and in such case it is more appropriate to define such analyses as "structural identification" processes rather than simple model calibration procedures.
Such "structural identification" can be based on direct or inverse procedures:

-       in the direct approach a standard direct analysis procedure is iterated and at each step the free parameters are modified on the basis of a criterion to measure discrepancy between expected and effective response and of a convenient mathematical method (Symplex method, Rosenbrook method, alternate variables method, etc.);

-       in the inverse approach equilibrium equations must be rewritten in such a way that the free parameters appear as independent variables. A number of different approaches have been proposed both for static and dynamic problems and in either deterministic or probabilistic procedures.

3.2   Input data treatment

Material properties are usually measured at a few isolated points where the flat jack test may be carried out or, exceptionally, samples may be extracted. In order to prepare a numerical model, however, appropriate values must be assigned to all other points in the structural model. Values can be selected in different ways:

- values measured at a specific point may be applied to a "tributary area" which is considered more or less homogeneous on the basis of visual inspection, historical information on the construction process or simplified experimental methods.

- values may be interpolated between measurement points. For example this is applicable in case discrepancies are ascribed to deterioration and the state of deterioration varies gradually within the structure;

- stochastic values (average values and statistical distribution) may be derived from the measured data set and applied uniformly.

Sometimes it may be convenient to solve an identification problem in order to extract from an experimental test the most reliable values of the needed structural parameters. For instance numerical simulation of the flat jack test was carried out and lead also to some improvement of the testing procedure [1]. The simulation, which also identified separate values for the elastic properties of bricks and mortar, should nowadays be revised and extended to take advantage of state of art knowledge on micromechanics of masonry.

3.3   Use of crack opening data

In many historical buildings cracks are too large to be ignored even though the lack of detailed information on structural material properties and the analytical complexity make unrealistic any attempt to model the cracking process [19,16,23,22,20]. In such cases the relative displacement of the two crack faces should be regarded as very meaningful information to be used for model calibration.

Probably the first case is which this approach was adopted is the analyses carried out in 1979 in view of the diagnostic and strengthening of the Palazzo della Ragione in Milano fig. 1.

This is a 13th century building which in the last two centuries housed the Notary archives of Milan [2]. The analyses before and after reinforcement were limited to the facade which exhibited severe cracking. The mesh was very detailed in order to model the main cracks as well as the reinforcement. (fig. 1). The aim of the analyses was to correlate the opening displacement of the main cracks with the settlement of the pillars. The analysis was carried out for unit settlements of each pillar, then a least square procedure identified the combination of settlements which minimizes the discrepancy between computed and measured crack opening displacements.
Note that this was the only possible way to identify the settlements and recover the stress distribution in the facade before reinforcement. The flat jack tests, used to identify the elastic properties of the masonry, also provided the stress values at a few control points, where the consistency of the procedure was checked.

Another important case history where the crack opening displacement plays a major role is the Brunelleschi dome in Florence. In the well known studies by Chiarugi, Fanelli and Giuseppetti [4] the main vertical cracks of the dome are correlated with the dead load while periodic opening / closing is associated with the periodic thermal loading due to seasonal temperature variations. More recently the crack opening displacement of Brunelleschi dome has been used by Chiostrini for identification of the most realistic value of the elastic module [19]. The analysis also leads to tensile stresses which are in agreement with the crack pattern. On the contrary the elastic module is not in agreement with that needed to fit the frequency of the first few eigenvalues of the dome.

The two examples mentioned above illustrate an approach (linearity of constitutive equations, explicit modelling of cracks) that is nowadays the most usual and well established.
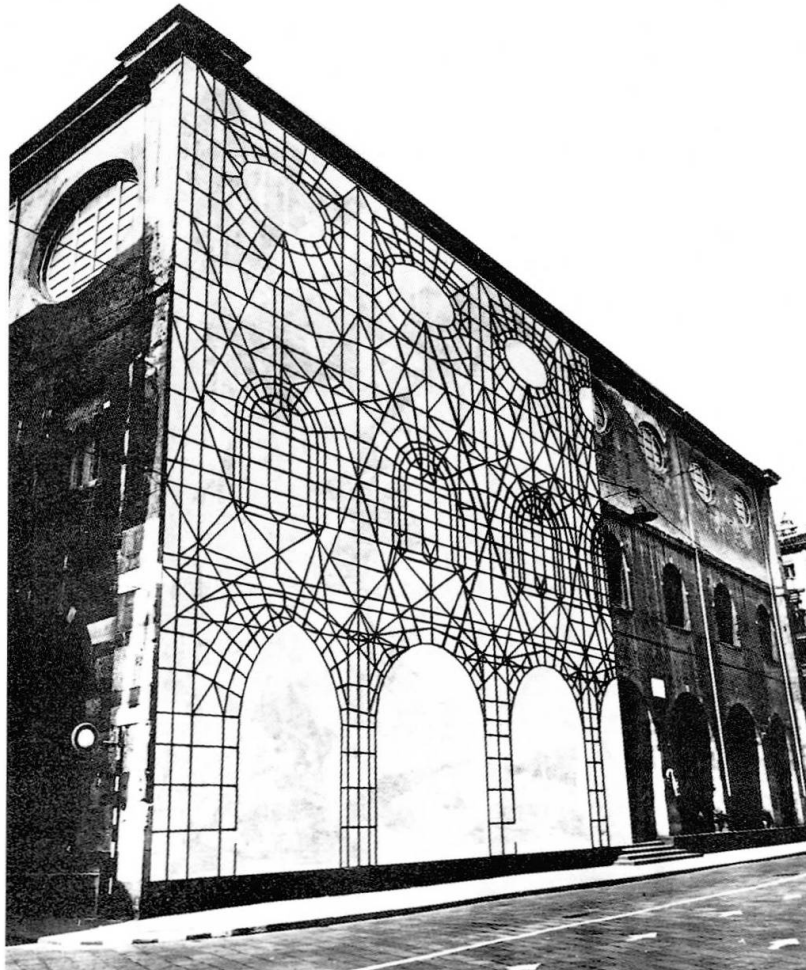

It could be surmised that this simple approach is dictated by reasons of convenience; namely by the uncertainties associated with the definition of a nonlinear material model and with the execution of complicated nonlinear analyses. On the contrary many case histories indicate that this simple approach is usually adequate to provide realistic results and it is far from a "force majeure" approach. The details of the practical implementation are however sometimes different. The approach first adopted in the analysis of the Palazzo della Ragione is crude: the only cracks modelled are the ones that exhibit a significant crack opening displacement; moreover the length of the cracks is determined in advance.

Figure 1: Palazzo della Ragione, Milano

Later the enormous reduction of computer costs has encouraged more sophisticated implementations even though the advantages are not always meaningful or easy to prove. The most interesting improvement is the execution of a non linear no-tension analysis instead of a linear elastic one. No-tension analysis has been developed for and extensively applied to concrete structures. When applied to historical buildings, it is crucial that the location of existing cracks is taken into account in the model. This is a partial remedy against lacking information on the variability of strength. The approach is as follows:

- cracks exhibited by the structure are taken into account during mesh preparation but they are initially closed; i.e. the model is initially undamaged;

- the full loads are applied or alternatively in case the loading changed during the life of the structure, such different phases of the load application are also simulated by the numerical model;

- no tensile stresses are admitted; therefore the boundaries of adjacent elements in regions of tensile stresses are disconnected and cracks are generated. This procedure is repeated step by step until complete relaxation of tensile stresses is achieved.

- A further refinement is to model no tension behaviour as a constitutive behaviour of masonry material in regions where no crack shape has been predetermined in the mesh. This is handled by introducing an anisotropic elastic model with zero elastic modulus in the direction parallel to tensile stresses. In this case the plausibility of computed results must be checked by investigating if a corresponding area of diffused microcracking exists in the real structure.

Of course this approach is much more computer intensive and occasionally numerically difficult than the linear elastic approach of many authors. On the other hand it may deliver two advantages that in some cases should not be neglected:

- first of all, in case loads are applied in loadsteps or tensile strength is reduced to zero in steps, it is possible to model the sequence of crack formation. This information may be compared with available historical records in order to collect evidence supporting the validation of the simulation or in order to interpret ancient strengthening interventions.

- Secondly, the consistency of the model is more carefully pointed out because it can be checked that cracks which do not open in the real building, also do not open in the numerical model.

One of the bolder masonry structures ever built, the Mole Antonelliana, provides an example of no tension analysis applied to the assessment of strengthening measures [5].

Finally it should be noted that another well established finite element technology, the use of joint elements, is rarely applied to monumental structures. Joint elements are widely used in rock mechanics and have found very useful applications in other engineering fields. Cracks in compression are also common in monumental buildings, there is however little experimental data on the constitutive equation of masonry joints.

3.4   Low amplitude dynamic data

The analysis of the dynamic behaviour is an important diagnostic tool to be used for validation of the numerical model, calibration of average material properties as well as investigation of the connectivity of different structural elements.
The dynamic excitation of the structure can be achieved in different ways:

- by means of environmental vibrations (traffic, wind, bells, microseismic noise, etc.). In this case the testing is easier and inexpensive but signal interpretation is more difficult [19,14,15];

- by means of devices which generate sinusoidal or random forces. In this case the test is costly and more difficult to set up (e.g. because of the need for authorization of load application). The main advantages are the better signal to noise ratio and the possibility to carry out tests at different levels of dynamic excitation [15,21,17].

The level of dynamic excitation is in both cases quite low. This is not so much a technological limit but rather a form of respect to the monument. As the dynamic stresses are small in comparison with the permanent stresses there is no doubt that linear elastic models are applicable even in case the investigation of the static structural behaviour points out nonlinear effects.

In table 2 are summarized the main dynamic test carried out by ISMES on monumental structures. The table shows that many tests, particularly the old ones, have been aimed mainly at characerizing the level of enviromental noise (traffic, wind, bells) in order to asses the risk of damage and therefore no numerical model was created to own knowledge neither by customer nor by others. After 1987 and the numerical/experimental studies carried on the Arnolfo Tower the numerical interpretation of the experimental tests has been performed when structural stability was under examination. Numerical models were set up also for some monuments previously tested (e.g. Marte Ultore Temple).

Year	Monument	Town	Wind	Traffic	Bells	Shaker	Modeling
1982/4	Duomo of Milan	Milan		x			
1984	Marte Ultore Temple	Rome	x	x		x	x
”	Flaminio Obelisk	”		x		x	
1985	Coliseum	”		x			
”	Trajan Column	”		x			
”	Minerva Temple	”		x			
”	Terme of Caracalla	”		x			
”	Trofei of Mario	”		x			
”	Arch of Costantino	”		x			x
1987	Arnolfo Tower	Florence	x			x	x
”	S.Maria del Fiore Cathedral	”	x				x
1989	Grotte di Catullo	Sirmione				x	x
”	S.Francesco Church	Arezzo		x	x		
”	Theater ”Alla Scala”	Milan		x			
1990	Majno Tower	Pavia	x				
”	Fraccaro Tower	”	x			x	x
1992	Campanone Tower	Bergamo	x		x	x	x

Table 2: Dynamic tests

Comparison between measured and computed response can be based on time hystories or other directly available data such as transfer functions. This approach is often numerically expensive during model calibration. Alternatively the measured data may be processed in order to extract natural frequencies and mode shapes. In this way the numerical effort can be more efficiently targeted to a limited number of low frequency modes.

The easiest and more common use of dynamic data for model calibration is the fitting of the first (or the first few) frequency (or frequencies) by adjusting the average elastic modulus. More powerful technologies for model calibration are available even though application to monumental buildings are missing yet. The most common ones are the "Theoretical stiffness matrix" and the "System error matrices" approaches. Both are able to identify and quantity global as well as local sources of discrepancy between computed and measured data.

4. SAFETY ASSESSMENT STUDIES

4.1 Role of numerical computations for safety management

Probabilistic risk assessment has been increasingly used to predict the level of safety or risk associated with structures. The real meaning of such analyses is not completely clear, when applied to unique or potentially catastrophic structures such as monuments, large dams or nuclear power stations [6,7]. Research in the nature of failures and disasters in a general sense has indicated that failure modelling itself fails to account for the occurrence of many failures. This is due to events and unforeseen combinations of events that fall outside the necessarily closed set of scenarios used in probability of failure calculations. Probability theory provides a theoretical framework for dealing with uncertainty, but does not take into account the problems of completeness associated with theories and models.

As the likelihood of failure of a unique structure is essentially unknowable, its safety should be approached as a problem of management. Whereas risk prediction is a calculation at some point in time, management of safety is a continuous procedure, similar to that used in HAZOP studies in the chemical industry, which is a structured discovery technique for identification of hazard in a project design and operation.
In this approach safety must be always under review and important structures must periodically undergo "Hazard Audits", aimed at detecting whether an accident is incubating by testing for the sort of factors which can lead to failure. Safety management is therefore centred on collecting and elaborating information through periodic check-up and, when appropriate, continuous monitoring of the structure. Of course elaboration of information concerning safety may also include, but is not limited to, probabilistic risk analysis.

The concepts introduced in the above summary, which is based on references [8,9], will now be applied to the field of monumental structures. A hazard audit should address three main obvious issues: the extent of our knowledge of the structure, the identification and interpretation of any anomalous trend in structural behavior and finally the capacity to resist exceptional loads or further deterioration. The model calibration studies discussed in the previous section are obviously very relevant to the first two issues. Infact the writer believes that computer interpretation of structural behaviour both as it evolved during the life of the monument and as measured under different test conditions is a cornerstone of the safety management procedure.

For what concerns the third issue, the availability and the actual use of advanced capabilities for estimation of structural capacity is well documented in these proceedings as well as in other previous technical literature. The methodologies presented cover both linear and nonlinear, deterministic and probabilistic approaches. Reviewing this valuable material is not possible in this short document. Here and in the next paragraph another well known, but usually unspoken of, crucial topic will be addressed: the interaction between safety assessment studies and the often extreme variability of structural properties.

A meaningful example is the collapse of the Civic Tower of Pavia documented in [10]. As the permanent load produced mean stresses much lower than the average strength but close to the 5% fractile values, it has been surmised that a local failure has occurred due probably to the combination of a poorly constructed zone in an area of stress concentration. Finite element computations have also proved that a local failure could trigger an overall collapse as the residual load capacity was limited.

This case history poses a crucial question: how could the risk have been diagnosticated in advance? Simplified analysis methods could have indicated the opportunity of further investigations only if

combined with very conservative masonry strength estimation. As the number of material tests is usually small, it is likely that the structure would have been considered safe. In conclusion the writer believes that the uncertainty of numerical results due to with incomplete material characterization is the main problem in safety management of monuments. Sensitivity analyses and probabilistic methods should be used in order to identify priorities and minimum standards for data collection.

In the next section a simplified example will demonstrate the possibility of carrying out such kind of analysis.

4.2   Simplified example of data completeness analysis

A typical medieval church of Southern Italy was selected as representative of a class of structures quite repetitive and widely diffused in Italy. The analyses carried out will be sketched only, as they are not yet completed. Only dead load has been considered and attention is focused on elastic stiffness uncertainties.

A preliminary analysis, based on best estimate material properties, was carried but in order to identify critical areas and to point out the most significant structural parameters, such as stresses or deflections.

Then a linear sensitivity analysis was used to identify the influence on the critical structural parameters of material property variations within the building. During this analysis the finite elements, which belong to the same structural element, are grouped together and the investigated material property perturbations are assumed constant within each structural element.

In our case the vertical stresses in some pillars are the main critical parameters. Of course the vertical stress is mainly influenced by material property variations within the pillar itself, but the sensitivity analysis identifies, which adjacent structural elements are of importance and the extent of the influence (in our case approximately one half of the influence of variations within the pillar itself).

Sometimes the state of stress is large and there is the need for increasing the level of confidence in the computed values by carrying out additional in situ tests for material property characterization. In this case the analysis provides also a rational tools for distributing the (scarce) additional tests among the various members.

As the number of material property tests is always limited the safety of the structure should be evaluated taking into account the effect of non-parametric bounds.

5.   APPLICATION OF ADVANCED MODELLING TECHNOLOGIES

The most advanced modelling technologies are gradually being transferred from other engineering domains to the analysis of architectural heritage. Here a few examples are briefly reviewed.

5.1   Geometric modelling

Solid modelling has been first developed in mechanical engineering for drafting applications. It has now spread to every kind of complex finite element analysis because it has the advantage of addressing separately two difficult tasks: the geometric description of complex shapes and the subdivision of a solid into a finite element mesh. This splitting of the difficulties is essential to keep the most complex problems manageable. Recently a second advantage has been achieved: the second

task, namely the mesh generation, has been completely automated thereby considerably reducing the cost and time required for the analysis.

A first and very substantial application of geometric modelling to architectural heritage is the modeling of Pisa Tower, demonstrated in these same proceedings [11]. The complexity of this model could not have been achieved with other sophisticated but more traditional approaches. A word of caution should however be spent on the automated mesh generation. Unfortunately meshes automatically generated are comprised only of tetrahedral elements. If a linear interpolation of displacement is used, tetrahedral are very stiff and an extremely fine mesh may be necessary to get reliable   results.

It is therefore important that a quadratic or higher interpolation of displacement be used at least in regions when the values of computed stresses is important. Algorithms to check the adequacy of the mesh and to improve the solution either by mesh or by polynomial level refinement should be used in combination with automated mesh generation techniques.

5.2 P-version modelling

The capability to improve the accuracy of the numerical approximation by increasing the polynomial order P of interpolating displacements is known as "P-version" of the finite element method. This capability is the most efficient numerically and it also opens the way to automated accuracy refinement and control [12] P-version may be applied in combination with geometric modelling and automated mesh generation techniques. The advantage is that the degrees of freedom may be assigned automatically in areas of stress concentration in order to improve the numerical results.
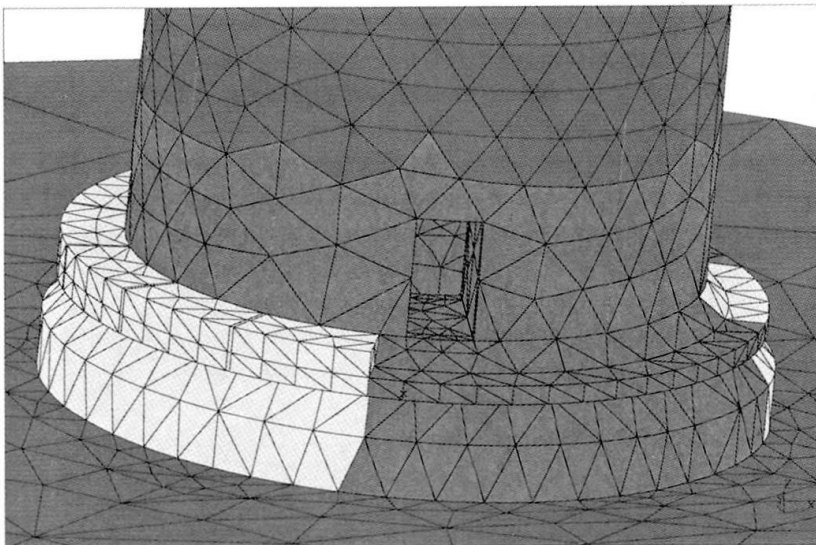

Fig. 2 Use of different polynomial levels according to specific computational tasks

5.3 Explicit integration in time of nonlinear problems

Complex nonlinearities such as opening and closing of joints, cracking, geometric effects and plastic behaviour usually lead to algorithmic difficulties and unmanageable computer costs. On the other hand successful results have been achieved in impact loading and rock mechanics problems by means of explicit time integration of nonlinearities and thanks to the stabilizing effect of inertia forces. Realistic modelling, if at all possible, of the seismic resistance of architectural heritage will be based on this approach, which is however nowadays inadequate to manage realistic problems, both for lack

of experimental validation and for excessive computational effort.

The use of distinct elements, proposed and by other papers [25] in these proceedings, should be further experimented and validated.

5.4   Knowledge-based systems

Artificial intelligence technologies have found interesting niche applications in civil engineering. One of the most relevant is the development of decision support systems.

For architectural heritage two prototypes are being experimented: one is related to interpretation of monitoring data [13] and the other to seismic resistance of masonry structures [15]. If a structural code applicable to architectural heritage will ever be developed, it has to be formulated as a knowledge based system, defining procedures for the management of safety.

6.   CONCLUSIONS

Substantial progress has been achieved with respect to the state of art illustrated by the 1983 IABSE symposium in Venice.

Modelling of architectural heritage is a rapidly exploding field of research, where significant results have already been achieved. Further progress relies on a close cooperation between numerical and experimental work, as both are often meaningless if not integrated.

REFERENCES

[1]   Ferrari da Passano C., Preservation of the Duomo of Milan, SEI, February 1993.

[2]   Jurina L., Peano A., Characterization of brick masonry stiffness by numerical modelling, 6th IBMAC, Roma, 1982.

[3]   Jurina L., Reinforcement of Palazzo della Regione, Milan, SEI, February 1993.

[4]   Chiarugi A., Fanelli M., Giuseppetti G., Analyses of Brunelleschi type Dome - Including Thermal Loads, IABSE Symposium, Venice 1983.

[5]   Nascè, V. and Arrigoni, R. and Pistone, G. and Strona, P.P., La Mole Antonelliana - Indagine Numerica sulla struttura originaria" in Alessandro Antonelli 1798-1888, Franco Rosso ed., Electa, Milano, 1989.

[6]   Macchi G., A note on the Structural assessment of Historical Buildings, Joint Committee on Structural Safety, Delft 1991.

[7]   Fanelli M., The safety of Large Dams, in Blockley D.I. Editor, Engineering Safety, McGraw Hill, London 1992.

[8]   Comeford J. B., Blockley D.I. Managing Safety and Hazard through Dependability, Journal of Structural Safety, 1992.

[9]   Comeford J. B., et al., The role of AI technology in Management of Dam Safety: the DAMSAFE System, Dam Engineering, Vol. III Issue 4, 1992.

[10]   Macchi G., Monitoring Medioeval Structures in Pavia, SEI, February 1993.

[11] Macchi G. et al., Structural Assessment of the Learning Tower of Pisa, IABSE Symposium on Structural Preservation of Architectural Heritage, Rome 1993.

[12] Peano A., Computer Aided Quality. Assurance of Finite Element Computations, SEI, November 1991.

[13] Lancini S. et al., Techniques and Methods for automatic Diagnosis of Anomalous Structural Behaviour of Pavia Tower and Cathedral, IABSE Symposium in Structural Preservation of Architetcural Heritage, Rome 1993.

[14] Carfagni M., Carfagni, S., Using Numerical and Experimental Modal Analisys in Building Conservation: the Case of the Medieval Belltower of the Church of Badia fiorentina in Florence, Italy, Proceedings of Florence Modal Analysis Conference, September, 1991.

[15] Fanelli M., A. Pavese, Diagnosis of Masonry Towers by Dynamic Identification Using Parametric Techniques, Proc. of IABSE Symposium on Structural Preservation of Architectural Heritage, Rome 1993

[16] Baggio, C., Computer analysis of Masonry Domes Following Castigliano's Suggestion. An example: the Dome of S. Pietro in Vaticano, Proc. of International Technical Conference, Athens, 1989.

[17] Bettinali F., C. Galimberti, M. Meghella, E. Pizzigalli, Identificazione Dinamica della Torre del Palazzo della Signoria in Firenze, Atti 5° Convegno Nazionale l'Ingegneria Sismica in Italia Palermo, Ottobre - Novembre, 1991.

[18] Chiarugi A., P. Foraboschi, Identificazione Strutturale nella Salvaguardia della Costruzioni Monumentali: Applicazione al caso di Palazzo Vecchio, Atti 4° Convegno Nazionale l'Ingegneria Sismica in Italia Milano, 1989.

[19] Chiostrini S., Un esempio di Modellazione numerica di Grandi Edifici Monumentali: La cupola del Brunelleschi a Firenze, Bolletino Ingegneri, 1991, volume 1-2.

[20] Blasi C., C. Borri, S. Chiostrini, Modellazione Numerica di Azioni Statiche e Dinamiche sulla Cupola di Santa Maria del Fiore, Bolletino Ingegneri, 1991, volume 1-2.

[21] Chiostrini S., A. Vignoli, Valutazione del Danneggiamento di Strutture in Muratura Attraverso un Modello agli Elementi Finiti, Atti 5° Convegno Nazionale l'Ingegneria Sismica in Italia Palermo, Ottobre - Novembre, 1991.

[22] Karantoni F., M.N. Fardis, Assessment of Analysis Methods and of Strengthening Techniques for Earthquake Resistant Masonry Structures, Structural Conservation of Stone Masonry - International Technical Conference, Athens, 1989.

[23] Cappi A., a. Fontana, Strengthening of Old Masonry Bridges, Structural Conservation of Stone Masonry - International Technical Conference, Athens, 1989.

[25] Pagnoni, T., N. Misticò, G. Canofeni, "Quasistatic Seismic Analisys of S.Maria Maggiore in Tuscania", Universitá degli studi "La Sapienza" Dipartimento di Ingegneria Strutturale e Geotecnica.

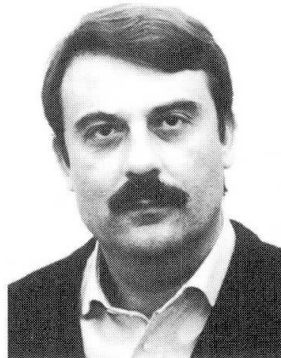Leere Seite

Blank page

Page vide

Analysis of the Seismic Response of Masonry Structures

Analyse du comportement séismique des structures en maçonnerie

Analyse des Erdbebenverhaltens der Mauerwerksbauten

Piero D'ASDIA
Assoc. Professor
Univ. "La Sapienza"
Rome, Italy

P. D'Asdia, born 1946, got his civil engineering degree in 1971 at the University of Rome "La Sapienza", where he worked as a researcher. In 1980, he became assistant professor and is now associate professor. Since 1971 he was involved in research in several fields of structural engineering, namely: elastic stability, structural optimization, finite element technique for the analysis of degrading and geometrically non-linear structures.

SUMMARY

For the analysis of the seismic response of masonry structures a number of procedures are available, which can be arranged in two groups: the first includes methods following the finite element approach, the second consists of procedures modelling only anticipated behaviour and collapse modes. Methods pertaining to both groups are taken into consideration, factors in favour or against their use for the analysis of different types of masonry structures are discussed. For evaluating the ultimate strength of walls subject to horizontal forces in their plane a method incorporating favourable features of both groups is proposed.

RÉSUMÉ

Pour l'analyse du comportement séismique des structures en maçonnerie, il existe de nombreuses procédures qu'on peut répartir en deux groupes: L'une comprenant les méthodes obtenues avec l'approche des éléments finis; et l'autre groupant les procédures qui modèlent les comportements et les modes de rupture déterminés préalablement. Cet article considère les méthodes des deux groupes et analyse les éléments en faveur ou contraires à leur emploi dans l'analyse de structures en maçonnerie. Afin d'évaluer la résistance des parois exposées aux forces horizontales dans leur plan, on propose une méthode qui présente des caractéristiques favorables des deux groupes.

ZUSAMMENFASSUNG

Für die Erdbebenanalyse der Mauerwerksbauten sind verschiedene Verfahren verfügbar. Sie sind in zwei Gruppen aufgeteilt: Die erste umfasst Methoden auf der Basis Finiter Elemente; die zweite Verfahren, nach denen voraussichtliches Verhalten und Bruchformen modelliert werden. Die Methoden beider Gruppen werden berücksichtigt und die zugunsten oder gegen ihre Verwendung bei verschiedenen Arten von Mauerwerksbauten wichtigen Elemente hervorgehoben. Um die Bruchfestigkeit der Wände gegenüber horizontal wirkenden Scheibenkräften zu bewerten, wird eine Methode vorgeschlagen, die geeignete Eigenschaften beider Gruppen verbindet.

1. INTRODUCTION

When the structural behaviour can be schematised as elastic-linear, the analysis of the dynamic response to seismic action is accurately performed through a mode-superposition procedure with the response spectrum thecnique. The ductility factor method allows the extension of such approach to structures characterised by elastic-perfectly plastic behaviour.

Even when the elastic behaviour is not linear (geometric non-linearity) or when the evaluation of the local ductility is required, the dynamic non linear seismic response of the structure can be analysed through the step by step integration of the equations of motion under a suitable set of accelerograms, recorded and/or numerically generated. Such approach requires a larger expenditure of computing effort, but the increase of personal computer power and the wide diffusion of general purpose non-linear programs (ADINA, ANSYS, etc.) implemented on personal computer, allow many designers to analyse with good accuracy the seismic response of large non-linear structures, as far as the constitutive law of structural material and elements can be reasonably assumed as elastic-plastic (even if hardening or softening and non-holonomic).

Unfortunately, the behaviour of most unrenforced masonry structures can't be assumed as plastic and is instead ruled by tension cracking, very low ductility in compression and shear strength variable according to the normal stress state, due to cohesion and internal friction. In such situation, the use of general purpose computer program (e. g. using in ADINA finite element ruled by the concrete law) for performing dynamic analysis provides significant results only associated to a high degree of discretization, usually attainable only for small structures.

Recently have been developed specific finite elements models (e. g. [1, 2, 3]) which represent typical features of masonry behaviour as an adequate schematization of the ultimate strength domain in the σ_1-σ_2-τ field, a satisfactory modelling of every allowable stress-strain path under monotone loading (descent branch included) and a sufficient ability to describe opening and closing of cracks and material degrading. They are a useful tool to understand the behaviour of typical structural elements under cyclic actions, allowing comparison with experimental results [4] and identification of the ruling parameter (see in fig. 1 the comparison between numerical and experimental results for a reinforced masonry panel under horizontal load [5]), but even they are non suitable for the analysis of the dynamic response of large masonry structures, non only for the intractable dimension of the problem, but also because many other uncertainties (e. g. the peculiar behaviour of the junctions between structural elements, often providing only unilateral constraints) add to the intricacy of the material behaviour.

If the above mentioned considerations point out that dynamic analysis is usually inappropriate or not appliable to define the response of masonry structures to seismic actions, then the evaluation of the ultimate strength to static forces (suitably simulating an approximate conservative distribution of inertia forces) appears more meaningful and the simpler procedures needed for such evaluation are less influenced by uncertainties on the material characteristics. That applies also and mainly to large and complex buildings like palaces and churches, dynamic analysis providing an important tool only for the analysis of simpler monuments, like columns and arches, made of large stone blocks simply superimposed, whose response is governed by the frictional behaviour of the joints, which is ruled by a degrading Mohr-Coulomb relationship between the limit shear stress and the normal stress [6, 7, 8, 9].

Assuming thus as a measure of seismic resistance the entity of suitable static loads which attains the ultimate strength of the structure, the distribution of such forces and the procedure for the evaluation of their limit value depend mainly on the structural type.

In the general case (churches, complex buildings and other structures) both horizontal and vertical forces have to be taken into account and their limit value should be evaluated through finite element modelling and non linear analysis procedure.

In the particular but frequent case, instead, of palaces where floors act as rigid diaphragms, being the seismic action sustained mainly by the strength of the walls in their plane, horizontal forces are normally of greater importance than the vertical ones and, for the evaluation of their limit value, a number of methods have been proposed which determine the ultimate strength of the walls according to one or more collapse mechanism (with better performance of those methods which take into account more mechanism and less arbitrary hypotheses on the stiffness of the elements involved).

In the next two sections the more suitable analysis procedures are considered for the two aforementioned cases.
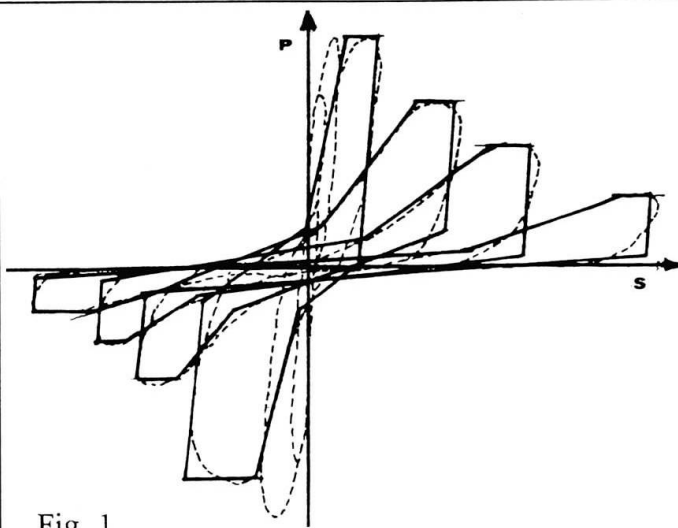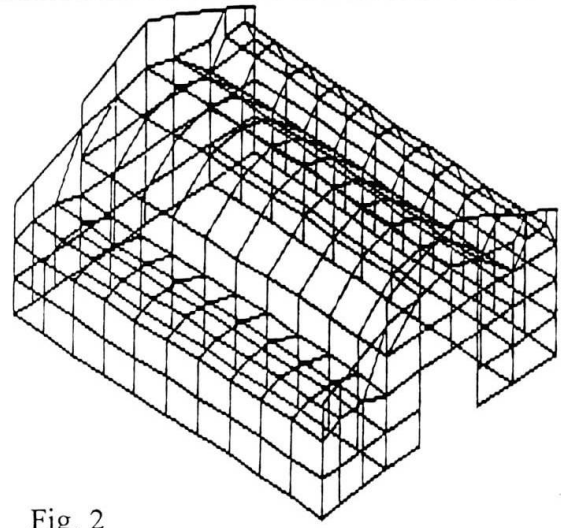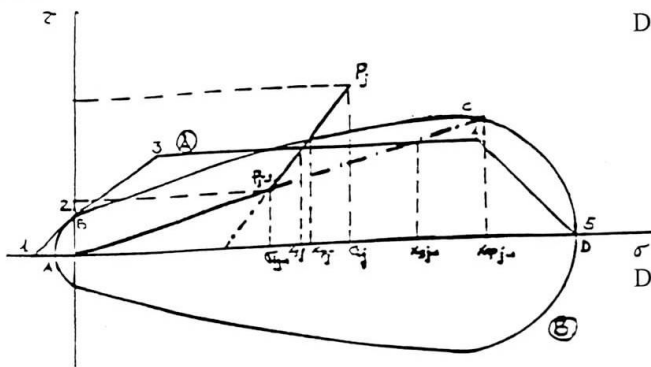
Fig. 1

Fig. 2

Fig. 3

Domain A. - point 1: $\sigma_1 = \sigma_{ut}$, $\tau_1 = 0$

- point 2: $\sigma_2 = 0$, $\tau_2 = \sigma_1 k_1$

- point 3: $\sigma_3 = C_1 \sigma_{uc} k_2 - \sigma_{ut}$, $\tau_3 = C_1 \sigma_{uc}$

- point 4: $\sigma_4 = \sigma_{uc}(1 - C_1 k_2)$, $\tau_4 = C_1 \sigma_{uc}$

- point 5: $\sigma_5 = \sigma_{uc}$, $\tau_5 = 0$

Domain B. - point A: $\sigma_A = \sigma_{ut}$, $\tau_A = 0$

- point B: $\sigma_B = 0$, $\tau_B = \tau_k$

- point C: $\sigma_C = \sigma_4$, $\tau_C = \tau_k \sqrt{(1 + 1.5 \sigma_4 / \tau_k)}$

- point D: $\sigma_D = \sigma_{uc}$, $\tau_D = 0$
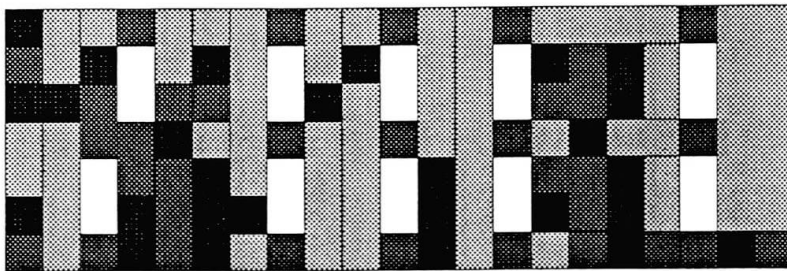
Fig 4.a
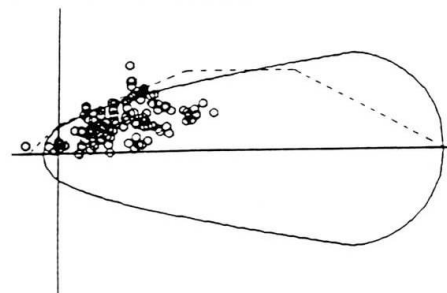
Fig. 4.b

Horiz. Force

Dead Load

SLIP
POR
ELAMOD (Domain A)
ELAMOD (Domain B
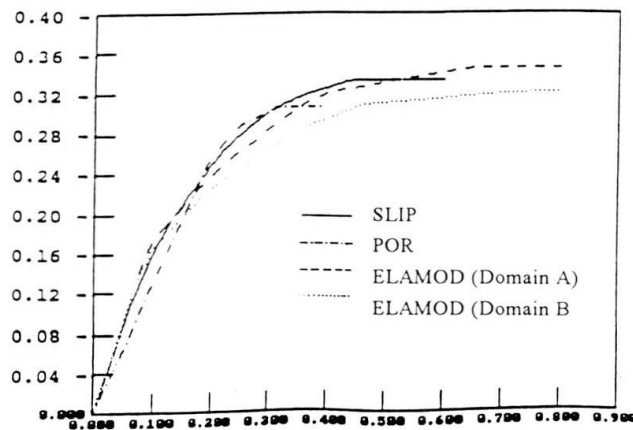
Displacemet (cm)

Fig. 5

2. GENERAL CASE: FINITE ELEMENT APPROACH

Static analysis to determine the collapse load can be performed following the non linear force-deflection path through already mentioned general purpose programs or specific ones. Using plate or shell (or brick) elements, with correct values of the uniaxial strength of the masonry, fragility in tension and prefixed (low) ductility in compression, even if the discretization is not refined, the ultimate strength domain is not completely correct and the elastic characteristic are only approximated, the results provided by the static analysis are usually quite significant.

An useful alternative to the use of non linear programs, which are still non familiar to many designers, is to perform an incremental analysis, piece-wise linear, through a procedure that automatically repeats subsequent runs of a well known linear program (SAP90, SUPERSAP, etc.) suitably changing the data files of the runs.

Synthetically the procedure (named ELAMOD [10]) can be described as follow:

- a data file is prepared describing for a linear program the structure (usually discretized into plate elements) with the dead loads and the live loads to be increased up to the collapse;

- another data file is prepared containing, for the different types of elements describing the structure, the limit domains σ-τ and the allowable ductility in compression along two orthogonal directions (alternatively three-dimensional σ_1-σ_2-τ domain could be used but that is normally not necessary and often non advisable as a too rigid constraint);

- a set of runs are done, the first under dead loads, the subsequent ones under unitary values of the live loads, for each of them a multiplier of the loads is computed which brings stresses or strains of an element, added to those of the previous steps, respectively to the border of a strength domain or to the end of the allowable ductility;

- after each run the structural data file is updated zeroing (or strongly reducing) the stiffness of the element attaining the domain border and/or cancelling the elements reaching the ductility end and applying to the remaining structure the forces carried by them up to that step;

- the procedure stops when the remaining structure can't carry more loads or when part of it is no more constrained.

In comparison with the use of non linear programs, the described procedure presents both advantages and disadvantages, namely:

- the procedure is easy to implement in any computer language (FORTRAN, BASIC, etc.) without being a skilled programmer, moreover, using widely adopted linear programs, it allows designers to prepare data files in the way they are used to; e. g. in fig. 2 is shown the sample presented in [10];

- limit domain shapes can be easily changed, in fig. 3 are shown two possible choices: domain A has a multilinear border (characterised by the three zones of collapse for overturning, shear and compression), domain B is formed by a POR-like curve $\tau_{ult} = f(\tau_k, \sigma)$ limited by circular arches in compression and in tension; analogously others typical features can be easily changed as the mutual influence of the checks along the two orthogonal directions (e. g.: a good choice can be to ignore a modest violation of the border in the tension side if the representative point in the other direction shows a stress state in compression inside the domain);

- reinforcements or frames can be taken into account easily, adding truss or beam elements to the mesh, if necessary a plasticity check of the reinforcements can be performed too;

- the interpretation of the results is easy; e. g. in fig 4 is shown one of the walls of the sample presented in fig. 2, in fig. 4a the element nearer to the border (or in ductile phase) are darker, in fig. 4b are presented the positions of the points representing the stress state of the elements;

- the results are in good agreement with those given by non linear programs, in fig. 5 is compared, for the sample of fig. 2, the equilibrium path obtained through the described procedure with the load-displacement curve given by the non linear program presented in [1, 3, 4]: the results obtained with the same procedure are very near and differ less than those given by the same procedure but with different domains;

- the procedure is numerically not efficient, the required computer time is considerably higher than for non linear programs (up to a few times);

Particular attention should be paid, in both cases of using non linear programs or the described incremental procedure, to the sensitivity of the results to the shape of the limit domains and to the extension of the ductile phase, as well as to the choice of the live load distribution, which should represent significantly the seismic action. In any case of high sensitivity, parametric analysis has to be performed.
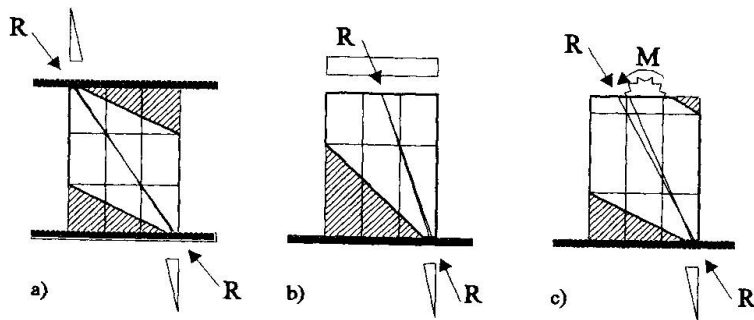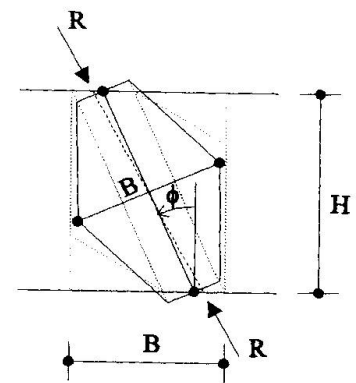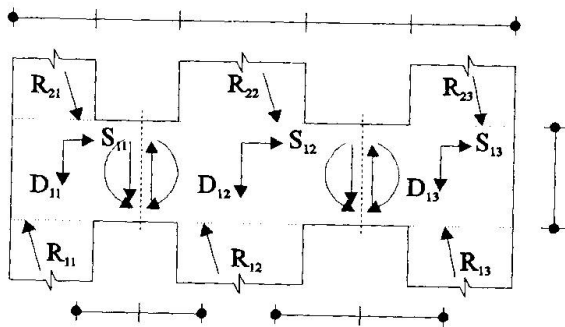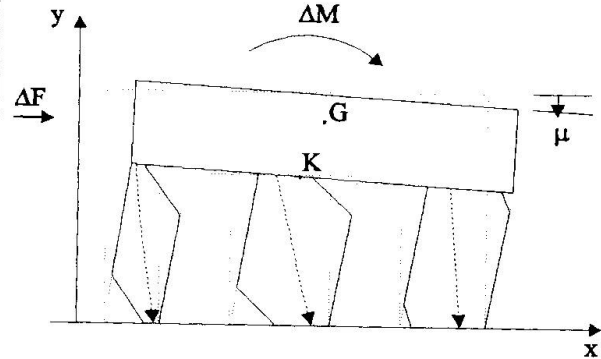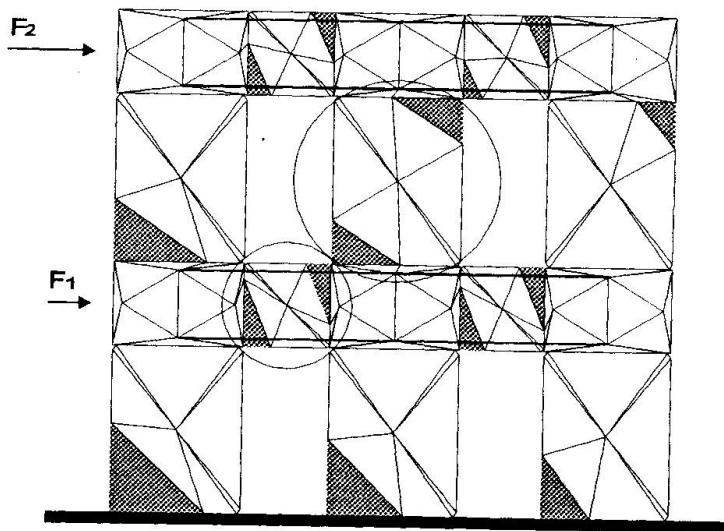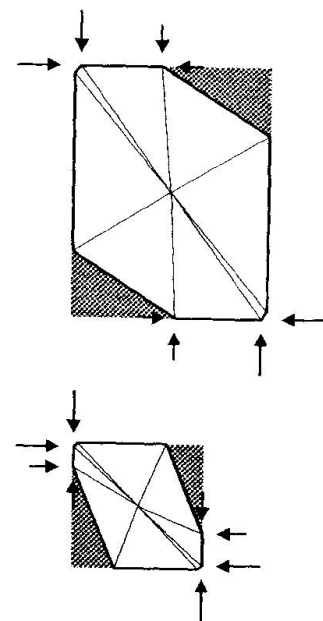
Fig. 6

Fig. 7

Fig. 8

Fig. 9

Fig. 13

3. PROCEDURES FOR EVALUATING MULTI-STOREY WALLS STRENGTH

As already mentioned, buildings with rigid floors, like many palaces, sustain global seismic forces through the strength of the walls in their plane; thus (provided a satisfactory behaviour of the walls with respect to the local action of forces acting in the orthogonal plane), the evaluation of the ultimate strength of the building is easily reduced to the problem of finding the collapse load of the walls.

Buildings damaged by earthquake can present most cracks (usually X shaped) either in the vertical panels between openings of the same floor, or in the horizontal bands between openings of two different floors; the first case represent a shear type behaviour where masonry bands between floors are stiffer and stronger than vertical panels, while in the second case the weaker bands crack first and vertical panels behave as multi-storey cantilever. It is worth noticing that, according to models providing no tensile strength to masonry, the first type of behaviour could not happen without reinforcements in the bands. It is also important to note that the collapse load of the wall, for equal dimensions and strength of the vertical panels, is higher according to the first type of behaviour than to the second one. In fact, in the shear-type behaviour the resultant of the vertical and horizontal forces rotates around the centre of the panel, fig. 6a (the horizontal sections where such resultant is out of the middle third part are partialized according to the low tensile resistance of the masonry). In the case, vice versa, of a cantilever-like behaviour the resultant of the forces rotates around the middle point of the upper section of the panel, fig. 6b. In the other (real) cases the resultant of the forces rotates around points situated between the centre of the panel and the middle point of its upper section, fig. 6c. Therefore, for equal values of vertical load and masonry strength, the shear-type behaviour leads to higher horizontal force at collapse.

For this reason technical rules in many countries prescribe to reinforce the horizontal bands between floors, and specific procedures have been proposed to evaluate the horizontal limit load (for each floor) according to that model of behaviour.

The first one was the well known POR method, which, even if it is still used by designers, was considered unsafe, as it takes into account only shear failure of the vertical panels. Two kinds of improvements were then proposed, the first one [11] adds, in a frame-like evaluation, a verification of the normal stress due to axial force and bending; the second one [12, 13] tests the axial and shear strength of the compressed beam of variable cross-section formed inside each vertical panel, inclined according to the direction of the vertical and horizontal forces resultant applied to the panel, fig. 7.

The last two approaches take into account (in different way) the three main mode of failure of each panel (overturning, shear and compression) and the local breaking of the continuity constrain between vertical panels and horizontal bands. The second procedure [13] provides also the amount and type of reinforcements in the bands necessary to fulfil the hypothesis that bands do not break, fig. 8, and, if the case, it takes into account both the contribution to equilibrium of the vertical reinforcements (prestressed or not) in the panels, and the variation of the ultimate strength in compression with the inclination of the resultant. The wall ultimate strength of each floor is computed separately through 3 equilibrium equation according to the hypothesis of rigid bands; it is worth noticing that in such way compatibility of the vertical panel displacements with the rigid band of each floor is automatically assured, while the evaluation of global effects, as transferring of vertical loads, is only approximate, fig. 9.

When the horizontal bands between floors are not enough strong and/or can't be adequately reinforced, as an alternative to the general procedures mentioned in the previous section, the following method can be employed, based on finite elements of variable shape, which presents some advantages in computer time and in easy understanding of results, while no hypothesis is introduced about the stiffness and strength of the wall elements (as in [11, 12, 13].

The procedure follows step by step the evolution of the resisting part of the wall; initially the structure (panel and band elements) is discretized through a mesh of triangular f. e., as shown in fig. 10 for a vertical panel. As the load increases, the shape of the elements is changed, fig. 11, eliminating the zones where the tension in the masonry is greater than zero or a small allowable value, in fig. 12 are shown both cases. The change of shape is obtained through a suitable translation of the joints, while the state of stress of the elements is changed in such a way to leave unchanged the resultant at each panel end (this condition is easy to obtain with triangular
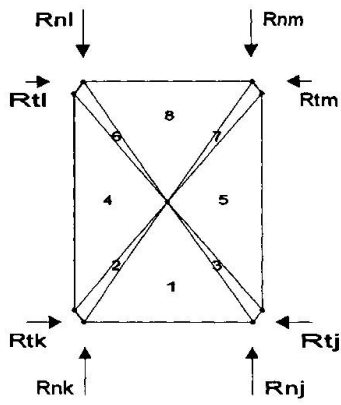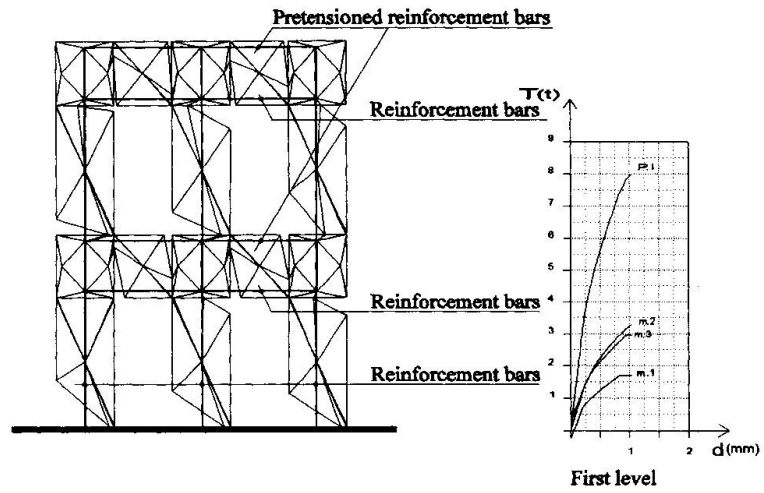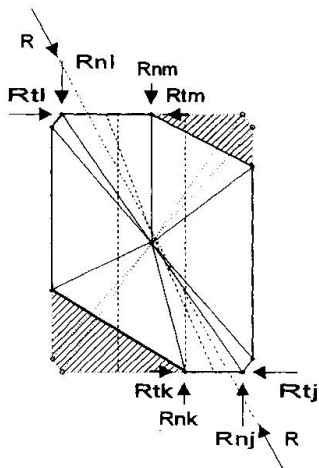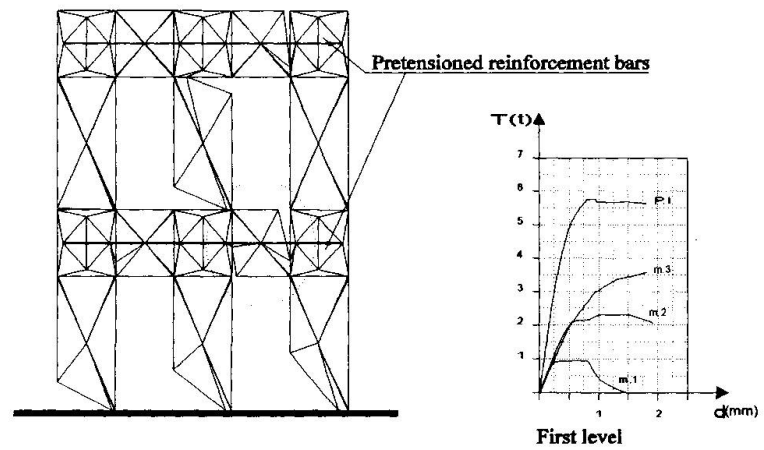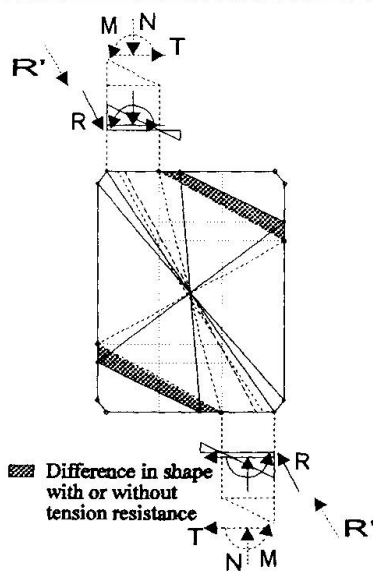
Fig. 10

Fig. 11

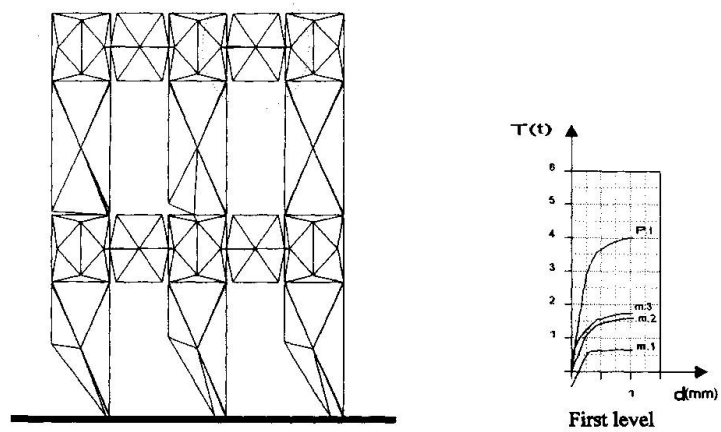Fig. 12

Fig. 14

Fig. 15

Fig. 16

constant strain f. e., and leads to results comparable, in term of generalised stresses, with those given by more complex f. e. approach).

Fig. 13 shows a typical situation of a wall during a loading history. The proposed procedure allows also easily the introduction into the model of reinforcements both horizontal in the bands and vertical in the panels (they can be linked to the joints of the bands also through slipping connection). Fig 14 shows the situation, at collapse, of a wall with reinforcements bars (prestressed in the bands and not prestressed in the vertical panels), in the same figure are shown also the horizontal force - displacement diagrams of the first floor panels and of the whole structure; it is interesting to compare such diagrams with those in fig. 15, regarding the same wall but with reinforcements in the centre of the bands only (same total amount of steel in the bands and same pretension), and with those in fig. 16, regarding the same wall without any reinforcement.

4. ACKNOWLEDGEMENT

The author is indebted to dr. Alberto Viskovic who implemented the computer program according to the procedure for evaluating the ultimate strength of walls proposed in the present paper.

5. BIBLIOGRAPHY

[1] U. ANDREAUS, M. CERONE, P. D'ASDIA, F. IANNOZZI, "A Finite Element Model for the Analysis of Masonry Structures under Cyclic Actions", 7-th IBMaC, Melbourne, 1985.

[2] F. MOTTA, "MASAN - Un codice di calcolo automatico per l'analisi non lineare delle strutture murarie", Atti Istituto di Scienza delle Costruzioni, Università di Catania, n. 74, 1987.

[3] G. CROCI, P. D'ASDIA, A. DI PAOLO, "Risultati e recenti sviluppi nella definizione teorica delle caratteristiche dei materiali e degli elementi murari", 3° Congresso Nazionale ASS.I.R.C.CO - Catania 1988.

[4] U. ANDREAUS, M. CERONE, G. CERADINI, P. D'ASDIA, "Masonry Columns under Horizontal Loads", 7-th IBMaC, Melbourne, 1985.

[5] P. D'ASDIA, "Influenza della legge· di degradazione nella modellazione dei legami costitutivi isteretici", Volume: "Omaggio a Giulio Ceradini", Università di Roma, 1988.

[6] U. ANDREAUS, P. D'ASDIA, A. DI PAOLO, "Sul comportamento di giunti fra conci lapidei: un modello di giunto attritivo", 3° Convegno Nazionale "L'Ingegneria Sismica in Italia ", Roma, 1987.

[7] P. D'ASDIA, D. D'AYALA, "L'Analisi del comportamento attritivo di murature costituite da grando blocchi a secco", 5° Convegno Nazionale "L'Ingegneria Sismica in Italia", Palermo, 1991.

[8] R. GIANNINI, A. GIUFFRE', R. MASIANI, "La dinamica delle strutture composte di blocchi sovrapposti: studi in corso sulla Colonna Antonina", 3° Convegno Nazionale AIMeTA, Torino, 1986.

[9] A. R. LIPSCOMBE, S. PELLEGRINO, "Rocking of rigid-block systems under dynamic loads", Applied Solid Mechanics, 3, London, 1989.

[10] G. CROCI, P. D'ASDIA, D. D'AYALA, "Verifica delle pareti murarie soggette al sisma e definizione degli interventi di rinforzo", 4° Convegno Nazionale "L'Ingegneria Sismica in Italia", Milano 1989.

[11] F. BRAGA, M. DOLCE, "A method for the analysis of antiseismic masonry multi-story buildings", 6-th International Brick Masonry Conference, Rome 1982.

[12] B. CALDERONI, P. MARONE, M. PAGANO, "Modelli per la verifica statica di edifici in muratura in zona sismica", Bradisismo e·fenomeni connessi, Napoli, 1987.

[13] P. D'ASDIA, F. PALOMBINI, A. VISKOVIC "Un modello di Setto Inclinato a Sezione Variabile per l'analisi delle pareti murarie", Quaderni del Dip. di Ingegneria Strutturale e Geotecnica, Università "La Sapienza", Roma, 1992.

Reinforcement Analysis in the Restoration of Masonry Monuments

Étude de renforcement pour la restauration de monuments en maçonnerie

Verstärkungsanalyse für die Restauration von Mauerwerksgebäuden

Donato ABRUZZESE
Civil Eng.
Univ. of Rome 'Tor Vergata'
Rome, Italy

Mario COMO
Prof.
Univ. of Rome 'Tor Vergata'
Rome, Italy

Giorgio LANNI
Assoc. Prof.
Univ. of Rome 'Tor Vergata'
Rome, Italy

SUMMARY

Within the framework of the studies on masonry structures that use the no-tension Heyman model of the masonry material, the paper aims to analyse the influence of the tie rods on the lateral strength of two archetype schemes of many masonry monuments and historical buildings: the plane multi-storey wall with openings and the vault with abutments walls.

RÉSUMÉ

Dans le cadre des études sur les structures en maçonnerie - utilisant en ce qui concerne les matériaux, le modèle non-tension de Heyman - ce travail a pour but d'analyser l'influence des chaînes sur la résistance latérale de deux dispositions types de nombreux monuments et bâtiments historiques: la paroi plane de plusieurs étages avec ouvertures et la voûte avec contreforts.

ZUSAMMENFASSUNG

Im Rahmen von Studien an Mauerwerkstragwerken, welche in Bezug auf die verwendeten Materialien dem zugspannungsfreien Heyman'schen Modell entsprechen, hat diese Arbeit zum Ziel, den Einfluss der Zugstangen auf die seitliche Widerstandsfähigkeit zweier Archetypen - der flachen mehrgeschossigen Wand einerseits und des Bogens mit aussteifenden Mauern andererseits - vieler gemauerten Monumente und historischer Bauten zu untersuchen.

1. INTRODUCTION

There is an increased need to understand the structural principles of the behaviour of masonry structures, mainly for the repair and the statical analysis of monuments and historical buildings. The assumption of a consistent model of the behaviour of the masonry is a fundamental starting point because, very seldom, the traditional linear elastic analysis can be useless. The response of masonry to the applied loads has an unilateral nature: this material, in fact, can carry compressive forces, but can resist only feable tensions [1,6]. In this context the pioneering studies of J. Heyman on the masonry arch [1,2,3,4] still to day represent fundamental results. According to this approach, to interpretate the masonry behaviour, four constitutive assumptions are made:
- sliding failure cannot occur
- masonry has not tensile strength
- masonry has an infinite compressive strength
- masonry is rigid in compression.

Very dangerous for the masonry structures are the actions of horizontal forces, particularly due to earthquakes. It is urgent therefore today the demand of simple and rational methods to control the lateral strength of masonry structures and, eventually, to calculate reinforcements. In progress with the research developed by the Authors on the argument [8,9,10,11], aim of this Paper is to analyse the influence of the horizontal connections, on the lateral strength of two archetypal structures that are the main resistant systems of many masonry buildings and monuments: the plane multistory wall with openings and the vault with abutments walls, both connected by metallic tie rods.

2. LATERAL STRENGTH OF MULTISTORY WALLS WITH OPENINGS AND CONNECTING TIES

Let us consider the plane multistory wall with a regular array of openings, with N_P stories and N_m piers. (Fig.1) The wall is subjected to the action of fixed dead loads G_{ij} and imposed horizontal loads, gradually increasing with the load factor λ.

The piers are connected by means of masonry architraves, eventually reinforced by steel platbands, and also by steel ties passing through the masonry at the floor levels. The platbands or architraves will be able to sustain only compressive forces. On the contrary, the steel ties can sustain only tractions.

Both the architraves and the steel ties can develop elastic strains. In a simplified model of the masonry walls we can take into account only the deformations due to the masonry fracturing. Consequently, under the action of seismic horizontal forces, piers will remain rigid as long as the local turn over failure does not occur. The horizontal displacements of the failed piers will be therefore due only to rotations around their toes. At a generic stage of loading, on a pier act:
- vertical dead loads G_{ij} applied at the pier i and at the story j. The position of the loads G_{ij} with respect to the bottom right toe are defined by the arms b_i.

- horizontal imposed loads λG_{ij}. The elevations of the various stories, where the forces are applied, are indicated by z_j.
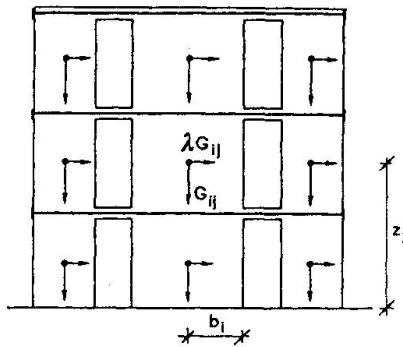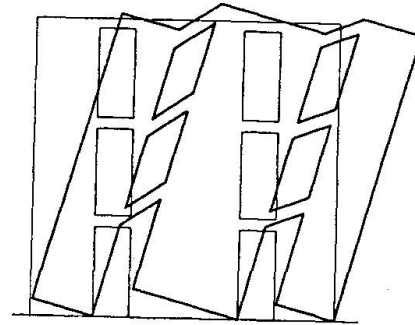
Fig.1 The multistory masonry wall

Fig.2 The sideway failure mechanism

- actions transmitted by the horizontal connections. According to the positions

$$M^S_i = \sum_1^{N_p} G_{ij} b_i \quad M^R_i = \sum_1^{N_p} G_{ij} z_j \quad M^N_i = \sum_1^{N_p} N_{ij} z_j \quad M^T = \sum_1^{N_p} T_j z_j \quad (1)$$

The quantities M^S_i , M^R_i , M^N_i, M^T_i respectively represent:
- the stabilizing moment of all the forces acting on the pier i;
- the turn-over moment of the imposed horizontal loads;
- the moment, related to the span i and respect to the pier base, of the axial forces acting in the architraves;
- the moment with respect to pier base of the tensions in the steel ties.

Each masonry pier is characterized by a proper lateral strength λ_{0i} defined by the limit value of the multiplier λ of the horizontal loads

$$\lambda_{0i} = M^S_i / M^R_i \qquad (2)$$

Under the gradually increasing lateral forces the local failure in the weakest pier is attained when the load factor λ reaches the value

$$\lambda^*_{0i} = M\ IN\ (\lambda_{0i}) \qquad (3)$$

The full lateral strength of the wall, on the contrary, will be attained when all the piers will have reached their proper failure condition under the limit value λ_0 of the load factor.
At the collapse of the wall the following equilibrium equations will be satisfied
- for the first pier

$$M^S_1 + \lambda_0 M^R_1 - M^N_1 + M^T = 0 \qquad (4)$$

- for the pier i

$$M_i^S + \lambda_0 M_i^R + M_{i-1}^N - M_i^N = 0 \qquad (5)$$

- for the last pier

$$M_{Nm}^S + \lambda_0 M_{Nm}^R + M_{Nm-1}^N - M^T = 0 \qquad (6)$$

Summing up these equations we obtain the collapse multiplier λ_0

$$\lambda_0 = \sum_1^{Nm} M_i^S \ / \ \sum_1^{Nm} M_i^R \qquad (7)$$

that is included between the minimum and the maximum values of the local collapse multipliers λ_{0i}. We immediately recognize the strengthening effect due to the introduction of ties. Because of the unilateral character of the horizontal connections, we have to associate to the equations (4), (5), (6) the following inequalities

$$M_i^N \geq 0 \qquad (i = 1, \ \ldots, \ N_m) \qquad (8)$$

At least one of the unknowns M^N_i , M^T must be equal to zero.
Let us suppose, in fact, that at the collapse the tensions in the steel ties are not equal to zero. It means that the horizontal fiber of the wall along any tie rod is stretched out. If, on the other hand, at any span of the wall the compression in the architraves were not zero, the same horizontal fiber should become shorter. Hence, to accept the stretching of the ties implies that at least in one span the compression in the architraves is zero.
On the contrary, if all the compression in the architraves were different from zero, the tensions in the steel ties will be equal to zero. Thus, since at least one of the unknown must be equal to zero, the system of equation (4), (5), (6) and inequalities (8) has an univocal solution. A simple procedure to obtain the solution of the problem has been proposed by the Authors in [11]. Once that the solution has been obtained, i.e. the collapse multiplier λ_0 together with the global moments M^S_i , M^R_i , M^N_i , M^T_i have been evaluated, it is necessary to define stresses in the ties. As usual, along the height ties are all equal each others ; thus we can write, according to the assumed model for the masonry behaviour

$$T_j = T_1 z_j \ / \ z_1 \qquad (9)$$

With this position the evaluation of the stresses in the tie rods at the ultimate state of the multistory wall can be immediately obtained.

3. VAULTED STRUCTURES

The evaluation of the vaults thrust, in order to design abutments able to stand firm against overturning, is a very old problem in the history of the mechanics of masonry structures [1]. The failure mechanism of the vaulted structure, with the determination of the position of the hinges, was another aspect of the same problem. Fig.3 shows the symmetric failure mechanism of this structure. A wide numerical investigation has been carried out by the Authors in the study of the symmetric collapse of the system with   a linearly increasing vertical load applied only on the vault and fixed loads on the abutments. The failure mechanism of the vault under the above defined system of vertical loads is characterized by the occurrence

of two hinges symmetrically placed at the intrados of the vault
(Fig.3) with an angle ϕ equal to 30° respect to the horizontal
chord. Fig.4, on the other hand, shows the multiplier λ_0 of loads
applied on the vault versus the ratio H/r, i.e. the ratio between the
height of the abutments and the radius of the vault at the intrados.
Contrary to the old De Durand [1] old rule, we can recognize the
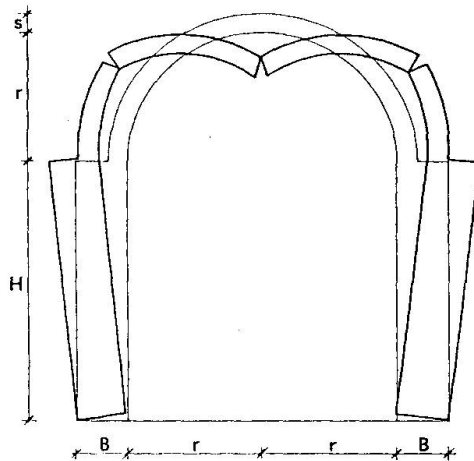influence of the abutments height on the multiplier $\lambda_0 sim$.

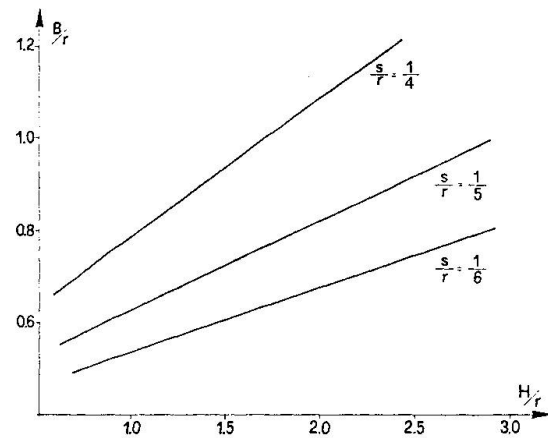<u>Fig.3</u> Symmetric failure mechanism
of the unreinforced vault

<u>Fig.4</u> The influence of H/r on the
collapse multiplier $\lambda_0 sim$

The vaulted masonry structure is very weak under horizontal loads.
On one side the thrust due to dead loads sums up to the thrust due
to the horizontal actions. The turnover failure of one abutment with
the occurrence of hingings in the vault is very frequent, as we have
shown in a previous analysis[8,9]. A chain just under the springings
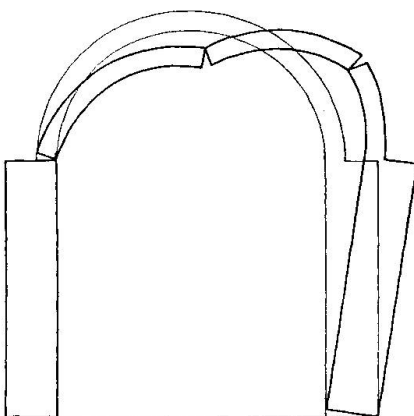of the vault is therefore often introduced.

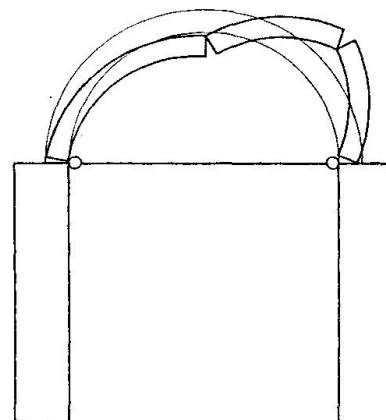<u>Fig.5</u> The four bar chain
mechanism

<u>Fig.6</u> The local sideways mechanism
of the vault alone

Let analyse therefore the vaulted structure of Fig.5 reinforced by a chain, passing through the head of the abutments. The introduction of the chain avoids the occurrence of the collapse mechanism of Fig.5, the so called four bar mechanism, with three hinges in the vault and a fourth at the toe of the right abutment.The collapse behaviour of the chained vaulted structure under horizontal loads is different. As the lateral loads increase in magnitude, the structure in fact will fail by one of the three different mechanisms:

a) *local sideways mechanism of the vault alone*
The masonry cracks in four sections of the vault with the development of a four bar mechanism with hinges only in the vault.(Fig.6)

b) *local sideways mechanism of abutments alone*
Cracks with hingings occur at the tops and at the toes of both the abutments walls. (Fig.7)

c) *global failure mechanism.*
The vaulted chained system can fail with a global "five bar chain" with the occurrence of hingings both in the vault and at the right toes of the abutments. (Fig.8) The study of this *global failure mechanism* of the vaulted system requires the analysis of the "five bar chains" with the localization of the rotation centers of the four rigid parts in which the system, at the failure, is subdivided. The presence of the chain require equal rotations θ around the toes of the two abutments. In the kinematical analysis at the collapse compatibility conditions require the opening of the fractures at the hinges.The collapse of type a) has been thoroughly examined in [8,9]. The collapse multiplier λ_0 corresponding to the mechanism b) can be easily obtained and is given by

$$\lambda_{0\,(b)} = \frac{G_v\left[\dfrac{(B-s)\,(r+s)}{(2r+s)} - s\right] + G_a B \cdot}{G_a\,H + G_v Y_{Gv}} \qquad (10)$$

where Gv and Ga represent the weights of the vault and of the single abutment, B and H the width and the height of the abutments, s and YGv respectively the thickness and the height of the center of gravity of the semicircular vault.

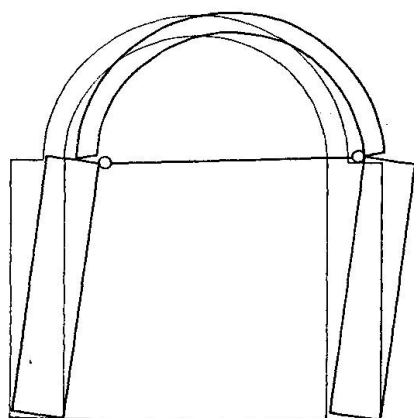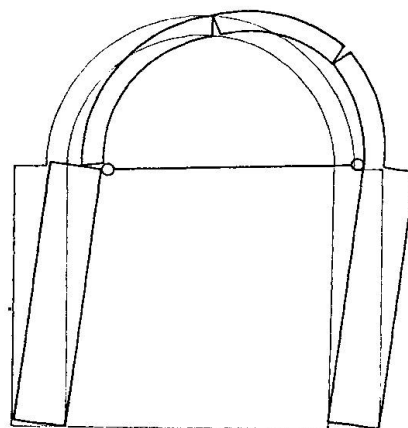Fig.7 The local sideways mechanism   Fig.8 The global failure mechanism
     of the abutments alone   of the vault

The occurrence of the various different mechanism and the corresponding values of the lateral strength of the structure, depends on numerous geometrical .factors. The collapse multipliers corresponding to the mechanisms b) and c) are very near each others. The contribution to the resisting work of the masses of the vault is mainly due to the lifting depending on the abutments rotation. Less relevant, in fact, is the contribution due to the lifting depending on the hinging in the vault.

From a practical point of view, when the collapse is not only localizes in the arch, the load multiplier can be therefore evaluated by means of the eq.(10).

Once the collapse multiplier λ_0 has been obtained, as minimum of the kinematical multipliers in the set of the admissible mechanism, type a), b) and c), the thrust line, passing through the hinges, has been traced in order to control the admissible state of stress inside the vaulted system at the failure (Fig.9).

An extended numerical investigation has been developed to evaluate the type of mechanism that occurs at the failure according the values of the most significant parameters of the structure geometry, expressed by the ratios H/r, B/r, s/r.

In Fig.10, if the point (H/r, B/r) representative of the vault, falls above of the straight line corresponding to the value of the ratio s/r, the collapse occurs with the development of the failure mechanism a).Otherwise, the failure occurs with the mechanisms b) or c).

It is interesting to evaluate the lateral strength increment obtained by the introduction of the chain with respect to same but unreinforced vaulted system. An investigation has been made to evaluate the dependence of this increment on the vaulted system geometry: the most significant parameter in this case can be represented by the above defined load multiplier λ_{0sim} concerning the symmetric collapse of the system. In Fig.11 is represented the ratio

$$\rho = \lambda_{0\ chain} / \lambda_{0\ no\ chain} \tag{11}$$
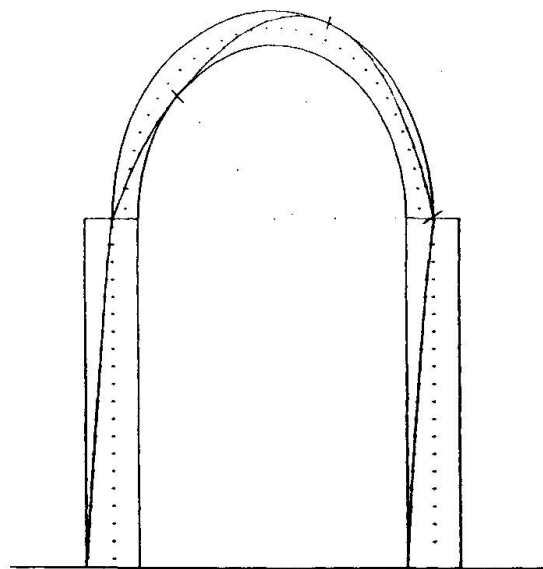

Fig. 9   The thrust line tracing to verify the results obtained by the kinematical procedure
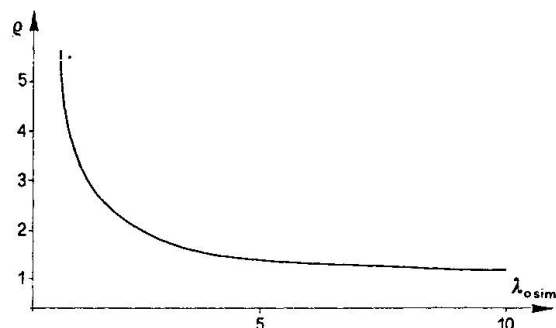
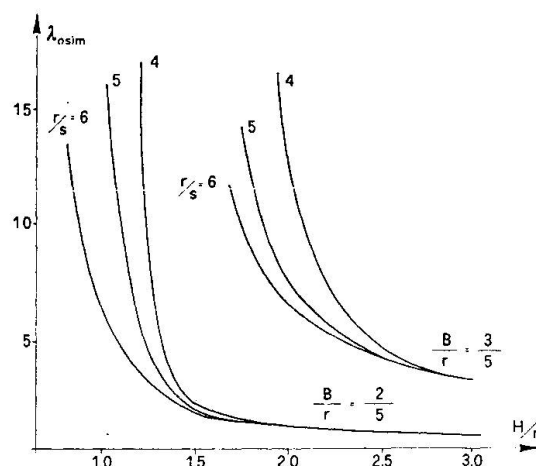**Fig.10** The occurrence diagram of the various failure mechanisms

Fig.11 Strength increment due to the introduction of the chain

versus the multiplier λ_{osim}. Of course, in presence of high values of λ_{osim} the influence of the introduction of the chain is not significant; the contrary occurs for small values of λ_{osim}.

REFERENCES

1.   HEYMAN J., The stone skeleton. Int.Journ. of Solids and Struct.,Feb.,1966.

2.   HEYMAN J., The safety of masonry arches.Int.Journ.Mech.Sci., Vol.11, 1969.

3.   HEYMAN J., Equilibrium of shell structures. Clarendon Press, Oxford,1977.

4.   HEYMAN J., The Masonry Arch.. Cambridge Press, Cambridge 1982.

5.   BENVENUTO E., An introduction to the History of Structural Mechanics. Part II, Vaulted Structures, Springer Verlag, 1991.

6.   COMO M., Equilibrium and collapse Analysis of masonry structures. Meccanica, Vol.27, No.3, Kluwer, Acad. Publ., 1992.

7.   COMO M., GRIMALDI A., An Unilateral Model for the Limit Analysis of Masonry Walls. Intern. Congr. on 'Unilat. Probl. in Struct. Analysis, Springer Verlag,1985.

8.   COMO M., LANNI G., Sulla verifica alle azioni sismiche di complessi monumentali in muratura, 3° Congr. Naz. Ing. Sism., Dip.Ing.Civile, Rep.n.11, Roma 1987.

9.   COMO M., GRIMALDI A., LANNI G., New results on the horizontal strength evaluation of masonry buildings and monuments. 9th World Conf. Earthquake Eng. ,Tokio,1988.

10.   ABRUZZESE D., COMO M., LANNI G., On the horizontal strength of the masonry cathedrals. ECEE,9, Moscow, 1990.

11.   ABRUZZESE D., COMO M., LANNI G., On the lateral strength of multistory masonry walls with openings and horizontal reinforcing connections. Proc.Tenth World Conf. Earthquake Eng. Madrid,. Balkema, Rotterdam, 1992.

Influence of Ashlar Inclusions on Behaviour of Masonry Walls

Influence des pierres de taille sur le comportement des murs en maçonnerie

Einfluss der Quadersteineinschlüsse auf das Mauerwerksverhalten

José B. IZQUIERDO
Structural Engineer
INTEMAC
Madrid, Spain

José B. Izquierdo, born 1948, earned his Civil Engineering degree at the Polytechnical University of Madrid, Spain. For the last 18 years, he has been in charge of the Pathology and Rehabilitation Department of INTEMAC. He is currently also President of Group IV, Maintenance and Repair, of the Spanish Section of the CEB.

SUMMARY

The behaviour of masonry facade walls can be strongly affected by the inclusions of ashlar pieces as ornate of doors, windows and corners and also on cornices. Their omission in the assessment may lead to errors on the unsafe side. In this paper a study using finite element analysis for a particular case illustrating this effect is shown.

RÉSUMÉ

Le comportement des murs en maçonnerie peut être fortement influencé par la présence de pierres de taille disposées comme ornement de portes, de fenêtres, d'angles ou de corniches. Il faut tenir compte de cette particularité dans l'évaluation de la résistance, car elle a en général un effet négatif. Un cas particulier, étudié à l'aide d'une analyse par éléments finis, est présenté dans cet article.

ZUSAMMENFASSUNG

Das Mauerwerksverhalten wird stark beeinflusst durch Quadersteineinschlüsse, die als Ornamente von Türen, Fenstern, Ecken oder Erkern dienen. Werden sie bei der Abschätzung des Verhaltens vernachlässigt, können daraus Fehler zur unsicheren Seite hin entstehen. Der Artikel beschreibt eine mittels der Finiten-Elemente-Methode analysierte Fallstudie.

1. INTRODUCTION

The internal performances of an ancient building's masonry walls are usualy not considered in detail when studies on structure rehabilitation are tackled by the Engineer. The Technician is not hardly enticed to carry out sophisticated analysis about actual behaviour of those elements due to their massive character.

For normal uses, assessing masonry walls as performed by an homogeneous, isotropic material, not taking into account the intrinsic complexity of their composition, may be used as a sufficiently precise approximation; particularly when vertical loads are predominant and compression stresses are high enough to ensure that friction forces will be developed in such a way that relative displacements between adjacent blocks and even between blocks and filling mortar will be restricted.

Classical redesign assumes the wall as a two-dimensional, linear-elastic member. Development of discharge arches on lintels is always taken into account, but the actual ability of the structure to develop internal vaults is very rarely considered, excepting, if even, on sandwich walls. Redesign is often made by calculating the mean stress along the wall, assuming that peak stresses are dissipated by the considerably high creep of the masonry. The presence of rigid element on lintels, cornices, corner and jambs, is neglected, and those elements are seen as just decorative pieces with no real influence on the general structural behaviour of the wall.

During the previous studies to the restoration of the Moorish Palace of "La Aljafería" (Saragossa), we noticed that this simplificating hypothesis could sometimes be on the unsafe side. The feeling that substituting a specific material by another of lower performance, on the assessment of the wall, should provide, in any case, a more unfavorable solution, pays no attention to the compatibility of their deformations. This may come to the point of not detecting concentration of stresses high enough to accelerate the collapse of the element.

In this particular case, the main tower of La Aljafería's Palace had the dungeon and ground levels build on sandwich walls, with two ashlar external leaves, about 80 cm thick, and an internal filler on massive rough masonry, with a plaster-based mortar matrix, about 2,0 m thick, which were the only layer of the four upper levels.

The huge difference of deformability and creep between both materials produced a considerably high channelling of loads towards the ashlar shell, having the masonry layers immediate to the top of the ashlar layers very high action effects, which surpassed their resistance capacity. Also the horizontal stresses generated by Poisson effect and plastification of the mortar produced a pressure on the internal face of the ashlar shell that favoured their inestability.

These effects were seen on a finite elements analysis of the cross-section of the wall. This result has made us rethink the convenience of detailed studying of the influence of rigid noble elements of facades in global wall behaviour.

2. MODELLING THE TOWER

This calculating model belongs to the Nordwest tower of Nuevo Baztán Palace, which stands in a village 30 kms away from Madrid, designed as an industrial town during early XVIII century for providing with ammonition, spirits and other various intendence to the royal army of Marie Louise of Savoia, Regent of Spain.

The set of buildings constituted by the Palace, the inevitable church, wine-presses, workshops and market surrounding a huge central square, besides worker lodgings, was designed by J.B. Churriguera, one of the best Spanish baroque architects. The Palace, thought as a "hunting hut" for the Lord and his Court, is a two-storey building with two towers in the corner of the North facade and an extra false tower in the corner of the west facade adjacent to the church.

Building's walls are made out of calcareous stone masonry with lime mortar. The corners, jambs, lintels and cornices are made out of ashlar of much better quality calcareous blocks. The modelized tower has a square section, 6,57 m long and walls of 1,50 m thick in ground, and two upper floors, lighting the wall in the last storey. Two of its facades are exterior ones in all their height while the other two are interior ones in their first two stories.

The thickness of the ashlar pieces that form the jambs, lintels and cornices of the exterior facades is only about 40 cm, been indented with the masonry that performs the wall. The higher body of the tower is also made by ashlar. The scarce entity of ashlar pieces in the lower floors was inviting to a classic manual calculus, but the experience with the Aljafería's Tower enticed us to use a more sophisticated model, introducing these elements with their greater relative rigidity.

Assessment was made modelling the tower with a total of nearly 4.000 knots and 3.000 brick elements, varying in size from $30 \times 30 \times 15$ cm^3 to $100 \times 70 \times 90$ cm^3, what is nearly elemental block level. The cover was represented with shell elements, and the floor loads were supposed punctual, located in the knots, affecting each knot with the load of the according floor surface. Two different types of foundation, rigid and elastic (springs) has been taken into account.

The early results of this study were exposed in the 1st International Conference of Rehabilitation of the Architectural Heritage and Buildings of Tenerife, on July '92. Further analysis taking into account different relationship between deformability modulus and also seismic forces are to be shown now.

3. RESULTS

a) Effect of inclusion of rigid zones

Figures Nº 1 and 2 show the stress levels in facade layer in both foundation hypothesis. In these graphics it is clearly appreciated the effect of development of inner discharge vaults among ashlar pieces. As it can be seen, wall compressions, far for having an uniform distribution from top to bottom, show a widely irregular stress distribution. The effect is better seen when they are confronted with similar sections in which the material is assumed to be homogeneous (Fig. 3) or with a lower relationship between deformation modulus (Fig 4). Also, it's shown how the closest masonry to the ashlar, is overloaded due to the reception of discharging arches.

The effect is also notable in the response of the structure to seismic actions. In fig 5 and 6 can also be seen the considerable difference existing in stress distribution along the structure whether we consider it as built with homogeneous materials and in the case in which we consider the existence of rigid inclusions on corners and around the holes.

In the whereabouts of the base, the stress distribution is strongly conditioned by the rigidity of foundation, but this effect is very

MIN IS   -.195E+03 <JOINT 13>   MAX IS   .493E+01 <JOINT 2555>

Fig 1 . STRESSES ON FACADES
RIGID FOUNDATION

MIN IS   -.217E+03 <JOINT 295>   MAX IS   .124E+02 <JOINT 2555>

Fig. 2 STRESSES ON FACADES
ELASTIC FOUNDATION

quickly disipated with height due to the great efficiency of discharging vaults. This comes to the point that as near as in the first floor level, stress distribution is nearly undistinguishable between both hypothesis.(Fig 7,8)
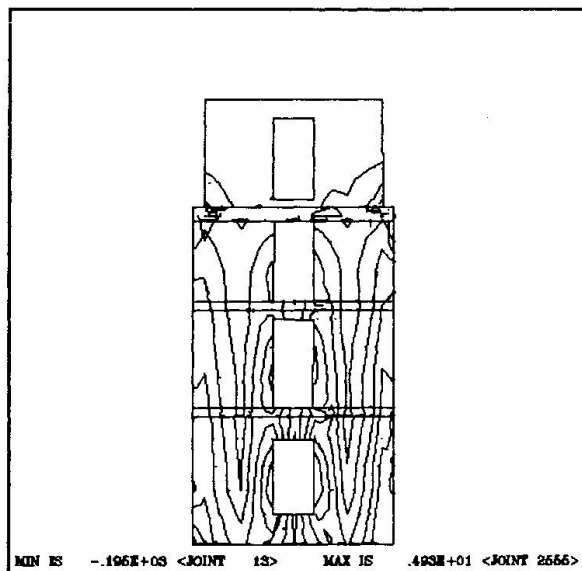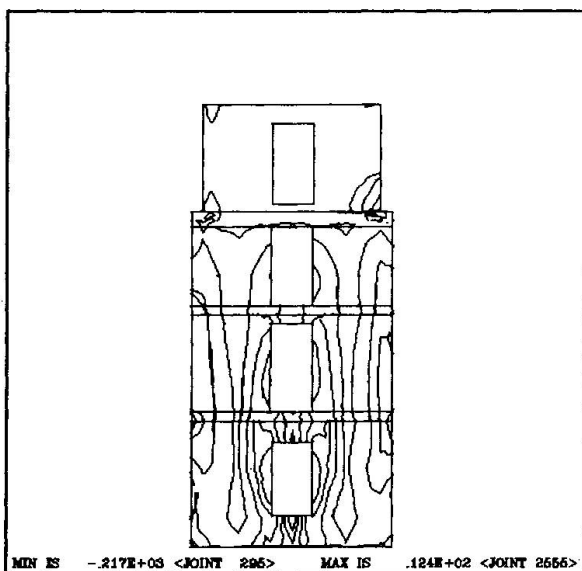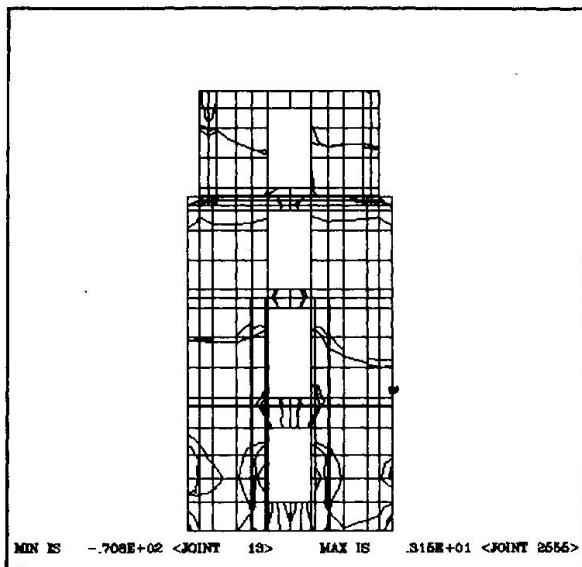
Fig. 3 STRESSES AT FIRST FACADES
        HOMOGENEOUS MATERIAL
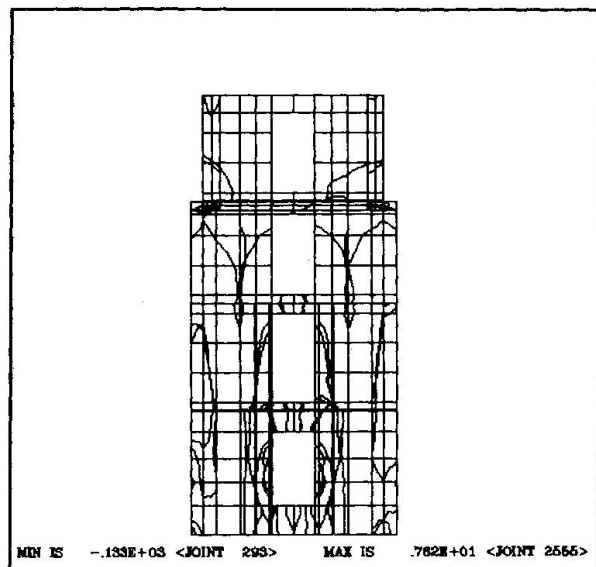

Fig. 4 STRESSES AT FACADES
        SLIGHTLY DIFFERENT MATERIALS
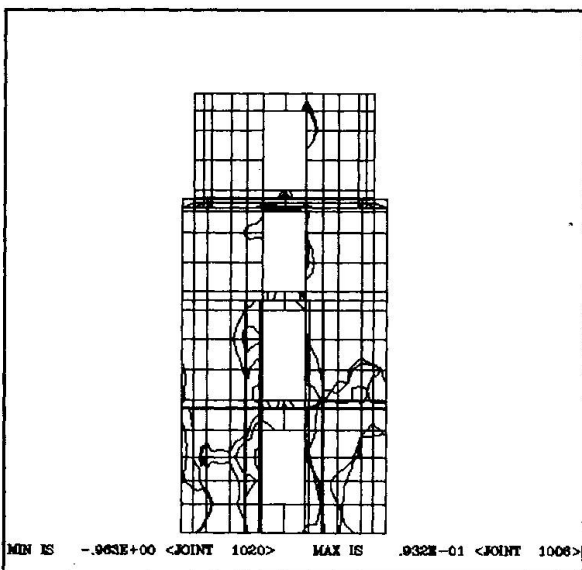

Fig. 5 STRESSES DUE TO SISMIC ACTIONS
        HOMOGENEOUS MATERIAL
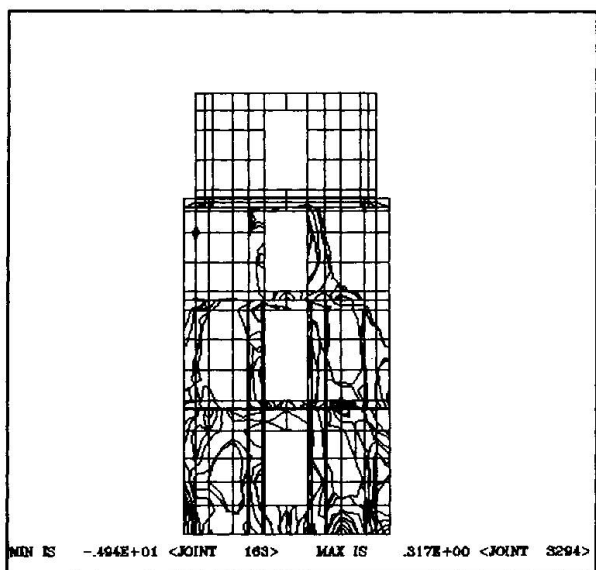
Fig. 6 STRESSES DUE TO SISMIC ACTIONS
        HETEROGENEOUS MATERIAL

An early and easy approximation to the evaluation of this effect can be done by simple substitution of the area of the ashlar elements by masonry elements whose area should be multiplied by the relationship between deformation modulus. Fig 9 and 10 show that this procedure is on the safe side on the evaluation of the action effects as well as in ashlar zones as in the mass of the masonry (zones far away from the rigid zones). The calculus, nevertheless is hardly on the unsafe side in masonry layers in contact with the ashlar pieces, being in the

safe side as soon as an intermediate stress between the one that stands the ashlar, and the calculated stress in the masonry according to this simplified method is adopted for this zone.
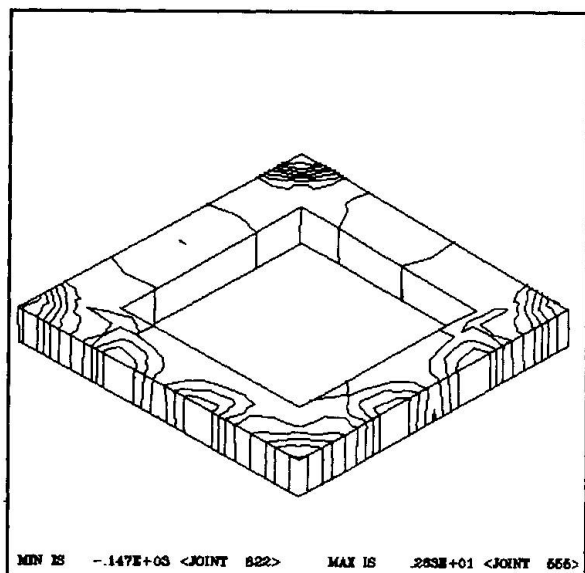

MIN IS   -.147E+03 <JOINT 822>   MAX IS   .263E+01 <JOINT 555>

Fig. 7 STRESSES AT FIRST FLOOR LEVEL
       RIGID FOUNDATION

MIN IS   -.137E+03 <JOINT 822>   MAX IS   .616E+01 <JOINT 620>
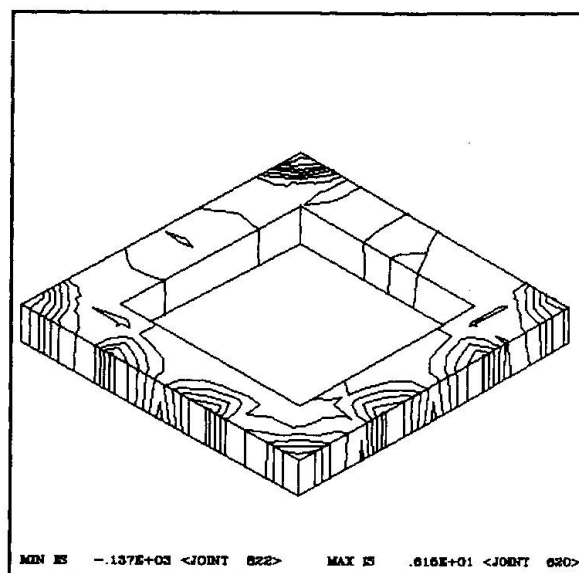
Fig. 8 STRESSES AT FIRST FLOOR LEVEL
       ELASTIC FOUNDATION
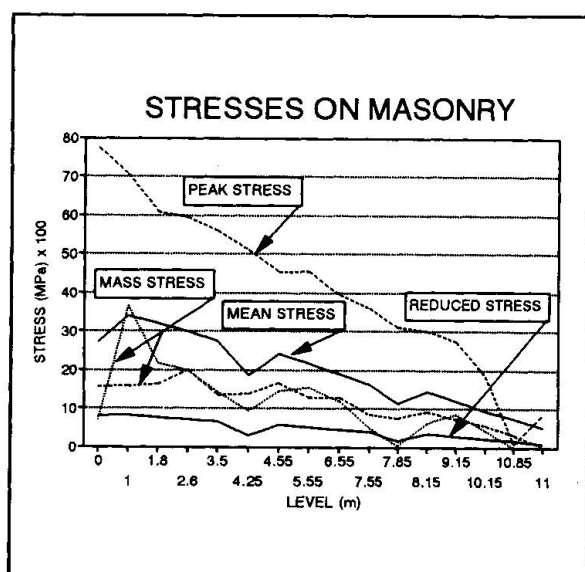
Fig. 9 ACTUAL STRESSES ON MASONRY
       RELATED TO CLASSIC METHODS
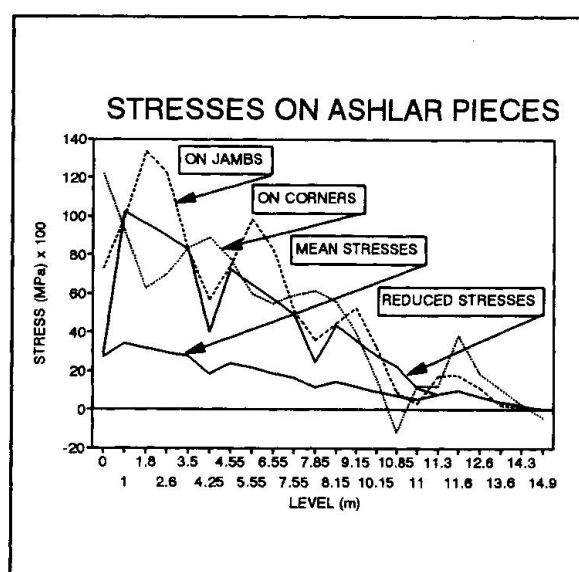
Fig. 10 ACTUAL STRESSES ON ASHLAR
        RELATED TO CLASSIC METHODS

A more accurate procedure requires a very fine net on the modelling of the wall in the neighbourhood of the ashlar pieces, due to the lack of accuracy that introduces the own finite element method in the determination of stress peaks in the proximity of a discontinuity. This takes a huge effort in modelling and interpretation of results, and the use of powerful calculus computers, which are

not within reach of normal projecting offices, so the greater precision achieved
is not rentable for normal cases. Furthermore only with the use of programmes
that allow the consideration of non-linearity of the stress-strain diagrams and
the plastic range is this greater precision turned into a greater accuracy and
thus in a better reflection of the actual behaviour.

8. CONCLUSIONS

-       The behaviour of a building's walls, when their thickness is considerable,
        is conditioned by the development of discharging vaults instead of
        traditional discharging arches. If no 3-D assessment is carried out,
        significant but punctual errors are given on the unsafe side.

-       The existence of ornates, tops, lintels and corners of ashlar included in
        the wall produce a high channelling of stresses, discharging the mass of
        the masonry and overloading the layers in contact with the rigid zones.

-       The classic assessment methods are not sufficient to carry out an accurate
        aproximation to the actual stresses. Nevertheless a more precise order
        of magnitude of its value may be achieved by determining the fraction of
        the load that the rigid pieces recieve by the traditional method of
        analysis of equivalent areas and by adopting a mean tension between the
        corresponding value of the rigid pieces and the one corresponding to
        remainder of the wall section.

Leere Seite

Blank page

Page vide

Investigations on the Load Bearing Behaviour of Multiple Leaf Masonry

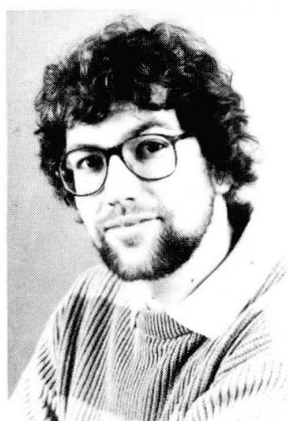Études sur le comportement des éléments multiplans en maçonnerie

Untersuchungen zum Tragverhalten mehrschaligen Mauerwerks

Ralph EGERMANN
Civil Eng.
Büro für Baukonstruktionen
Karlsruhe, Germany

R. Egermann, born 1958, has for seven years been research assistant with a special research programme of the Univ. of Karlsruhe "Preservation of historic buildings - single and multiple leaf old masonry". Since October 1992, he is engaged as consulting engineer in building conservation and repair.

SUMMARY

The aim of the research has been to minimise the amount of strengthening and repair of multiple leaf masonry by a better understanding of its bearing and failure behaviour. By simplified mechanical models, finite element analysis and compressive tests on small size walls, it is shown that the deformation process of multiple leaf masonry has two phases. From a knowledge of the crushing strength of the outer skins, the infill, as well as the relative volume proportions of each, the ultimate carrying capacity of the composite system can be estimated with sufficient accuracy.

RÉSUMÉ

Cet article fait le point sur des travaux de recherche dont le but est de minimiser les mesures de restauration grâce à une meilleure connaissance du comportement mécanique des éléments multiplans en maçonnerie. A l'aide de modèles simplifiés, de calculs d'éléments finis et d'essais de compression sur modèles, il a été démontré que les éléments multiplans suivent deux phases de déformation. En connaissant les résistances à la compression des parois extérieures et intérieures, ainsi que la répartition de leurs volumes, les charges de rupture de ce type de mur peuvent être déterminées avec une bonne précision.

ZUSAMMENFASSUNG

Es wird aus einer Forschungsarbeit berichtet, deren Ziel es ist, durch möglichst genaue Kenntnis des Trag- und Bruchverhaltens mehrschaligen Mauerwerks sanierende Eingriffe auf ein Minimum zu beschränken. Mit Hilfe von einfachen Tragmodellen, Finite-Elementberechnungen und Modellversuchen wird dargelegt, dass mehrschalige Mauerwerkswände ein zweistufiges Verformungsverhalten aufweisen. Die Bruchlasten derartiger Wände lassen sich bei Kenntnis der Bruchfestigkeiten von Aussenschalen und Zwischenschicht sowie der Volumenanteile dieser Komponenten mit hinreichender Genauigkeit vorhersagen.

1   INTRODUCTION

When dealing with preservation or restoration of historic buildings the question frequently arises as to how to assess the residual strength of the existing masonry. In order to evaluate the residual structural capacity the manner of response to loading of the structure in question must be understood. Detailed knowledge of the structural behaviour only permits a static check; but together with testing of the building materials it allows the safety level of the structure to be assessed.

Historic masonry was commonly built using multiple leaf walls consisting in general of two outer walls and a more or less heterogeneous infill; the total thickness being not less than 50 cm. This method of building is around 4000 years old and exists in a variety of forms. Therefore a detailed understanding of the behaviour of these structures is essential, in order to reduce any intervention for the purpose of strengthening or repair to a minimum. Thereby can historic buildings be maintained as authentic as possible.

In this respect the aim of the presented research was to analyse the load bearing and failure behaviour of multiple leaf masonry walls as well as to estimate the ultimate strength.

2   INVESTIGATION METHOD

The load bearing behaviour of multiple leaf masonry was investigated by a three-way approach:

- theoretical identification of the loading of the components by simplified mechanical models
- linear and non-linear finite element analysis
- experimental analysis of multiple leaf masonry wallets under vertical loading

The overlay of the results provided an idea of the load path through the cross sections and enabled a prediction to be made of the ultimate strength of these constructions.

The investigations presumed that all loadings were vertical and uniformly applied. Additional (eccentric) loads caused by wind, hogging or sagging, shaking by traffic or earthquake, are the subject of future research work.

2.1   Mechanical models

2.1.1 Multi-material model

Fig. 1   Multi material model
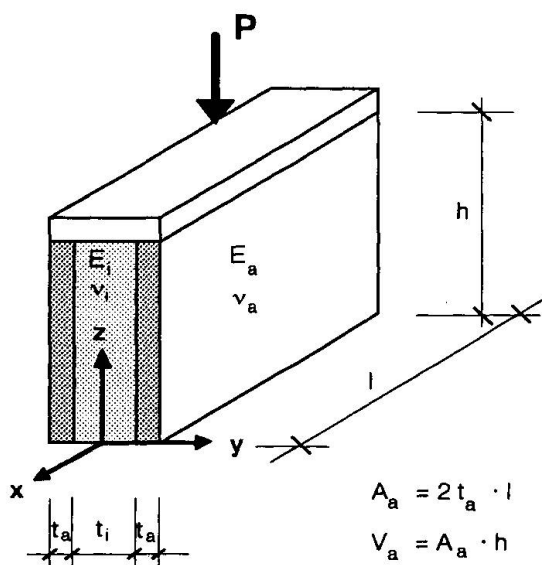
The following conditions were presumed for the validity of the model:

- the system is formed by two parallel situated components (outer skins, infill),
- the outer skins are of similar geometry and materials,
- a stiff loading platen distributes load to the components
  (uniform vertical strain: $\varepsilon_a = \varepsilon_i = \varepsilon_z$),
- the wall is restrained from rotation about the lines of external loading,
- the wall is "long" ($\blacksquare$ plain strain conditions apply: $\varepsilon_x = 0$),
- all components are linear elastic.

If the influence of lateral strain is neglected, the multi-material model can be simplified to the *spring model* [1]. The mechanical behaviour of the components can be described by different springs so that the stresses of outer skins ($\sigma_{zz,a}$) and infill ($\sigma_{zz,i}$) only depend on the ratios of stiffness (E) and geometry (t, A):

$$\sigma_{zz,a} = \frac{E_a}{E_i} \cdot \sigma_{zz,i} \tag{1}$$

$$\sigma_{zz,i} = \frac{P}{A_i} \cdot \frac{1}{1 + 2\dfrac{E_a \cdot t_a}{E_i \cdot t_i}} \tag{2}$$

The modulus of elasticity of the multiple leaf wall can be calculated as:

$$E_{ml} = \frac{A_a}{A} \cdot E_a + \frac{A_i}{A} \cdot E_i \tag{3}$$

The formula forms the basis of predicting the ultimate strength. The condition of compatibility requires the same vertical strains in all components and with the knowledge of the stress-strain behaviour of the components the actual stress of the system can be generally derived from the component stresses and their volume ratios:

$$\sigma = \frac{V_1}{V} \cdot \sigma_1 + \frac{V_2}{V} \cdot \sigma_2 \tag{4}$$

The upper limit of strength is reached if the ultimate strains of the components are equal. In the normal case the ultimate strength of the system depends on the crushing strength of the component with the lower peak strain and the relating stress level of the remainder:

$$f = \frac{V_1}{V} \cdot f_1 + \frac{V_2}{V} \cdot \sigma_2 \tag{5}$$

with

$$\sigma_2 = E_2 \cdot \varepsilon_{u,1} \tag{6}$$

If the influence of the lateral strain is considered the bending moments in the outer skins can be qualitatively calculated by the use of the analogy of the elasticly bedded beam [2].

2.1.2 Silo model

In a endless high silo compartment the cohesionless infill causes a horizontal pressure $(p_{h,a})$ on the outer skins:

$$\max p_{h,a} = \frac{\gamma_i \cdot A_i}{\mu \cdot U_i} \tag{7}$$

If the silo model is valid the load bearing capacity of multiple leaf masonry would directly depend on the density (γ_i), the friction coefficient (μ) and the geometric ratio of area / perimeter (A_i/U_i): the thicker the infill the lower the crushing strength of the wall. One aim of the experiments therefore was to check this hypothesis. Certain features of silo theory bring its veracity into question as a suitable analogue for multiple leaf masonry:

– masonry cannot be filled with a cohesionless material without tilting of the outer skins at a critical filling height [2]

– the silo pressure causes high bending moments in the outer skins; the resulting tension stresses cannot be suppressed by the compressive stresses induced by vertical loads. Therefore multiple leaf masonry walls could not exist if the silo pressure $(p_{h,a})$ is acting [2].

2.2 Finite element analysis

The aim of the finite element analysis was to investigate how different parameters influenced the stresses of the outer skins. The sensitivity study varied the following:

– the ratios of the elastic constants (Young's modulus E, Poisson ratios v)
– boundary conditions at the wall crest
– application of the vertical loading: deformation or average applied stress
– bond between outer skins and infill

- thickness ratio of the components
- stress-strain behaviour of the infill (material law)

A selection of the results will be presented later for comparison with the experimental work.

The FE-Program ADINA 5.0 was used on the mainframe. Outer skins and infill were modelled by quadratic 2-D-SOLID elements (9 integration points). The material of the outer skins was considered homogeneous with linear elastic stress-strain behaviour. By the use of the symmetry and the plain strain condition the number of elements varied between 318 and 742 depending on the thickness ratio (t_i/t_a = 1, 3, 5). The geometry of the models provided an analogue of the test specimens. For the non-linear analysis the Drucker-Prager material law was applied to the infill as a generalised version of the Mohr-Coulomb failure criterion.

2.3   Experimental analysis

The testing programme was run on the basis of a developed typology [2] with:

- the thickness and the properties of the outer shells held invariant
- the thickness and the stiffness of the infill varied as standard parameters.

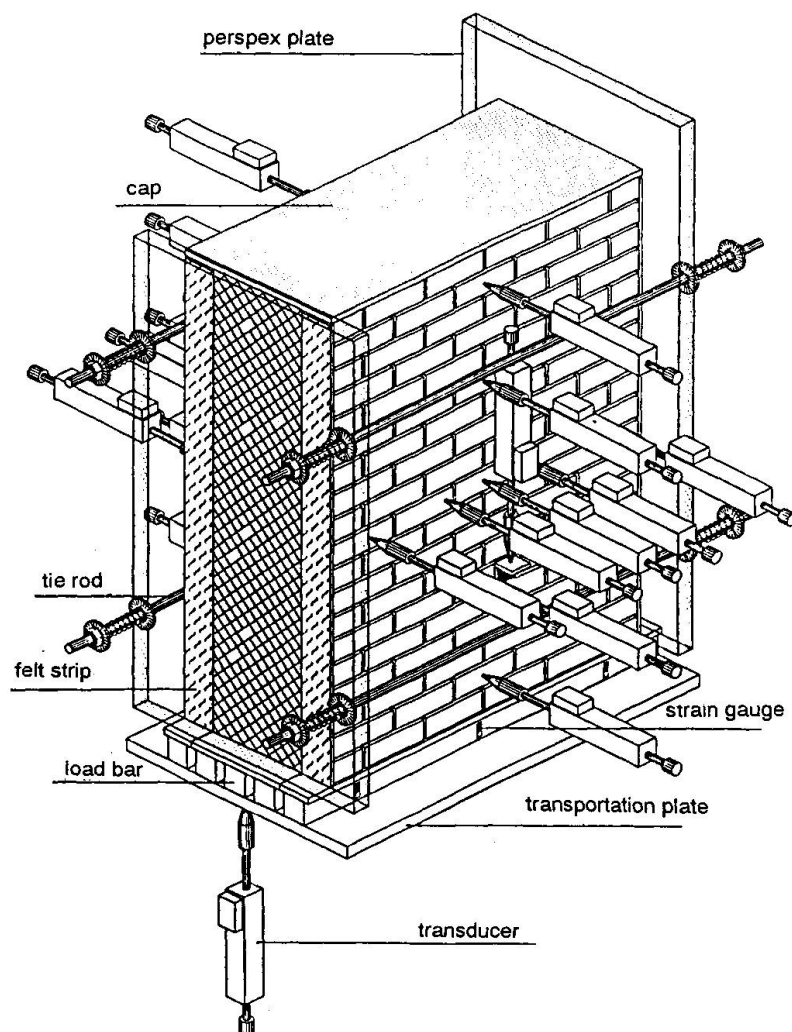Five different infills were used for the specimens:

Fig. 2   specimen (t_i/t_a = 3) with the measure equipment

perspex plate

cap

tie rod

felt strip

load bar

strain gauge

transportation plate

transducer

infill L: 3 reference-specimens (t_i/t_a = 3) kept unfilled (= infill air) and were tested under the same conditions as the other wallets.

infill B: 5 specimens (t_i/t_a = 3) were filled with mortar of a high binder content. The compressive strength and the stiffness of the infill were higher than the relating properties of the outer skins.

infill F: 1 specimen (t_i/t_a = 1), 6 specimens (t_i/t_a = 3), and 1 specimen (t_i/t_a = 5) were filled with mortar of a extremely low binder content. The compressive strength and the stiffness of the infill were lower than the relating properties of the outer skins.

infill K: 5 specimens (t_i/t_a = 3) were filled in a sandwich pattern: layers of mortar followed layers of gravel, giving cohesionless zones in the infill and a high specific volume.

infill Z: four specimens each (t_i/t_a = 1, 3, 5) were filled with a mixture of crushed bricks and
mortar. The mechanical properties of the infill were similar to the characteristics of infill
K.

All 33 specimens were built as quarter scale masonry wallets. The thickness of the specimens
varies between 90 mm (t_i/t_a = 1) and 210 mm (t_i/t_a = 5), the height was 400 mm and length
313 mm. The model-brick skins had a slenderness of 13,4. There was a simple bond only
between the outer skins and infill; consequently the tests investigated the worst scenario to give
the lower limit of the bearing capacity. The mortar capped specimens were continuously loaded
up to the failure by means of a 600 kN hydraulic test machine. Nine transducers on each outer
shell measured the horizontal deformations during the test. Further measurements were taken of
longitudinal deformations and the load distribution within the outer and inner layers at the base
of the specimens (fig 2). A data logger and computer stored all measurements at five-second
intervals.

Test cubes were made up from the material of the outer skins (masonry pillars) and the infill. The
pulse velocity was measured ultrasonically and the results are used to determine the dynamic
modulus of elasticity. The separate component behaviour was studied through compression tests
on the cubes. Their stress-strain curves formed the basis of the comparison with their behaviour
in the composite system.

3   RESULTS AND THEIR INTERPRETATIONS

3.1   Load bearing behaviour

The deformation behaviour of central loaded multiple leaf masonry is seen to have two phases:

Phase I: There is complete bonding between the outer skins and the infill, with the lateral
deformations increasing linearly with vertical load. The normal stresses in the
components are estimated by the use of the dynamic modulus and geometry of the
components (spring model). In this load phase no damage in the outer skins can be
recognised, cracks in the stones, gaping or squeezing bed joints, horizontal
deformations or bending.

Phase II: This starts with the onset a bond failure between outer skins and infill (outer skins
tear off). Because of the reduced lateral restraint (ε_q) the linear increase of the lateral
deformations is higher than in phase I. The beginning of phase II depends on geometry
and the ratio of the elastic constants between components, the boundary conditions of
the outer skins, the load application and the structural bond between the components.

At a definitive load level the infill starts to yield, at the same time lateral deformations
increase disproportionally (compare fig. 3 and fig. 4). The yield-load depends on the
triaxial stress-state in the infill influenced by the normal vertical stress and the
resistance to lateral strain. The yielding effects an increase of the normal stress and a
constant horizontal loading of the outer skins. The height of the edge pressure results
from the normal load and the bending moments. In that load step the outer skins
clearly belly out. According to the spread-direction these deflections either cause an
opening-up of the bed joints or vertical bending cracks.

3.2   Behaviour at failure

The behaviour at failure depends on the stiffness ratio of the components:

–   If the infill is stiffer than the outer skins the collapse of the system is caused by the
compressive failure of the infill. The vertically low-stressed skins are not able to bear the load
transfer from the infill to the outer layers and the horizontal loading arising immediately
before failure. The failure of the composite system occurs suddenly and without advance
warning.

lateral strains depending on the area load

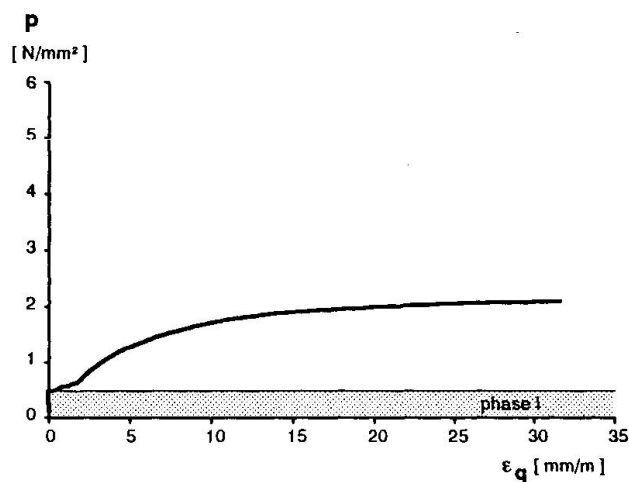## stress rate curves

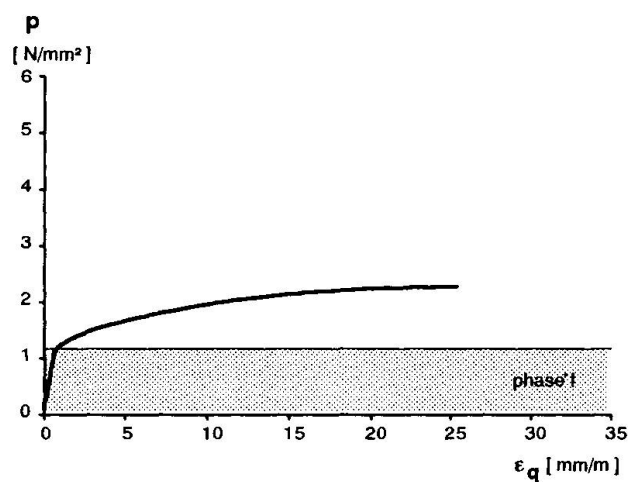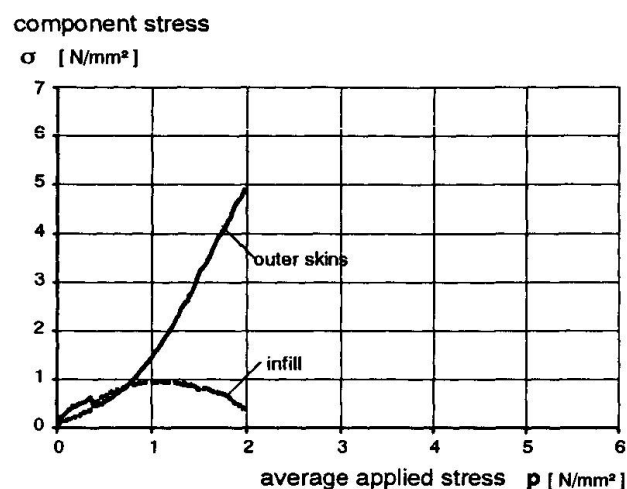Fig. 3a specimen with weak infill F

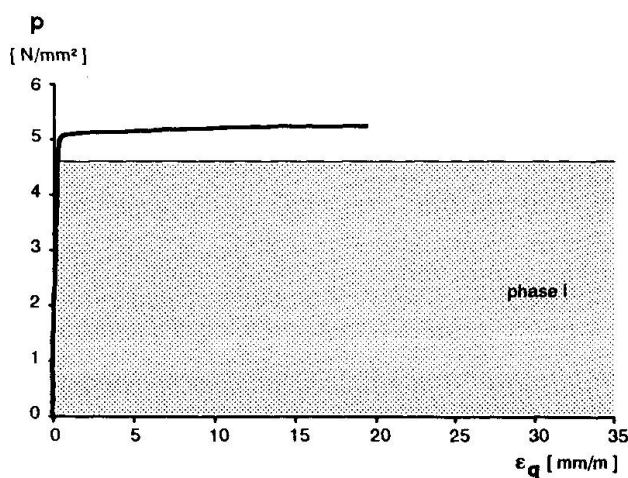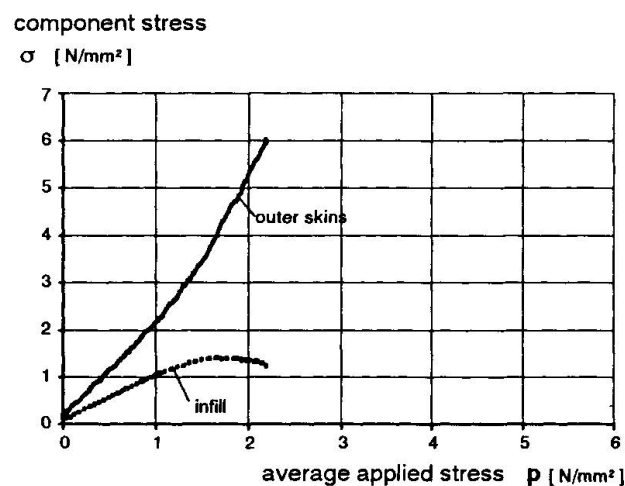Fig. 3b specimen with heterogeneous infill K

Fig. 3c specimen with stiff infill B
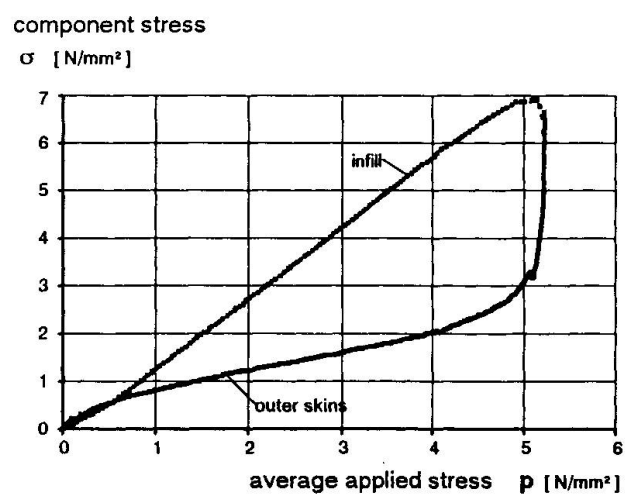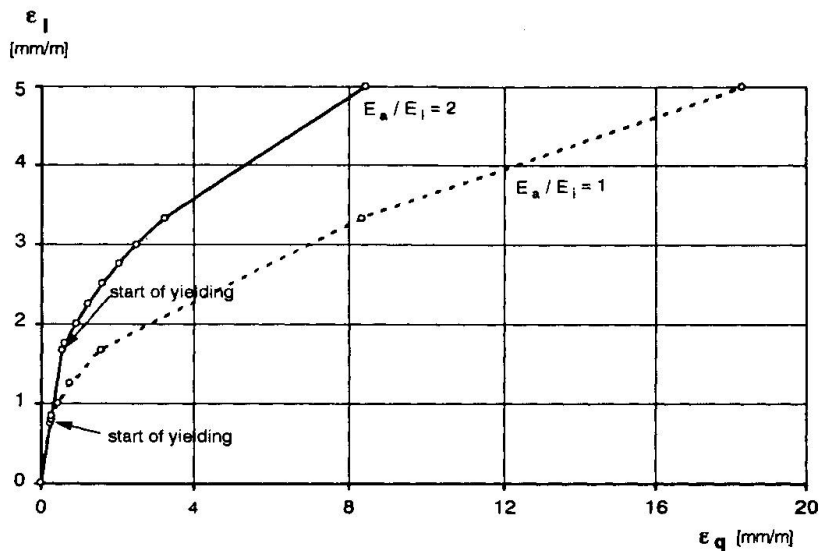
Fig. 3   Lateral strain curvature and stress rate curves of three specimens with different infills

ε_l [mm/m]

E_a / E_i = 2

E_a / E_i = 1

start of yielding

start of yielding

ε_q [mm/m]

— In the case of a weaker infill the collapse of the system is caused by a compressive edge failure due to bending of the outer skins. Large bending deflections combined with gapping of the bed joints or bending cracks announce the failure long time before. The slenderness and the boundary conditions of the outer skins have an important influence of the load bearing capacity of multiple leaf masonry.

Fig. 4: Relation between the vertical (ε_l) and the lateral strain (ε_q) of the FE-model (at $h/2$)

3.3 Estimation of the load bearing capacity

The finite element analysis together with the experimental results showed that the thickness ratio (t_i/t_a) and the compressive strength of the components are the most important parameters to influence the load bearing capacity. By a linear finite element analysis for different thickness ratios and ratios of the elastic constants (E_a/E_i) the average applied stress p was computed which caused an edge pressure of 5 N/mm² in the outer skins (fig. 5). The dashed curve represents the air-filled cross-section. Fig. 6 shows the results of the experiments on three air-filled specimens plus one specimen with the infill F and four specimens with the infill Z in which properties vary slightly. Notice that the linear elastic calculation lies close to the experimental results. Although the load bearing behaviour can only be simulated by a non-linear calculation a linear analysis suffices to describe failure behaviour in qualitative terms. Even in the case of very weak infills the experiments concluded that the thicker the infill the higher is the ultimate strength of the specimen; that is in fact a contradiction to the silo theory which would anticipate lower ultimate strengths for thicker infills. Therefore the silo model is inappropriate for estimating the horizontal loading on the outer skins, its use would lead to an overprediction of the stresses and therefore to inadequate repairing methods.

p [N/mm²]

infill air

E_a/E_i = 3; ν_i/ν_a = 1

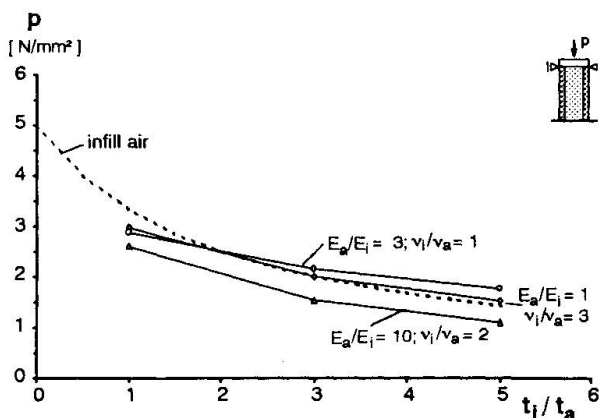E_a/E_i = 1
ν_i/ν_a = 3

E_a/E_i = 10; ν_i/ν_a = 2

t_i / t_a

Fig. 5 FE-analysis: maximum of average applied stress (p) for reaching the critical edge stress at different thickness ratios (t_i/t_a)
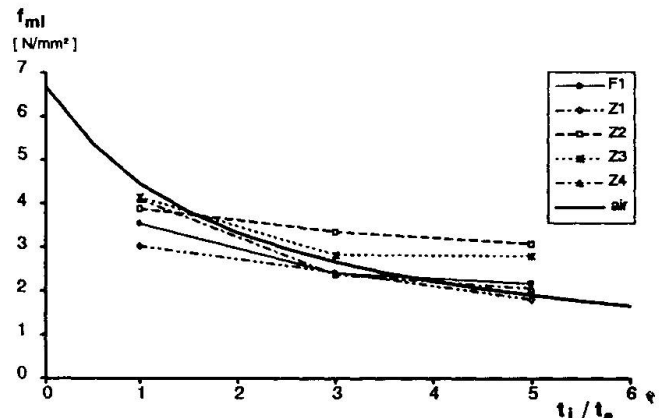

f_ml [N/mm²]

F1
Z1
Z2
Z3
Z4
air

t_i / t_a

Fig. 6 Experiments: crushing strengths (f_{ml}) of filled and unfilled specimens of different thickness ratios (t_i/t_a)
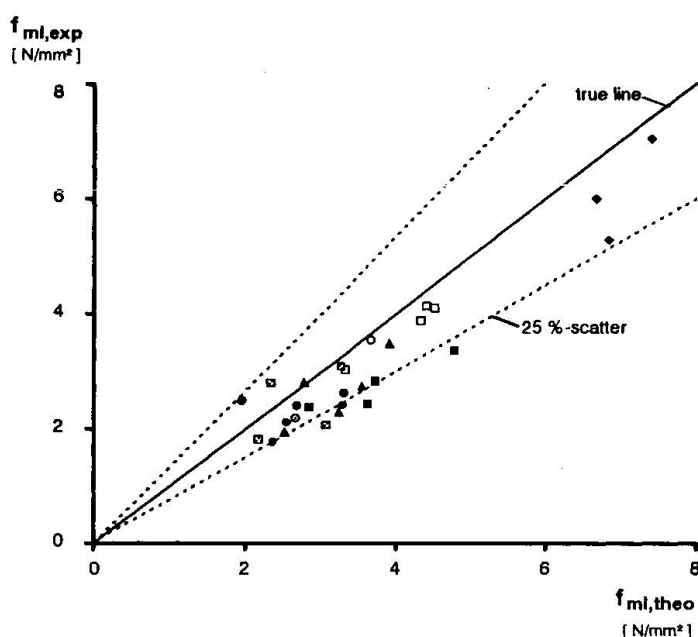
Fig. 7   Relation between the calculated and the measured crushing strength of the wallets

Through *load bars* at the base of the specimens the normal stresses in the components could be measured (fig. 2). So it became possible to check the validity of the multi-material model by the use of equation (4). For σ_1 we put in the measured strength of the outer skins at the failure $(\sigma_{a,u})$ and for σ_2 the corresponding value of the infill $(\sigma_{l,u})$. Fig. 7 presents the comparison between the theoretic crushing strength $(f_{ml,\ theo})$ according to eq. (4) and the experimental results $(f_{ml,\ exp})$. The 45°-line gives the stress path for conformity and the diagram shows points lying near to that line, with only 14 % are outside a masonry-usual scatter of 25 %.

Equation (4) is not suitable for the structural analysis because the component stresses at the failure load are not known. Therefore a failure criterion was developed which estimates the crushing strength of a multiple masonry wall (f_{ml}) on the basis of the failure loads of its components $(f_{a,k}, f'_l)$. The comparison of the stress-strain relationships between the components in- and outside of the composite system showed that the criterion can be derived out of the triaxial stress relationships:

– In the composite system the infill reaches a higher compressive strength than under uniaxial loading. The reason is the triaxial compressive stress state caused by the vertical stress and the hindered lateral deformations. The correcting factor (Θ_l) which describes the ratio between the component stress at failure $(\sigma_{l,u})$ and the uniaxial compressive strength (f'_l) generally is larger than one and depends on the structure of the infill.

– The compressive strength of the outer skins in an unfilled system $(f_{a,k})$ are never reached in a multiple leaf cross section, because of the horizontal loading through the yielding infill. The correcting factor (Θ_a) depends on the bending stiffness, the boundary conditions and the bending moments. Its value is smaller than one.

The crushing strength of a multiple leaf masonry wall can be estimated as:

$$f_{ml} = \frac{V_a}{V} \cdot \Theta_a \cdot f_{a,k} + \frac{V_l}{V} \cdot \Theta_l \cdot f'_l \tag{8}$$

4   OUTLOOK

Continuing research work will investigate the amounts of the correcting factors in relation to different types of multiple leaf masonry wall [2]. Then low-destructive test methods will be developed to identify the determining parameters for structural analysis.

REFERENCES

1. BINDA, L.; FONTANA, A.; ANTI, L. , Load transfer in multiple leaf masonry walls. Proceedings of the 9th International Brick/Block Masonry Conference, Berlin, 1991, pp. 1488-1497.

2. EGERMANN, R. , Ein Beitrag zum Tragverhalten mehrschaliger Mauerwerkskonstruktionen. Universität Karlsruhe, Fakultät für Architektur, Diss., in preparation

Floor and Wall Interaction in Unreinforced Masonry Buildings

Interaction plancher-paroi dans les bâtiments en maçonnerie

Wechselwirkung von Wand und Decke in unbewehrten Mauerwerksbauten

W. Bradford CROSS
Assist. Professor
Southern IL Univ.
Edwardsville, IL, USA

Nicholas P. JONES
Assoc. Professor
The Johns Hopkins Univ.
Baltimore, MD, USA

SUMMARY

This paper focuses on the application of a finite element technique that has been developed to model the friction and impact characteristics of a wood joist bearing on a brick wall. A traditional yield model was used for friction, in conjunction with an innovative impact formulation which uses a stiff spring and damper to approximate the energy lost in impact between a floor or roof diaphragm and a wall. The nonlinear, dynamic interaction between the wood floor diaphragm and the wall at the interface is shown to be significant and the finite element procedure developed can represent both the retrofitted and unretrofitted conditions.

RÉSUMÉ

Cette communication traite d'une technique par éléments finis qui a été développée pour reproduire les caractéristiques de friction et d'impact d'une solive appuyée sur un mur en brique. Un modèle traditionnel a été employé pour la friction appuyée avec une formulation innovatrice de l'impact utilisant un ressort rigide et un amortisseur pour représenter la quantité d'énergie perdue dans l'impact d'un plancher ou d'un toit avec un mur. L'interaction dynamique et non linéaire entre le plancher et le mur est importante et la technique par éléments finis qui a été développée peut représenter également les conditions avec ou sans restauration.

ZUSAMMENFASSUNG

Es werden Anwendungen eines Finite-Element-Modells der Reibungs- und Aufprallcharakteristiken eines Holzbalkenauflagers auf einer Mauerwand vorgestellt. Dabei ist die Reibung herkömmlich als Fliesskriterium modelliert, während für den Energieverlust beim Aufprall zwischen einer Decken- oder Dachscheibe auf die Wand eine neuartige Feder-Dämpfer-Formulierung entwickelt wurde. Wie gezeigt wird, ist die dynamische Wechselwirkung im Auflager bedeutend. Das Verfahren ist für Zustände mit und ohne Verstärkungsmassnahmen geeignet.

1. INTRODUCTION

Typically, joists bearing on masonry walls are modeled as frictionless rollers in an equivalent static analysis. Since this model rarely satisfies conditions for structural stability, the engineer designing a structural retrofit is required to assume a pinned condition in the structural model, for which an approximate pin is constructed at the joist-wall interface when the actual building is retrofitted. All such details are currently designed based on the assumption that during an earthquake, the unretrofitted joist-to-wall connection has no lateral load capacity. In reality, however, the joist bearing has some lateral load capacity due to friction and contact between the elements. In order to assess the dynamic affects of motion between the joist end and the wall, and more accurately analyze retrofit alternatives, an analytical model that accounts for this motion has been developed.

2. THE ANALYTICAL MODEL

The analytical model must be capable of capturing the dynamic friction behavior of a joist bearing connection. It must also take into account impacts that might occur when the joist end comes into contact with the end of the joist pocket.

2.1 Friction Model

The fact that, in general, there is frictional resistance to sliding of one body on another occurs due to relative motion has been known for centuries, and classical models considering static and dynamic friction components have been developed (e.g., Coulomb). A finite element friction model which accounts for the dynamic friction behavior of a joist bearing on a brick wall has been developed by the author and explained in detail elsewhere (Cross 1992, Jones and Cross 1991).
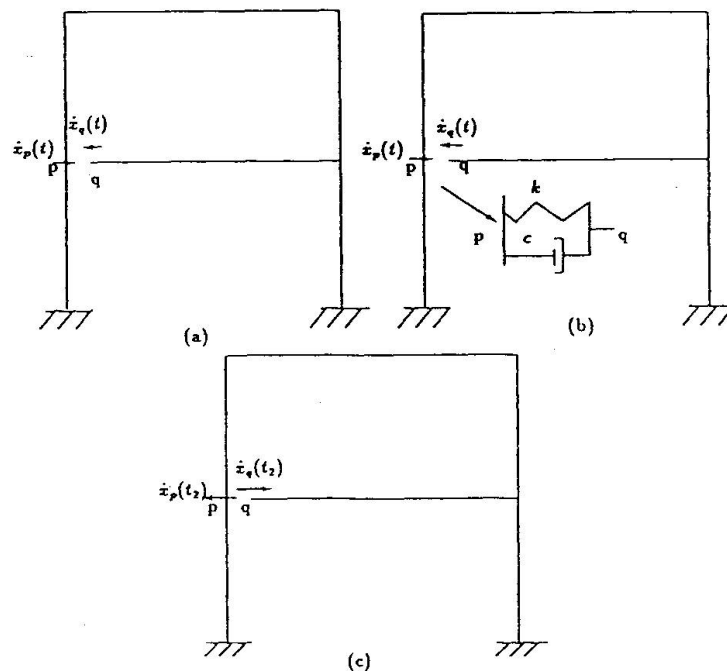
2.2 Impact Model

Figure 1: (a) Before Impact, (b) During Impact, (c) After Impact

The impact formulation developed for this research is a coefficient-of-restitution method, using an equivalent spring-damper placed at the point of impact for the duration of impact. The structure immediately prior to interior impact is modeled as shown in Figure 1(a), during impact as shown in Figure 1(b), and after impact as shown in Figure 1(c). The stiffness and damping properties of the model change as the structure goes through the three states. Full details of the derivation of the impact procedure briefly described above are given in Cross and Jones (accepted for publication 1993).

3. APPLICATION OF THE METHOD

The finite element procedure described above has been applied to an actual unreinforced masonry structure. Since the building was instrumented before the Loma Prieta earthquake, data from the structure were gathered during that earthquake. The connection analysis procedure derived in this research will be applied to this structure, and comparisons made to recorded data. In addition, the role of the retrofit strategy used in this building will be examined.

3.1 The Gilroy Historic URM Building

The structure to be investigated in this study is an historic unreinforced masonry building in Gilroy, California. It is currently used for commercial space. The original part of the building was constructed in 1890 and survived the 1906 earthquake. The building was surveyed in 1990 and as-built drawings with details are available. The building is a two-story, brick masonry structure with story heights of about 3.73 meters (the second floor unbraced height varies due to differences in roof elevations). The 30.5 cm, 3-wythe brick walls act as shear walls, and the wood floors are horizontal diaphragms to resist lateral load. These floors consist of 25.4 mm by 101.6 mm diagonal wood sheathing nailed to timber joists that are supported by wood beams at the second floor framing and wood trusses at the roof. Floor joists measure 50.8 mm by 355.6 mm, and the roof rafters are 50.8 mm by 152.4 mm.

The diaphragms and the walls are tied by 19.05 mm diameter steel rods anchored in the outside wythe of the walls by a hook, and with or without a hook in the diaphragms. These ties are placed every 1.55 m nominally at the east and west walls, and every 1.83 m at the south, center, and north walls. The building is founded on spread footings whose dimensions and depth were not determined by a field survey. (CSMIP 1990, Tena-Colunga 1992). The structure was instrumented by the California Strong Motion Instrumentation Program (1990).

3.2 Finite Element Model of the Gilroy URM Building

A two-dimensional, linear-elastic, finite element model was chosen for the wall and floor elements of the Gilroy building. This was done for two reasons: First, that the actual response of the structure was in the linear range during the Loma Prieta event (Tena-Colunga 1992), and second, the influence of connection nonlinearities on global structural response was to be examined in this research. The two-dimensional model was based on an east-west cross section of the building, the dimensions of which are shown schematically in Figure 2.
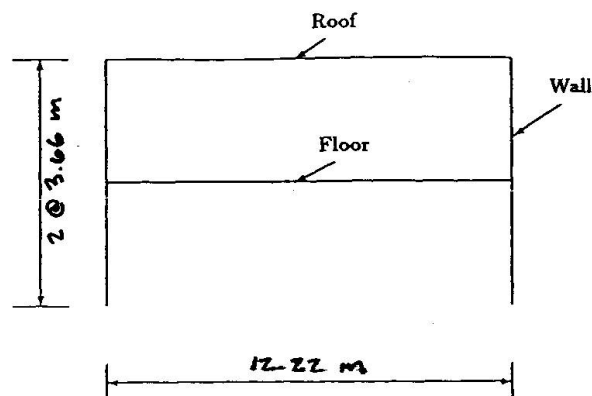
Fig 2: East-West Cross Section of the Gilroy Historic
Commercial Building

The cross section at the center of the original portion of the structure was modeled, because it was at this location that horizontal diaphragm deflections would be the largest, and hence the relative motion between the floor and the wall was potentially greatest at this location. A 1.83 metre section of the wall was chosen as a tributary width to correspond to the nominal spacing between the 19.05 mm wall anchors. This particular width was also found to correspond well to the width required to obtain the appropriate generalized mass for a simple beam spanning horizontally between shear walls. The 1.83 m section was also used to obtain floor and roof properties.

Shear walls were modeled by placing stiff vertical members at the center of the model, which were in turn attached to horizontal springs connected to the floor and roof members. The horizontal springs were used to model diaphragm flexibility. Additionally, the transverse stiffness of the bearing walls at each level was modeled by horizontal springs attached to the shear walls. This permitted the outside walls to behave as beams spanning horizontally between shear walls. The stiffness of this spring could be adjusted to account for a shorter span between floor-to-wall anchors. The foundations were modeled as per the recommendations of the NEHRP provisions (FEMA 1989).

4. ANALYSIS OF THE GILROY HISTORIC 2-STORY COMMERCIAL BUILDING

4.1 Retrofitted Structure

As a calibration of the model, the retrofitted structure with wall ties was analyzed, and the results were compared to actual recorded values from the Loma Prieta Earthquake of 1989. The input parameters for the model were those discussed in the previous section. Base acceleration was input as the east-west component of the Loma Prieta Earthquake. The linear finite element approximation gave results that are close to the recorded results. The maximum predicted roof acceleration relative to the base is .78g, while the maximum recorded acceleration relative to the base was .75g.

Field observations of the structure (Tena-Colunga 1992) suggest that the structure responded in its elastic range to the Loma Prieta earthquake. This is verified by the stresses computed by the finite element model; in no case did the stresses in the retrofitted structure exceed their ultimate limits. Maximum tensile stress in the outside walls approached 689.48 kPa, which is close to the ultimate tensile strength of brick (258.4 kPa as measured by Ali and Page (1988)). Ten percent damping was used for the masonry material; additional damping would lower this stress value.

4.2 Unretrofitted Structure

In the study presented in this section, the possible response of the unretrofitted Gilroy structure (i.e., the structure without wall ties) to the Loma Prieta Earthquake of 1989 is examined. Different input parameters for the pocket element were considered, including coefficients of friction of .2 and .4, coefficients of restitution of .25 and .5, and distance to the end of pocket of 2.54 mm and 25.4 mm. These quantities will be varied while using the default values discussed above for all other parameters. For these analyses, the system limit states are considered to be either forces high enough to initiate cracking of the brick masonry, or displacement response great enough to make the joist fall off of the wall. The effects of coefficient of friction and distance to the wall will be examined in reference to the system limit states.

4.2.1 Nonlinear Gilroy Model

The complete Gilroy nonlinear finite element model described above, with the joist pocket elements incorporated, was analyzed using the finite element method. The initial parameters for the pocket element were $\mu = .2$, distance to wall $= 25.4$ mm, and $e = .5$. The graphs of absolute displacement indicated that the floor and roof joists begin to slide at about 3.2 seconds. For this coefficient of friction (0.2), sliding continues throughout the record for both roof and floor pockets. The relative displacement between the joists and the walls is high (Figure 3). If only 50.8 mm of bearing exist for each joist, the right roof would fall at 4.5 seconds, and the left roof would fall at 4.4 seconds. A full 69.9 mm of bearing is required to assure that the left roof joist would stay on its bearing for the ten-second time history. The relative displacement at the floor level is lower. About 38.1 mm of relative motion occurs between the joist and the wall, with the maximum occurring at 4.5 seconds.

The joist-falling-off-bearing condition does not assure collapse, but it indicates a possibly high-risk condition. Joist bearing lengths can vary in older structures from as much as 152.4 mm (or higher) to merely 25.4 mm. The actual bearing state depends greatly on the individual structure and joist in question, and can vary from joist to joist in even a well-constructed building.

The forces developed at the wall interface are relatively low until an impact occurs, varying between μN and $-\mu N$. When an impact occurs, the horizontal force at the joist bearing increases. The largest magnitude impact force occurs at the left roof pocket, with a magnitude of 2363 N. For the 1.83 m section of roof used in the analysis, the cross-sectional area is 144 in^2. If it is assumed that this is the contact area during impact, the contact stress between the joist and the wall is 406.79 kPa. This stress is well below the ultimate stress required to crush the brick or the wood in bearing. The punching stresses would be even lower, and would not be large enough to cause the joist to punch through the brick wall.

The maximum moment occurs at 4.4 seconds in the lower section (below the first floor) of the right wall, with a magnitude of 37.97 KN-m. This would cause a bending stress in the brick wall of 1344.5 kPa (after accounting for axial compression). This stress is higher than the ultimate tensile stress for typical brick masonry (689.5 - 758.4 kPa), and indicates that the force of the impact between the diaphragms and the walls could cause bending failure in an unretrofitted wall (note that the maximum moment occurs at the same time as the impact of the floor with the wall). The maximum shear force in the wall was 12.4 kips, with a corresponding average shear stress of 99.3 kPa for a 1.83 m section of wall, which is within reasonable limits, even for conservative analysis. Maximum axial loads were low.
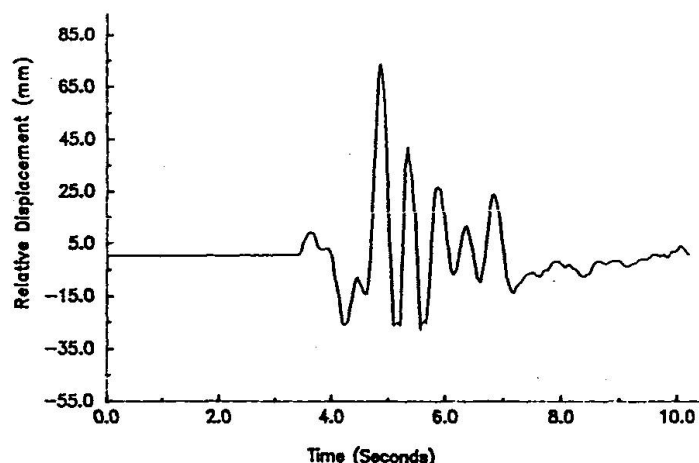
Fig 3: Relative Displacement ($\mu = .2$, Left Roof)

4.2.2 Friction Coefficient of .4

A second run was made, with all parameters the same as the first nonlinear run, except for a higher coefficient of friction at the bearing. The coefficient of friction used in the first run (.2) is lower than the static coefficient of friction specified in Machinery's Handbook; it is possible that the actual coefficient of dynamic friction between wood and brick could be closer to the coefficient of static friction. Also, since in this study the effects of vertical accelerations have not been taken into account, an effective coefficient of .4 between the joist and its bearing is not unreasonable.

The maximum relative displacement for the $\mu = .4$ case is 44.45 mm, occurring at 5 seconds at the left roof pocket. This is 25.4 mm less than the 69.85 mm relative displacement occurring in the $\mu = .2$ run. The implications for this for retrofit design are clear: a 50.8 mm bearing condition would prevent the joist from falling off the wall for the .4 coefficient of friction. Clearly, further experimental tests of wood bearing on brick would allow more certainty in the choice of the coefficient-of-friction value.

The wall is impacted only twice at the right roof pocket, with a maximum moment in the right wall of 293 in-k. This would cause a net tensile stress of 999.7 kPa. This stress is still higher than the ultimate tensile strength of brick in bending, but with only two high intensity impacts occurring, the wall may not suffer catastrophic failure. Further of modeling of the full nonlinear response of the brick masonry may be warranted in this case.

4.2.3 Coefficient of Restitution of .25

A run was made with the coefficient of restitution between brick and wood set at 0.25. All other parameters were at their default values; in particular, μ was .2, and the distance to the end of the pocket was 25.4 mm. The response was very similar to the $e = .5$ case, which indicates that the system response is not very sensitive to the choice of e.

4.2.4 Distance to End of Pocket of 2.54 mm

The final run for the Gilroy structure was made using the default parameters described in the previous section, with a distance to the end of the joist pocket of 2.54 mm. In actual field conditions, the joist may be grouted at the end of the pocket, or loose bricks or other debris can

limit travel to the end of the pocket. Also, the proximity of the floor sheathing to the wall can be very close in some structures, which would effectively limit the distance that the joist may travel before impact. Therefore, it is not unreasonable to assume that the end of the pocket is 2.54 mm.

The results from this analysis are very interesting. It is immediately apparent from the output that the relative displacements are lower than those for the first example (with a 25.4 mm distance to end of pocket). The maximum relative displacement occurs at the right roof, where the relative distance is 53.34 mm. This is less than the 69.85 mm relative displacement computed for the 25.4 mm pocket. This seems to indicate that if the distance from the end of the joist to the end of the pocket is minimized, a smaller bearing length is required.

The force of impact, however, is apparently higher with the shorter pocket distance. The maximum force can be seen to occur at the floor pockets, with a magnitude of just over 2780 N. This is still relatively low, however, compared to the bearing strength of wood and brick. The maximum moment occurs in Element 17, which is in the second level of the right wall. It has a magnitude of 25.42 kN-m, which would cause a corresponding maximum tensile bending stress of 813.6 kPa. This stress is just over the ultimate tensile stress for brick masonry (689.5 - 758.4 kPa), and is 40% lower than the stress in the 25.4 mm pocket case. It is possible that the shorter end distance is producing a partial bracing effect, at least between the end of the pocket and the joist. This would explain the higher impact forces: since wall horizontal motion is more fully restricted, the joists are acting more fully as stiff supports throughout the time history and taking more load. Another possible explanation for this effect is that the lack of motion in the direction of the wall produces less energy loss due to frictional work, and this could raise the momentum associated with the impact.

Thus, it can be seen that in terms of the bearing distance required for the joist and the moment response of the exterior walls, a reduction in pocket depth is desirable. To produce this result in actual structures, the joist pockets could be grouted (effectively reducing any travel distance). This procedure would be relatively easy and inexpensive with existing equipment. It is not currently a recommended retrofit procedure. It should be noted that this could increase the force between the wall and the joist. If a wythe separation condition is of concern, then the attachment of the brick wythes at the floor and roof levels should be examined carefully before grouting.

5. CONCLUSIONS

Failure of this 2D model of the structure was observed in two distinct cases. The first failure mode occurs when the joists move sufficiently far relative to the wall to cause the joists to fall of the wall. Although in some cases it may be possible for the joists to move back on to the wall (this would require a 3D analysis), it is a highly undesirable event which could lead to catastrophic collapse. This failure mode is dependent on the length of the bearing, however, and in the worst case for this structure, a 114.3 mm minimum bearing length for the joists would have been sufficient to avoid this type of failure.

The second failure mode would be collapse of the wall in out-of-plane bending. Interestingly, the movement of the joist relative to the wall causes impact of the floor or roof diaphragm with the wall in all cases examined. These impact forces can be high enough to cause tensile bending failure of the brick wall. Such a failure is very dangerous, because bearing wall structures usually exhibit little redundancy. The collapse of a bearing wall could lead to total collapse of the structure. Although the forces do not appear to be high enough to cause bearing or punching failure of the wall at the floor and roof levels, it is possible that the impact forces could cause wythe peeling, a common

failure in brick buildings during earthquakes.

If properly accounted for in analysis and design, the mobilization of some joints between the floor or roof and the wall in a URM building may allow for a minimization of retrofit construction (allowing some of the joists to remain unattached to the wall, for example), which could reduce repair costs. Additionally, for historic buildings, the minimization of retrofit interventions might allow more of the existing structure to remain intact, which is a primary goal of preservation architects.

In conclusion, it is clear that the dynamic interaction between the floor and roof diaphragms and the bearing wall would have been significant in the Gilroy structure if it had not been retrofitted. The retrofitted structure responded elastically to the Loma Prieta earthquake.

REFERENCES

Ali, S.S. and Page, A.W. (1988) "Finite Element Model for Masonry Subjected to Concentrated Loads," *J. Struct. Div. ASCE., 114*(8).

California Strong Motion Instrumentation Program (CSMIP 1990) *Data for the Set of Records from the Santa Cruz Mountains (Loma Prieta) Earthquake of 1989,* California Department of Conservation, Division of Mines and Geology, Sacramento, California.

Cross, W.B. and Jones, N.P. (accepted for publication 1993) "Sesimic Performance of Joist-Pocket Connections I: Modeling," *J. Struct. Div. ASCE.*

Cross, W.B. (1992) *Analysis of the Seismic Performance of Connections in Historic Unreinforced Masonry Structures,* Ph.D. Dissertation, The Johns Hopkins University, Baltimore, Md.

Federal Emergency Management Agency (1989) "NEHRP Recommended Provisions for the Development of Seismic Regulations for New Buildings. Part 2. Commentary." FEMA-95, October.

Jones, N.P. and Cross, W.B. (1991) "Seismic Response Prediction of Unreinforced Masonry Structures," *Structures Congress Abstracts,* ASCE, New York, NY.

Machinery's Handbook (1957) Industrial Press, New York, New York.

Tena-Colunga, A. (1992) "Seismic Evaluation of Unreinforced Masonry Structures with Flexible Diaphragms," *Earthquake Spectra, 8*(2) 305-318.
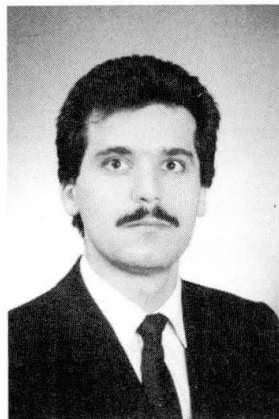
Seismic Adequacy of Old Stone Masonry Buildings

Résistance aux séismes d'anciens bâtiments en pierres de taille

Seismische Widerstandsfähigkeit alter Mauerwerksbauten

Samir E. CHIDIAC

Dr. Eng.

National Research Council

Ottawa, ON, Canada

S.E. Chidiac, born 1961, obtrained his PhD degree in civil engineering and engineering mechanics from McMaster Univ. Hamilton, Ontario. For the last two years, he has been involved in investigations of seismic adequacy of stone unreinforced masonry subjected to moderate earthquakes.

SUMMARY

This paper examines different approaches available to determine the seismic resistance of unreinforced stone masonry buildings. First, the requirements of the National Building Code of Canada for unreinforced masonry walls are examined, then a method developed in California is briefly explored with respect to this type of construction. Both simple and sophisticated analytical models that have been proposed in the literature for the evaluation of in-plane and out-of-plane dynamic behaviour of stone masonry are reviewed.

RÉSUMÉ

L'article examine différentes méthodes pour la détermination de la résistance aux tremblements de terre de bâtiments en pierres de taille. Les exigences du code de construction canadien pour les murs en maçonnerie sont examinés, de même qu'une méthode développée en Californie est analysée pour ce type de construction. Les modèles analytiques simples et compliqués proposés dans la littérature pour l'estimation du comportement dynamique de maçonneries en pierres de taille, plan et dans l'espace, sont passés en revue.

ZUSAMMENFASSUNG

Der Bericht prüft verschiedene verfügbare Methoden zum Bestimmen der seismischen Widerstandsfähigkeit von unbewehrten Mauerwerksbauten. Als erstes werden die für unbewehrte Mauerwerkswände bestehenden Bauvorschriften Kanadas geprüft, dann wird eine in Kalifornien entwickelte Methode hinsichtlich derartiger Konstruktionen kurz vorgestellt. Sowohl einfache als auch anspruchsvolle analytische Modelle, wie in der Literatur für die Ermittlung des dynamischen Verhaltens von Steinmauerwerk innerhalb der Scheibenebene und quer zu ihr vorgeschlagen, werden begutachtet.

1. BACKGROUND

Many of today's historic monuments were built to express national or local pride and as a result, good workmanship and high material quality were used during their construction. Some old buildings, not intended as monuments, have also withstood the challenge of time. These structures have therefore, by their survival, demonstrated that they had the needed capacity to support all the loads, which also sometimes included earthquakes. However, natural deterioration coupled with limited maintenance may not guarantee continuing future stability, and thus a proper assessment is warranted.

In North America, a large number of historic buildings were constructed with three basic components: lime mortar, natural stone units and clay bricks. These old structures are labeled unreinforced masonry (URM) and were constructed in the absence of mandatory seismic requirements. Their poor performance under seismic activities, however, in the last decades, is a testimony to their vulnerability [1-3]. To address this problem, a multiyear project was sponsored by the National Science Foundation in the USA to review the unreinforced masonry construction and develop a methodology to mitigate the seismic hazards inherent to these buildings. This project was carried out by a joint venture of specialists and is known as the ABK [4].

Although the ABK study was comprehensive, the scope of the project did not extend to cover thick masonry and walls constructed with natural stone units. This is understandable given the limited number of buildings that fall in this category. In eastern Canada, however we have some historic monuments that were built with natural stone and lime mortar and in view of the projected seismic risk, an assessment of their present safety is felt necessary. This gave life to a study of the seismic vulnerability of these structures, is expected to take three years to complete, and is made up of various steps. For a specific project, a tower was selected and is shown in Fig. 1. In this paper, only that part of the investigation is given which briefly examines the relevant mathematical models reported in the literature. Also the applicability of both the ABK methodology and the national building code of Canada to stone masonry buildings are discussed.

2. STANDARDS & GUIDELINES

2.1 Design Code Requirements

Modern codes are intended as requirements for new construction and should not be applied to historical monuments [5]. This statement can easily be substantiated by examining the National Building Code of Canada, NBCC 1990, which requires that the building be designed according to a minimum seismic base shear force, V given by

$$V = \left(V_e/R\right)U \qquad \text{and} \qquad V_e = vSIFW \qquad (1)$$

in which R is the force reduction factor, equal to 1.0 for unreinforced masonry and U the calibration factor, equal to 0.6. V_e is the elastic base shear, v is the zonal velocity ratio, S the seismic response factor, I the importance factor, F the foundation factor, and W the weight of all the reactive masses that induce inertia forces in the structure. The code also requires a minimum reinforcement for all members that are either load bearing or that resist lateral loads in moderate seismic zones, although for small buildings the NBC Part 9 allows some walls in seismic zones without reinforcement. It is however clear that many stone masonry walls do not comply with the current seismic standards. Further, the Canadian design standard for masonry, CSA 1984 [6], requires that all structural members be designed according to either the elementary principles of elastic mechanics of materials coupled with a semi-empirical relationship to account for load eccentricity effects, or to empirical rules relying on the compressive stresses coupled with a limit on the wall slenderness ratio.
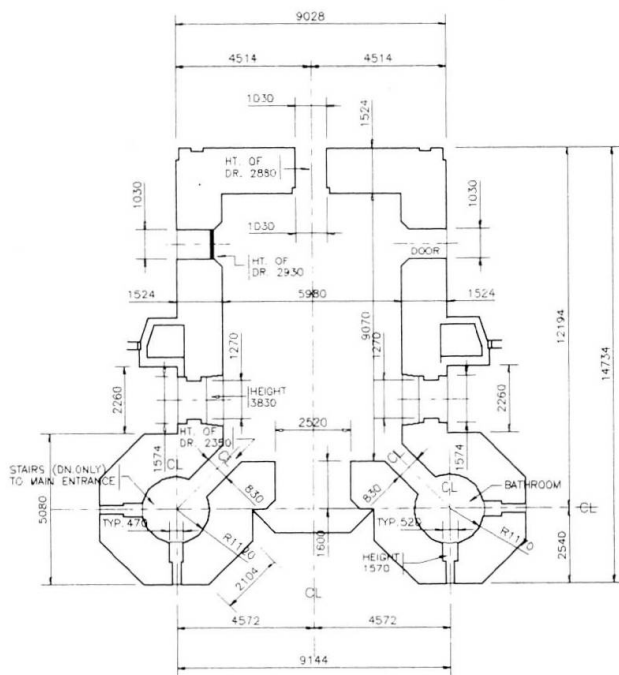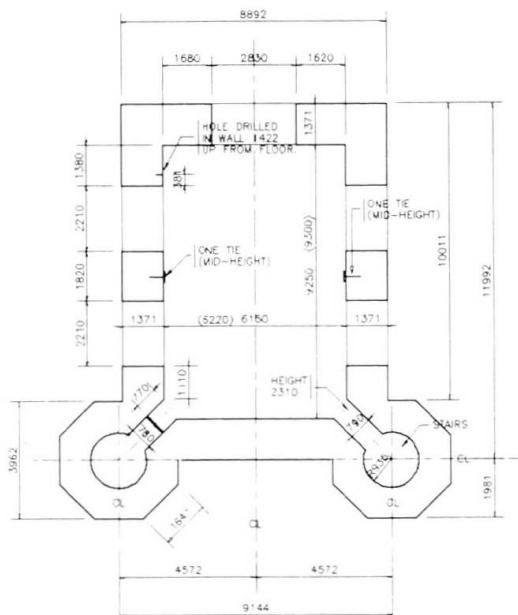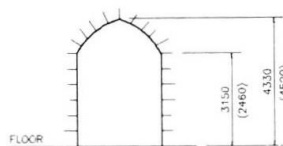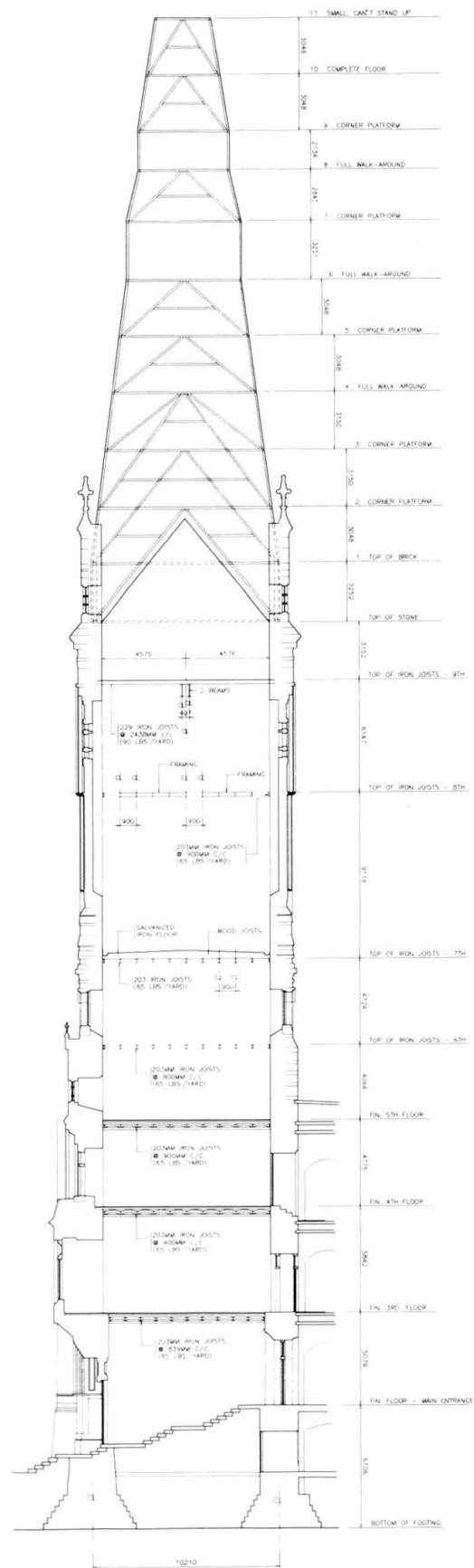
Fig. 1   Elevation and cross-sectional
view of the tower.

2.2 The ABK Methodology

The objective of the ABK-Joint venture of three Southern California engineering consultant firms was to develop a methodology to mitigate the seismic hazards associated with URM buildings [7]. Their task included a survey of URM buildings, an experimental testing program and development of a procedure that structural engineers can follow to investigate the adequacy of an existing URM building. The detailed description and review of all aspects and steps of the proposed methodology falls beyond the scope of this paper.

The methodology was primarily focused on the common features noticed during the survey of URM buildings. Wooden floors and roofs were found in low rise commercial buildings, and cast-in-place concrete floors in important and large multi-storey structures. URM buildings through out the USA were found to be consistently not designed to resist seismic loads, but at the same time URM buildings have survived earthquakes of varying intensity and sometimes in spite of major structural deficiencies. Accordingly, static and dynamic testing of floor diaphragms and URM walls for out-of-plane motion were conducted with emphasis on the non-linear hysteretic behaviour. The walls examined are primarily 3 wythe common brick, clay block and concrete blocks of height/thickness ratio ranging from 14 to 25. After a comprehensive investigation, ABK recommended that limits are required for out-of-plane dynamic stability and for the demand/capacity ratios for diaphragms. However these limits were derived for regions of high seismic risks or for places where the soil condition will lead to ground amplification. In their study, ABK made two major assumptions; i) the in-plane response of a URM is infinitely rigid and, ii) the ground motion is directly transmitted unmodified to each floor by the end walls parallel to the direction of earthquake.

The ABK methodology made a major contribution for assessing seismic adequacy of URM. Most of their recommendations have been incorporated in new guidelines to assist engineers in the assessment of seismic adequacy [8,9]. However the method is not suitable when investigating stone masonry walls with the height/thickness ratio ranging between 2 to 8 are involved (as is the case shown in Fig. 1) and for regions where structures are subjected to a seismic activity of moderate intensity, as is the case in the eastern part of North America.

3. ANALYTICAL METHODS

3.1 General Considerations

The use of any numerical simulation of a historic structure must be founded on detailed preliminary studies designed to provide realistic data on the construction and the behaviour of the building. The historical knowledge of how it was constructed and why certain features are present are often missing. Once such a preliminary survey has been completed, the information can be used in analytical models and thus identify the weak points in the overall structure.

A sophisticated mathematical model can give very detailed information about the structural behaviour, while a coarser model can give information which may suffice in given circumstances. A fundamental difference between a coarse and a detailed model lies not only in the amount and quality of data needed to describe the structure but also in the interpretation of the results. Both input to, and output from a coarse model is usually simple and the interpretation of the results can be integrated into a design procedure in a clear and complete manner. Detailed models, on the other hand, require specific experimental studies but are usually more representative of the structure at hand.

3.2 Simple Models

Out-of-plane and in-plane simple models have been developed in the past to assist engineers in their assessment of structural safety. The out-of plane models are mostly developed on the basis of static stability conditions. Priestley [10] has modified the ABK recommendations and proposed a model for clay brick masonry based on energy considerations. For in-plane modelling, there are two approaches: either it is assumed that the pier is solid and that the spandrel beam will crack as given in Reference [11] or that the spandrel beam is solid and that the pier will crack under lateral load as given in References [12]. These models are conservative and examine only one part of the structure.

3.3 Material Constitutive Models

The behaviour of masonry while subjected to dynamic excitation has proven to be very complex due the heterogeneous nature of the mortar and brick, and the layering patterns. To overcome this difficulty, researchers and engineers have in the past assumed and still treat masonry as a linear, elastic, homogeneous and isotropic material. However, others have decided to take on the challenge of treating this complex material in a realistic manner and a brief summary of their findings follows.

The first attempt to model the behaviour of masonry consisted of developing a mathematical model that can simulate both the brick and mortar by a continuum mechanics approach and by the mathematical theory of mixture [13]. The model was shown to properly depict the linear elastic dynamic behaviour of URM walls. However, it was recognized that it is costly and a substructuring method was then proposed by Ali and Page [14]. Though substructuring did reduce the scale of the problem it was still not feasible to analyze a complete structure using such a technique.

The attempt to model the three-dimensional nonlinear behaviour of unreinforced masonry was first proposed in Reference [15] and is based on the idea that the nonlinear effects can be represented using the linear equivalent method, LEM, which was previously used in nonlinear soil-structure interaction. Mengi et al. [16] have assumed that the behaviour depends on two parameters, namely the shear modulus G, and its viscous counterpart G'. Based on experimental studies, the variations of G and G' with the shear strain can be described by bilinear and trilinear functions, respectively. In a more recent study, Tanrikulu et al. [17] have recognized that the bilinear and trilinear functions are only applicable to burned-clay bricks and that the suggested parameter $c = \tau_c/\overline{\tau}$, where τ is the shear stress, should be part of the constitutive model. This has led to a more general relation between G and the shear strain γ:

$$G = \begin{cases} \overline{G} & for |\gamma| \le \overline{\gamma} \\ f(\overline{G}, |\gamma|, \overline{\gamma}, \gamma_c, c) & for |\gamma| > \overline{\gamma} \end{cases} \tag{2}$$

where the bar over a symbol denotes effective. A damage criterion similar to Reference [15] was also proposed for monitoring the amount of damage in the wall. Although the model is not hysteretic, during an earthquake excitation Tanrikulu et al.'s model predicted hysteresis loops similar to those observed experimentally. This model was shown to capture the dynamic behaviour of both clay brick and stone masonry.

The criterion by Benedetti and Benzoni [18] appears to be one of the few that have proposed a material model that is hysteretic in nature. The material model is based on the static shear tests carried out on single piers, requires seven parameters, and is constructed by superimposing three bilinear hysteretic shear sub-elements failing in a brittle manner at a prescribed strain intensity. Each sub-element is defined by its own

mechanical properties, G, τ, γ and is limited by γ_c. The resulting shear panel hysteretic curve is obtained by direct summation of all individual sub-elements; the ones that have exceeded the limits, γ_c are excluded. This model was derived from tests on stone masonry and agreement with experimental results is very promising.

3.4 Modelling of Stone Masonry

A large number of proposed analytical models are found in the literature of which only a representative few are selected here. Modena [5] stated that the sophisticated analytical and numerical models, which require the knowledge of relevant material and structural properties, can be inadequate for interpreting the actual behaviour of such complex and special masonry structures. He went on to say that the process of properly analyzing these monuments is iterative and is accomplished by upgrading a simple model to a level that can simulate structural damage that has been historically recorded. This view is echoed by some other researchers who are attempting to model the behaviour of stone masonry.

In an attempt to check the safety of an ancient church located in a seismic area, Vestroni et al [19] acknowledge that a model that correctly takes into account the detailed aspects of nonlinear dynamic behaviour of the monument is practically out of the question, especially since the monument has a spatially distributed structure which, even if discretized, requires a large number of variables. Furthermore, the material is quite complicated and strongly anisotropic, and the incomplete knowledge of the structural integrity makes the analytical description more uncertain. In view of the foregoing, two models of different complexity were employed. The first was a linear 3D finite element model used to develop a detailed stress analysis of the structure as a tool to identify the weak components. The second model was a nonlinear single-degree-of-freedom oscillator that was used to study the nonlinear response of a substructure.

Turnsek et al. [20] provided some insight on the seismic resistance of stone masonry by investigating the damage caused by the medium-strength Slovenia earthquake of 1974 and the two-successive strong earthquakes which hit the Friuli region in Italy and the Soca valley region in Slovenia in May and September 1976. A model that computes the shear strength of the masonry building was developed based on the assumptions that i) for each individual wall a shear strength ductility diagram can be constructed on the basis of characteristics obtained from laboratory tests; ii) displacement due to torsional rotation about the enter of rigidity can be superimposed; and iii) failure of individual walls occurs when a limiting ductility is reached. The model was verified by comparing the computed results with an actual two-storey building that was subjected to two different earthquakes. The results obtained from this model are in the form of base shear coefficients. The computed values appear to be in agreement with the ground acceleration values from the MSK-64 scale.

3.5 Comparative Study of Analytical Models

Karantoni et al. [21] have used the 1986 Kalamata earthquake in Greece to compare a finite element modeling, a three-dimensional space-frame model and an approximate hand-calculation method for performing seismic response analysis of unreinforced stone masonry structures. The objective of these analyses was to assess the ability to predict both the location and severity of seismic damage for a given seismic excitation. Damage and failure are taken in the form of and originate from macro-cracking, which for stone masonry is taken to occur when the magnitude of the principal stress exceeds the strength of masonry in uniaxial tension.

For the three buildings investigated, Karantoni et al. found from eigenvalue/eigenmode analysis that the first significant mode of vibration consists solely of bending

deformations with a natural frequency of 4 Hz. The in-plane displacement was almost nil. The second mode was found to have a natural frequency of 7.5 Hz and the deformation of two opposite exterior walls was mainly in-plane, with some bending of the other two walls. The authors stated that the bending and the in-plane action of the walls are generated by different and widely separated modes of vibration, and for the frequency content of their earthquake, bending was the dominant form of deformation.

The analysis performed was linear elastic and the equivalent static load was uniformly distributed along the height according to the distribution of mass. This approach was chosen in order to include the hand calculation method as one of the alternative techniques. It was concluded that the finite element analysis, which accounts for both in-plane and out-plane behaviour, was the only one to capture the key behaviour of the walls. The space frame idealization with rigid joints yielded a behaviour not observed in reality and gave an overestimate of principal tensile stresses. The hand-calculation approach, a shear beam model, accounts only for in-plane action and produced results that are lower and have an incorrect distribution of damage. In their final conclusion, Karantoni et al. noted that the finite element analysis revealed that the out-of-plane bending in walls is responsible for most of the observed damage and that this dominant behaviour is often overlooked in design.

4. SUMMARY

As has been briefly presented in this paper, different approaches are available to assess the seismic adequacy of old stone URM structures. It needs be recognized that such monuments are "unique" structures and that modern codes do not apply; therefore special requirements need to be developed.

Simple models have traditionally been the tools used by engineers to study behaviour and to check the safety of URM structures. However, it was found that these simple methods do not always apply and are not necessarily conservative. It should be recognized that the dynamic behaviour of stone URM is complex and nonlinear, and therefore an investigation of the safety of these monuments requires more sophisticated approaches. Consequently, more sophisticated models that employ the finite element method are increasingly used for the analysis. However, the usefulness of this approach is so far limited by the practical difficulty of adequately characterizing the material behaviour and of properly assessing the structural integrity. Further work toward realizing the potential of this method needs to be undertaken.

ACKNOWLEDGMENT

REFERENCES

1. ERGUNAY, O., and ERDIK, M., Turkish Experience on the Earthquake Performance of Rural Stone Masonry Buildings, Int. Conf. on Natural Hazards Mitigation Research and Practice: Small Buildings and Community Development, New Delhi, October 1984.

2. COMITE' NATIONAL D'URSS de l'ICOMOS, La Sauvegarde du Patrimoine Architectonique de L'Armenie, Icomos Information, April/Juin 1989.

3. ALLEN, D.E., FONTAINE, L., MAURENBRECHER, A.H.P., GINGRAS, M., The 1988 Saguenay Earthquake: Damage to Masonry Construction, Internal Report No. 584, Institute for Research in Construction, National Research Council Canada, October 1989.

4. ABK, A Joint Venture, Methodology for Mitigation of Seismic Hazards in Existing Unreinforced Masonry Buildings: Categorization of Buildings, ABK-TR-01, Seismic Input, ABK-TR-02, Diaphragm Testing, ABK-TR-03, Wall Testing, out-of-plane, ABK-TR-04, Agbabian Associates, El Segundo CA, 1981.

5. MODENA, C., Italian Practice in Evaluating, Strengthening, and Retrofitting Masonry Buildings', chapter 2, 1991.

6. CSA, CAN3-S304-M84, Masonry Design for Buildings, Candian Standards Association, Rexdale, Ontario, 1984.

7. ABK, A Joint Venture, Methodology for Mitigation of Seismic Hazards in Existing Unreinforced Masonry Buildings: The Methodology, ABK-TR-08, Agbabian Associates, El Segundo CA, 1984.

8. ATC, Seismic Evaluation of Existing Buildings, Applied Technology Council Report ATC-22, Redwood City CA, 1989.

9. IRC, Guidelines for Seismic Evaluation of Existing Buildings, Institute for Research in Construction, National Research Council Canada, December 1992.

10. PRIESTLEY, M.J.N., Seismic Behaviour of Unreinforced Masonry Walls, Bulletin of The New Zealand National Society for Earthquake Engineering, 1985.

11. ENGLEKIRK, R.E. and HART, G.C., Earthquake Design of Concrete Masonry Buildings, Vol. 2: Strength Design of One-to-Four Story Buildings, Prentice-Hall, Englewood Cliffs, New Jersey, 1984.

12. GRANVILLE, J.I. and HATZINIKOLAS, M.A., Engineered Masonry Design, Winston House Enterprises, Winnipeg Manitoba, 1989.

13. MENGI, Y. and McNIVEN, H.D., A Mixture Theory for Elastic Laminated Composites, International Journal of Solids and Structures, 1979.

14. ALI, S.S. and PAGE, A.W., Finite Element Model for Masonry Subjected to Concentrated Loads, Journal of Structural Engineering, 1988.

15. McNIVEN, H.D. and MENGI, Y., A Mathematical Model for the In-plane non-linear Earthquake Behaviour of Unreinforced Masonry Walls, part 2: Completion of the Model, Earthquake Engineering and Structural Dynamics, 1989.

16. MENGI, Y., McNIVEN, H.D. and TANRIKULU. A.K., A Model for Nonlinear Earthquake Analysis of Unreinforced Brick Masonry Buildings, Computers and Structures, 1991.

17. TANRIKULU. A.K., MENGI, Y. and McNIVEN, H.D., The Nonlinear Response of Unreinforced Masonry Buildings to Earthquake Excitations, Earthquake Engineering and Structural Dynamics, 1992

18. BENEDETTI, D. and BENZONI, G.M., A Numerical Model for Seismic Analyis of Masonry Buildings: Experimental Correlations, Earthquake Engineering and Structural Dynamics, 1984

19. VESTRONI, F., GIANNINI, R. and GRILLO, F., Seismic Analysis of an Ancient Church and a Proposal of Strengthening Repairs, Structural repair and maintenance of historical building II, Spain 1991.

20. TURNSEK, V., TERCELJ, S., SHEPPARD, P. and TOMAZEVIC, M., The Seismic Resistance of Stone Masonry Walls and Buildings, 6th European conf. on Earthquake engineering, Yugoslavia, 1978.

21. KARANTONI, F.V. and FARDIS, M.N., Computed versus Observed Seismic Response and Damage of Masonry Buildings, Journal of Structural Engineering, ASCE, 1992.

Modeling Masonry Behaviour using Distinct Elements

Modélisation de la maçonnerie par la méthode des éléments distincts

Modellierung von Mauerwerk mittels distinkten Elementen

Christian DIALER
Civil Engineer
Munich, Germany

Ch. Dialer, born 1959, got his civil engineering degree and PhD from the Techn. Univ. Munich, Germany. After one year in a construction firm, he spent two years as a Visiting Scholar at the Univ. of Colorado at Boulder, USA, and at the Univ. of California at Berkeley, USA. Currently, he is working as a structural engineer.

SUMMARY

Masonry made out of natural stones and bricks is among the most common building materials which at present need to be preserved. However, there is still a big gap between actual material behaviour and a sound understanding of how to model or analyze its behaviour. One way to describe discontinuous material behaviour is by using Distinct Elements; a 'continuum' is subdivided into distinct blocks which are able to undergo large motions and rotations. This numerical method is introduced to masonry and critically reviewed.

RÉSUMÉ

La maçonnerie de pierres naturelles et de briques représente un type de construction commun qui mérite d'être conservé de nos jours. Pourtant, nous manquons encore de modèles analytiques qui décrivent véritablement le comportement de la maçonnerie. L'utilisation des élément distincs offre un tel modèle d'analyse. Dans la méthode des éléments distincts, un 'continuum' est divisé en différents blocs qui peuvent soutenir de grands déplacements et rotations. Cettte méthode numérique est appliquée à la maçonnerie, et elle est passée en revue.

ZUSAMMENFASSUNG

Mauerwerk aus natürlichen und künstlichen Steinen gehört zu jenen klassischen Baumaterialien, deren Erhaltung heute grosses Augenmerk geschenkt werden muss. Dennoch mangelt es an Kenntnissen, wie grundlegendes Materialverhalten von Mauerwerk zu modellieren oder analysieren ist. Ein möglicher Weg besteht in der Anwendung von Distinkten Elementen. Dabei wird ein 'Kontinuum' in Blöcke unterteilt, die grossen Translationen und Rotationen unterworfen werden können. Diese neuere numerische Methode wird für Mauerwerksprobleme angewandt und kritisch beleuchtet.

1. INTRODUCTION

Preservation of the Architectural Heritage demands first an assessment of the structural serviceability of, in most cases, blocky materials. Brick or block arches, stone bridges and masonry walls in general, they all exhibit more or less a discontinuous material behavior due to their jointed nature. Modeling techniques which do not consider this discontinuous behavior of blocky structures can only model the over-all behavior. For a closer and more detailed look at the deformation and load bearing behavior, one has to use numerical schemes which account for the jointed behavior of e.g. masonry.

It is doubtful that new and advanced techniques would have saved the classic Tower of Babel (Fig. 1), but, at least we might have gained a deeper insight why, if not for a biblical spell, the structure failed.
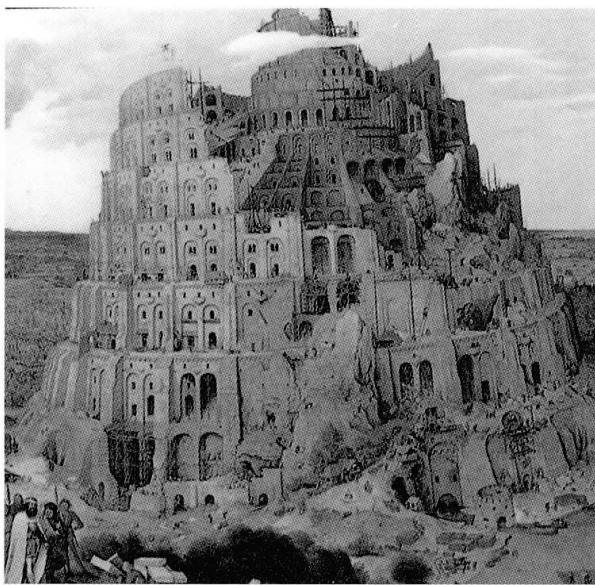
Fig. 1 The Tower of Babel by Peter Brueghel (1525/30-1569), cut

Thus, this paper introduces the Distinct Element Method (DEM) as proposed by Cundall [1] as an alternative modeling technique. The code was developed to model the behavior of discontinuous media, such as jointed rock masses and for other geotechnical applications (e.g. dam engineering). However, as certain restrictions are kept in mind, this method is also well suited to model masonry.

Tests on shear walls from a previous investigation by the author [2,3] at the Technical University of Munich were used to model those results applying the program UDEC [6].

2. CLASSIC MASONRY

Dealing with historical masonry, one has to consider the big difference between classic masonry and e.g. North-American Masonry made of concrete blocks. In the former, there is no reinforcement and no grouting. The mortar joints act as a real plane of weakness. Therefore, unreinforced ungrouted plain masonry has to be treated as a real discontinuum.

3. EXPERIMENTAL RESULTS

3.1 Test set-up

Experimental results following a test set-up as described in Figure 2 yielded the equations 1 to 3. A more detailed description of these tests and derivations is given in [2,3].

σ_I, σ_{II} applied principal stresses

σ_x, σ_y average normal stresses

τ_{xy}, τ_{yx} average shear stresses

$$X = \frac{\sigma_x}{\sigma_y} \quad , \quad Y = \frac{\tau_{xy}}{\sigma_y}$$

μ coefficient of friction in the joints

c   cohesion

$\beta_{t,b}$ tensile strength of bricks

β_c compressive strength

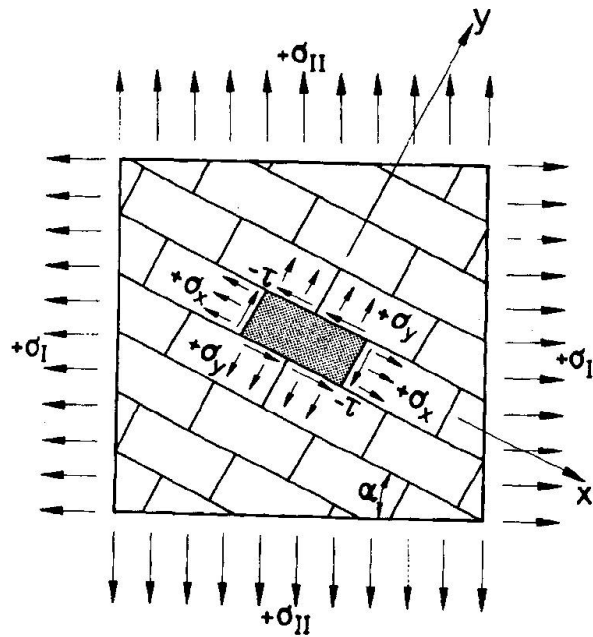$$v = \frac{2\Delta y}{\Delta x} \text{ see Fig. 3}$$

$$w = \frac{1}{v} \quad \text{see Fig. 3}$$

Fig. 2 Test set-up, assumption of a homogeneous state of stress

3.2 Model for ultimate strength

Figure 3 shows a model proposed by [5] and expanded by [2] for a non-uniform stress distribution as a result of the unbalanced shear stresses in the head and bed joints.
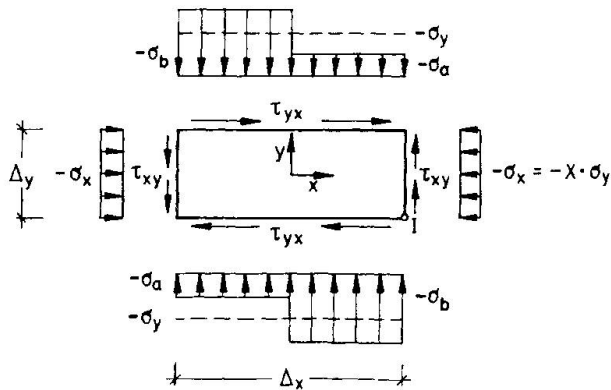
Fig. 3 Model

Three different failure modes can be distinguished. An opening of the bed joints was not observed, as tensile stresses in the bed joints have not been investigated in these tests. Furthermore, considering $c_{xy} \neq c_{yx}$ and $\mu_{xy} \neq \mu_{yx}$ leads to:

Shear failure of the bed joints:
$$\tau_{yx} = \frac{c_{yx} - \mu_{yx}\sigma_y + v\mu_{yx}(c_{xy} - X\mu_{xy}\sigma_y)}{(1 + v\mu_{yx})} \tag{1}$$

Tensile failure of the brick:
$$\tau_{yx} = \frac{1}{2}(c_{xy} - X\mu_{xy}\sigma_y) + \frac{\beta_{t,b}}{2.3}\sqrt{1 - \sigma_y\frac{(1+X)}{\beta_{t,b}} + \frac{X\sigma_y^2}{\beta_{t,b}^2}} \tag{2}$$

Compression failure of the panel: $\tau_{yx} = c_{xy} + w\beta_c + \sigma_y(w - X\mu_{xy})$ (3)

4. DISTINCT ELEMENT METHOD

4.1 Introduction

There are a couple of ways to analyze a structure: experimentally, analytically or using a numerical scheme. Analyzing large and more complex structures, one normally is forced to use numerical approaches. As there are three major groups of numerical models, one should be precise in using terminology. The different methods in use for discretizing a structure are:

Finite Elements   (FEM)
Boundary Elements   (BEM)   Discrete Elements
Distinct Elements   (DEM)
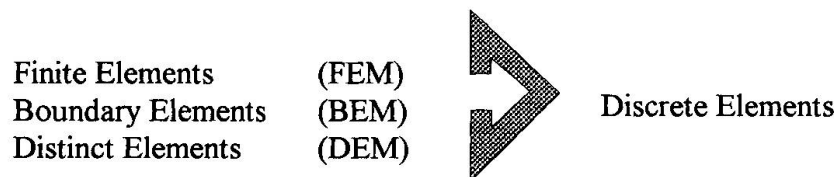
All these three methods together should be called Discrete Elements to avoid confusing terms.

In the Distinct Element code a medium is simulated as an assemblage of blocks which interact through corner and edge contacts. At these contacts, either rigid or fully deformable blocks are connected by spring like joint-normal and joint-shear stiffness, k_n and k_s, respectively (Fig. 4).
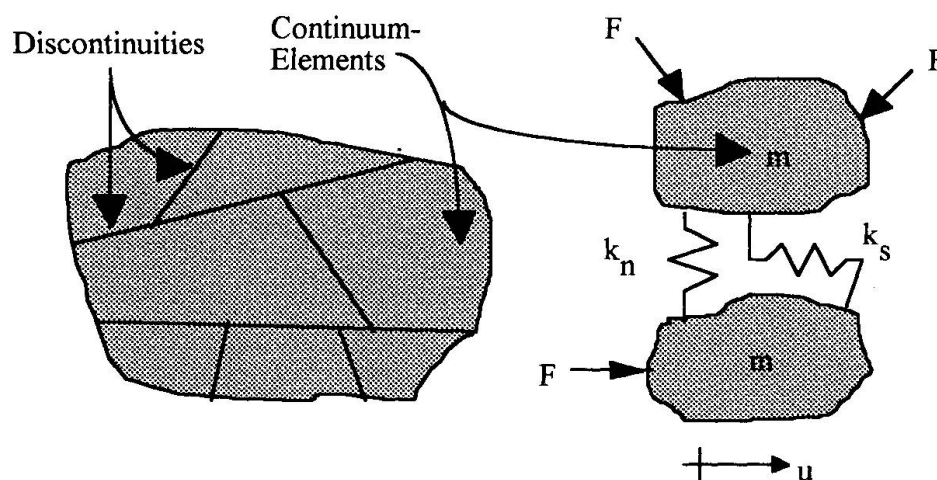
Fig. 4 Basic separation in a Distinct Element formulation

4.2 Theory and Background of the Code

Alike in FEM, the unknowns in DEM are the displacements and rotations of the blocks. However, unlike FEM, these unknowns are solved explicitly by solving the dynamic equilibrium of motion. For a single mass, avoiding matrix notation, this can be written in a general form (Newton's 2nd Law):

$$m\ddot{u}^t + c\dot{u}^t + ku^t = F^t \tag{4}$$

with

m	mass
$u, \dot{u}, \ddot{u}$	displacements and their derivations, respectively
c	damping
k	joint stiffness
F	loads
t	time

A similar equation can be written for rotations. A damping must be provided, otherwise, an elastic system oscillates forever. The static solution is interpreted as the end result of a long time oscillation (dynamic relaxation scheme).

The main task of the scheme is to determine a set of displacements by iteration that brings all elements into a state of equilibrium, or, if not possible, will indicate a failure mode.

Thus, the blocks in the system can develop large deformations and rotations, while compatibility is always satisfied. No stiffness matrix has to be formed and non-linearities can be implemented in an incremental form.

5. APPLICATIONS

5.1 Calibration tests

First computational runs on small two-brick specimen were carried out to investigate the correct stress distribution in joints and to check the overall behavior.

5.2 Masonry Shear Walls

Shear tests on biaxial loaded small scaled specimen have been carried out and have been reported in [3]. The panel in Figure 5 has been loaded in uniaxial compression with an inclination of the joints of $\alpha = 28.7$ degree. Thus, producing an averaged inner stress ratio with $X = \sigma_x : \sigma_y = 0.30$ and $Y = \tau_{xy} : \sigma_y = -0.55$ (Notations see Fig. 2). Figure 5 shows a typical crack pattern of the joints at shear limit as a result of a UDEC-simulation using a Mohr-Coulomb-failure criterion for the joints. The failure pattern correlates well with real test data.
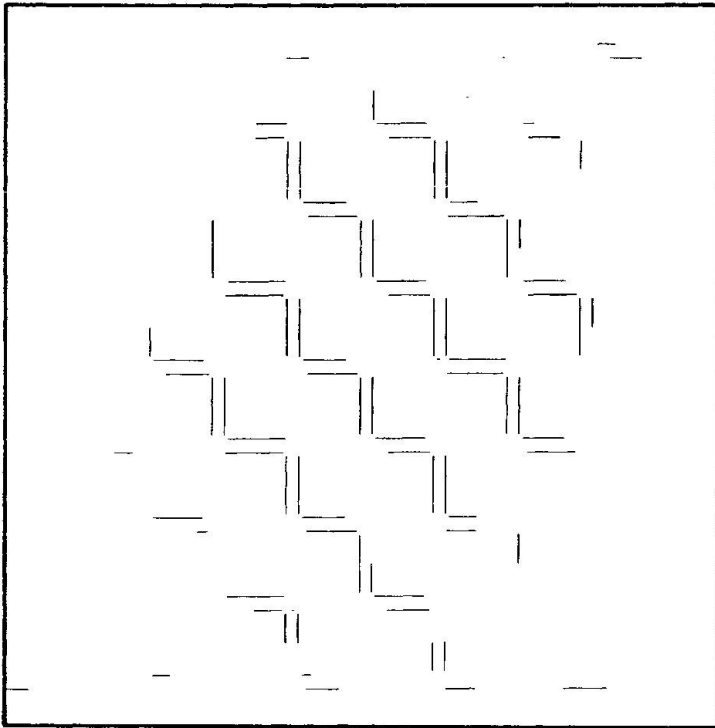
Fig. 5　Crack Pattern

The influence of the joints is remarkable for blocky structures. Furthermore, the qualities of joints in different directions are also different, being the basis of several shear failure criterions. This behavior was experimentally verified in [2], where it was shown that the bricks start to rotate in shear stressed masonry until a new state of equilibrium is reached.

To save calculation time, the mortar in the joints of the panels was now simulated using an equivalent joint stiffness, which was different for bed and head joints. Thus, for the same example as in Fig. 5, Fig. 6 shows the clockwise rotation of the bricks before failure. A calculation of the stresses is given in [4].
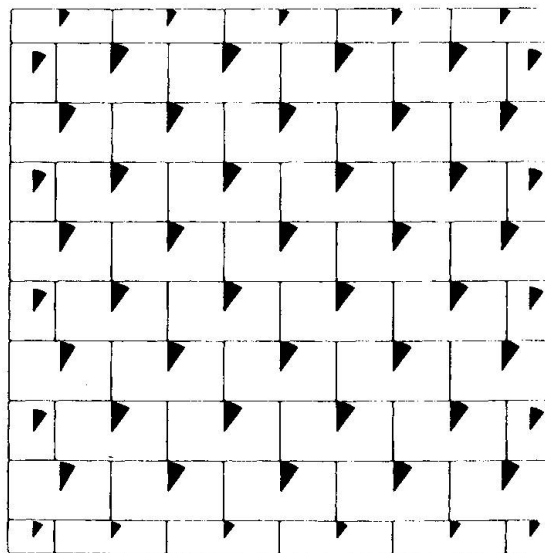

Fig. 6　Modeled brick rotations in shear stressed masonry

5.3 Infilled Frames

Structures made of infilled frames were already common hundreds of years ago. Although this example shows an infilled concrete structure, the basics remain the same. There is still little known about the fundamental load bearing behavior. Obviously, the influence of the joint between concrete and masonry is one of the driving factors for the bearing capacity. Fig. 7 shows the horizontal x-displacements of the frame and the infill as an example.
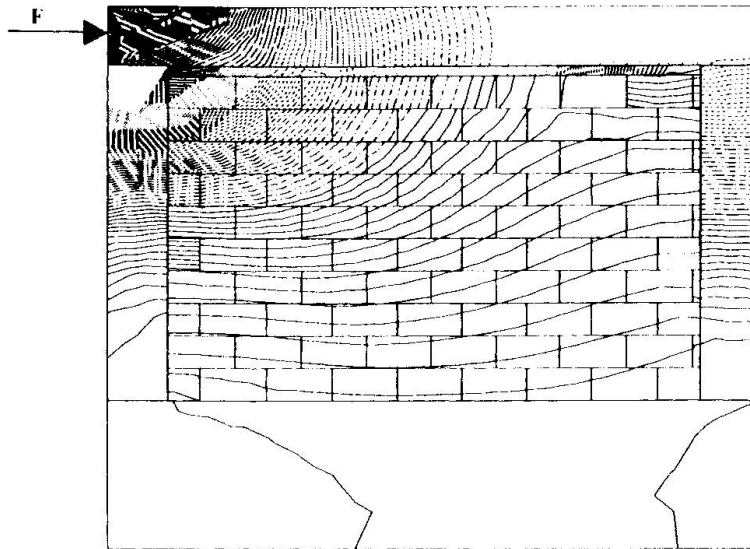

Fig. 7 Horizontal displacements of an infilled frame under a horizontal load.

6. CONCLUSIONS AND QUALIFIERS

The Distinct Element Method (DEM) solves the dynamic equilibrium for each body and boundary interaction forces. Each body communicates with surrounding bodies via boundary contacts which may change as a function of time. The forces which are generated between the contacts can obey various interaction laws.

Simulating different qualities of bed and head joints (cohesion and friction), the numerical results show brick rotations (Fig.6) and stress distributions along the joints which correlate very well with the test results. Furthermore, modeling techniques and a critical review of advantages and disadvantages for a further use of Distinct Elements in masonry are presented.

As the code was mainly developed for geotechnical applications where plane strain conditions are widely assumed, this state of strain is certainly not true for masonry and has to be considered.

For clay brick masonry, one typical failure mode is an internal split-off due to different Poisson's ratios of brick and mortar. Mortar, in general, has a Poisson's ratio which is twice as large as a brittle clay brick. Therefore, the mortar tears the brick apart. This out-of-plane characteristic, obviously, cannot be described with a plane program.

Furthermore, if one is interested in a more detailed deformation analysis, an orthotropic material law has to be derived and incorporated in the code. This would make the analysis for masonry more realistic.

Some of the driving code parameters which still need further investigation are:

- joint stiffnesses k_n , k_s
- damping factor c
- time step Δt.

These factors influence the solution process and, therefore, the state of equilibrium has to be checked by the user.

ACKNOWLEDGMENTS

REFERENCES

1.   Cundall P.A., A Computer Model for Simulating Progressive Large Scale Movements in Blocky Rock Systems, Proc. of the Symposium of the Int. Society of Rock Mechanics, Nancy, France, 1971, Vol. 1, Paper No. II-8

2.   Dialer C., Bruch- und Verformungsverhalten von schubbeanspruchten Mauerwerksscheiben, zweiachsige Versuche an verkleinertem Modellmauerwerk, Dissertation, Berichte aus dem Konstruktiven Ingenieurbau, Technische Universität München, 1990, Ph.D.-thesis in German

3.   Dialer C., Some Remarks on the Strength and Deformation Behavior of Shear Stressed Masonry Panels under Static Monotonic Loading, Proceedings of the 9th Int. Brick Masonry Conference (IBMaC), Berlin, Vol. 1, 1991 pp. 276 283

4.   Dialer C., A Distinct Element Approach for the Deformation Behaviour of Shear Stressed Masonry Panels, 6th Canadian Masonry Symposium, Saskatoon, Saskatchewan, 1992, pp. 765-776

5.   Mann W., Müller H., Versuche zur Bruchtheorie von querkraftbeanspruchtem Mauerwerk, Proc. of the 4th Int. Brick Masonry Conference, Brügge, 1976, p. 4.a.4

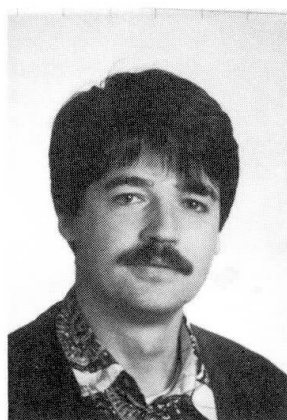6.   UDEC: Uniform Distinct Element Code, Version IGG 1.6, Itasca, Minneapolis, Minnesota, 1991

Modèle considérant la maçonnerie comme matériau non-résistant à la traction

Zugspannungsfreies Werkstoffmodell für Mauerwerk

Non-Tension Material Model for Masonry
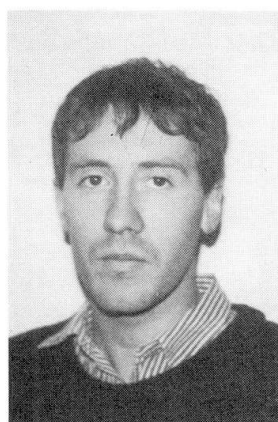
Koen VAN BALEN
Dr. Sc. Appl.
K. U. Leuven
Leuven, Belgique

K. van Balen, né en 1956 a obtenu le diplôme d'ing. architecte à la K.U. Leuven. Il a travaillé pour la restauration du patrimoine architectural avant de se concentrer sur la recherche dans le domaine des structures et matériaux historiques.

Pierre SMARS
Maître en Sc. Appl.
K. U. Leuven
Leuven, Belgique

P. Smars, né en 1966, a obtenu le diplôme d'ing. architecte à la K.U. Leuven. Il s'est spécialisé en conservation des monuments au Centre d'études pour la conservation du patrimoine architectural et urbain où il travaille en tant que chercheur dans le domaine des calculs des structures anciennes.

RÉSUMÉ

La définition de la maçonnerie ancienne comme un matériau ne résistant pas à la traction, permet de reproduire différents comportement typiques de structures anciennes. L'intégration de cette hypothèse dans un modèle aux éléments finis permet d'individualiser dans la maçonnerie des parties structurelles simples, telles que des barres ou des arcs. Suite à des fissurations, ces zones s'isolent de la partie de la maçonnerie qui ne fonctionne que comme remplissage et poids mort. Ce nouveau type de modèle est illustré sur différents exemples simples.

ZUSAMMENFASSUNG

Indem das Mauerwerk als ein Material ohne Zugfestigkeit definiert wird, können verschiedene typische Verhaltenserscheinungen bei alten Tragwerken nachvollzogen werden. Die Integration dieser Hypothese in ein Modell mit finiten Elementen erlaubt die Identifikation unterschiedlicher struktureller Partien, wie Bogen oder Balken, innerhalb des Mauerwerks. Als Folge von Rissbildungen heben sich diese Zonen vom übrigen Teil des Mauerwerks, das nur als Füllmaterial dient, ab.

SUMMARY

Defining masonry as a non-tension material allows to reproduce different well known behaviours of ancient masonry structures. When this hypothesis is included in a finite element model, different structural zones like arching, thrust and dead-load areas can be identified within the masonry. The presented model is illustrated for different simple masonry structures.

1. INTRODUCTION.

Les méthodes de calcul employées pour le calcul des structures anciennes en maçonnerie ont beaucoup évolué depuis que Méry a introduit sa méthode graphique pour la définition de la ligne de poussée. Les nouvelles théories des charges limites ont permis à différents auteurs, souvent en s'appuyant sur les recherches de J. Heyman [5], de démontrer la validité de l'emploi des lignes de poussée pour des structures composées de blocs rigides.

Durant les derniers décades l'introduction de la méthode des éléments finis a bouleversé les différentes aires de la science des matériaux. On a, en particulier, chercher à l'appliquer pour décrire le comportement des maçonneries. Comparés aux modèles de lignes de poussée les modèles aux éléments finis ont l'avantage de permettre, pour autant que le comportement des matériaux soit décrit correctement, d'étudier parallèlement les tensions et les déformations dans la structure [4][9]. Graduellement différents chercheurs ont essayé d'adapter ces modèles, considérant initialement les matériaux comme isotropes et élastiques, à la réalité du comportement de la maçonnerie. Il s'est avéré que ce matériau n'est que très peu élastique et que les importantes déformations dues entre autre à la fissuration constituent plutôt la règle que l'exception.

La simple observation de maçonneries historiques suffit à expliquer la difficulté ou même l'incapacité [1] de bien décrire son comportement. Afin de l'étudier nous avons employé un nouveau matériau: le NTM (Non Traction Material [2], n'ayant aucune résistance à la traction) [5]. Celui-ci tient compte d'une caractéristique essentielle de la maçonnerie: sa faible résistance à la traction et des éventuelles fractures qui peuvent en être la conséquence.

Un programme de calcul de type éléments finis a été développé [7] dont les éléments sont constitués de "NTM". Le modèle constitué est relativement simple et permet ainsi de garder un certain contrôle sur la qualité des résultats fournis. En outre, le NTM, étant plus fragile que la maçonnerie, peut servir de base à des calculs de vérification de sécurité.

2. MODELISATION DE LA MACONNERIE.

2.1. Principes de base du modèle [2]

Le matériau NTM ne possède aucune résistance à la traction. Cela signifie que, en tout point, et pour toute direction, la contrainte normale sur une section parallèle à cette direction est négative ou nulle. Cette condition équivaut à dire que les contraintes principales sont non-positives.

$$\sigma_1 \leq \sigma_2 \leq 0 \tag{1}$$

Le problème consistera alors en la recherche d'un champs de contraintes vérifiant, outre les équations d'équilibre, également les conditions (1) sur le tenseur. En général, une structure constituée d'un tel matériau se décomposera en trois zones aux propriétés différentes:
- la zone R_0, où les deux contraintes principales sont nulles ($\sigma_1 = \sigma_2 = 0$)
- la zone R_1, où seule une contrainte principale est non nulle ($\sigma_1 = 0$, $\sigma_2 < 0$)
- la zone R_2, où les deux contraintes principales sont négatives ($\sigma_1 < \sigma_2 < 0$)
Un problème subsiste, on sait bien que, à un champs de contrainte arbitraire donné, ne correspond pas nécessairement des déplacements possibles; il faut que les équations de compatibilité soient vérifiées. Dans le cas qui nous occupe, si la solution NTM diffère de la solution standard, les équations de compatibilité ne seront pas vérifiées: sous l'influence des forces extérieures le matériau se sera fracturé. Afin de pouvoir a nouveau intégrer le système, c'est à dire déterminer les déplacements on peut , dans le cas de l'utilisation d'un

programme aux éléments finis, représenter les fractures au mouyen de
déformations initiales Δ (pour autant qu'elles restent petites en regard aux
dimensions des éléments).

On comprend aisément qu'il existe deux types élémentaires de fractures: celles
d'ouverture (type Δ_ϵ) et celles de glissement (type Δ_γ): toute fracture
générique étant une combinaison de ces deux types fondamentaux (Fig.1).

Comme pour les contraintes, il y aura
certaines conditions sur le tenseur des
fractures. Pour qu'il n'y ait pas
d'interpénétration de matière, il faut
que les fractures ∈ soient d'ouverture
et non de fermeture, ce qui implique que
le volume de la fracture doit être
positif (trΔ ≥ 0).

Il existe aussi des relations entre les
fractures et les contraintes. Nous
envisageons successivement les trois
zones R_0, R_1 et R_2.

Dans une zone R_0, aucune contrainte ne
doit être transmise, le matériau ne
pouvant absolument pas résister à la
séparation de ses parties, il peut être
entièrement fracturé.

Dans une zone R_1, les contraintes
doivent être transmises dans *une*
direction; sans nuire à la généralité,
nous pouvons la fixer comme étant y
(σ_y=0). Pour que cette transmission soit
possible, il ne peut y avoir de

Fig. 3   Fractures élémentaires et
leur représentation sous
forme de déformation
initiale.

fractures Δ_x (ouverture dans le sens y), par contre, les déformations Δ_y
(ouverture dans le sens x) et Δ_{xy} (glissement) sont possible; aucun effort ne se
transmettant perpendiculairement aux fractures.

Dans une zone R_2, les contraintes doivent être transmises dans les deux
directions, il ne peut y avoir aucune fracture. Dans cette zone le matériau NTM
se comporte exactement comme un matériau standard.

Ces observations peuvent se résumer en disant que, en tout point, les tenseurs
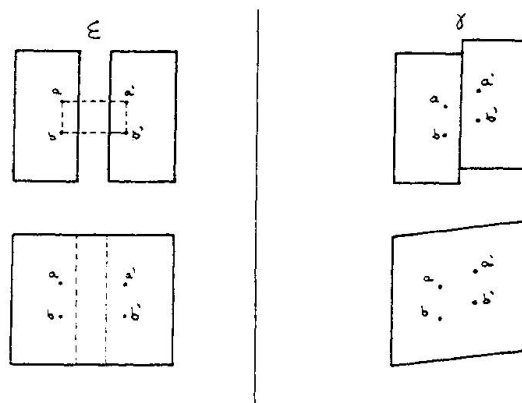des fractures et des contraintes sont orthogonaux ($\Delta^T\sigma$ = 0).

2.2. Présentation du programme CALPA

Un programme aux éléments finis a été écrit. Il utilise une discrétisation en
éléments triangulaires à contrainte constante [10]. Les inconnues sont les
déplacements des noeuds. Les éléments sont constitués de matériau NTM (n'ayant
aucune résistance à la traction).

Le problème étant non-linéaire, une procédure itérative doit être utilisée, on
utilise la méthode de Newton-Raphson modifiée (modifiée car il se peut que, à un
moment du calcul, la structure ou certaines de ses parties devienne
hypostatique) [3],[10].

$$^{n+1}u = {}^nu + du$$

$$du = -[R(^0u)]^{-1}[R(^nu)^nu - F]$$

(2)

A chaque itération, la matrice de raideur R est recalculée. En fonctions des

déplacements des noeuds, on décide du type de comportement d'un élément [4].

- Comportement bi-directionnel (zones R_2)

Si les déplacements conduisent à des déformations dont le tenseur vérifie les conditions

$$\operatorname{tr} D < 0$$
$$(1-\nu^2)\det D + \nu \operatorname{tr}^2 D \geq 0 \tag{3}$$

On se trouve dans une zone R_2 et la matrice K, liant les contraintes aux déformations, est du type

$$K = \frac{E}{1-\nu^2} \begin{bmatrix} 1 & & \nu \\ & \frac{(1-\nu)}{2} & \\ \nu & & 1 \end{bmatrix} \tag{4}$$

- Comportement uni-directionnel (zones R_1)

Si le tenseur des déformations vérifie les conditions

$$\det D < 0$$
$$\operatorname{tr} D \geq -(1-\nu)\sqrt{\frac{-\det D}{\nu}} \tag{5}$$

On se trouve dans une zone R_1 et la matrice K, anisotrope, est construite en effectuant une rotation d'un angle β (orientation de la fracture) de la matrice K'

$$K' = E \begin{bmatrix} 1 & & \\ & 0 & \\ & & 0 \end{bmatrix} \tag{6}$$

- Absence de réaction (zones R_0).

Si le tenseur des déformations vérifie les conditions

$$\operatorname{tr} D \geq 0$$
$$\det D \geq 0 \tag{7}$$

On se trouve dans une zone R_0 et la matrice K est nulle

$$K = \begin{bmatrix} 0 & & \\ & 0 & \\ & & 0 \end{bmatrix} \tag{8}$$

Si le processus itératif utilisé converge on peut être sûr de deux points.
- Le champs de contrainte est admissible et respecte les équations d'équilibre.
- Les fractures obtenues finalement sont orthogonales au tenseur des contraintes.
Or, dans un problème d'élasticité standard (avec résistance à la traction), si

l'on ajoute des déformations initiales orthogonales aux contraintes, la solution statique n'est pas modifiée, l'expression de l'énergie complémentaire (9) restant identique.

$$\mathbb{C} = \frac{1}{2} \int_\Omega \sigma^T K \sigma \, d\Omega + \int_\Omega \sigma^T \Delta \, d\Omega \qquad (9)$$

On peut en déduire que le champs de contrainte donné par le programme aux éléments finis est bien la solution statique du problème NTM étudié.

Comme on peut le démontrer, la solution cinématique à un problème NTM n'est pas unique, l'expression de l'énergie potentielle totale n'étant pas influencée par certaines fracturations.

Les déplacements trouvés par le programme CALPA, utilisant uniquement des fractures d'ouverture, sont acceptables, mais pas forcément "économiques" [7].

Nous allons à présent étudier un certain nombre de problèmes simples afin de voir comment le programme se comporte à leur égard.

2.3. Modélisation d'un arc

La maçonnerie résistant mal à la traction, pour couvrir un espace efficacement, on a toujours eu recourt à des systèmes visant à faire descendre les charges au sol sans créer de tractions dans la structure. L'arc, à cet égard, peut être considéré comme l'élément structurel typique de la maçonnerie (la voûte et la coupole étant d'autres systèmes plus complexes).

Suite aux recherches de Coulomb et ensuite en suivant la formulation classique définie au XIX$^{\text{ième}}$ siècle, on calculait les arcs en utilisant la méthode des lignes de poussée. Cette méthode, basée sur l'utilisation du polygone funiculaire, permet de fixer une limite inférieure et une limite supérieure aux poussées d'un arc sur les structures sous-jacentes.

Heyman a montré que cette méthode était toujours la plus efficace. Le choix entre la poussée minimale et la poussée maximale se fait en analysant la situation (une voûte s'ouvre en général).

Il est intéressant de voir comment se comporte le programme CALPA vis-à-vis de telle structures et plus particulièrement s'il fournit des résultats comparables à ceux obtenus en utilisant la méthode des lignes de poussée. Nous avons, à cette fin, testé un arc brisé successivement soumis à un écartement des appuis et à un rapprochement des appuis. Les résultats sont présentés à la Fig.2 joints à une analyse graphique.

On remarque que, pour la poussée minimale, des rotules se forment aux reins pour un angle d'environ 60° de part et d'autre de la clef de voûte. Il est également à noter qu'il y a deux zones (1 et 1') non soumises à contrainte. Ces zones ne sont pas en équilibre. Le matériau NTM, absolument incapable de résister à la traction, ne peut, en toute circonstance, assurer l'intégrité des structures qui en sont constituées; pour une poussée minimale les parties 1 et 1' tombent.

Pour obtenir des renseignements sur le comportement d'un arc d'une précision comparable à celle obtenue avec la méthode des lignes de poussée il faut utiliser un grand nombre d'éléments (nous en avons utilisé 500). L'avantage est que, pour une structure complexe, formée d'un ensemble d'éléments structuraux simples, le programme détermine -en tenant compte de l'élasticité des matériaux et de l'interaction des éléments- une combinaison de poussées (variant entre H_{min} et H_{max}) conduisant à la formation d'un champs de contrainte admissible pouvant donc servir de base à une analyse aux charges limites.
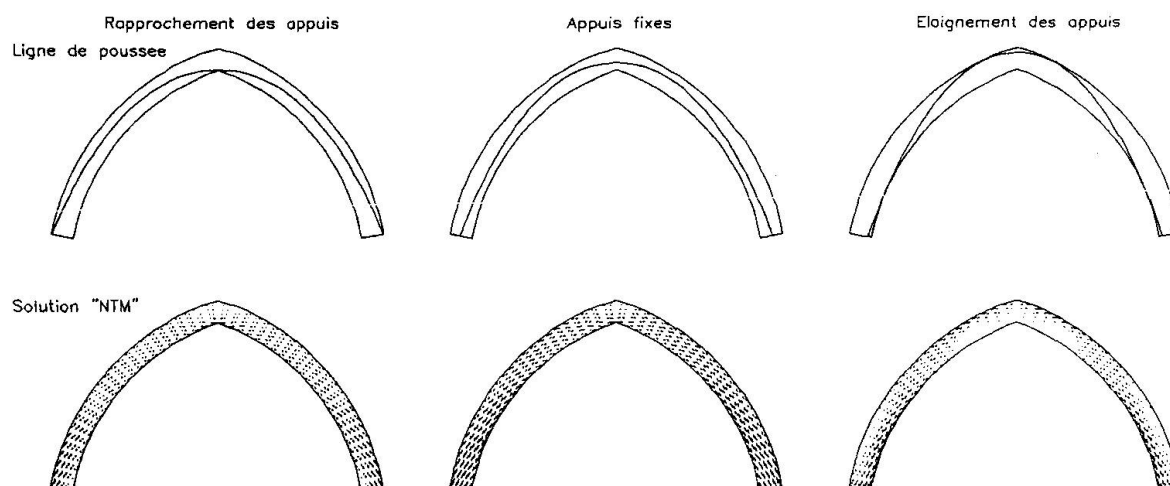
Fig. 4 Arc soumis à un éloignement et à un rapprochement de ses appuis.

2.4. Modélisation d'un panneau de maçonnerie

Le programme CALPA a principalement été développé pour l'analyse de structures bidimensionnelles. Nous l'avons testé sur un élément bidimensionnel élémentaire pour lequel nous possédons une solution théorique, un panneau rectangulaire.

On sait [2] qu'une force appliquée sur un tel panneau ne diffuse absolument pas à l'intérieur de celui-ci. Ce résultat se retrouve bien en utilisant le programme.

On a également testé l'influence d'une force latérale de confinement. Si la force de confinement est égale à la force verticale, la solution NTM est identique à la solution standard, cette dernière étant acceptable ($\sigma_1 < 0$ partout). Si la force de confinement est beaucoup plus faible (5 fois par exemple), l'interprétation est plus complexe. Il est néanmoins possible de distinguer dans le panneau les zones R_0, R_1 et R_2. Pour un panneau constitué d'un matériau standard, les isostatiques sont courbes alors que pour un panneau de NTM, il y a des zones R_1 où elles sont droites (formant des barres structurelles) et des zones R_2 de transition entre celles-ci.

PANNEAU ENTIER

STANDARD   NTM   STANDARD   NTM
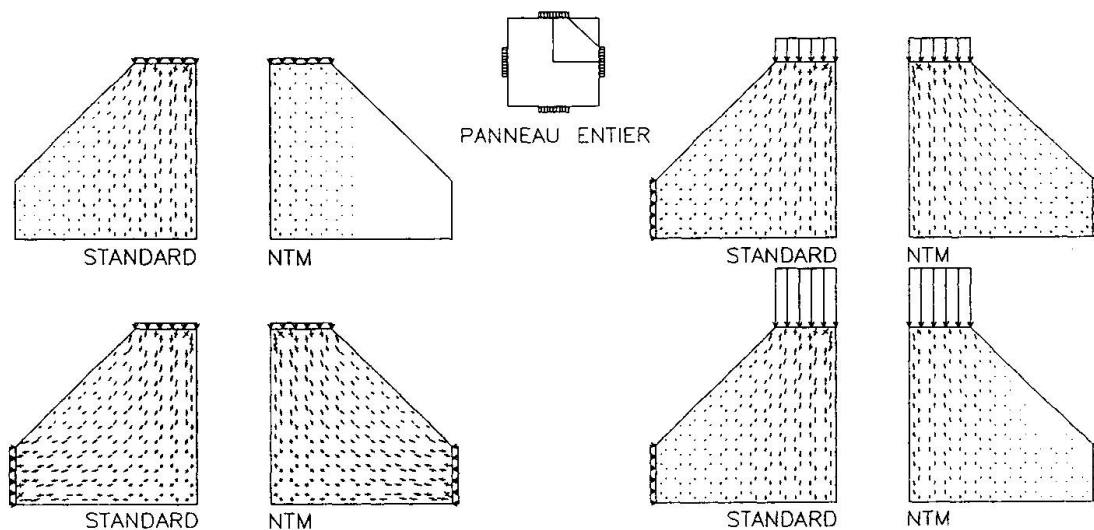
STANDARD   NTM   STANDARD   NTM

Fig. 5 Panneau de matériau NTM soumis à différentes charges.

La soudaine transition de zone R_0 à la zone R_1 s'exprime dans les structures réelles par des fissures. Celles-ci se présentent souvent sous les appuis des poutres maîtresses dans les structures traditionnelles en brique et bois.

On analyse également un panneau rectangulaire posé à ses extrémités. La formation à l'intérieur du panneau d'un ensemble d'arcs est bien visible.
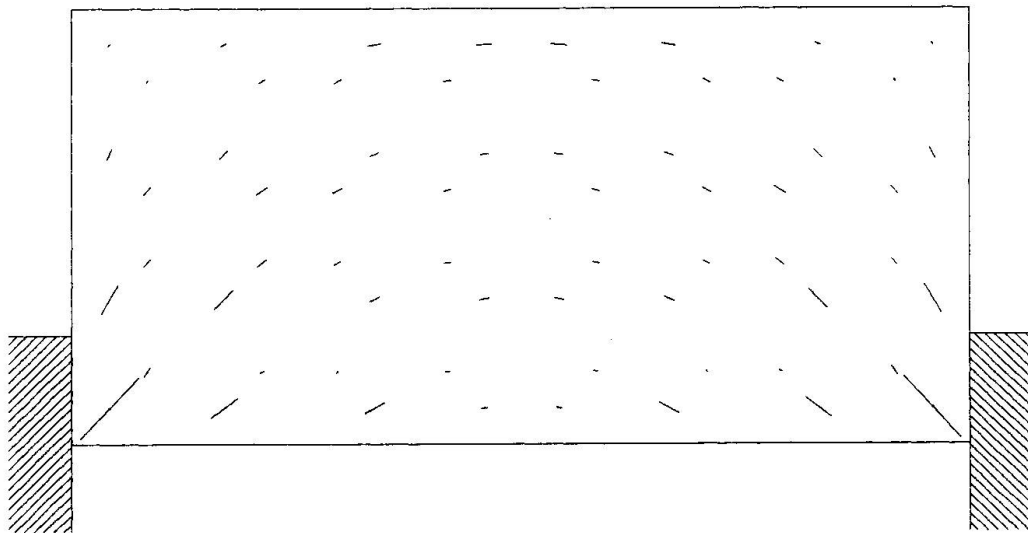
Fig. 6 Panneau de NTM sur deux appuis et soumis à son propre poids.

L'emploi du modèle illustre bien la séparation de la maçonnerie en zones structurelles et de remplissage. L'ouverture des appuis du panneau de la Fig.4 conduirait ainsi à la chute de la partie basse (comme les zones 1 et 1' de la Fig.2) et à la formation d'un arc structurel soutenant la partie supérieure. Ce type de comportement, caractéristique de la maçonnerie a conduit les maîtres maçons de l'époque à la recherche des formes structurelles optimales.

3. CONCLUSIONS

Les exemples donnés montrent que le modèle NTM présenté fournit des résultats très différents des modèles élastiques, plus proches de la réalité et comparables au résultats des anciens modèles (utilisants la méthode de Méry) pour des problèmes simples tout en conservant l'avantage de la méthode des éléments finis, apte à traiter des problèmes extrèmement généraux.

NOTATION

σ_1, σ_2 : contraintes principales.
Δ : matrice du tenseur des fractures.
D : matrice du tenseur des déformations.
$\text{tr}\Delta$: trace de la matrice Δ.
$\det\Delta$: déterminant de la matrice Δ.
$^n u$: vecteur déplacement à l'itération n.
R : matrice de rigidité de la structure.
F : vecteur des forces extérieures.
ν : coéfficient de Poisson.
$\mathbb{C}$: énergie complémentaire.

REFERENCES

1. BENVENUTO E., L'ingresso della storia nelle discipline strutturali, in Palladio, n°1 giugno 1988.
2. DI PASQUALE S., Statica dei solidi murari, teoria ed esperienze, preprint dipartimento di costruzioni, Firenze, 1984.
3. DOLTSINIS I.St., Nonlinear concepts in the analysis of solids and structures, in CISM courses and lectures n°300, pp.1-79, Springer Verlag, Wien New-York.
4. GIAQUINTA M., GIUSTI E., Researches on the equilibrium of masonry structures, in Arch. Rat. Mech. Analysis, 88, 1985.
5. HEYMAN J., The stone squeleton, in Int.J.Solids and structures,vol.2, 1966, pp.249-279.
6. HEYMAN J., The masonry arch, Ellis Horwood, Chichester, West Sussex, 1982.
7. SMARS P., Etudes sur les structures en maçonneries, mémoire présenté au Centre d'Etudes pour la Conservation du Patrimoine Architectural et Urbain R.Lemaire, K.U.Leuven, 1992, 221 p., Leuven.
8. STABLE-UNSTABLE, La consolidation des structures anciennes, actes du colloque, Leuven University Press, Leuven, 1988.
9. VAN BALEN K., Karbonatatie van kalkmortel en haar invloed op historische strukturen (La carbonatation de la chaux et son influence sur le comportement des structures anciennes), thèse de doctorat, Faculté des Sciences Appliquées, K.U.Leuven, décembre 1991, 281 p., Leuven.
10. ZIENKIEWICZ O.C., The finite element method, McGraw-Hill, London, 1977.

Earthquake Resistant Capacity of the Parthenon

Résistance du Parthénon aux tremblements de terre

Erdbebenwiderstand des Parthenon

Makoto WATABE
Senior Man. Dir.
Shimizu Corp.
Tokyo, Japan

Hitoshi AOKI
Dep. Dir.
Minist. of Constr.
Tokyo, Japan

Toshikazu HANASATO
Research Eng.
Tajimi Eng.Serv. Ltd
Tokyo, Japan

SUMMARY

The anticipated ground motions required to examine the earthquake resistant capacity of the Parthenon have been generated through the probabilistic approach. Seismic response analyses of the columns have been conducted to study their feasibility to safely withstand the simulated ground motions. Static shear tests on the model marble columns have been carried out to investigate the effect of the shear keys on earthquake resistant capacity.

RÉSUMÉ

C'est à l'aide d'une approche probabilistique que les mouvements du sol permettant l'examen de la résistance du Parthénon aux tremblement de terre ont été produits. Les analyses du comportement sismique de colonnes ont été réalisées afin d'étudier leur capacité à résister au mouvement du sol simulé. Les essais au cisaillement statique dans des colonnes types de marbre, ont été exécutés afin d'étudier l'effet des clés de cisaillement sur la capacité de résistance aux tremblements de terre.

ZUSAMMENFASSUNG

Die voraussichtlichen Bodenerschütterungen, für die der Erdbebenwiderstand des Parthenon zu überprüfen war, wurden nach dem Wahrscheinlichkeitsprinzip generiert. Das seismische Antwortverhalten der Säulen wurde analysiert, um deren Widerstandskraft gegen die simulierten Bodenerschütterungen zu studieren. An marmornen Säulentrommeln wurden statische Schertests durchgeführt, um die Auswirkung der Scherenverzahnungen auf den Erdbebenwiderstand zu prüfen.

1. INTRODUCTION

The various historical monuments constructed in seismic regions have been subjected to a number of destructive or damaging earthquakes during their histories and they have survived by grace of their excellent design and construction or by chance owing to the characteristics of the earthquakes. The inherent structural complexity, variability of buildings and foundation materials, as well as, their final state of repair, make each historical monument a special case of study. In this study, our attention will be focused on Parthenon which is one of the main historical monuments in Greece. Parthenon's behavior under seismic actions for 25 centuries was completely satisfactory. However, during the various phases of the monument's history, radical alterations have occurred concerning the geometric configuration, the interconnection of structural members and the state of materials. For example, the 1981 Corinth Earthquake was reported to cause slight damage to the columns. It was considered that the wooden shear keys inserted between the drums could not withstand the seismic load due to the material weathering. The aspect mentioned above all impose the necessity to study Parthenon's earthquake resistant capacity. It was reported that Parthenon has been partially strengthened, but at that moment, earthquake resistant design has not been accomplished. The scope of this paper is to study the feasibility for the monument, in its existing state, to withstand safely the earthquake ground motions, probabilistically derived from seismological data of the region, and to conduct an experimental study for the aseismic retrofitting.

2. REFERENCE GROUND MOTIONS REQUIRED TO EXAMINE EARTHQUAKE RESISTANT CAPACITY

2.1 General

The input ground motions required to examine the earthquake resistant capacity of Parthenon were generated through the probabilistic approach. The procedure was explained in detail by Theofanopoulos in reference [1] and Theofanopoulos and the authors in reference [2].

2.2 Seismic hazard analysis

A data base of the earthquake records with magnitude greater than 5.0 which occurred in the area of Greece during the period between 1900 and 1986 was referred in this study. The region of Greece was divided into 19 seismic areas on the basis of the seismotechtonic criteria. Within each area, earthquakes were assumed to occur uniformly, randomly and independently as they were assumed to follow the Poisson process. By use of the historical earthquake records, the parameters for the seismic risk analysis, such as the annual occurrence rate of events, the b-value of Gutenberg-Richer's equation and the upper bound magnitude were estimated. Some of these parameters formulated the probability density function for each area. Furthermore, the probability density of distance between the shortest distance and the longest one from the site to the source-area was calculated for each of 19 areas. To obtain the anticipated response spectra at the site, the attenuation equation for spectral acceleration proposed by Kawashima [3] was introduced in this study,

$$S_A(M,\Delta,T) = a(T)10^{b(T)M}(\Delta + 30)^{-1.178} \tag{1}$$

where M is the earthquake magnitude, Δ is the epicentral distance, and T is the natural period. Since it is necessary to consider the uncertainties of the normalized response spectra among the ground motions whose magnitudes and epicentral distances were the same, the coefficient of variation was assumed as 0.3 for all periods between 0.1 and 3.0 seconds [4]. Through the above procedure, the probability of exceedance per year of the ground motions for all the control points were calculated. Fig.1 shows an exampled hazard curve for the natural period of 0.2 sec. Another significant task is the selection of acceptable levels of risk which should be determined on a specific project as Parthenon's retrofitting. These were directed; 1) To prevent structural and most architechtural damage due to those earthquakes reasonably anticipated to occur several times during the life of the monument (Level 1). ii) To prevent total collapse, due to the maximum credible earthquake
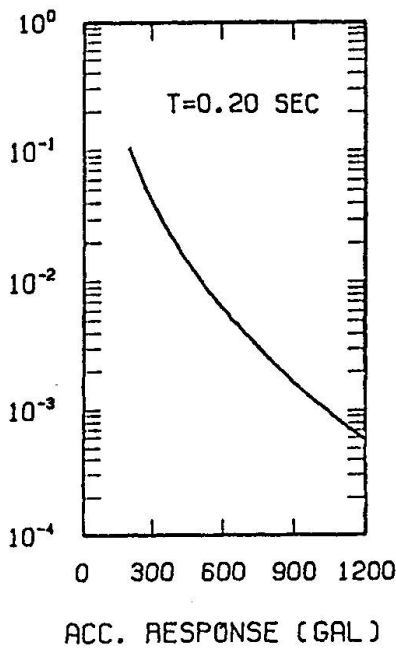
T=0.20 SEC

ACC. RESPONSE (GAL)

Fig.1 Seismic hazard curve for the control natural period of 0.2sec

PARTHENON. 1000 YEARS
PARTHENON. 100 YEARS
PARTHENON. 50 YEARS

PERIOD (SEC)
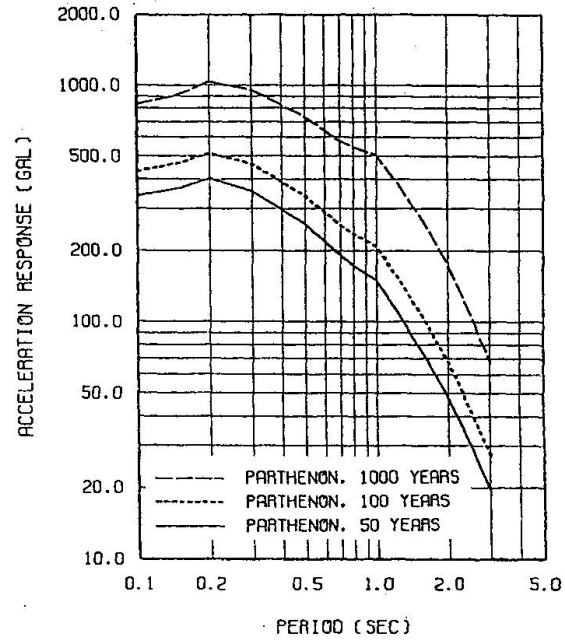
Fig.2 Uniform hazard spectra at the base of Acropolis hill for return period of 50, 100, and 1000years

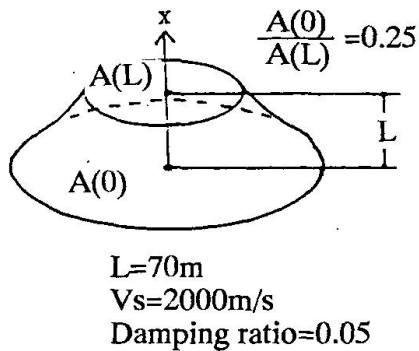$$\frac{A(0)}{A(L)} = 0.25$$

L=70m
Vs=2000m/s
Damping ratio=0.05

Fig.3 Elastic shear beam model to calculate the topographical effect of Acropolis hill

RETURN PERIOD 1000 YEARS (LEVEL 2)

RETURN PERIOD 100 YEARS (LEVEL 1)

DAMPING = 5%

TOP OF HILL

BASE OF HILL

PERIOD (SEC)

MAX = 579 GAL
TOP OF HILL
RETURN PERIOD 100 YEARS (LEVEL 1)

TIME (SEC)

MAX = 1051 GAL
TOP OF HILL
RETURN PERIOD 1000 YEARS (LEVEL 2)

TIME (SEC)

Fig.4 Synthetic earthquake ground motions for return period of 100 and 1000years, along with the target spectra

Fig.5 Drum's interface and shear key (After Penrose,C.K.(1973))

anticipated to occur (Level 2). In this study, a return period of 100 years was adopted to represent the earthquake motions of level 1 and a return period of 1000 years for the earthquake motions of level 2. The acceleration response spectra for return periods of 100 and 1000 years were obtained from the seismic hazard curves for all the control points. Fig. 2 shows the anticipated acceleration response spectra at the base of Acropolis hill for return periods of 50, 100 and 1000years.

2.3 Simulation of synthetic earthquake ground motions

Earthquake ground motions compatible with the anticipated response spectra for return periods of 100 and 1000 years were generated by the superposition of sinusoidal waves with a set of phase angles uniformly distributed in the interval between 0 and 2. The stationary waves were multiplied by the envelope functions proposed Theofanopoulos et al. [5]. These envelope functions correspond to earthquake magnitudes and distances, relative to active faults in the vicinity of Athens with potential to generate earthquake motions of level 1 or of level 2 , respectively.

2.4 Topographical effect of the hill and resulted motions

The Acropolis hill where Parthenon is located was modeled as a linearly elastic shear beam with an exponentially varying cross-section (See Fig.3). Since the height-to-width ratio of the hill is small, it may be reasonable that primary response of the hill due to earthquake motions at its base will be principally in shear. The resulted ground motions at the top of the hill for return periods of 100 and 1000 years, along with the response spectra at the base and at the top of the hill, are shown in Fig.4. Comparing the acceleration response spectra at the top of the hill with those at the base, the spectral amplitudes at the top are about 1.4 to more than 5 times greater than those at the base in the period range between 0.04 and 0.2sec. Thus, it seems feasible for the shear waves of the motion at the base, with period of about 0.1sec, to cause resonance, because the wavelength of them are compatible to the dimension of the hill. On the other hand, the maximum acceleration amplitudes of the ground motions at the base of the hill are 201gals for return period of 100years and 460gals for return period of 1000years, and consequently the amplification ratio of the maximum accelerations at the top to the base takes values of 2.3-2.9. The synthetic ground motions at the top of the hill will be used as the input motions for the seismic response analysis in the following chapter.

3. SEISMIC RESPONSE ANALYSES OF MASONRY COLUMNS

3.1 General

Dynamic analyses of Parthenon's columns have been conducted to study their feasibility to withstand the given ground motions safely. The analytical methods were explained in detail by the authors in reference [6] and [7].

3.2 Structural conditions

The column has a height of 9.6m, composed of 11 drums and a capital. The diameter of the drum ranges from 1.9m at the base to 1.5m at the top, of which average height is o.87m. The material used for the construction is white Penteric marble. Fig.5 describes the condition at the interconnection between the drums [8]. In the present state, the most of columns have beams and pediments on their capitals, while some of them have not. This structural condition was also taken into account in the linear response analysis.

3.3 Linear response analysis

Thirteen or twelve lumped mass systems were assumed, and rotational and translational modes at each level of drum's separation were considered. In this study, three models were assumed as follows. Model (A) represents a column with a beam and a pediment on its capital, subjected to seismic loads perpendicular to the longitudinal direction of its beam(See Fig.6). Model (B) is similar to Model (A), but it is subjected to seismic loads in the longitudinal direction of its beam.
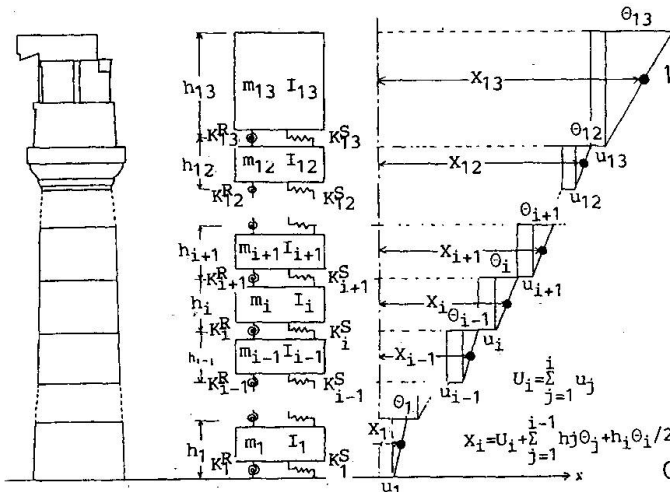
Fig.6 Model for linear response analysis of a masonry column with a beam and a pediment on its capital (Model(A))

Fig.7 Fourier spectra ratio of microtremor records at Zeus–Olympeion Athens ; the ratio between the top and the base of the column

(T1=1st mode , T2=2nd mode)

T:NATURAL PERIOD OF THE COLUMN

PERIOD (sec)

Table 1 Natural periods of Zeus–Olympeion column ; Comparison of measurements with analysis

	Natural period (sec)	
Mode	measurement	analysis
1st	0.525	0.531
2nd	0.101	0.101

Table 2 Estimated natural periods of Parthenon columns

Mode	Natural period (sec)		
	Model(A)	Model(B)	Model(C)
1st	0.583	0.275	0.236
2nd	0.086	0.037	0.046

RETURN PERIOD = 100 YEARS

O MODEL (A)
□ MODEL (B)
△ MODEL (C)

RETURN PERIOD = 1000 YEARS

O MODEL (A)
□ MODEL (B)
△ MODEL (C)

MAXIMUM SHEAR COEFFICIENT

Fig.9 Assumed characteristics between load and displacement for non-linear response analysis

Q(shear force)

strengthening

μ·W

weathering of pivots

μ:friction coefficient
W:Weight

δ(displacement)

RETURN PERIOD = 100 years

RETURN PERIOD = 1000 years

Case 2 Case 1 DRUM LEVEL Case 1 Case 2

Case 1:without shear key
Case 2:with shear key

Case 1:without shear key
Case 2:with shear key

MAXIMUM SHEAR COEFFICIENT

Fig.8 Results of linear response analysis ; Distribution of the maximum shear coefficients along height of columns
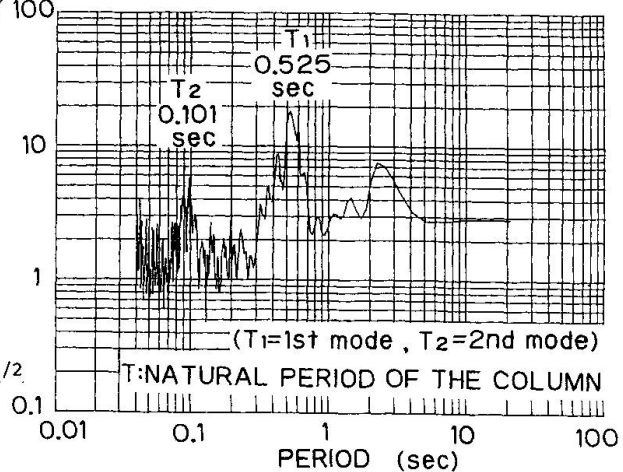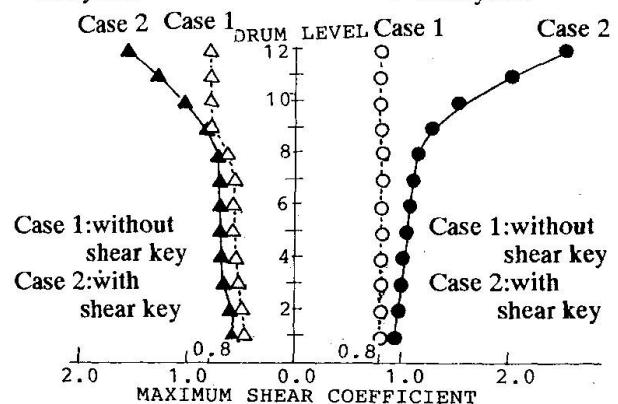
Fig.10 Results of non-linear response analysis ; Distribution of the maximum shear coefficient along height of a column without beam and pediment on its capital

Model (C) represents a column without any member on its capital. Since the dynamic characteristics of Parthenon such as natural periods of its column was not available, the natural periods, as well, as the other parameters for the analysis were estimated, considering the microtremor records at Zeus-Olympeion Athens and the difference in the dimensions between Parthenon and Olympeion. Fig.7 shows the Fourier spectral ratio of the records obtained at the top to that of the records obtained at the base of the Olympeion's column, in which the natural periods of the column for the 1st and 2nd modes are presented. For the linear analysis, the rotational spring constant K_R at each interface was assumed as the following equation.

$$K_R = \alpha \sqrt{\sigma_V} r^4 \tag{2}$$

where σ_V is the normal stress, r is the interface's radius, and α denotes the proportionality index evaluated through the eigenvalue analysis of Olympeion's column in order to obtain the natural periods equal to the estimated ones by the microtremor analysis (See Table 1). Using the estimated value of α, K_R at drum's interface of Parthenon were evaluated. Furthermore, the translational spring constant K_H was evaluated from the elastic deformation characteristics of the drum. The eigenvalue analysis using these parameters provided the natural periods of the column, as shown in Table 2. The columns have the fundamental periods longer than the predominant period of the anticipated ground motions. This results may explain that, although the recent earthquake was reported to cause the slight translational displacement at the drums' interfaces, the earthquake which hit Athens did not destroy the columns due to overturning. As results of the linear response analysis utilizing the assumed MDOF systems to the synthetic ground motions for return periods of 100 and 1000 years, the distributions of the maximum response accelerations along the height of the columns are presented in Fig.8. The shear coefficient of Model (C) attains rather high values compared to those obtained by the other models. In the case when the shear keys at the interfaces between drums of the column without any member on its capital have already weathered and they can not resist seismic loads, translational displacements may occur due to earthquake motions. This result is consistent to the fact that the differential displacements were caused by the 1981, Corinth Earthquake at the drum's interfaces of some columns.

3.4 Non-linear response analysis

A lumped mass system with only a translational degree of freedom at each drum's interface was introduced. The spring constants were determined so that the natural periods and modal shapes of the column should coincide with those of the model of the linear response analysis. To represent non-linear characteristics, bi-linear type of load-displacement relationship shown in Fig.9 was assumed. The non-linear response analysis was carried out for the Model (C) under the condition that the effect of the shear key was not taken into account due to weathering (Case 1) and that the shear keys made of titanium alloy was replaced to strengthen the columns (Case 2). The resulted distributions of the maximum shear coefficients shown in Fig.10 indicates that the shear keys can undertake the excess seismic loads, and that the overloading beyond the critical friction resistance will occur for the column without shear keys. The effect of the shear keys on the aseismic retrofitting will be investigated in the following chapter.

4. STATIC SHEAR TESTS ON MODEL MARBLE COLUMNS FOR ASEISMIC RETROFITTING

4.1 General

The static shear friction tests among the marble drums were conducted to understand their behavior when the drums undertake the seismic translational loads, and to investigate the effects of shear keys designed for the aseismic retrofitting. The tests were explained by the authors in reference [9].
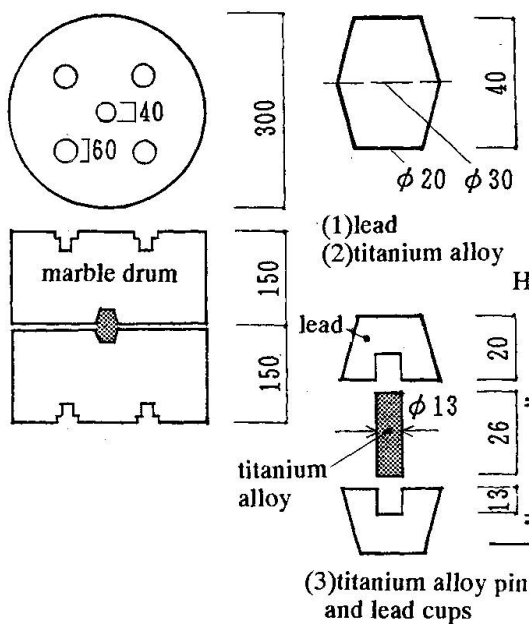
(1)lead
(2)titanium alloy

marble drum

lead

titanium
alloy

(3)titanium alloy pin
and lead cups

Fig.11 Model marble drums and shear keys
for the static shear tests

Steel plate   500   Translational load
            Normal load
                                          H-shaped beam
Hydraulic cylinder
Load transducer   Specimen
Displacement transducer
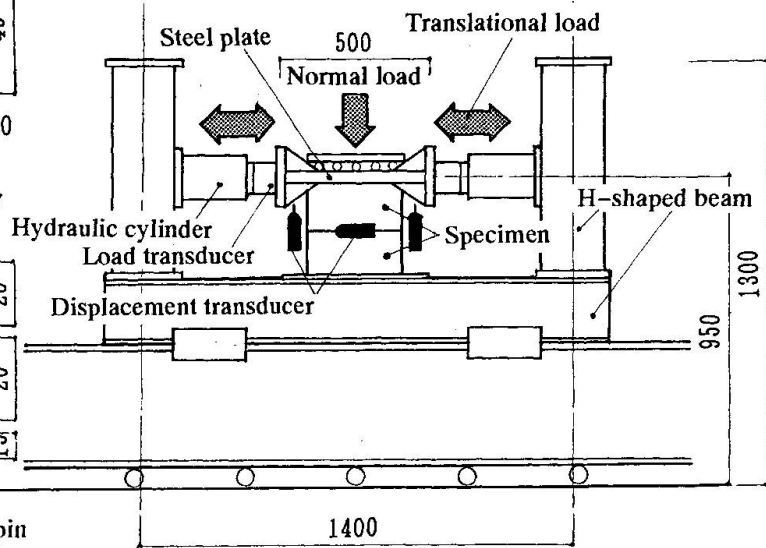
Fig.12 Apparatus for the static shear tests

titanium alloy shear key
lead shear key
without shear key

N=1060kgf
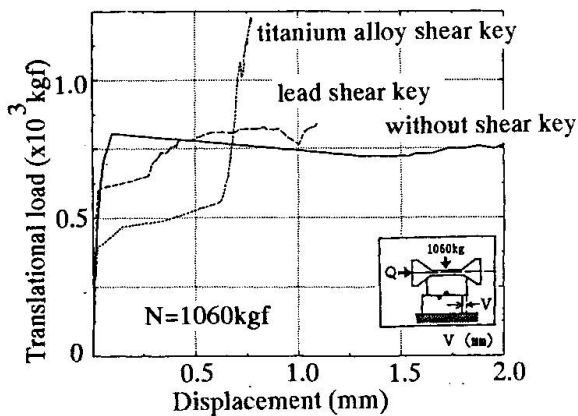
Fig.13 Load–displacement relationship of the
monotonic loading tests of the drums
with lead shear key, with titanium shear
key, and without shear key

shear key composed of titanium
alloy pin and lead cups

N=1060kgf
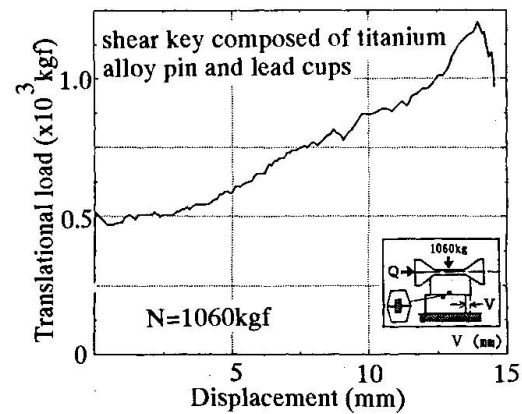
Fig.14 Load–displacement relationship of the
monotonic loading tests of the drums
with shear key composed of titanium
pin and lead cups
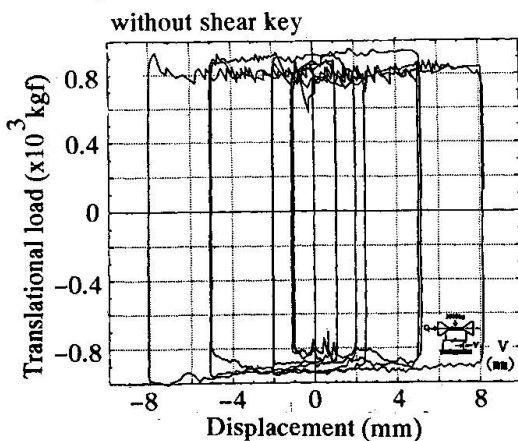
without shear key

Fig.15 Behavior of interface without shear key
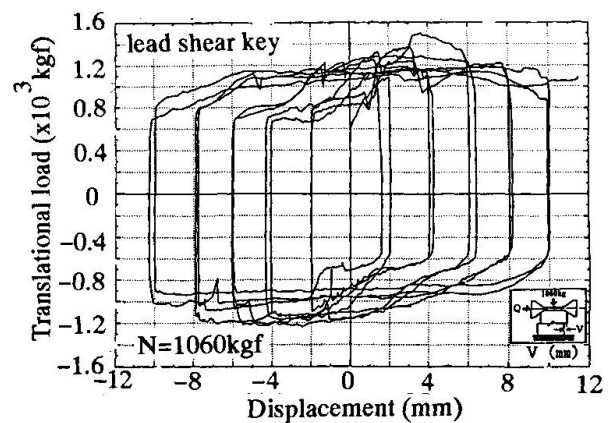under cyclic loading

lead shear key

N=1060kgf

Fig.16 Behavior of interface with lead shear key
under cyclic loading

4.2 Test materials and procedure

The cylindric marble drum, a one-sixth scale model of Parthenon column, was used, and the three types of shear keys were examined in this experimental study (See Fig.11). Fig.12 shows an apparatus for the simple static shear tests.

4.3 Experimental results

The load-displacement relationships of the one-way monotonic loading tests and of the cyclic loading tests are described in Fig. 13, 14 and in Fig. 15, 16, respectively. These figures demonstrate that the shear keys undertake the loads beyond the critical friction resistance (friction yielding), and that the load-displacement relationship after the friction yielding were affected by the material properties and structures of the shear keys. The experimental results indicate that the shear keys such as the one composed of titanium alloy pin and lead
cups, proposed in this study, have the effect on increase of the earthquake resistant capacity.

5. CONCLUSIONS

Parthenon's behavior under seismic actions for 25 centuries has been satisfactory due to its excellent design and due to the characteristics of the earthquake ground motions. However, when the shear keys among the drums lose their function due to weathering, the seismic loads may cause damage to the columns. Replacing the old shear keys by the new ones are suggested to be adopted for the aseismic retrofitting. Future study will be needed on the overturning behavior of this structure under strong ground motions.

ACKNOWLEDGMENTS

REFERENCES

1. Theofanopoulos, N., Input Earthquake Motions for the Response Analysis of Various Important Structures, Doctor Thesis, UniversityofTokyo Metropolitan, 1989.
2. Theofanopoulos, N., Hanazato,T. and Watabe, M., Probabilistic Approach to Generate the Reference Motion for the Protection of Historical Monuments against Earthquakes, Proc. of 1st International Conferenceon Structural Studies, Repairs and Maintenance of Historical Buildings (STREMA89), pp.289-298, 1989.
3. Kawashima, K. et al., Attenuation of Peak Ground Motions and Absolute Acceleration Response Spectra, Proc. of 8th WCEE, Vol.II, pp.257- 264, 1984
4. Itoh, T. et al., Development of Seismic Hazard Analysis in Japan, Trans. of 9th SMiRT, Vol. K1, pp.69-74,1987.
5. Theofanopoulos, N., Watabe, M. and Matsukawa, K., Strong Motion Duration and Intensity Function, Proc. of 9th SMiRT, Vol. K1, pp.31-36, 1987
6. Hanazato, T., Theofanopoulos, N. and Watabe, M., Seismic Response Analysis of Parthenon Columns, Proc. of STREMA89, pp.339-348, 1989.
7. Theofanopoulos, N., Hanazato, T., Matsukawa, K. and Watabe, M., Analysis of Microtremor Recordsat Zeus-Olympeion Athens and Assessment of its Safety by Employing Dynamic Response Analysis, Proc. of STREMA89, pp.319-328, 1989
8. Penrose, C. K., An Investigation of the Principles of Athenian Architecture, Mc Growth Publishing Company, Washington D.C., 1973.
9. Mabuchi, Y., Hanazato, T. and Watabe, M., Static Shear Friction Tests on the Model Marble Columns of Parthenon for the Aseismic Retrofitting, Proc. of STREMA93, (submitted), 1993.

Limit Analysis of Block Masonry Shell Structures

Analyse limite des dôme en pierres de taille

Grenzwertanalyse von Gewölbestrukturen aus Quadersteinen

Piero D'ASDIA
Assoc. Professor
Univ. of Rome 'La Sapienza'
Rome, Italy

P. D'Asdia, born 1946, got his civil eng. degree in 1971 at the Univ. of Rome 'La Sapienza', where he worked as a researcher. In 1980, he became assist. prof. and is now assoc. prof. Since 1971, he has been involved in research in several fields of structural engineering.

Dina D'AYALA
PhD Student
Univ. of Rome 'La Sapienza'
Rome, Italy
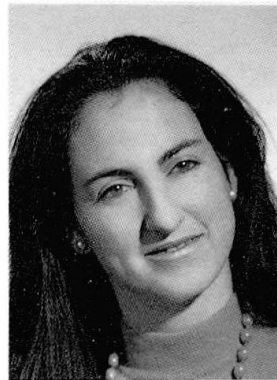
D. D'Ayala, born1962, graduated in civil engineering at 'La Sapienza' in 1988. She is now working on a PhD at the Structural Engineering Dep. and part of it has been spent at the Cambridge Univ. Engineering Dept. She has been involved in a number of restoration projects.

SUMMARY

The paper presents the limit-state analysis of three-dimensional masonry structures with special interest focusing on domes. A lower bound approach using linear programming techniques has been developed and improved with respect to the 'simplex method' formulation. The duality theorem and an algorithm have been applied to handle three-dimensional mechanisms resulting from sliding and rotating, or both, at the blocks interface. The results are compared with those obtained from experimental work carried out on a masonry dome model in order to study the crack pattern.

RÉSUMÉ

Ce document décrit l'analyse limite de structures tridimensionnelles en maçonnerie, en particulier des dômes. On a développé une méthode statique avec des techniques de programmation linéaire qui a été améliorée concernant la formulation du 'simplex method'. Le théorème de la dualité et un algorithme ont été adoptés pour traiter les mécanismes tridimensionnels résultant de combinaisons de glissements et rotations à l'interface des blocs. Les résultats ont été comparés avec ceux d'essais réalisés sur un modèle de dôme, afin d'étudier le modèle de rupture de ce type de structure.

ZUSAMMENFASSUNG

Dieser Beitrag beschreibt die Grenzwertanalyse dreidimensionaler Mauerwerkstrukturen, insbesondere Kuppeln. Eine statische Methode wurde mit linearer Programmierungstechnik entwickelt und in bezug auf die Formulierung der Simplex-Methode verbessert. Unter Verwendung des Dualitätstheorems wurde ein Algorithmus entwickelt, um die dreidimensionalen Mechanismen zu behandeln, die durch Gleiten und Rotation oder beides kombiniert an der Innenflächen der Quadersteine entstehen. Die gewonnenen Erkenntnisse werden mit denjenigen aus Experimenten an einem Gewölbemodell verglichen, um das Bruchverhalten dieser Strukturen zu untersuchen.

1. INTRODUCTION

The limit-state analysis method was first applied to the collapse analysis of masonry structures by Heyman [1] [2]. The scheme for the material consist of rigid blocks and joints incapable of carrying tension stress, with friction coefficients high enough to prevent sliding. Subsequently Livesley [3] developed a numerical procedure for the analysis of plane single span arches with in-plane loading, which he recently extended to multi-span arch structures, considering both hinging and sliding [4].

The more recent applications directly involved in the masonry dome analysis have followed two different approaches: the one mentioned above and the finite-element method, which considers the structure in either its uncracked or cracked state. The works of Bridle-Hughes [5] are based on the first approach and propose an energy method in which the arch geometry and stiffness are modified according to the fracture evolution; Oppenehim et al. [6] also deals with an analytical approach that leads to a closed form solution of the fundamental differential equilibrium equations in the case of axisymmetric loads under the assumption of zero hoop stress. This greatly simplifies the problem reducing it to a monodimensional case. The assumption is correct for the lower part of the dome, but not for the upper part, this being more extensive as the ratio between rise and span of the dome is bigger, therefore it can be assumed to be within the lower bound of the possible solutions.

The necessity of the solution of a full three-dimensional problem is first assessed by Melbourne [7] in 1991. He isolates the barrel vaults that constitute the structure of masonry bridges in order to define through a number of experimental test the collapse mechanism due to variable restraint conditions along the abutments and non symmetric loads.

The limit-state analysis therefore appears as a fundamental tool for the assessment of the safety levels of such structures, and in the following sections a fully three-dimensional analytical method is presented.

2. DEFINITION OF CONSTITUTIVE LAWS

The Coulomb failure criteria is assumed to rule the mechanical behaviour of a structure of material whose tensile imaginary strength is due to friction. The criteria states that there will be sliding in every point of the material where the applied shear (τ) overcomes the friction strength (defined by the coeff. μ and cohesion c_o). It also states that the two sides of the sliding surface will separate if compressive stress (σ) is not applied on the surface:

$$\tau \leq c_o + \mu \sigma \tag{1}$$

In the block-work masonry sliding movements can occur at the joint surfaces only, and therefore the sliding layers are a known of the problem; other possible mechanisms are rotations around axes parallel or orthogonal to the sliding surface, or around an edge or a vertex of the block, or a superposition of any of these primary mechanisms.

The choice of whether the contact surfaces should be thought slightly convex or concave (i.e. 1 point or 4 points contact in space; 1 or 2 in the plane), does not affects the collapse load factor in two-dimensional problems, but is fundamental when the kinematic chain and the applied action that produces it are not in the same plane. The hypothesis of a convex surface (a simple contact point) that is usually assumed in two-dimensional problems, no longer applies here; actually with this type of surface the collapse load factor will be always zero, unless it is somehow coupled with an additional torsional constraint. It is therefore evident that in those cases the contact should be realised on a concave surface, that can eventually degenerate in a line or a point. The least number of nodes are then 3, if the surface is flat, and 4 in the case that a finite curvature is present. In each of these points orthogonal and tangential stresses develop, the tangential ones oriented in any direction but retaining equilibrium.

Because in real structures blocks are quadrangular parallelepipeds and the contact surfaces will not in general be flat, the present formulation is written for a 4 contact points with normal to the surface not necessarily parallels.

For structures with simple curvature Livesley [4] showed how the elimination of one of the contact points only slightly reduces the collapse load factor while it does not affect the mechanism, so that the contact surface can be well enough approximated by a plane. The same cannot be said for double curvature structures, as will be shown later, this involving a strong constraint for the collapse thrust surfaces.

Taking the centre of gravity as origin of the coordinates, in the case of contact along only one direction and assuming the block has not curvature of its own, the equilibrium equations and the constraint expressions for a single block, are as follows:

$$\mathbf{H\,r = p} \tag{2}$$

$$\sqrt{t_i^2 + s_i^2} \leq c_0 + \mu q_i \qquad\qquad i = 1,4$$

where : **r** is a vector whose elements are s, t, q (generalised stresses),
   H is a matrix of linear geometrical relations,
   p is the vector of dead and live loads

In the case of a single block the matrix **H** is a 6 x 12 (3 generalised stress components for each contact point) for one contact surface only, 6 x 24 if the contact surfaces are two.
The constraints in (2), which are quadratic, represents a conical limit surfaces with vertex **q** = 0 and circular section on the plane s-t.

3. OUTLINES OF THE PROPOSED METHOD

To be able to formulate an algorithm in linear programming terms the constraints (2) have to be linearised, i.e. the conic surface has to be approximated by a pyramid. Different approximating polygonals on the plane s-t are proposed in literature, from a minimum of 3 edges to a maximum of 12. In the present case an 8 edges polygonal has been chosen, obtained by introducing two auxiliary variables, u and v, in order to define the two directions at an angle of 45° with respect to s and t, and 8 new constrained variables ω_i (while s, t, u, v are unconstrained), one for each orientation of the four primary directions.
With the introduction of these new variables, the dimension of the global system becomes 46 x 52 for each contact surface. The system has 6 redundant variables.
The position of the optimisation problem takes then the canonic form:

$$\max \{ \lambda \; : \; \lambda\,\mathbf{p} + \mathbf{w} = \mathbf{H\,r} , \; -\mathbf{r}_L \leq \mathbf{r}^- , \; \mathbf{r}^+ \leq \mathbf{r}_U \} \tag{3}$$

The linear programming algorithm used works extracting the maximum rank sub-matrix of the system, choosing the variable to be maximised in relation with the correspondent known vector and the active constraints, computing the increment in the load factor associated with the maximisation of the variable, and then operating a substitution between the column of this variable and one, appropriately chosen, external of the present sub-matrix.
The first problem that arises in a limit-state analysis approach is the fact that the normality rule does not apply when sliding is involved, because the generalised stress limit surface and the generalised strain limit surface do not coincide: the first one is a cone and the limit value of the shear linearly depends on the normal stress, while the corresponding sliding of the associate mechanism will take place without any change in volume. Alternatively applying the normality rule to the conical limit surface, the generalised strain vector ε_{pl}, assumed to be normal to it, will show a component along the q direction that implies separation of the facing nodes; but this is not possible if $q \neq 0$.
The numerical methods and their optimising strategies can be different according to the object and size of the analytical problem. It is worthwhile noting that the adopted algorithm, a series of Gauss-Jordan reductions, with forward and backward substitutions, has the advantage of operating only on the meaningful portion of the matrix (all the equations but only the primary variables, so that the matrix to be stored is a 46 x 12 instead of 46 x 52 for each block) and of exploiting the dual nature of the problem so as to obtain from the same solution the collapse load factor and the associated mechanism. The back substitution is actually carried out at the end of the forward process to obtain the sliding displacement component, associated with the variables s, t, u, v that are unconstrained, as independent from q and therefore observing the normality rule.

4. APPLICATION TO SHELLS AND DOMES

Two versions, applicable to structure of double curvature will be proposed: the first aims to define the collapse of the material medium from a local approach, the second is intended to

define the collapse load factor on a global scale. In the former the equations are written for the individual block constituting the masonry work. Each block is in contact with 6 adjacent ones and, if each interface is defined by 4 contact points, the number of generalised primary stresses will be 6 x 4 x 3 = 72. Some of the points (vertices of the block), being common to two normal surfaces, can be regarded as a single one with six applied generalised stress components, fig. 1. The middle points, related with the staggering, can be thought as common to the considered block and the two above and below, fig. 2, so to have a single node. In this way the increment in matrix dimension is only due to the increased number of stresses in each node, while the bandwidth of the matrix is considerably increased according to the complex contact scheme. Therefore the coefficient matrix **H** of the equilibrium equations takes a three-diagonal form, while the limit constraints duplicate to take into account the friction constraint onto the parallel surface of the block as well as onto the meridian ones.

As far as the equilibrium equations are concerned, dimensions of each block matrix are 6 x 24, plus 80 equations for the auxiliary constraints. As it can be seen, the size of the problem quickly increases even if a limited number of elements are treated (i.e. hundreds in order to simulate a part of a real structure), CPU time growing with the power of 2 of the matrix dimension.

In order to reduce the problem dimensions, a simplification can be introduced by extending the shear reciprocity rule ($t_{12} = t_{21}$) to the plastic field; it is worthwhile noticing that this assumption provides approximated values, on the conservative side, of the collapse load factor λ.

If no external load is applied to the block, the equilibrium equation along the direction tangent to a generic parallel becomes :

$$\frac{\partial(t_{12}R_2\sin\varphi)}{\partial\varphi} + R_1\frac{\partial q_2}{\partial\vartheta} - t_{21}R_1\cos\varphi = 0 \qquad (3)$$

being R_1 and R_2 the two local radii of curvature, φ and θ the spherical coordinates. If $q_2 = 0$ then also $t_{21} \leq c_o$ because of the friction relation, and locally approximating the surface with a sphere:

$$t_{12}(R_2\cos\varphi - R_1\cos\varphi) + \frac{\partial t_{12}}{\partial\varphi} = 0 \qquad (4)$$

The first element is 0 and thus the variation of t_{12} along the meridian.

The simplification $t_{12} = t_{21}$ therefore reduces of 1 the number of variables. The other assumption is that, the flexural stiffness along the parallel being much greater than the one along the meridian, generalised stress s normal to the surface will develop only on the parallel faces of the element (of normal q_1) while their variation along the meridian line is equilibrated by the normal component of q_2. This reduces the number of generalised stresses for each node to 4 and only one conical surface is needed for the constraints, checking the t variable as function of the lesser between q_1 and q_2, so that the block matrix is 46 x 16.

This formulation has been used to study the local behaviour and collapse mechanism of 1/8 of the experimental dome for an outward horizontal displacement. The result has also been compared with the one obtained for a spherical dome (fig. 3).

It is evident that the present formulation is not only unsuitable for analysing global mechanisms but is also unnecessary at the global scale. Therefore a slightly different algorithm has been prepared that derives from the observation of the most common structural layout and associated failure patterns of domes. The shell may be divided into not less than 8 slices with straight sliding surfaces along a discrete number of meridian and parallel curves, fig. 4. The meridian surfaces represent the meridian cracks, while the parallels are the lines where an hinge along the meridian arch is most likely to occur.

In this way the entire structure can be modelled with a small number of macro-elements. For each one of these the equilibrium equations must take into account the relation between q_1 and q_2 due to the finite double curvature of the element and the discontinuity conditions at the sliding interfaces. Equilibrium equations are as follows:

$$2\pi R_2 q_1(\sin\varphi)^2 + 2\pi R_2 s \cdot \sin\varphi \cdot \cos\varphi = \gamma \int 2\pi R_2\sin\varphi \cdot d\varphi$$

$$R_2q_1(\sin\varphi) + R_1q_2(\sin\varphi) + \frac{\partial(R_2 s \cdot \sin\varphi)}{\partial\varphi} = \gamma R_2 R_1 \sin\varphi \cdot \cos\varphi \tag{5}$$

$$\frac{\partial(R_2 q_1 \sin\varphi)}{\partial\varphi} - R_1 q_2 (\cos\varphi) - R_2 t \cdot \sin\varphi = \gamma R_2 R_1 (\sin\varphi)^2$$

While the discontinuity condition for a material (with φ = polar coordinate in the vertical plane and $\alpha = \pi/2 - \varphi$) are:

$$q_n = \frac{q_1 + q_2}{2} - \frac{3}{2}[(q_1 - q_2)\sin\alpha] \qquad n = 1, 2$$

$$\tag{6}$$

$$\tau = \sqrt{s^2 + t^2} = \frac{(q_1 - q_2)\cos\alpha}{2}$$

The equilibrium differential equations can not straight be integrated and linearised in the general form. Once a curve has been chosen to approximate the real curve that generate the dome, however, is then possible to define an analytical expression for R_1 and R_2 and therefore the equation that represents the curve can be written in the Hessian normal form choosing φ as the parameter. Substituting these in the system (5) and applying the hypothesis of a uniform stress state in the block when the ultimate state is reached, leads now to linearised equations. The method has been applied to structure whose approximating curve are sections of circles, cycloids and ellipses.

Load factor and collapse mechanism, for a given c_0 and μ, depend on several parameter as: radius, variable thickness, ratio between rise and span of the generating curve, and relative position of the discontinuity surfaces.

As it can be seen from fig. 5, where the relation between the load factor and one of these parameters has been drawn, normalising the load factor value with respect to the dead load value, the relation is not monotone but reaches in general a maximum for a certain value and then decrease exponentially for the others. This depends on the fact that the geometrical parameters are not independent.

Other peculiar characteristic of dome structure is the fact that, the behaviour being mainly ruled by the shear strength, the mechanism shows an antisymmetric pattern even if the action is symmetric. More in general once the first crack has open the symmetry is lost and the final collapse mechanism evolves toward an highly non symmetric pattern.
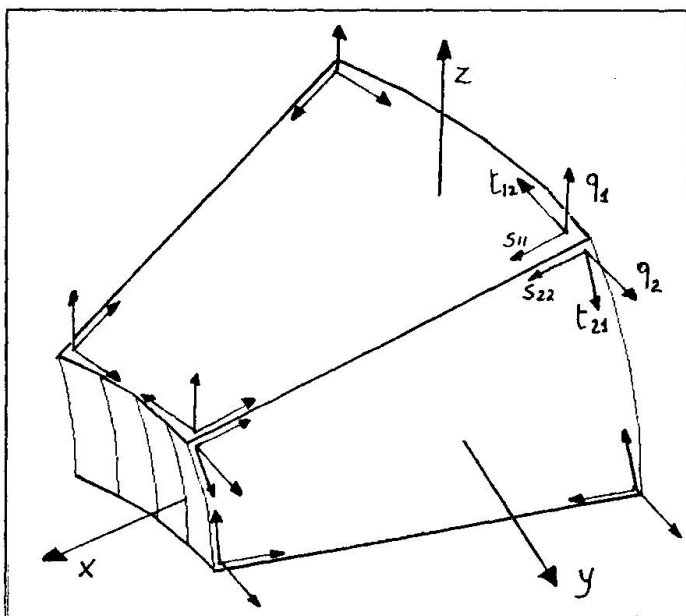

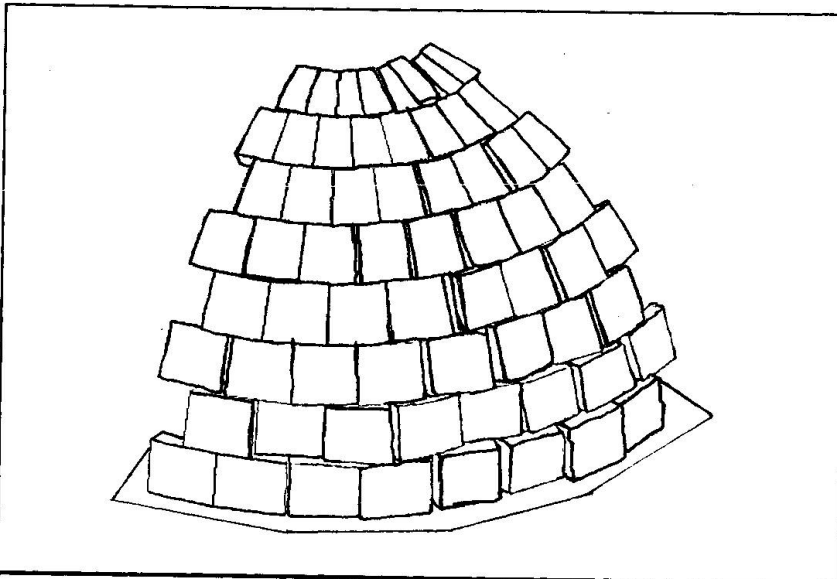fig. 1 - Coordinate system and generalised nodal stresses for a block

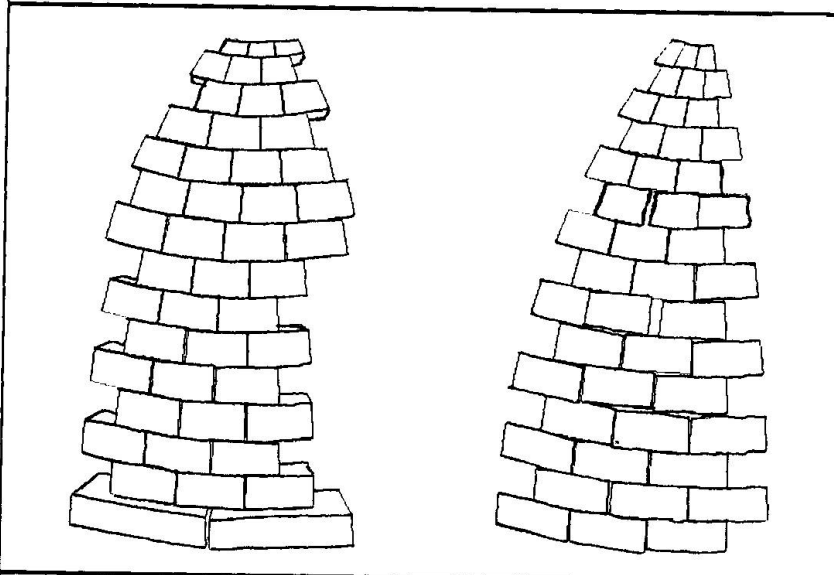fig.2-A 90° sector of a spherical dome subjected to horizontal outward action on the second row

fig. 3 - Collapse mechanism for a 45° sector of the experimental dome ($\lambda = 0.55$) and of a spherical dome ($\lambda = 0.325$) for outward horizontal sliding of the base
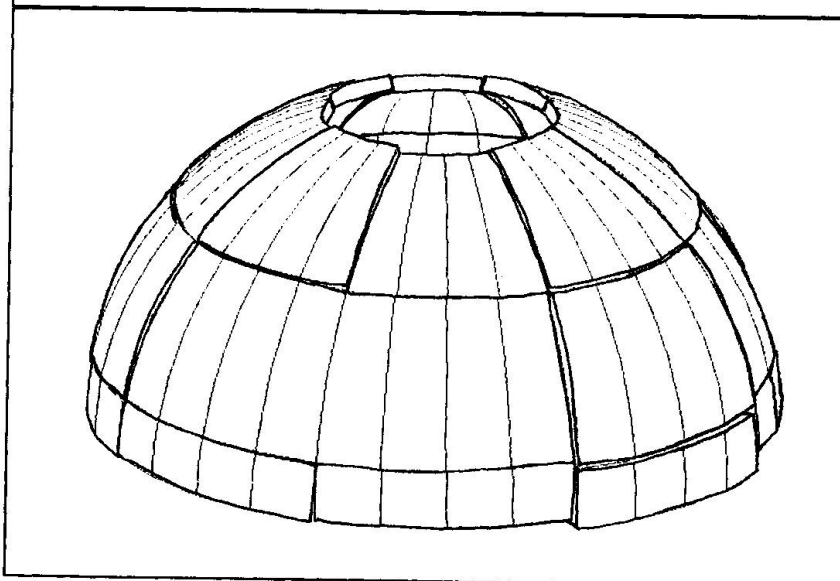
fig.4 - Global collapse mechanism for a spherical dome with hinges positioned at 45° and 80° for the settlement of one basis.

5. CONCLUSIONS

The analytical method described above is part of a Ph.D. research program which also investigates the behaviour of masonry domes affected by foundation movements, through laboratory testing. For this purpose a model dome (fig. 6) has been built in the Laboratory of the Cambridge University Engineering Department, U.K. [8]. One of the most interesting tests involves the sliding out of one or two of the sectors of the base ring which simulate the lower structure. The change in shape of the dome and the relative movement between blocks are recorded by means of special transducers. Results show that the damping behaviour for elastic shells still applies, even if the thickness cannot be thought of as significantly smaller than the radius (fig. 7). Therefore the crack pattern only develops in a region close to the point of application of the action. When the action is further increased, the crack pattern tends to extend and flow in the one caused by an upper load, simulating the lantern effect, and a series of local hinging mecanisms take place at the single block level (fig. 8). The load factor has been deduced from the decrease in the level of bearing capacity of the dome (for the upper imposed load) when the base is moved out. The values and shape of the mechanism show good correspondence with the results obtained by the analytical model in fig. 4.

6. REFERENCES

[1] HEYMAN J., "On shell solution for masonry domes" - Int. J. Solid Struct. 3, 1967.
[2] HEYMAN J., "Equilibrium of shell structures" - Oxford Engineering Science Series - 1977.
[3] LIVESLEY R.K., "Limit analysis of structures formed from rigid blocks" - Int. Journ. for Numer. Methods in Engineering - 12 1978
[4] LIVESLEY R.K., A Computational Model for the Limit Analysis of Three-Dimensional Masonry Structures, Meccanica 27-3,1992
[5] BRIDLE R.J., HUGHES T.G., An energy method for arch bridge analysis, Proc. Inst. of Civ. Engrs., Part 2, 89, 1990
[6] OPPENHEIM I.J., GUNARATMAN D.J.,ALLEN R.H., "Limit State Analysis of Masonry Domes", J. of Structural Engineering ASCE n.4 april 1989
[7]MELBOURNE C., The Assessment of Masonry Arch Bridges, 9th International Brick/Block Masonry Conference, Berlin 1991
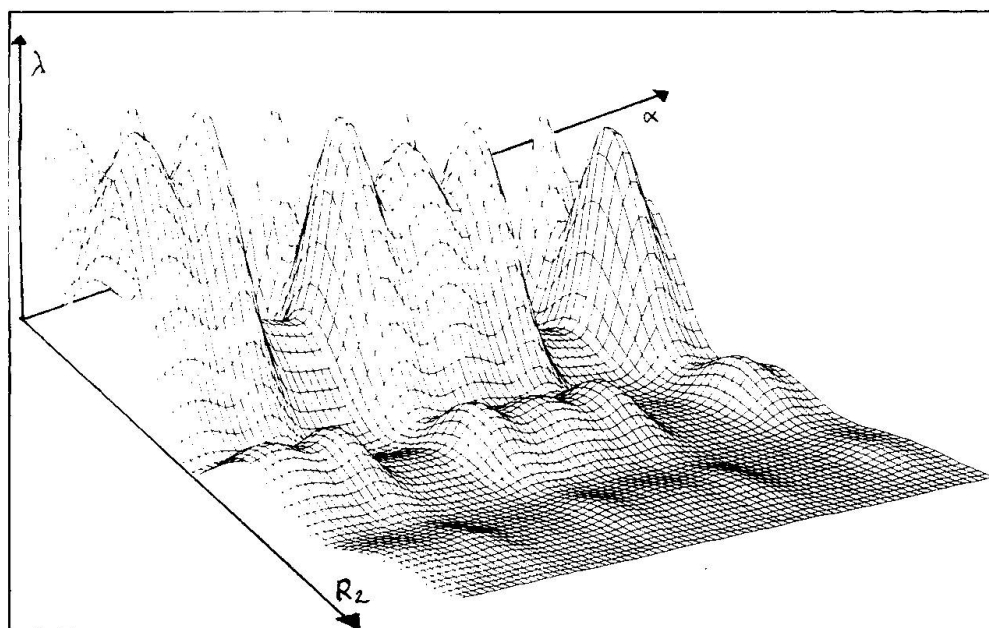

fig.5 -
Load factor variation
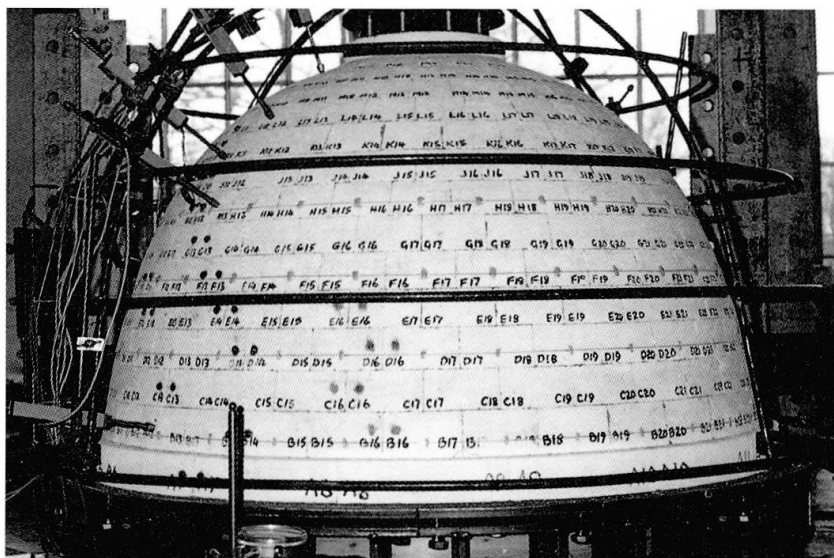for different dimension
of the base blocks

fig.6- The model dome is realised with 380 small concret blocks casted in situ. To simulate the friction caractheristiques of the stone sandpaper has been interposed between surfaces.
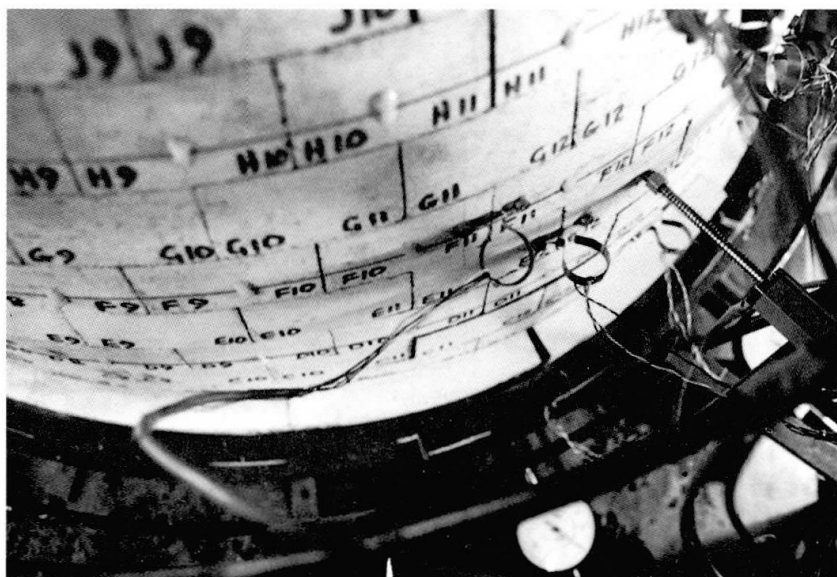

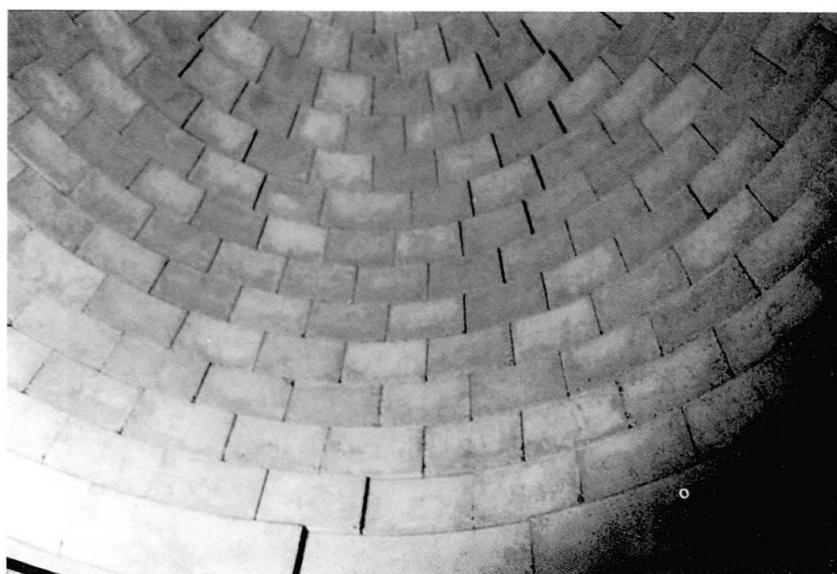fig. 7 - Crack pattern for outward horizontal sliding of the base

fig.8 - An inside view of the collapse mechanism.

Dynamic Response of Models Subjected to Horizontal Motions

Comportement dynamique de modèles soumis à des forces horizontales

Dynamisches Verhalten von Modellen unter horizontaler Anregung

Milton DEMOSTENOUS
Civil Engineer
Aristotle University
Thessaloniki, Greece

M. Demosthenous, born in 1962, got his Civil Eng.degree and post-graduate studies (1988 - 1993) at the Univ. of Thessaloniki. He has five years experience with the Earhquake simulator facility and elastic and inelastic analysis of structures.

George C. MANOS
Assoc. Professor
Aristotle University
Thessaloniki, Greece

G. C. Manos, born 1948, got his Civil Eng. degree at the Univ. of Thessaloniki and PhD at the Univ. of Durham, UK. He is Assoc. Professor at the Univ. of Thessaloniki and Director of the Inst. of Engineering Seismology and Earthquake Engineering (ITSDAK).

SUMMARY

This paper presents predominant modes of response shown by ancient monuments in Greece that can lead to damage during strong earthquakes. Observations from an experimental and analytical investigation of the seismic behaviour of model ancient columns are also presented, utilising the Earthquake Simulator of Aristotle Univ. of Thessaloniki.

RÉSUMÉ

Cette étude présente les modes de réaction prédominants de monuments de la Grèce antique, face à des tremblements de terre de grande intensité, pouvant conduire à des dommages. Des observations provenant d'une étude expérimentale et analytique du comportement séismique de modèles de colonnes anciennes sont aussi présentées. Ces observations sont basées sur l'utilisation du simulateur de tremblements de terre de l'Université Aristote de Thessalonique.

ZUSAMMENFASSUNG

In der vorliegenden Arbeit werden die wichtigsten Verhaltenscharakteristiken antiker Monumente in Griechenland gezeigt, die nach starken Erdbebenbeanspruchungen zu erheblichen Tragfähigkeitsverlusten führen können. Weiterhin werden Ergebnisse experimenteller Untersuchungen an charakteristischen antiken Säulen gezeigt, die in der Erdbebensimulationsanlage der Aristoteles-Universität Thessaloniki gewonnen worden sind. Diese Ergebnisse werden mit denjenigen numerischer Untersuchungen verglichen.

1. EARTHQUAKE DAMAGE TO ANCIENT MONUMENTS.

Ancient Greek and Roman type structures composed of large heavy members that simply lie on top of each other in a perfect fit construction without the use of connecting mortar type materials are distinctly different from relatively flexible contemporary structures. The material used for the formation of ancient columns was usually limestone or marble of an average bulk density 2.7 t/ m^3. For rough contact surfaces peak values of the angle of static friction are approximately 35^0 to 40^0. However, drums were caused to revolve around a central pivot until, by the addition of sand inserted for the purpose, they rested, with no overlap whatsoever, on the drum beneath in which case the angle of static friction would have been reduced to about 28^0 to 35^0.

For the monuments of Ancient Greek or Roman type, discussed in this paper, an earthquake may bring about the damage or collapse of the relatively rigid, freestanding columns in one (or a combination) of the following ways:

1) By causing the column to slide off its base or at joints higher up between drums (fig. 1).
2) By setting the column to large amplitude rocking response resulting in overturning (fig. 2).
3) By progressively inducing excessive permanent tilting of its foundation (fig. 3).
4) By causing drums of weak or damaged stone material to fail in compression.
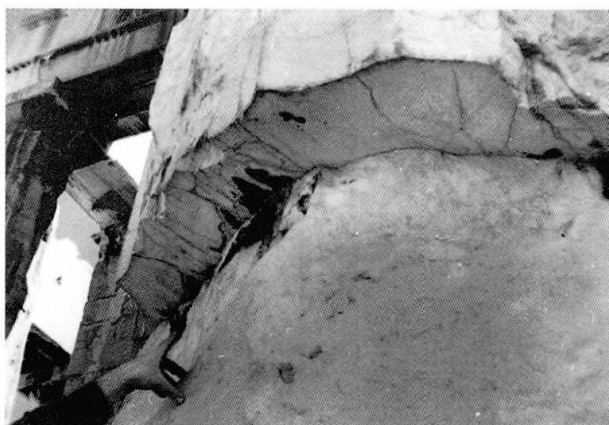

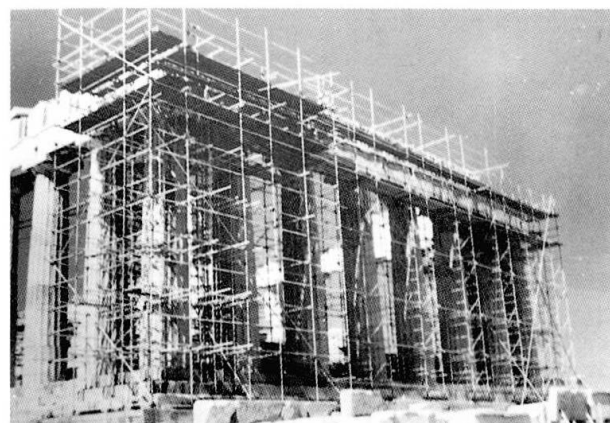
Fig. 1 Drums showing a sliding response.

Fig. 3 The NE side of Parthenon after the EQ of 1981.

Fig. 2 Overturned monolithic column.

Fig. 4 The ancient city of Philippi, Macedonia - Greece.

Apart from the partial damage resulting from the earthquake response of the main supporting elements (columns or colonnades) listed above, the cumulative damage of such elements in large numbers led to the partial or total destruction of urban centers which had structural forms of this type. The destruction of cities, reported by ancient historians due to strong earthquake motions such as the ancient city of Sparti (464 B.C.), the city of Eliki (373 B.C.) , the city of Philippi at Macedonia in Greece (597 A.D.) (fig. 4) [1] can be seen as happening in the way described above.

The scientific and engineering achievements of this century have also been spreading slowly to the field of the seismic response of historical monuments due to the necessity of repair and preservation of these cultural landmarks for human civilization. The inherent structural complexity and the variability of building and foundation materials, makes each historical monument a unique case for study requiring special consideration. Because of this, rational proposals for the repair of such monuments need special attention and utilisation of the most advanced techniques in the field of engineering, and in depth knowledge of certain aspects of earthquake engineering in particular. The experimental investigation discussed in what follows, which employs advanced dynamic excitation techniques and measurement media, can be classified as one of the advanced tools available today in the engineering community. The results of such an investigation can be utilised in the repair effort of ancient monuments of the Greek and Roman type shown in the photographs of this paper.

2. AN EXPERIMENTAL INVESTIGATION INTO THE EARTHQUAKE RESPONSE OF MODELS OF ANCIENT COLUMNS.

The seismic response mechanisms that develop on this solid-block structural system during strong ground motions can include sliding and rocking, thus dissipating the seismic energy in a different way from that of conventional contemporary buildings. The seismic behaviour of this type of structure (ancient Greek and Roman monuments) or of their components can be investigated by studying the earthquake response of solid or sliced rigid bodies during simulated base motions.

The present study deals with the dynamic response of three different geometries of solid or sliced rigid - block type bodies (fig. 5). The solid and sliced specimens are either square prisms, cylinders or truncate cones and are assumed to represent models of prototype structures 20 times larger. Two basic categories of practically non-deformable bodies were studied. The first one deals with whole solid bodies of certain geometry whereas the second category includes non-deformable bodies of the same geometry but this time these bodies are formed with slices that lie on top of each other without any connecting material. The tests performed include sinusoidal sweep tests within a chosen range of frequencies and amplitude as well as earthquake simulated tests using the El Centro 1940 record as will be explained below.
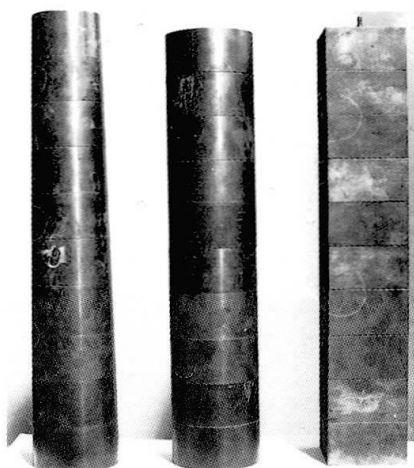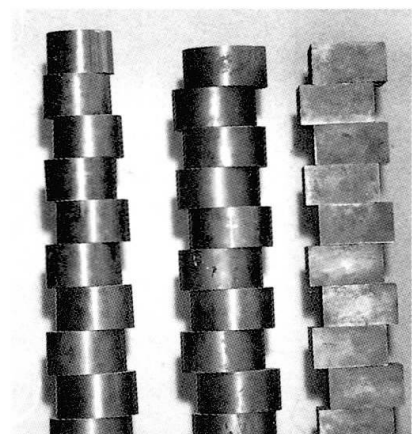

Fig. 5. Solid and sliced rigid bodies

The behaviour of solid-block structures supported on either rigid or flexible foundation, when subjected to earthquake ground motions, has been researched for quite sometime. Housner (1963) investigated the dynamics of a solid block on a rigid base, Aslam et.al. (1980) investigated the sliding and rocking response of solid rectangular concrete blocks on the earthquake simulator facility of the University of California at Berkeley, Priestley et.al. (1978) has dealt with the problem in a way that also included experiments with a shaking table. Yim et.al. (1984), Spanos et.al. (1984), Oppenheim et.al. (1986) and Koh et al. (1990) have also been investigating this problem treating it with various analytical approaches. Ishiyama has also studied this problem and among other things gives a comprehensive survey of the rigid-block research (1980).

2.1. Behaviour of solid bodies.

2.1.1 Preliminary free vibration test

Free vibration tests were performed for the solid specimens with the aim of assessing the coefficient of restitution of the test structures. Figures 6a, 6b and 6c depict with a solid line the rocking angle response for each specimen. Superimposed on each graph is a dashed line curve that corresponds to a predicted rocking response with a coefficient of restitution that gave the best fit to the experimental measurements.

The predicted rocking response was derived from the linearised equations of motion (Aslam et al. 1980). Whereas there is good correlation between predicted and observed rocking response for the prismatic specimen certain discrepancies are apparent at the initial large amplitude rocking stages for the cylindrical and conic specimens. As was also stated by Koh (1990) this must be attributed to 3-D rocking, since rocking in a perfect plane for a 3-D model requires exacting initial conditions and the slightest out of plane disturbance will cause rocking to be three dimensional.
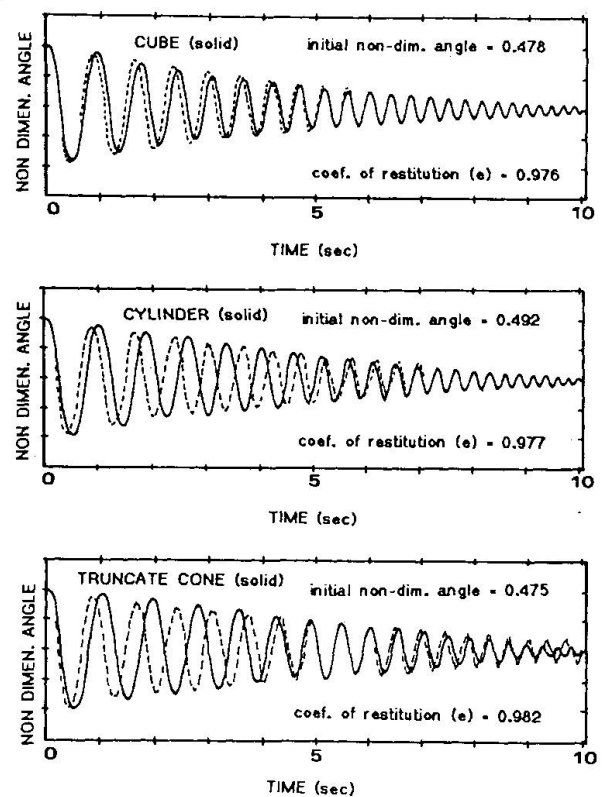

Fig. 6. Free vibration response

2.1.2 Sinusoidal tests for the solid specimens.

During these tests the frequency of motion was varied from 1Hz to 7Hz, in steps of 1Hz. This resulted in groups of tests with constant frequency for the horizontal sinusoidal motion for each test. In the various tests belonging to the same group of constant frequency, the amplitude of the excitation was varied progressively from test to test. The above stages are graphically portrayed in the plot of figure 7. The ordinates in this plot represent the non-dimensional amplitude of the base motion whereas the absiscae represent the non-dimensional frequency given by the following formulae :

$$A \quad = \quad x/(\theta * g), \qquad \Omega = \omega/p, \qquad p^2 = WRc/Io \tag{1}$$

A = The non-dimensional base acceleration amplitude .

x = The actual horizontal peak acceleration of the sinusoidal motion.

θ = The critical angle that indicates overturning of the specimen (rads).

g = The gravitational acceleration

Ω = The non-dimensional frequency

ω = The actual sinusoidal frequency (Hz).

p = The natural rocking frequency of the specimen (Hz).

W = The weight of the Block

Rc = The distance of the center of gravity from the pole of rocking

Io = The mass moment of inertia of the block with respect to the pole of rocking
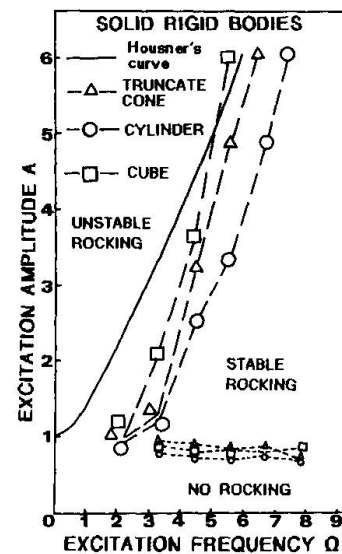
Fig. 7. Summary of sinusoidal tests for solids

The dotted lines in this plot represent the stage where rocking was initiated for the first time during the tests whereas the dashed lines represent the state of overturning of the specimen during the experimental sequence. The same figure depicts with a solid line the stable-unstable boundary of a solid block with properties the same as the ones used in the experiments, as predicted by Housner (1963), when this specimen is subjected to one half-cycle sine-wave. The following observations summarise the main points:

-For all specimens the initiation of rocking occurs for non-dimensional amplitude (A) almost equal to 1.0 for all examined frequencies.

-The non-dimensional unstable rocking amplitude increases rapidly with the non-dimensional frequency, which indicates greater stability of the solid blocks for higher frequencies.

-For small values of the non-dimensional frequency the transition range in terms of non-dimensional amplitude from no-rocking to overturning is very small and it occurs with a minor amplitude increase.

-The behaviour predicted by Housner (1963) overestimates the stability for all the used specimens, especially for small non-dimensional frequencies.

A further numerical analysis has been performed, aimed to simulate the dynamic response of the solid prism used in the experiments (cube), using the non-dimensional linear equations for sinusoidal excitation, as given by Spanos et al. (1984), and the coefficient of restitution, as evaluated from the free vibration tests. This analysis has been performed for various combinations of amplitude and frequency. Figure 8 presents these results in a summary form and as can be seen they exhibit fairly good agreement with the corresponding experimental measurements.
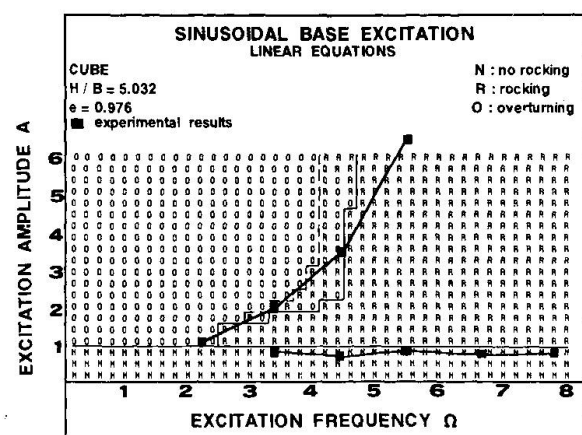

Fig. 8. Summary from numerical analysis

2.1.3. Simulated earthquake test for the solid specimens

A number of tests were performed, based on the 1940 El Centro earthquake record, with progressively increasing intensity. The base acceleration and displacement response was measured together with the rocking response of each specimen. The principal objective of these tests was to observe again the stable-unstable behaviour of the studied specimens, as shown in figure 9. The following points summarise the most important findings:

- During small intensity tests the solid blocks developed either slight rocking or no-rocking at all. In this case the maximum rocking angle is less than 30% of the critical angle.

- For peak base displacement between 10mm and 16.25mm the maximum rocking angle becomes approximately 60% of the critical.

- There was no considerable difference in the intensity of base motion during which all three specimens overturned [9].
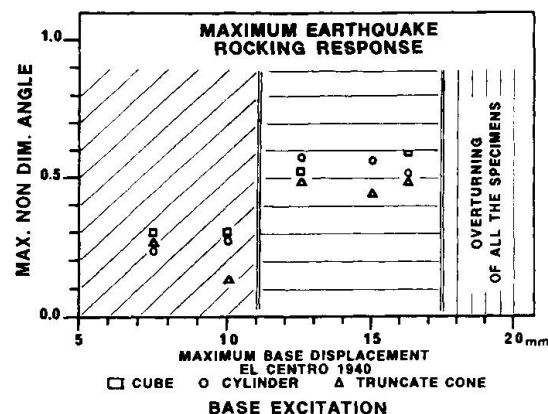

Fig. 9. Maximum earthquake rocking response

2.2. Behaviour of sliced specimens.

2.2.1 Sinusoidal tests with the sliced specimens

This sequence included similar tests with the ones performed for the solid specimens in order to assess the stable- unstable boundaries by studying the response with varying frequency and amplitude of the base motion. One important observation this time is that the response of all the sliced specimens for large amplitude excitations involved sliding as well as rocking in more than one slice contact-level. The overturning this time was caused by large sliding as well as rocking displacements. The measured stable-unstable boundary is depicted in figure 10 in terms of the same non-dimensional amplitude and frequency parameters that were used before and are based on the corresponding solid specimens as was already explained (Eq. 1).
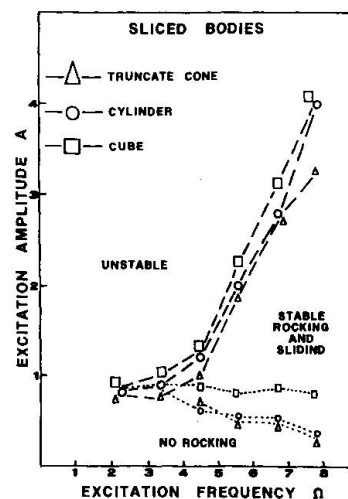

Fig 10. Summary of sinusoidal tests for sliced bodies

The following points can be made:

- From the comparison of the stable- unstable boundary between the solid and the sliced specimens of the same geometry (Figs. 7 and 10) it can be seen that all sliced specimens appear to be more unstable than the corresponding solid specimens.

- Because the sliding displacements are coupled this time with the rocking displacements the overturning or the sliding failure is also dependent on the maximum value of the relative sliding displacement that develops at its slice level as compared with the critical value that it can be allowed from the geometry of the specimen at the same level.

2.2.2. Acceleration response of the sliced specimens

In order to further investigate the response of the sliced specimens during the sinusoidal base motions the following tests were performed [11][12]; the results are presented below in non-dimensional form.

a) The first group of tests includes base motions where the non dimensional peak base acceleration was kept constant equal to 0.6 while the non-dimensional frequency was varied from 2.2 to 7.8 with steps of 1.117 for each test. For the cylindrical specimen the measured response for this series of tests is plotted in figure 11. The following points summarize the most important findings:

- For low non-dimensional frequency values the acceleration response of all the slices was in phase with that of the base motion and with the same amplitude, thus signifying no-rocking.

- For high non-dimensional frequency values, where sliding and rocking develops at many slices along the height, the acceleration response at the various slices is out of phase with that of the base and with amplified peak acceleration values as compared with the base acceleration response. The distribution of the peak acceleration along the height of the specimen changes significantly from that corresponding to low frequency values, thus reflecting the sliding and rocking response mechanisms that develop at the various contact surfaces.

b) The second group of tests included base motions where the non-dimensional excitation frequency was kept constant equal to 5.57 while, for the four tests performed for each specimen, the non-dimensional peak base acceleration took the values 0.45, 0.60, 0.75, 0.90 respectively. For the cylindrical specimen the measured response for this series of tests is plotted in figure 12. The following summarise the most important points:

- For relatively low values of peak base acceleration the slices of all the specimens responded in phase with that of the base motion. A no-rocking stage is indicated from the distribution of the acceleration response along the height.

-For relatively high non-dimensional values of the peak base acceleration the distribution of the peak acceleration changes, thus reflecting the sliding and the rocking response mechanisms involving more than one of the slices.
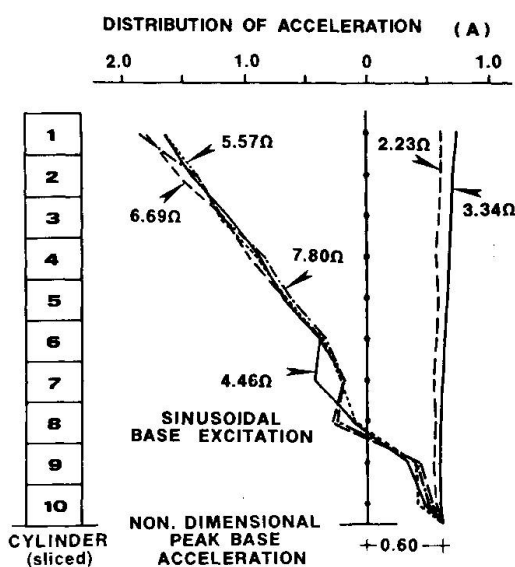
Fig. 11. Acceleration response of sliced
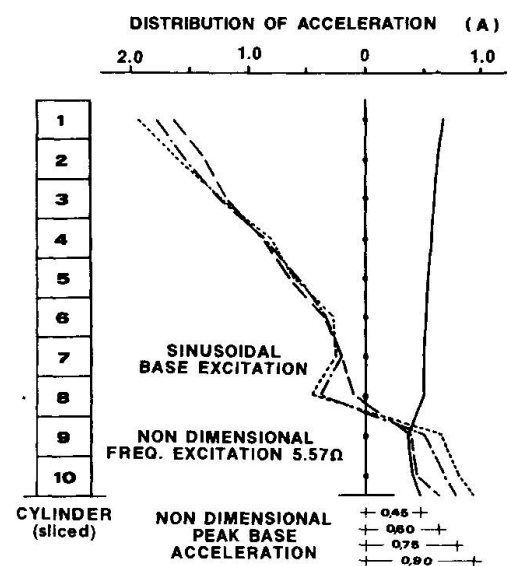bodies with constant base acceleration

Fig. 12. Acceleration response of sliced
bodies with constant base motion frequency

3. CONCLUSIONS

1. The coefficient of restitution can be defined with sufficient accuracy from the free vibration test results in combination with the performed numerical analysis, despite complications from the three dimensional rocking.

2. Similar stability behavior was observed for the three solid specimens of different geometry, as was assessed from the sinusoidal and the simulated earthquakes tests.

3. The numerically predicted upper-bounds for the stable-unstable rocking of the solid prismatic specimen, subjected to sinusoidal base motions, agrees well with the observed behaviour.

4. The stability of the sliced specimens during sinusoidal tests appears to be inferior to that of the solid specimens and it involves both sliding as well as rocking at various levels.

5. All solid as well as all sliced specimens responded out-of-plane of the excitation axis during large in-plane rocking and sliding amplitudes; naturally, this was more pronounced for the cylinder and the truncate cone specimens.

ACKNOWLEDGEMENTS

REFERENCES

1. B. PAPAZACHOS and K. PAPAZACHOU, "The Earthquakes of Greece", Thessaloniki 1989.

2. G. W., HOUSNER, "The Behaviour of Invented Pendulum Structures During Earthquakes", Bulletin of the Seismological Society of America, Vol. 53, No. 2, 1963.

3. M. ASLAM, W. G. GODDEN and D. THEODORE, "Earthquake Rocking Response of Rigid Bodies", J. Struct. Div. ASCE, pp. 337-392, 1980.

4. YUJI ISHIYAMA, "Review and Discussion on Overturning of Bodies by Earthquake Motions", BRI Research Paper No. 85, Building Research Institute, Ministry of Construction, 1980.

5. M. J. N. PRIESTLEY, R. J. EVISON, A. J. CARR, "Seismic Response of Structures Free to Rock on their Foundations", Bullet. of the New Zealand National Society for Earthquake Engin., Vol. 11, No. 3, 1978.

6. I. J. OPPENHEIM, I. J. BIELAK, R. H. ALLEN, A. R. PARKEV, "Dynamics of Multistory Rigid Prism Assemblies", Project Report, Department of Civil Engineering, University of Carnegie Mellon, Pittsburg, 1986.

7. POL. D. SPANOS, AIK- SIONG KOH, "Rocking of Rigid Blocks Due to Harmonic Shaking", Journal of Mechanics Division, ASCE, Vol. 110, No' EMII, pp. 1627-1642, 1984.

8. S. C. S. YIM and A. K. CHOPRA, "Dynamics of Structures on Two-Spring Foundation Allowed to Uplift" Journal of the Engineering Mechanics Division, ASCE, Vol. 10, No. EM7, pp. 1124-1146, 1984.

9. G. C. MANOS and M. DEMOSTHENOUS, "The behaviour of solid or sliced rigid bodies when subjected to horizontal base motions", Proc. of Fourth U. S. National Conf. on Earthquake Engineering, Palm Springs, California, Vol. 3, pp. 41-50, 1990.

10. AIK- SIONG KOH and G. MUSTAFA, "Free Rocking of Cylindrical Structures" Journal of Eng. Mechanics, Vol. 116, No. 1, pp. 35 - 54, 1990.

11. G. C. MANOS and M. DEMOSTHENOUS, "Comparative Study of the Dynamic Response of Solid and Sliced Rigid Bodies", Proc. of Florence Modal Analysis Conference, pp. 443 - 449, Firenze, Italy, 1991.

12. M. DEMOSTHENOUS and G. C. MANOS, "Dynamic Response of Rigid Bodies Subjected to Horizontal Base Motions", Proc. of 10th World Conf. on Earthquake Engineering, Vol. 5, pp. 2817 - 2821, 1992.

Mechanical Models for Behaviour of Block Structures

Modèles mécaniques du comportement de structures rigides assemblées

Mechanische Modelle des Tragverhaltens von Blocktragwerken

Anna SINOPOLI
Prof. of Struct. Mechanics
Inst. Univ. di Archit.
Venezia, Italy

A. Sinopoli got a degree in Physics from the Univ. of Padova in 1993. Assistant Professor of Applied Mechanics in the same University, she moved to the Architecture Univ. of Venice, where she has taught Structural Mechanics since 1976. Her main interests lay presently in structural dynamics and contact mechanics.

Giuliano AUGUSTI
Prof. of Struct. Mechanics
Inst. Univ. di Archit.
Venezia, Italy

G. Augusti got a Civil Eng. degree from the Univ. of Napoli in 1958 and a PhD at Cambridge, UK, in 1964. He became a Full Prof. of the Univ. di Firenze in 1973 and moved to 'La Sapienza', Rome, in 1985. His main research interests are presently in structural reliability, earthquake and wind eng.

SUMMARY

The aim of this paper is to review and discuss recent studies on the mechanical behaviour of unconnected large block structures, like those of ancient temples. The main aspects which determine the structural behaviour will be discussed, namely, the identification of the load-bearing structures and the stability of the most probable mechanism. Recent results obtained with regard to free and forced motions will be summarized and their relevance with regard to the understanding of the actual structural behaviour under seismic actions, discussed.

RÉSUMÉ

L'article passe en revue les résultats de récentes études sur le comportement mécanique de structures composées de grands blocs rigides assemblés, comme ceux des temples antiques. On analyse les aspects qui déterminent le comportement dynamique; c'est-à-dire le problème de l'identification des éléments porteurs et la stabilité de l'ensemble. Une synthèse présente des résultats obtenus en étudiant la dynamique libre et forcée et leur implications afin de comprendre le comportement réel en présence d'une action sismique.

ZUSAMMENFASSUNG

Der Bericht schildert und diskutiert kürzlich gemachte Studien über das mechanische Verhalten von Tragwerken aus grossen Einzelblöcken, wie jene antiker Tempel. Die wichtigsten das Verhalten der Strukturen bestimmenden Faktoren werden besprochen, besonders die Identifikation der tragenden Teile und die Stabilität der wahrscheinlichsten Mechanismen. Eine Synthese präsentiert die betreffend freier und forcierter Dynamik gewonnenen Resultate und erklärt ihre Bedeutung für das Verständnis des Tragverhaltens unter seismischen Einwirkungen.

1. INTRODUCTION

The evaluation of vulnerability and risk with respect to environmental influences and accidental loads should be a prerequisite of any preservation policy for architectural heritage, in order to allocate rationally the available resources. Notwithstanding the active interest aroused in the accademic and professional communities on these themes, and the many studies developed in the last couple of decades, much still remains to be done.

In a previous paper [7] an extensive review has been presented on the mechanical models relevant in the study of the free and forced dynamics of structures made by large blocks without mortar, such as the structures of Grecian and Roman temples. The present paper will underline some aspects particularly important in view of applications aimed at conservation and restoration.

2. STRUCTURAL MODELLING

The main purpose of a consistent mechanical model is to identify the most relevant aspects of the response, with the minimum of a-priori restrictions, and to recognize for each given structure a "safe domain", i. e. a domain in the load space (space of the parameters of the external actions: tipically in case of seismic excitations, an "intensity" and a significative "frequency") within which the examined structure survives. This must be done taking into account all possible dynamics modes.

The structures dealt with in this paper are made of blocks, rigid by assumption, in contact with each other and with the support planes. Relevant aspects of the motion are rocking and relative rotations with consequent impacts, slidings with friction of blocks on one another, loss of equilibrium due to excessive rotations and/or relative displacements; these last ones determine permanent changes of the geometry.

The absence of connections between the elements and the consequent unilateral constraints give rise to several possible mechanisms with different centers of relative rotations and different planes of relative slidings; consequently, in each dynamic mode different values of mechanical and geometrical features appear.

Then, in the load space, a large number of evolutive regions with time dependent boundaries can be identified corresponding to the different dynamic modes; it is also possible that these regions overlap each others.

Which mechanisms are important depends on the present features of the structure; that can be a whole temple with a well preserved entablature, but also a surviving colonnade portion or even an isolated column.

In the following, it will be shown that all these structures can be assimilated to two mechanical models: an isolated column, possibly with an added mass at the top, or a combination of two columns supporting a lintel (trilith). This result gives a-posteriori significance to the great number of papers on the dynamics of slender rigid bodies, which have been spurred by the well known work by Housner[1] and include most of the papers purported to tackle the dynamics of columns and temples. But, during the dynamics evolution, it can happen that, depending on the values of geometrical and mechanical parameters, one mode is dominant with respect to the other ones, which can be considered like some perturbations induced on the masses, on the geometry and on the restoring forces of the system. The first step is to analyze the most probable mechanism, at the instant in which the motion starts.

3. STARTING MECHANISMS

3.1. The column

Let us examine now the starting motion of a rigid column subjected to a given horizontal ground excitation; the governing forces are gravity and Coulomb dry friction.

Consider, first, a monolithic column of height h, base b, and mass m simply supported on a rigid ground (Fig. 1), in presence of a ground acceleration $a_0 = k_0 g$.

The relative values of the acceleration coefficient k_o, the static dry friction coefficient μ_s and the size ratio b/h decide whether the column remains at rest, or starts to rock, to slide or to slide-rock.
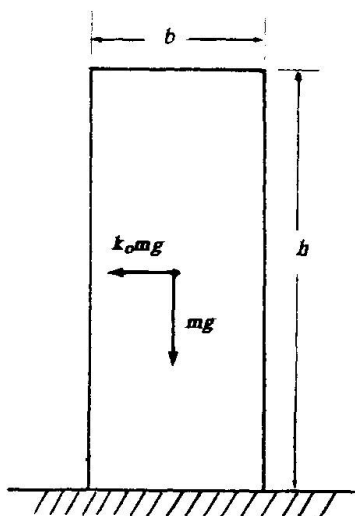

FIG. 1. *Monolithic column.*

FIG.2. *Sliding regions in the plane* (λ_1, λ_2) *of horizontal and vertical reactions.*

Let us analyze separately the possible mechanisms.

First, assume that only sliding can occur. The column slides if k_o is larger than μ_s ; the region of "no motion" is the so-called Coulomb cone (Fig.2).

Instead, whether the rocks starts depends on the relative values of k_o and b/h. In fact, with respect to the possibility of rotation, the system is at rest in a potential well (Fig.3) similar to the situation of two inverted pendulums leaning on an oblique plane of slope equal to arctg b/h. (Fig.4).
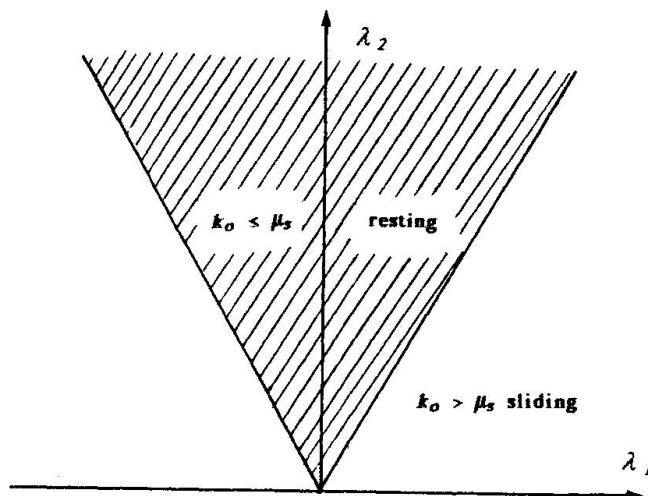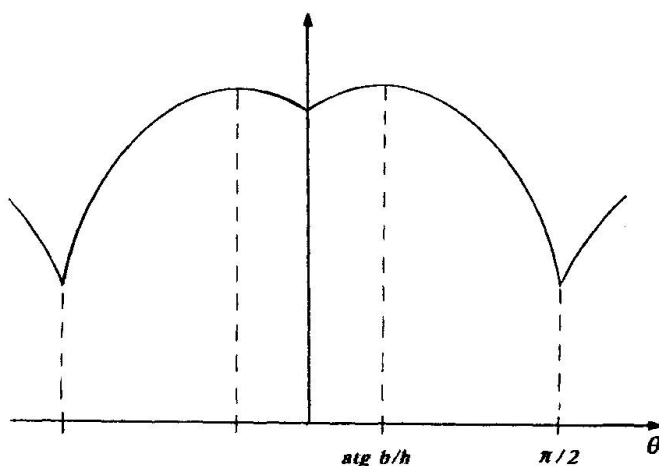

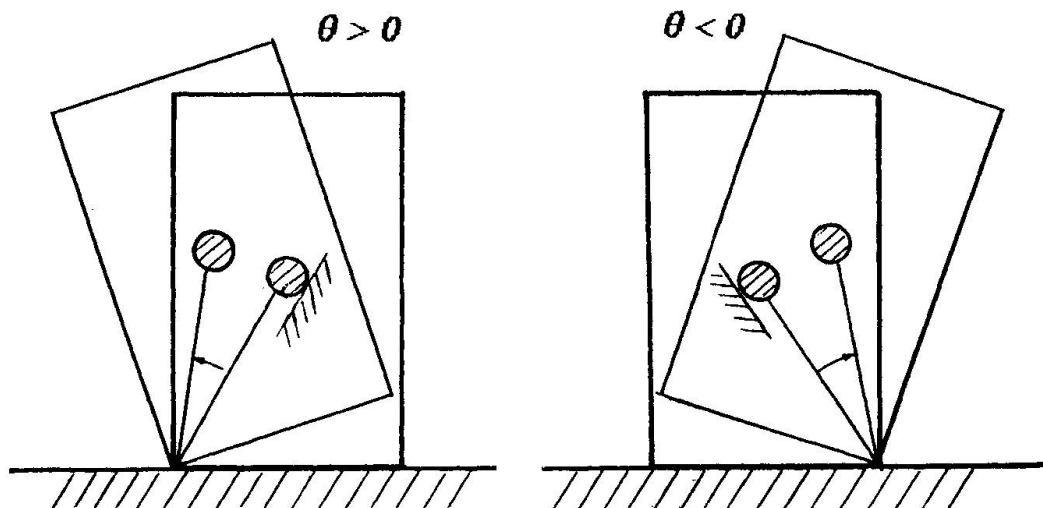FIG. 3. *Gravitational potential energy.*

FIG. 4. *Equivalent systems for positive and negative angle.*

The regions of possible or impossible rocking are shown in Fig. 5, in the plane of the restoring gravitational moment M_r and unstabilizing moment M_u.
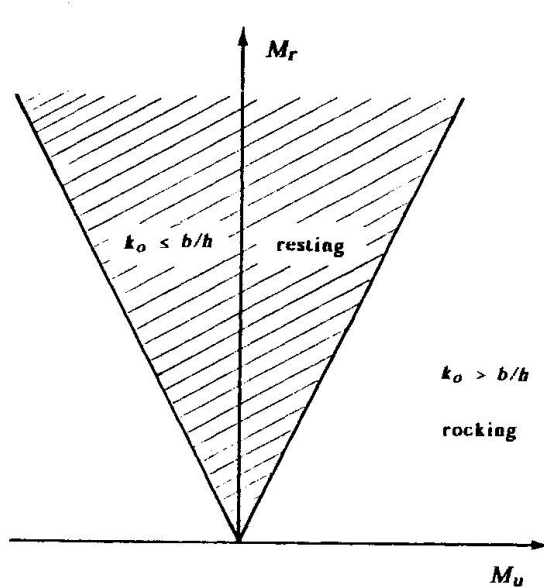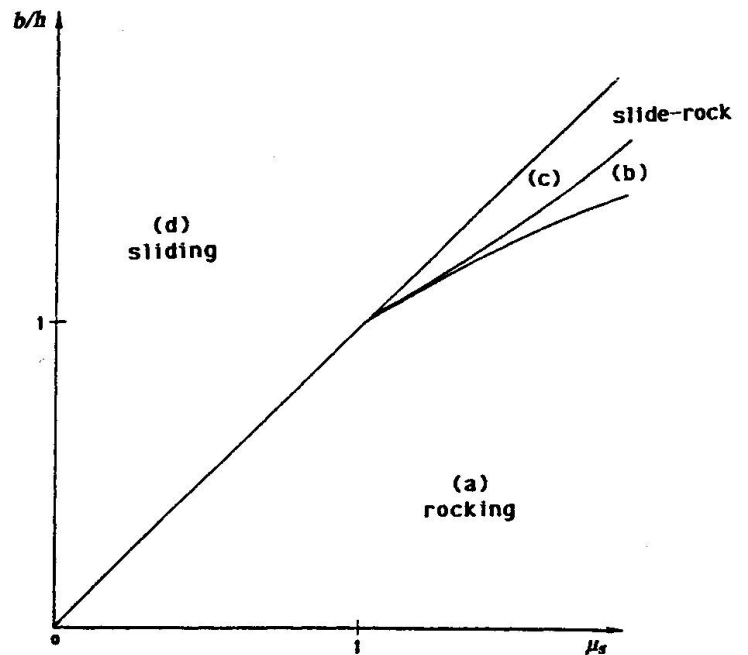

FIG. 5. *Rocking regions.*   FIG. 6. *Regions of rocking, sliding or sliding-rocking.*

Assume now that rocking and sliding are both allowed. If k_o is smaller than μ_s and b/h, obviously the column does not move. Otherwise, different situations arise depending on whether b/h is smaller, equal or larger than μ_s, as illustrated in Fig. 6. In fact, it has been demonstrated [3] [10] that, if b/h is larger than μ_s, the motion always starts as a sliding; on the contrary, if $b/h \le \mu_s$, regions of sliding, coupled sliding-rocking and rocking appear when $\mu_s > 1$. Discarding this latter case, which is unrealistic in the contact between stone blocks, it can be said that the starting motion of a monolithic column is either sliding or rocking.
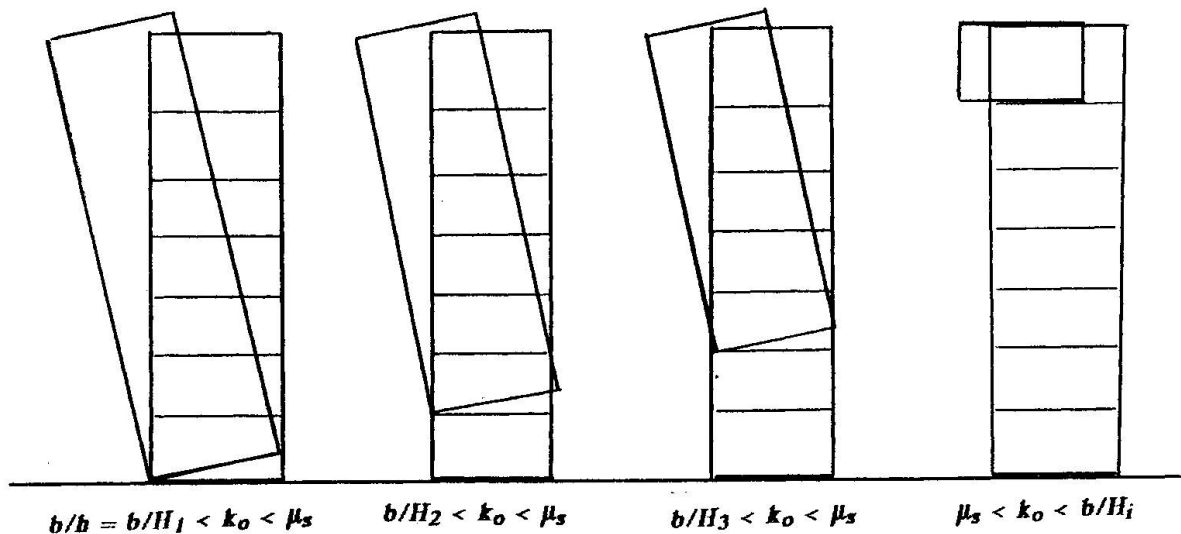

$b/h = b/H_1 < k_o < \mu_s$ $b/H_2 < k_o < \mu_s$ $b/H_3 < k_o < \mu_s$ $\mu_s < k_o < b/H_i$

FIG. 7. *Multiblock column.*

3.2. The multiblock column

In case of a multiblock column, either relative slidings or rotations between adjacent blocks can be activated. But relative movements in different contact joints imply different size ratios b/H_j: in fact, H_j must the height above the involved joint (Fig. 7).
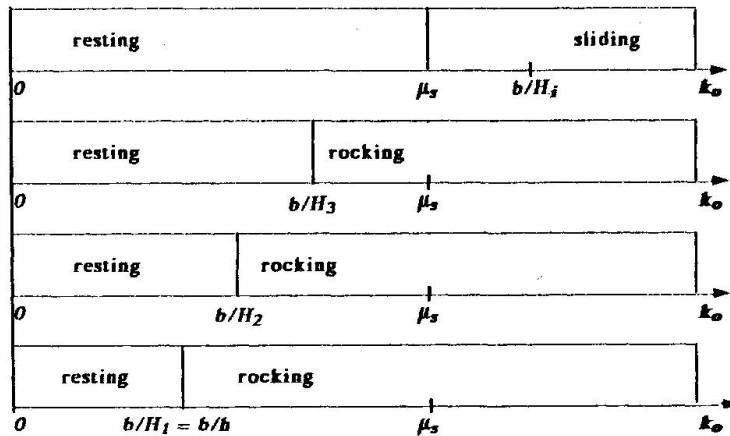

FIG. 8. *Starting modes for multiblock column.*

The number of activated d.o.f. then depends on the value of k_o (Fig. 8): assuming that $b/H_j < \mu_s$ when $j < i$ and $b/H_j \geq \mu_s$ when $j \geq i$, only rocking can start in the joints below the i-th, sliding in the joints above.

Then, for multiblock columns, the rocking of the whole column is in all cases activated whenever k_o is larger than b/h, while activation of the other d.o.f. requires larger and larger values of k_o, so that relative slidings are improbable in the starting motion for usual geometric ratios of ancient columns and values of k_o.

3.3. The trilith and the temple

The same situation above occurs for a trilith (Fig. 9 a); it starts with an one d.o.f. mechanism, the rocking of the two columns, whose behaviour is also governed by Fig. 6 [9]. It can be easily demonstrated that the motion of a colonnade in the plane defined by the columns, and the motion of a whole temple in the plane of the excitation (taking into account the axial simmetry of the columns and assuming efficient connection between the entablatures) can be modelled like that of a trilith.

The motion of a colonnade out of its plane can be assimilated to that of a higher column. In conclusion, the most probable mechanism for any kind of monumental structure, either monolithic or multiblock, can be modelled at the instant of starting motion like a single column, i.e. an inverted pendulum with appropriate values of masses and possibly added masses on the top.
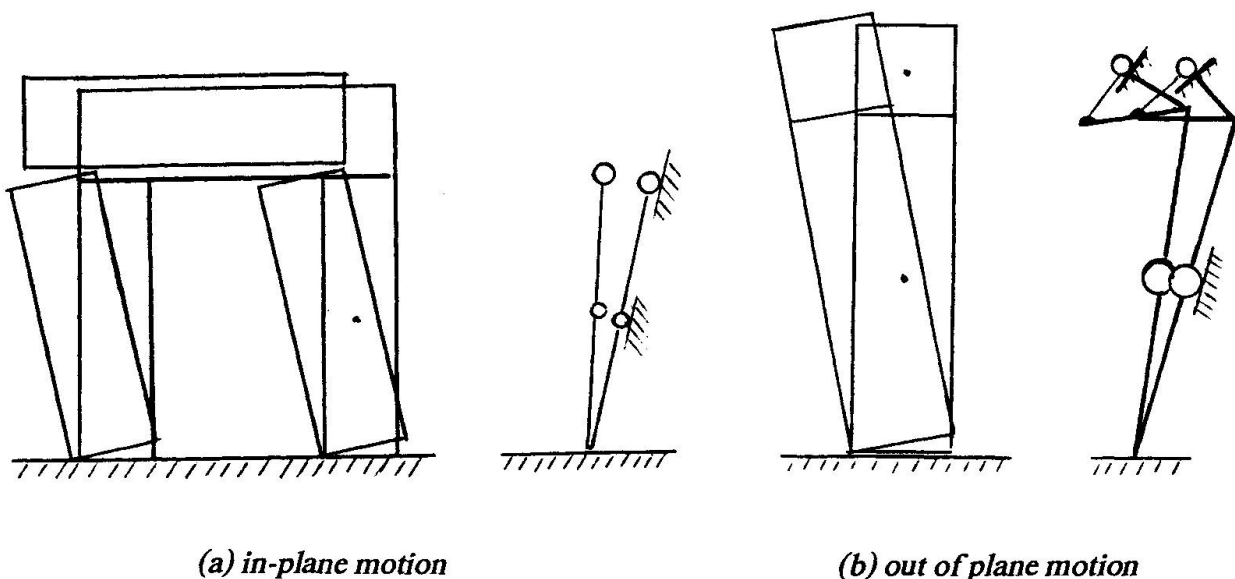

(a) *in-plane motion*   (b) *out of plane motion*

FIG. 9. *One d.o.f. trilith mechanism.*

4. DYNAMIC EVOLUTION AND FAILURE MODES

In time, the dynamical behaviour of a multiblock structure can become more and more different from that of a monolithic column. In fact, the variations of the inertia forces and of the restoring gravitational moments, with respect to the instantaneous value of the excitation, change the "threshold" conditions at different heights of the column and can allow the starting of new mechanisms. But, if rocking has already started, the above variations must be evaluated in such a mechanism for each element of the structure.

The dynamic analysis of the rocking response is then mandatory for any multiblock structure; the actual effects of the impact depend on the number of the blocks and on their geometry [4][5].

Let us refer to a column under a harmonic excitation. The dynamics of the rocking mode for small angles and any kind of periodic response (symmetric or not, and with any number of impacts per period) is governed by a damped forced Hill equation [5][7], in both cases of monolithic and multiblock column:

$$u" + p(\tau) u' + q(\tau) u = f(\tau) \tag{1}$$

Equation (1) is typical of a system with parametric resonance. It is impossible to obtain closed form solutions for $f(\tau) = 0$; the identification of stable oscillations for the column would require that all kinds of periodic response are analyzed, with given initial conditions.
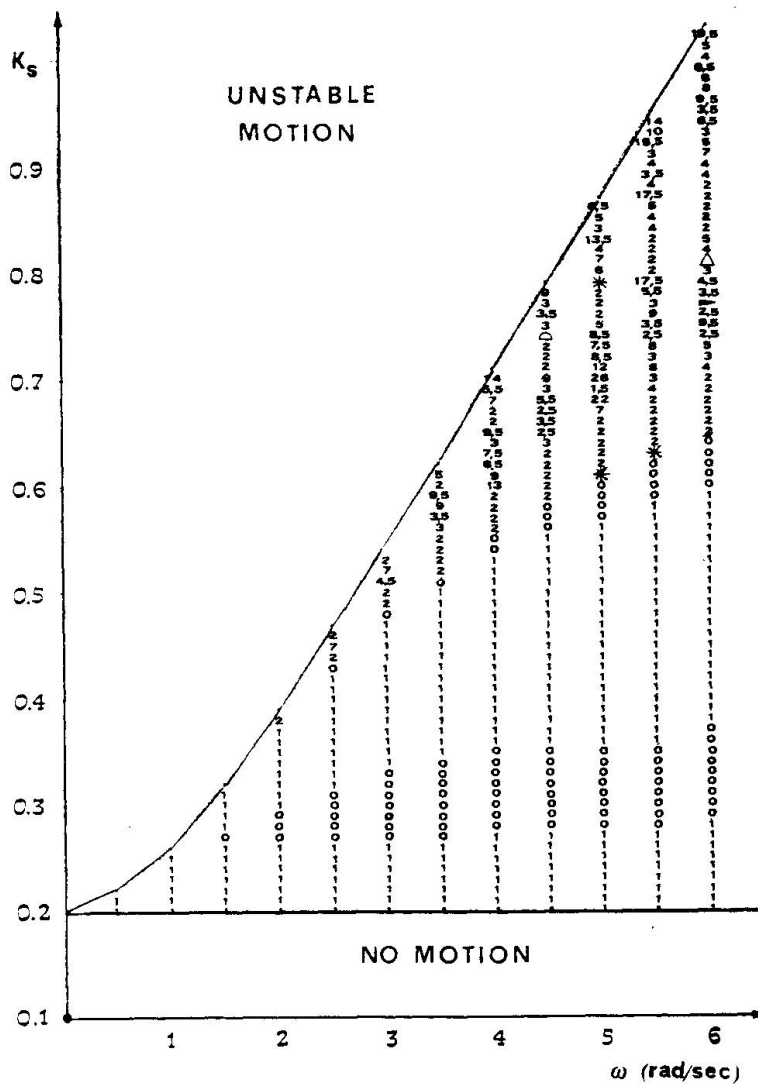

This result seems discouraging: fortunately, conditions of existence and of stability coincide; therefore, it is sufficient to perform numerical investigations to obtain the regions of either stable (periodic) or unstable (exponentially increasing amplitude) motions as functions of the parameters (ω, K_s) of the excitation.

This is shown in Fig.10 for $b/h = 0.2$ and $h = 10m$, geometrical features of the multiblock columns of the E-3 Temple in Selinus (Sicily).

Fig. 10 is limited to values of ω in the range 0-6 rad/sec: in fact, the response amplitude increases systematically with K_s and decreases quickly with ω increasing, tending asynptotically to zero; the amplitude becomes neglegible for ω larger than 6 rad/sec.

If the same column is subjected to a generic stationary excitation, the linear character of the system between two impacts and the small values of the amplitude of the stable oscillations allow to obtain the response by summation of the responses to each harmonic component defined by the Fourier spectrum of the excitation.

For $\omega > 6$ rad/sec, the global amplitude of the oscillation is negligible; the angular velocities and the relative slidings consequent to the impacts are of the same order of magnitude.

FIG. 10. *Multiblock column: stable or unstable motions [5,7].*

The amplitude of the column response becomes significant for values of angular frequency below ω = 6 rad/sec and increases with ω tending to zero. In this range new mechanisms can start.
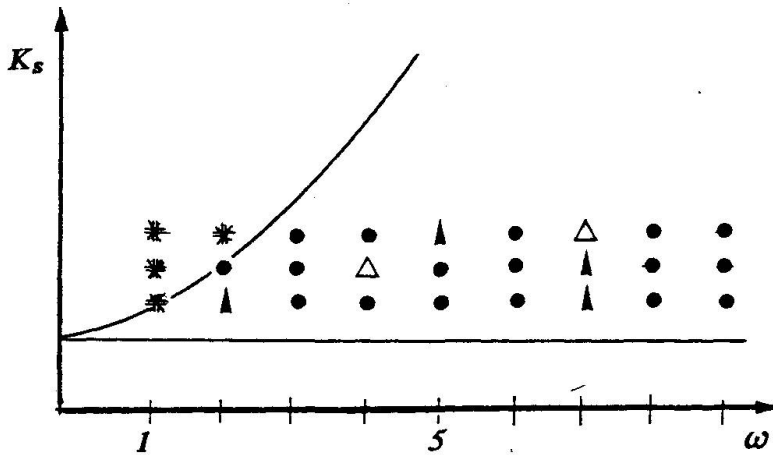

FIG.11. *Trilith: stable or unstable motions*

* *Immediate overturning,* ▲ *overturning after one or more impacts,* △*collapse due to excessive slidings,* ● *bounded motions.*

An analysis of the relative importance of slidings displacements on the upper elements of the structure has been performed studying the behaviour of a trilith under harmonic excitation [9]. It has been assumed that relative slidings are possible only between the lintel and the two columns. The geometric features are derived from a colonnade of the E-3 Temple in Selinus. The numerical investigation performed confirms that before the first impact only the rocking mechanism is activated; after this instant, relative slidings appeared for all values of K_s and ω.

Examples of the distributions of the maximum angular responses of the column in simple rocking and of the maximum sliding displacements in the trilith motion, in a given time interval, are shown in Fig. 12 and Fig. 13 respectively.

In the latter, the average absolute relative sliding S_m is reported, defined as

$$S_m = 1/t \ \left[\int_0^t (| S_l | + | S_r |) \right] dt \qquad (2)$$

where $S_l(t)$ and $S_r(t)$ are the instantaneous relative slidings respectively on the left and the rigth support of the lintel. The average displacement S_m increases monotonically with time.
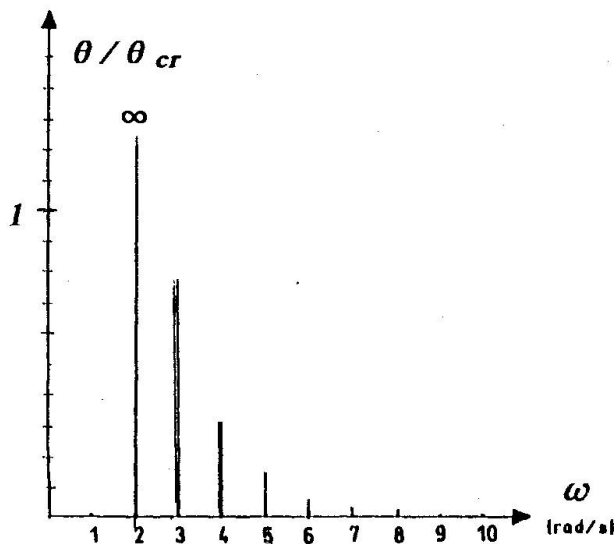

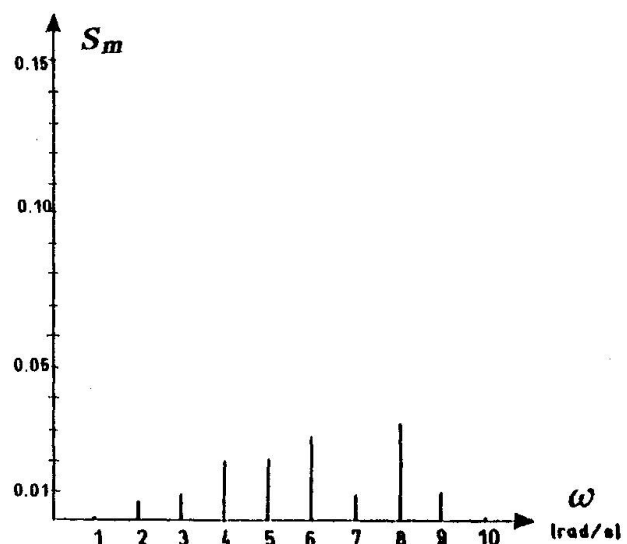FIG.12. *Typical distribution of max. rotation for the column of Fig. 10.*

FIG. 13. *Typical distribution of max. relative displacement for the trilith of Fig. 11.*

Comparison between Fig.12 and Fig.13 shows that the responses in the uncoupled rocking and coupled sliding-rocking vary with ω in a very different way.

5. CONCLUDING REMARKS

In conclusion, the dynamical behaviour of block structures, in particular under earthquake-type loads, is a well developed field of research, which has already yielded very significative results (cf. the numerous references listed in [7]). Much less developed appear the applications of these studies to actual problems: even in the few cases in which the importance of the problem almost forced a systematic program of studies parallel to the actual works, like the restoration of the Parthenon, the dynamic aspects have been somewhat undervalued, and the structural analysis followed the quasi-static approach [2].

The present paper was conceived as a modest attempt towards bridging this gap.

The results synthetically illustrated in the preceding sections show that overturning by overall eccessive rotation is a rather improbable mode of collapse under seismic loads, both for isolated columns made of stocky blocks and well preserved temples. On the other hand, rocking does not lead to any apparent damage of the structure, unless the repeated impacts weaken the material and cause fractures and "spalling", a process that may be enhanced by previous wheatering. This phenomenon has not been studied yet in sufficient depth, but some preliminary results [8] seem to indicate that it becomes relevant under extreme conditions only.

On the contrary, sliding causes permanent displacements [6][9] that alter the geometry. However, impacts and sliding displacements dissipate energy and therefore tend to stabilize the structure.

For all these reasons, it appears that blocks must not be tied or rigidly connected to each other: the only sensible "maintenance" policy is the elimination of permanent displacements and, possibly, the restoration of the damaged basis of column so to preserve the original size ratio.

Further studies are still very much needed with an eye not only at academic results but also at real possibilities of applications.

ACKNOWLEDGEMENTS

REFERENCES

1. HOUSNER, W.G., 'The behavior of inverted pendulum structures during earthquakes', *Bull. of Seism. Society of America*, 53, 1963, pp.403-417.

2. VV. AA., *Proceedings of 2nd International Meeting for Restoration of the Acropolis Monuments: PARTHENON*, Athens, 1983.

3. SINOPOLI, A., 'Dynamics and impact in a system with unilateral constraints. The relevance of dry friction', *Meccanica*, 22, 1987, pp.210-215.

4. SINOPOLI, A., 'Kinematic approach in the impact problem of rigid bodies', *Applied Mechanics Review, ASME*, Vol.42, 11, Part 2, 1989.

5. SINOPOLI, A., 'Nonlinear dynamic analysis of multiblock structures', Kratzig, W.B., et al (Eds.): *Structural Dynamics*, Vol. 1, A.A. Balkema, Rotterdam, 1991, pp.127-134.

6. SINOPOLI, A., 'Dynamic analysis of a stone column excited by a sine wave ground motion', *Applied Mechanics Review, ASME*, 44 (10), Part 2, 1991.

7. AUGUSTI, G., SINOPOLI, A., 'Modelling the dynamics of large block structures', *Meccanica*, Vol. 27 (3), pp. 195-211, 1992.

8. AUGUSTI, G., CIAMPOLI, M., CICCHETTI, G., 'An introduction to the dynamics of degrading rigid blocks', in *Proc. of III Pan American Congress of Applied Mechanics*, pp. 53-56, 1993.

9. SINOPOLI, A., SEPE, V., Coupled motion in the dynamic analysis of a three-block structures', in *Proc. of III Pan American Congress of Applied Mechanics*, pp. 65-68, 1993.

10. SINOPOLI, A., 'Base excitation of rigid bodies. I. Formulation', (Discussion), *Journal of Engineering Mechanics, ASCE*, 119 (EM1), January 1993.

11. SINOPOLI, A., 'A variational principle for non-smooth dynamics of rigid bodies', In preparation. 1993.

Strength Assessment of Ancient Masonry Vaults

Evaluation de la résistance d'anciennes voûtes en maçonnerie

Tragwiderstansbestimmung alter Mauerwerksgewölbe

Aldo CAUVIN
Prof. of Struct. Eng.
Univ. of Pavia
Pavia, Italy

Giuseppe STAGNITTO
Research Engineer

Pavia, Italy

SUMMARY

An overview of available methods for the safety assessment of ancient vaulted structures is given, specifying the limitations and fields of application of each approach. Suggestions are given for an appropriate use of the Finite Element Method. The validity of classical equilibrum methods based on the pressure line concept is emphasized and a simplified incremental method of non-linear analysis is proposed to evaluate the ultimate load and the influence of cracking in masonry arches and vaults.

RÉSUMÉ

L'article passe en revue les méthodes existantes pour l'évaluation de la sécurité d'anciennes structures voûtées. Il précise les limites et les domaines d'application de chaque méthode. Des propositions sont faites pour l'emploi de la méthode aux éléments finis. La validité des méthodes classiques de l'équilibre, basées sur le concept de lignes de pression, est soulignée. Une méthode simplifiée d'analyse non-linéaire est proposée pour évaluer la charge ultime et l'influence des fissures dans les arches et voûtes en maçonnerie.

ZUSAMMENFASSUNG

Es wird eine kritische Gesamtübersicht über die verfügbaren Methoden zur Bestimmung der Tragsicherheit alter Gewölbekonstruktionen und deren Anwendungsgebiet und -grenzen gegeben. Geeignete Einsatzmöglichkeiten der Finiten-Elemente-Methode werden vorgeschlagen Die Gültigkeit der klassischen, auf dem Drucklinienkonzept basierenden Gleichgewichtsmethode wird unterstrichen und eine vereinfachte inkrementelle Methode vorgeschlagen, um in nichtlinearer Berechnung die Traglast und den Einfluss der Rissbildung in gemauerten Bögen und Gewölben zu ermitteln.

-Introduction

Vaulted structures have been built for a long period of time using,until the advent of modern methods,materials unable to resist tension;in fact,apart from wood,which is a perishable and not always easily available material,the only available building materials were bricks and stone masonry;on the other hand,the only way to cover reasonably large spans using "no tension" materials was by adopting the "arch" scheme.

The dimensioning of arches and their derivatives,barrel and cross-barrel vaults has been performed in the past using purely empirical criteria,translated into geometrical rules.Only in more recent times rational verification methods were developed ,that is the well known equilibrium methods of graphical statics whose origins date back to the sixteenth century,but were formalized in a definitive way by Culmann [4]in the nineteenth century.

On the other hand,the modern evolution of elastic structural analysis and,most recently,of the finite element method,has provided a new tool of investigation also for this kind of structures.

However the finite element method,expecially if applied in the linear elastic field,could lead in these applications to unreliable results,as it ignores the influence of cracking,and of the highly anisotropic characteristics of the materials involved.

At last the development of nonlinear analysis methods permits to overcome ,at least partially,these limitations.

As will be later explained,the uncertainties which arise from these problems can be reduced by evaluating the results deriving both from "traditional" and "modern" methods of analysis:

in fact it is certain that traditional methods,being based on the "pressure line" concept retain a considerable validity as far as "no tension" materials such as masonry are concerned.

In this paper,using the experience accumulated by the authors in the field of ancient vaults restoration, the following topics are discussed:

-Validity of results given by the finite element method in the elastic field.
-Differences of behaviour between short barrel vaults on rigid supports and arches
-Possibility of adopting one dimensional schemes for vaults
-Importance of the "pressure line" concept
-Simplified methods of nonlinear analysis of masonry vaults and arches
-Procedures to be followed in structural analysis both of non restored damaged and restored vaults.
-Criteria to be followed for a rational restoration of vaults.

Examples of calculations performed on eighteenth century vaults are also,as available space permits, given.

-Problems arising from the use of the FE method in analysis of masonry vaults

The use of the FE method for the analysis of vaulted structures permits to model geometrically the structure in a very precise way and thus to define boundary conditions quite accurately(fig.1).

However this kind of analysis is not in itself enough to evaluate the structural safety for the following reasons:

A-The material does not resist tension and therefore cracks,altering the distribution of stresses,are present.Besides the material behaviour is highly nonlinear ,nonelastic and anisotropic.

Large cracks due to past settlements can be accounted for by introducing discrete cracks in the mesh according to the survey of visible cracks[2].However non visible tension cracks can only be accounted for by performing a nonlinear analysis.Nonlinear FE methods using "layered" elements have been prepared for reinforced concrete shells[9].

However nonlinear analyses are reliable provided that constitutive laws for the materials can be accurately defined.The problem is already difficult to solve for concrete which is a much more homogenuous material than masonry;the problem of definition of constitutive laws for masonry in two dimensional state of stress as is found in shells seems very difficult to solve.The problem can be simplified if it is possible to consider an equivalent one dimensional state of stress as will be explained later.

B-Commercial FE graphic postprocessors usually represent results in the form of "isostress"lines.

This is all right if ,as normally happens,the program is used to analyze materials with symmetrical behaviour such as steel.In the case however of material subject to cracking the given results both are inaccurate and do not permit to give an interpretation of the structural behaviour.
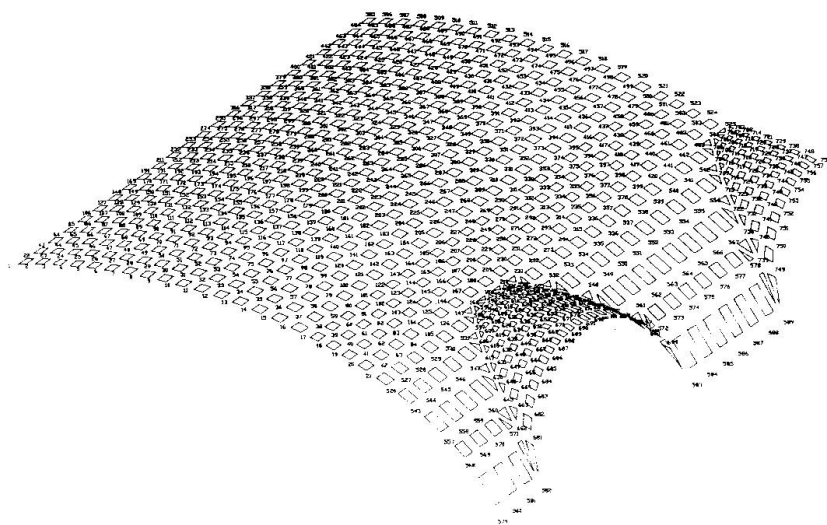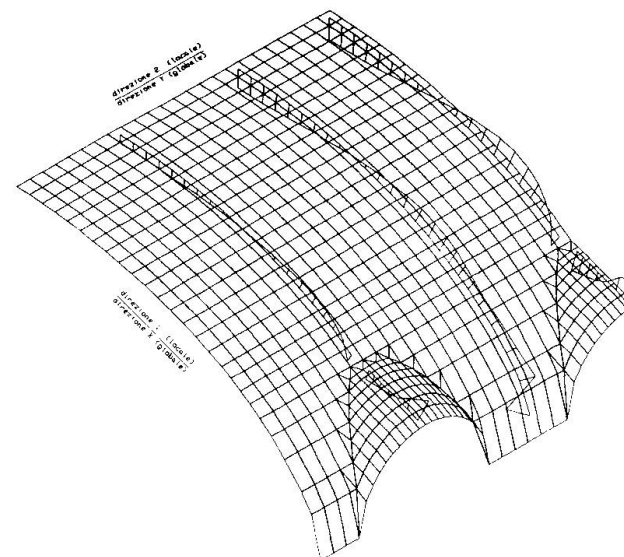
Fig.1-FE mesh of a barrel vault

Fig.2-Moments in barrel vault

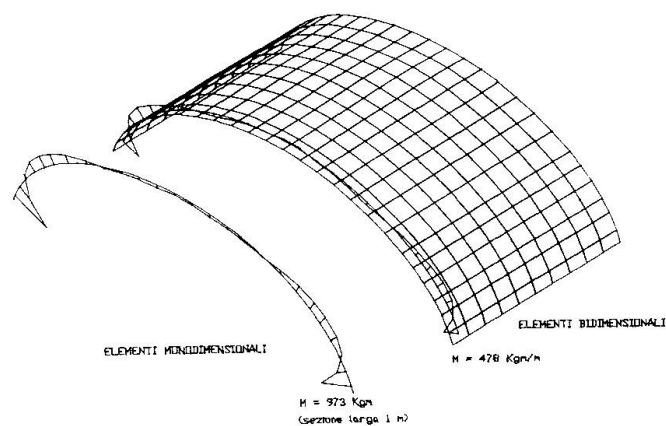
ELEMENTI MONODIMENSIONALI

ELEMENTI BIDIMENSIONALI

H = 478 Kgm/m

H = 973 Kgm
(sezione larga 1 m)

Fig.3-Torsional effect in barrel vault

minimum thrust PL

max thrust PL

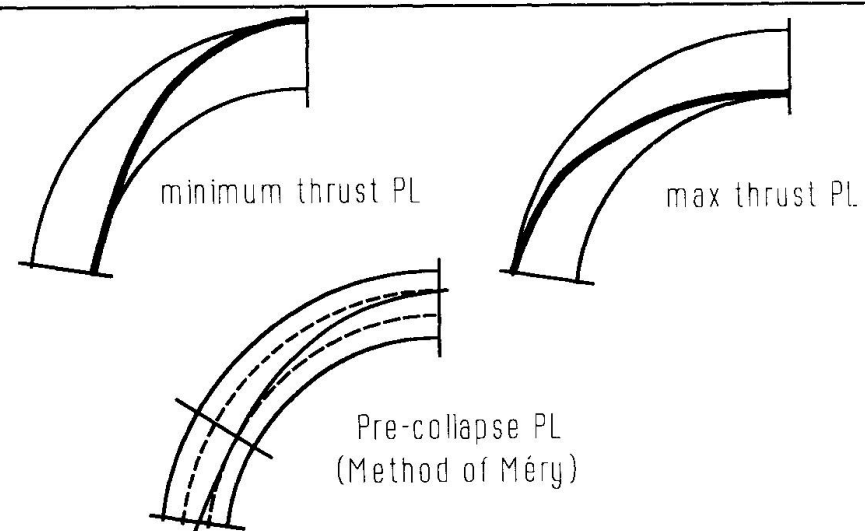Pre-collapse PL
(Method of Méry)

Fig.4-Limit pressure lines in arches

For this reason a specialized post-processor which permits to represent the diagrams of action effects along given alignments was prepared.The program was written in autolisp(the particular form of lisp language which can be used within the AUTOCAD program)and therefore can exploit the enormous grafic possibilities of the AUTOCAD system.Details concerning this subject can be found in [11].On fig.2 an example of this kind of representation is given.

This kind of representation permits to interpret in a very intuitive way the structural behaviour;in particular it permits to establish when a simplified structural scheme(such as a plane one-dimensional one)can be reasonably adopted to perform nonlinear analyses.

This postprocessor also permits to represent the state of stress in terms of isostatic lines.This reppresentation can also be useful for the same reason.

C-FE analyses permit to evaluate the state of stress and strain but not ,at least directly,the structural stability of a vaulted structure made of a "no tension" material.This subject will be considered later.Let us observe now the following facts concernig historical structures:

-Mean stresses are normally(but not always) very low and much below the material resistance.Besides when higly stressed zones are found,they have a very limited extension and are therefore unable to produce a danger of global collapse.

In fact the empirical rules used by ancient builders were normally very conservative;on the other hand the very fact that these structures have survived for so many years is a symptom of the presence of low stresses.

-Large deflections are normally due to foundation settlements which occurred in the past and which are usually stabilized;deflections due to applied loads are normally very limited and therefore not critical in the verification process.

It may be concluded that results from FE analyses,although necessary and important are not usually the crucial part of this process as far as structures composed of "no tension" materials are concerned.

-Possible simplifications of structural schemes:reduction to arch structures

As known ,in the classical methods of analysis,the study of vaulted structures is reduced to one dimensional problems:in other words the vault is imagined as composed of arches and each type of arch is studied separately.

One might wonder whether this method can,at least to some extent and for the simplest vaults(such as barrel vaults)be accepted.

Let us consider the barrel vault of fig.3 which has been analyzed both using two-dimensional finite elements and considering it as a series of independent parallel arches.In the first case the maximum moments along the arches are much smaller (about 50% less for the central arch)due to the collaboration of adjacent arches which in the second case has been disregarded.

Apparently the Finite Element calculation is more "exact".It must be noticed however that,with reference to the central arches, this collaboration takes place mainly because of the torsional stiffness of "fibers" orthogonal to the "arches".In fact,if the torsional stiffness of finite elements is assumed as zero,the results are exactly the same as for the one dimensional analysis.

Assuming an homogeneous elastic material,the torsional stiffness of transverse fibers in a shell structure like this is considerable(as the ratio between the sides of the shell is about one).

It is not easy however to evaluate torsional stiffness of a brick panel and to which extent this stiffness can be relied upon,as,to our knowledge,experimental evidence is lacking.

Common sense suggests however that this stiffness be both low and unreliable.

We might conclude therefore that the one-dimensional approach,at least in these cases,is to be preferred ,not only because it is on the safe side,but also because it is after all the more likely to approach reality.

-The individuation of "pressure lines"

As known the individuation of the possible pressure lines is essential to assess the overall equilibrium of an existing arch structure made with a "no tension" material,as stated by the Hayman's principle[1].

If a linear elastic behaviour is assumed the pressure line is univocally individuated and can be derived from the elastic analysis.In the same way it is possible to derive the pressure line corresponding to a nonlinear analysis.However,given the uncertainties in the evalution of the "true" pressure line,it is also important in the diagnosis and restoration process to consider limit pressure line such as those represented in fig.4:
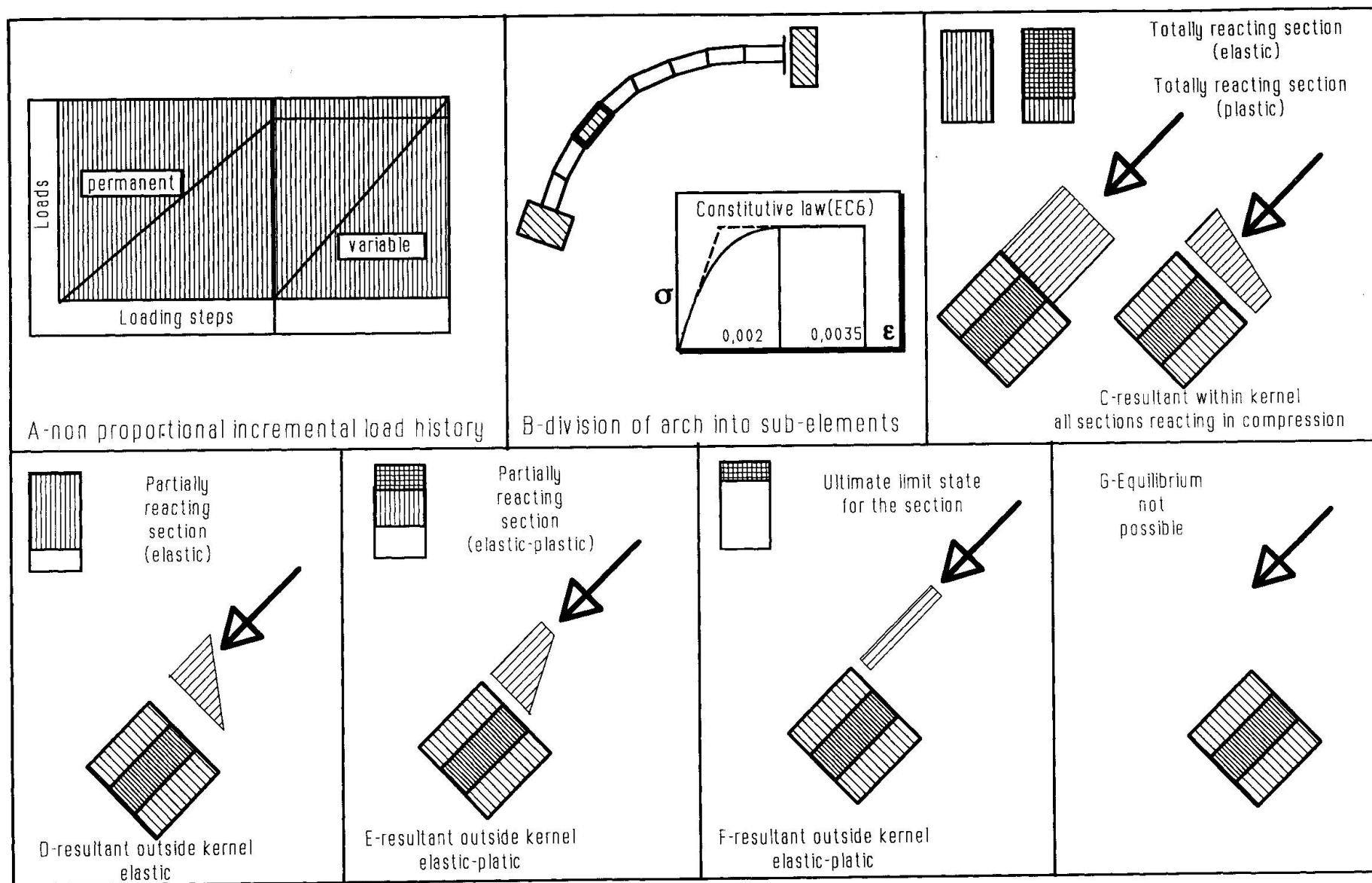
-The pressure line corresponding to maximum thrust

A. CAUVIN · G. STAGNITTO

A-non proportional incremental load history

B-division of arch into sub-elements

Totally reacting section (elastic)

Totally reacting section (plastic)

C-resultant within kernel all sections reacting in compression

Partially reacting section (elastic)

D-resultant outside kernel elastic

Partially reacting section (elastic-plastic)

E-resultant outside kernel elastic-platic

Ultimate limit state for the section

F-resultant outside kernel elastic-platic

G-Equilibrium not possible

Constitutive law(EC6)

Fig.5-Simplified nonlinear analysis

381

-The pressure line corresponding to minimum thrust
-The pressure lines corresponding to the pre collapse phase in which critical sections begin to(or are already) cracked.The pressure line based on the classical method of Mery belong to this category.
In these cases elastic analysis cannot help and the equilibrium methods of graphical statics must be used[4].
In particular the method for the tracing of the only funicular polygon connecting the applied loads and passing through three determined points must be applied.
However,in the computer era,graphical constructions are considered too laborious , time consuming and not easily integrated in the design or analysis process.
To overcome this inconvenience an analytical procedure has been elaborated by the authors and a computer program prepared for the instant tracing of pressure lines passing through three predetermined points[12]
In this way the limit solutions which "brackets" the unknown physical situation can be rapidly determined.

-Simplified nonlinear analysis of masonry arches and vaults.

A simplified procedure for nonlinear analysis of masonry was prepared which permits to obtain,in the case of one dimensional plane structures the following results:
-Evaluation of the collapse load
-Evaluation of second order effects in slender arches
-Evaluation of the influence of cracking.
The program is based on the same phylosophy which was adopted by the first author in the preparation of programs for nonlinear analysis of Reinforced Concrete Structures[5],[7],[8],which can be summarized as follows(while details on the procedure are reported in [6]):
-The solution procedure is incremental,non proportional;permanent loads are applied first,then variable loads are applied step by step until collapse of the structure(fig.5/A)
-A "smeared" cracking "concentrated"plasticity approach is adopted,that is:
-Each element is divided into sub-elements(fig.5/B)
-The stiffness of each element is reduced,during the loading process,to take account of cracking,according to the criteria which are summarized in figg.5/D-E.
-The stiffness of each element is reduced to take into account second order effects
-Plastic hinges are introduced in critical sections when full plasticization is reached in a critical section(figg.5/C,F)
-The structural equilibrium is checked section by section and step by step(fig.5/G)
Although the accuracy of this approach should not be overemphasized,it can give useful informations in the verification process of a vault structure such as a reasonably accurate evaluation of collapse load(certainly more accurate than the one given by conventional "plastic"methods),of the "trend" in redistribution of action effects due to cracking,and of the importance of second order effects.
A constitutive law such as the one suggested by EC6(fig.5/B)[3]can be adopted for masonry,as it is appropriate for the degree of accuracy required by the method.

Use of the "pressure line" concept for rational restoration of barrel vaults. An example.

An example of the use of pressure lines of barrel vaults is given in fig.6.
Eighteenth century masonry vaults,having a span of 10 meters,had to be repaired and strengthened.
The rubble infill originally used to level the exterior part of the vault(fig.6/A) had to be removed,a r.c. cap was added and a light overstructure was built in place of the rubble infill(fig.6/B).
In addition to FE analyses,the pressure lines for the two loading cases were traced and it was noticed that,despite the great reduction in permanent load,and the increase in arch cross section,the state of stress in critical sections had really worsened because of the increased excentricity of the pressure line with reference to the arch axis(figg.6/A1,A2,6/B1,B2).In fact the ancient builders were well aware of the concept of "funicular arch" and designed the vault accordingly.
An edge r.c. beam was therefore added to increase the section height of the arch near the abutment.
An alternate solution would have been to evaluate the distribution of overloads in the new situation,corresponding to an assumed pressure line,approaching as much as possible the arch axis.
This can be done using well known equilibrium criteria.

A-original state of vault

A1-loads and action effects diagrams

A2-Pressure line in vault

B-restored vault with lightened overstructure

B1-loads and action effects diagrams

B2-Pressure line in vault

C-restored vault with lightened overstructure and ballast

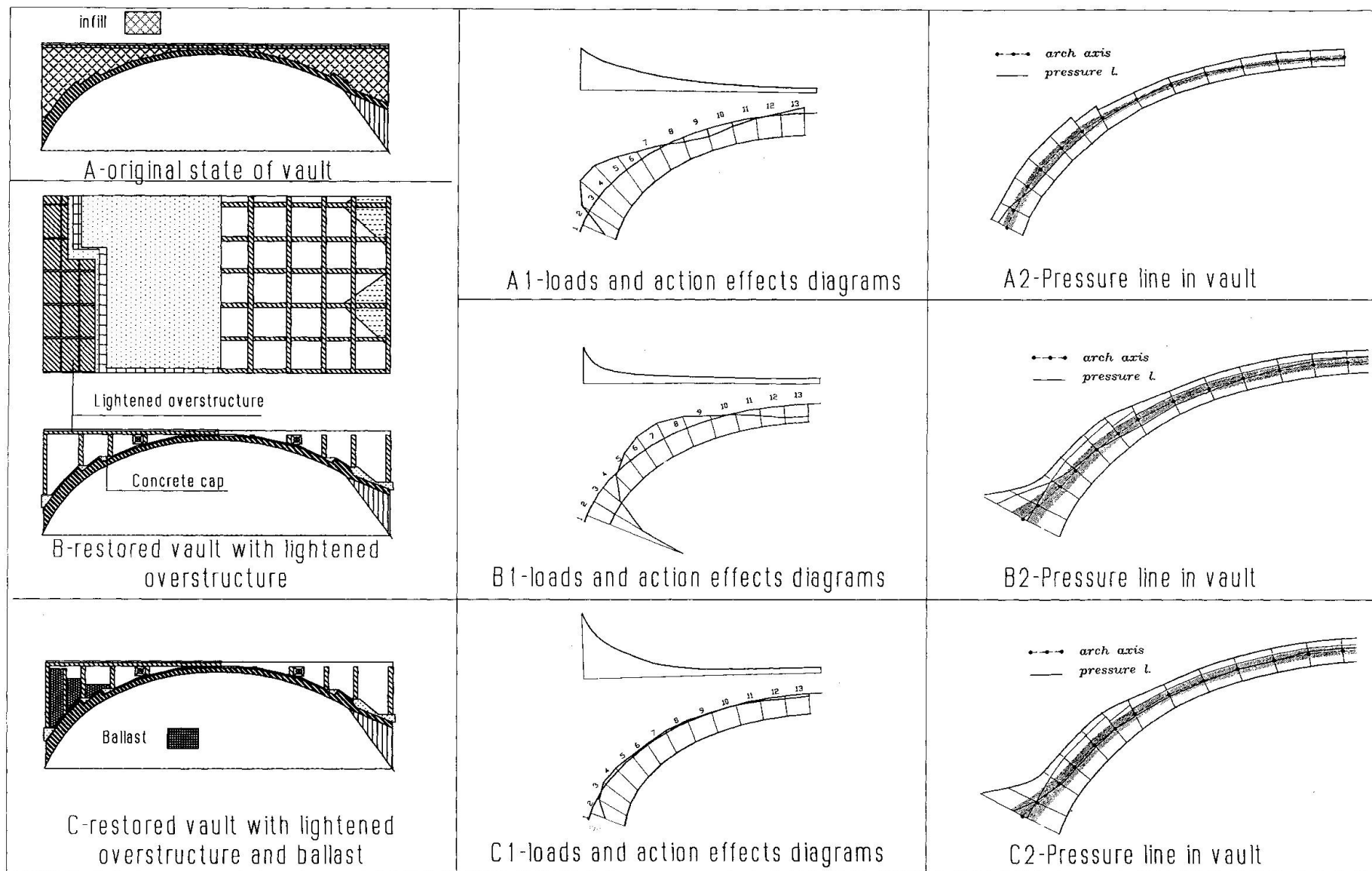C1-loads and action effects diagrams

C2-Pressure line in vault

Fig.6-Example of restoration design of a masonry eighteenth century barrel vault

As a result,it was verified that by filling some of the cells of the overstructure with sand ballast a much more favourable pressure line could be obtained(fig.6/C,6/C1,6/C2)

Conclusions

The assessment of the degree of safety of masonry vaults is a complex procedure which requires the use of different approaches:
-The FE method in the linear elastic field permits to evaluate the state of stress and displacement of the structure assuming realistic structural schemes and boundary conditions.However cracking and nonlinear behaviour cannot be accounted for and the overall equilibrium of a structure made of "no tension"material cannot be directly established.
Suitable graphic representation of results permit in many cases to adopt realistically one-dimensional simplified structural schemes,which improve structural understanding,and simplify analysis.
-Whenever this is possible,the tracing of pressure lines using graphical or,better,analytical procedures permit to assess the structural stability and,in case,to alter permanent loads,during design of restoration, to increase this stability.
-A simplified nonlinear approach can also be useful to evaluate the ultimate load and the influence of cracking and second order effects.
-The use of more sophisticated FE nonlinear approaches is hampered by the difficulty to establish realistic two-dimensional constitutive laws and,in particular,to assess torsional behaviour.

References

1-Heyman J.,The care of masonry buildings.The engineer's contribution.,from the volume:structural repair and mantainance of historical buildings,edited by C.A.Brebbia,Computational Mechanics Publications Birkhauser,Basel 1989
2-Ignatakis C,Stylianidis K.,Stavrakakis E.,Design of intervention in domes.The importance of consideration of cracking,from the volume:structural repair and mantainance of historical buildings,edited by C.A.Brebbia,Computational Mechanics Publications Birkhauser,Basel 1989
3-Eurocode n.6,Unified Common Rules for Masonry Structures,Commission of the European Communities,Industrial Processes,Building and Civil Engineering,Predraft document,1991
4-Culmann Karl,Traité de Statique Graphique,Dunod,Paris,1880
5.-Cauvin A,Analisi non lineare di telai piani in CA.,Giornale del Genio Civile;fascicolo 1,2,3-1978
6-Cauvin A, Stagnitto G.,"MAS-NL" a computer program for the nonlinear analysis of one dimensional plane masonry structures,Research report,Department of Structural Mechanics,University of Pavia,Pavia,Italy,1993
7.-Cauvin A,Incremental Nonlinear Analysis of r.c. frames using microcomputers,from"Microcomputers in Engineering",edited by Schrefler B.A. and Lewis R.W.,Pineridge Press,Swansea,1986
8.-Cauvin A,Nonlinear analysis of Coupled Shear Walls in Tall Buildings,from"Numerical methods for nonlinear problems",edited by Taylor,Owen,Hinton,Damjanic,Pineridge Press,Swansea,1986
9.- Scordelis A.C.,Finite Element Analysis of reinforced concrete structures,Proceedings of the Conference on Finite Element Methods in Civil Engineering,Montreal 1972.
10-Cauvin A,Stagnitto G.,Problems concerning strength assessment and repair of Historical Vaulted Structures,to be published on the proceedings of the IASS Symposium"Public Assembly Structures from Antiquity to the Present",Istambul,1993
11-Cauvin a.,Stagnitto D.,Stagnitto G.,Postprocessing of Finite Element Analyses in "AUTOCAD"environment.Research report,Department of Structural Mechanics,University of Pavia,Pavia,Italy,1993
12-Cauvin A.,Stagnitto G.,Tracciamento mediante computer delle linee delle pressioni negli archi(Computer tracing of pressure lines in arches)Research report,Department of Structural Mechanics,University of Pavia,Pavia,Italy,1993

Aknowledgements

Examination of Masonry Arch Assessment Methods

Examen des méthodes d'évaluation des ponts-arcs en maçonnerie

Vergleich von Bewertungsverfahren für Mauerwerksbrücken

Parag C. DAS
Princ. Civil Eng.
Dep. of Transport
United Kingdom

P.C. Das obtained his Doctorate in civil engineering in 1968 from Southampton Univ. He joined the Dep. of Transport as a bridge engineer. and has since been involved with research, design and technical approval of bridges. He is now a Principal Civil Eng. responsible for formulating standards.

SUMMARY

This paper gives brief descriptions of a number of masonry arch bridge assessment methods developed in the United Kingdom in recent years. It also describes the findings of an investigative study of the methods involving comparisons with collapse tests on full-scale bridges.

RÉSUMÉ

Cet article donne des renseignements sur quelques méthodes, récemment développées au Royaume-Uni, du calcul de la résistance restante des ponts-arcs en maçonnerie. Il présente les principes de ces méthodes sur la base de comparaisons avec des essais à la rupture sur des ponts prototypes.

ZUSAMMENFASSUNG

Dieser Beitrag beschreibt verschiedene Bewertungsverfahren für existierende Bogenbrücken aus Mauerwerk, die in letzter Zeit in Grossbritannien entwickelt wurden. Es liegen die Ergebnisse einer Studie vor, die diese Verfahren mittels Bruchversuchen an Originalbrücken untereinander vergleicht.

1. INTRODUCTION

1.1 Background

There are approximately 35,000 masonry arch highway bridges in the United Kingdom and a similar number on the country's railways. All of these are of considerable age and many are excellent reminders of the country's architectural heritage. It is important therefore not only to maintain these bridges in good condition but also, when necessary, to be able to estimate their load carrying capacity as accurately as possible so that the numbers needing replacement are kept to the minimum.

1.2 Masonry Arch Research In The UK

The UK Bridge Census and Sample Survey [1], published in 1987, indicated that almost 10 per cent of the masonry arch road bridges would be found to be substandard according to the commonly used assessment method given in the Department of Transport Advice Note BA 16/84 [2]. The Department therefore sponsored a coordinated programme of research aimed at improving on the method, known as the MEXE method, which was generally suspected to be conservative. This programme, which, in addition to the theoretical work, involved the collapse testing of 8 redundant bridges and 2 full-scale models [3], resulted in the development of three different computer-based analytical methods of assessment.

The ultimate load capacities of the test bridges calculated by using the three methods were compared with the test results. A further study was also undertaken to examine in greater detail the theoretical implications of the methods. This paper contains the results of the comparisons and the additional study.

2. ASSESSMENT METHODS

2.1 The Modified MEXE Method

This method is described in Advice Note BA 16/84. It is based on the earlier MEXE method which was originally developed for military purposes. It involves the use of a nomogram, or optionally, an equation which gives a provisional axle loading (PAL) for a given span and a given total thickness of the masonry plus fill at the crown. The PAL is then modified by a number of factors which deal with the specific geometry, materials and the condition of the bridge to give a modified allowable axle load. The allowable axle load can be converted into permissible gross vehicle weights with the help of a table.

2.2 The Modified Pippard Method

The precise theoretical basis of the MEXE method is not known. However, it was almost certainly based on the simple elastic method of Pippard [4], which involved the elastic analysis of a parabolic arch, shown in Fig.1, assuming its cross-sections to be able to take tension but using a permissible limit of compressive stresses. It has been confirmed by recent investigative work that if Pippard's arch were analysed by replacing the single axle with a two axle bogie, the original Pippard results would approximate to the modified MEXE values.

The Modified Pippard method, developed in the Department, involves the use of any frame analysis computer program to carry out the Pippard analysis, with two significant differences. Firstly, any arch, fill or loading configuration may be considered without the Pippard simplifications. Secondly, instead of using a

permissible compressive stress limit,the compressive strength of the masonry is used to calculate the ultimate applied load. This is then reduced by the MEXE Condition and Joint Factors and a load factor of 3.0 to obtain the permissible axle or vehicle load.
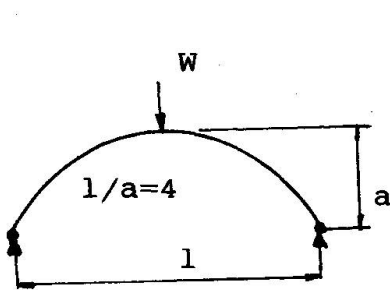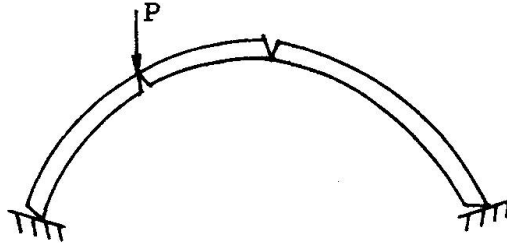
Fig.1 Pippard arch   **Fig.2** Failure mechanism

2.3 The Dundee Mechanism Method

The Mechanism Method, developed by Heyman [5], envisages that the arch shown in Fig.2 will, under increasing load, ultimately fail by forming the four hinges as shown. The method states that the line of thrust, i.e the line through the resultants of the compressive stresses in successive cross-sections of the arch, approaches the extrados and the intrados at the four potential hinge positions as the applied load increases. At the point of collapse, the thrust line touches the extrados and the intrados at the four points as shown in Fig.2. Since at these points moments are zero, it is possible to obtain the applied load which will cause the arch to collapse by taking moments of the reactions and forces about the hinge points, the system being statically determinate. The Heyman method assumes that the deformations are negligible and that the masonry has infinite compressive strength. The method also assumes that the surrounding fill only acts as vertical dead weight on the arch.

The Heyman method has been modified in a computer program by Harvey [6] of Dundee University to incorporate horizontal fill resistance. Since the method does not involve any elastic analysis, the fill resistance is applied as fixed fractions of the ultimate passive pressure of the soil.

2.4 The Cardiff Elastic Method

The Cardiff elastic method [7] is based on the Castigliano [8] method and involves an elastic analysis of the linear arch, the cross-section of which is successively reduced in order to eliminate the areas with tensile stresses. The Cardiff method employs a computer programme to carry out the necessary iterations at increasing levels of the applied live load. At the end of the iterations, at any load level, the resultant cross-section becomes as shown in Fig.3. The centre-line of the solid (uncracked) cross-section is also modified at each load level to take account of the deformations occurring up to that load. As the applied live load increases the deformations increase more rapidly as shown in Fig.4 until failure occurs.The Cardiff method assumes that the ultimate compressive strength of the masonry does not influence the analysis. The method represents fill resistance by a series of horizontal springs.

3. COMPARISONS WITH TEST RESULTS

3.1 The Full Scale Tests

Ten full-scale tests to collapse have been carried out under the supervision of the Transport Research Laboratory in order to provide a datum for comparing the merits of different assessment methods. These tests, involving carefully selected typical road bridges and two models, have been fully described by Page [3]. The more significant details of the ten bridges are given in Table 1. The arches were loaded with a line load across widths at quarter span positions as indicated in Fig. 3.
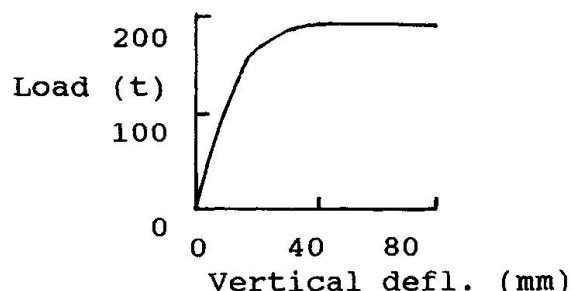
Fig.3 Section after thinning   **Fig.4** Cardiff load deflection

Bridge	Span	Rise	Ring	Width	Failure Loads (tonnes)		
	(m)	(m)	Th.(m)	(m)	Test	Castigliano	Mechanism	MEXE/Pippard
Bridgemill	18.30	2.85	.711	8.30	310	183	278	245
Bargower	10.36	5.18	.558	8.68	560	601	336	350
Preston	5.18	1.64	.360	8.70	210	184	130	181
Prestwood	6.55	1,43	.220	3.60	22	0	2	7
Torksey	4.90	1.15	.343	7.80	108	103	91	124
Shinafoot	6.16	1.19	.542	7.03	250	268	204	296
Strath'ie	9.42	2.99	.600	5.81	132	118	142	112
Barlae	9.86	1.69	.450	9.80	290	232	216	320
Dundee	4.00	2.00	.250	6.00	104	90	23	123
Bolton	6.00	1.00	.220	6.00	117	41	39	124

Table 1 Comparisons with test results

3.2 Comparisons

The three methods were used to calculate the collapse loads for the ten bridges which are given in Table 1. The methods took account of the different conditions and defects of the arches as far as these could be accommodated. It should be noted that the calculations were carried out with the knowledge of the test results. Some of the parameters required by the methods, for example some of the compressive strengths of the masonry, were not recorded for all the bridges. Such missing items had to be assumed for the calculations.

It can be seen that all three methods give generally safe results. However, regarding the two more advanced methods, the following features have been observed. Compared to the test results, the Cardiff method gives generally low capacities for the flatter arches. Many of the Dundee results are very low. Obviously no theoretical method can be expected to provide uniformly accurate collapse loads for bridges in different degrees of deterioration, some of which also contained special features such as internal spandrel walls. Nevertheless, the results of these two

methods for the two laboratory controlled model bridges and the Bridgemill bridge, all of which were in very good condition, are disappointing. The Pippard method gives both higher and lower results in equal numbers, the 'error' being mostly within +/- 20%, which is a desirable characteristic of an assessment method.

4. THEORETICAL INVESTIGATION

4.1 Failure Modes

In the first stage of the theoretical investigation a general frame analysis computer program MINIPONT, modified to carry out the Castigliano type elimination of the tensile part of the cross-section, was used to analyse the arch shown in Fig.5, the three loads P, W and R approximately representing the applied live load, the fill dead weight and the passive soil resistance respectively. At a typical longitudinal position (say X) the stress condition, derived from the bending moment and axial force present at that position, would be as shown in Fig.6, which also shows the position of the resultant thrust line in terms of its eccentricity 'e'from the intrados. The following three cases were analysed :-
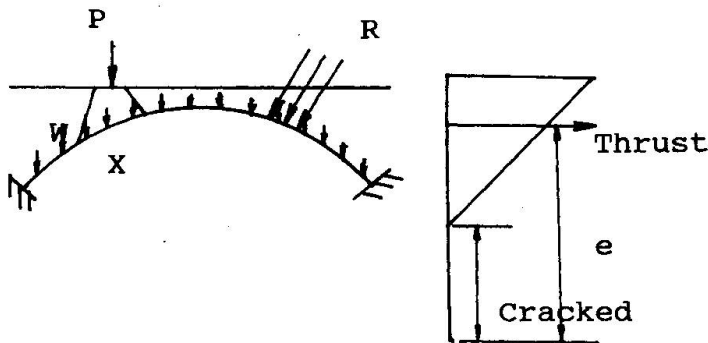
Case A : P increasing, W constant, R=0

Case B : P and R increasing in constant proportion, W=0

Case C : R increasing more slowly than P, W=0

The load deflection curves for the three cases are shown in Fig.7a and the changes of the thrust line eccentricity e is shown in Fig.7b.

Fig.5 Analysis loads   **Fig.6** Stress at X

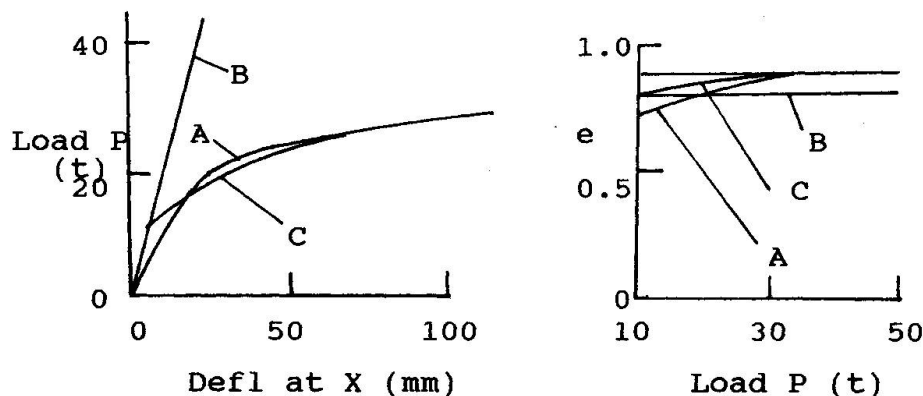Defl at X (mm)   Load P (t)

Fig.7a Load v deflection   **Fig.7b** Load v ecc.

In Case A, only one unknown load parameter is involved and any single position of the thrust line corresponds to a unique value of the applied load. The Mechanism method and the Cardiff method can both model this situation. In this analysis it has been assumed that the masonry has infinite crushing strength and the deflections have been assumed to be negligible.

In Case B, which represents a very rigid soil condition, the thrust line does not move as the loading increases and the failure can only be initiated by the

compressive stresses reaching a limit at successive parts of the longitudinal section. Since in such cases a single position of the thrust line can correspond to any magnitude of the applied loading, the Mechanism method is not strictly applicable. The Cardiff method is also not suitable because it does not consider (i.e. model) material crushing. However, more recently, finite element methods using line elements have been developed [9] for arch analysis which incorporate material crushing. Such a method would be suitable for this type of failure. The behaviour of the arch being linear, at least between successive hinge formations, the Modified Pippard method may also be appropriate for such cases, provided the compressive stresses developed in a cracked arch could be reasonably predicted by the non-thinning Pippard analysis, and the arches can be assumed to be pinned at the supports, which is probably quite realistic. It has been found in the above finite element analysis that the arch fails shortly after the the masonry crushes at the third hinge position, which is the limiting condition of the Modified Pippard method.

Case C represents a failing soil condition and the Cardiff method would be the only appropriate method in such cases. Although the failure is by forming a mechanism, more than one unknown load parameter is involved, which makes the Mechanism method unsuitable.

In the discussions above, deflections are assumed not to influence the arch behaviour. However, in theory at least, deflections added to the analysis as the load increases can speed up the collapse. However, for arch bridges of realistic dimensions, when the analysis was repeated in this manner this effect was found to be negligible. This is not to say that, for arches of more slender proportions, and especially for those without backfill, a deflection-aided failure can be precluded.

4.2 Finite Element Plane Stress Analysis

In order to examine which of the failure modes described above are likely to be relevant for typical highway arch bridges, a two-dimensional plane-stress finite element computer program SAFE [10] was used to analyse the ten test bridges with increasing applied load. All ten test bridges were idealised, as shown typically in Fig.8, and analysed for increasing load levels, approximately up to the test collapse loads. At each load level, iterations were performed to eliminate the areas with tension. In essence this analysis was identical to the Cardiff type
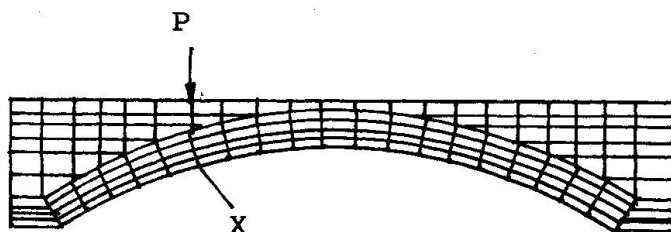

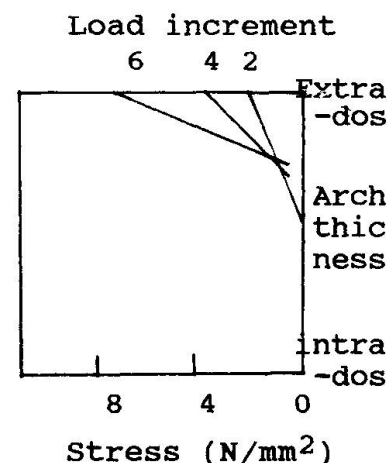Fig.8 Finite element plane stress idealisation

Fig.9 Stresses at X

analysis except that no simple linear stress distribution through the thickness of
the arch was assumed (i.e plane sections remaining plane). The soil model used in
the analysis was capable of yield in accordance with the Mohr Coulomb criterion.No
crushing strength limit was used. Deflection correction was also not used.Stress
distributions across the thickness at different load levels for one of the bridges
are shown in Fig.9. These indicate that the stress blocks are basically triangular
in shape and the extreme fibre compressive stresses are somewhat proportional to
the load increments. The thrust lines appear to move at the early stages of the
loading but then become stationary.

Comparisons of extreme fibre compressive stresses at the critical third hinge
position (X) between the plane stress finite element analysis and the modified
Pippard analysis are shown in Fig.10. This shows that in general there seems to be
a constant relationship between the two sets of stresses. It should be noted that
a lower Pippard stress could result in a potentially unsafe ultimate load estimate
since in the Modified Pippard method the ultimate capacity is almost inversely
proportional to the extreme fibre compressive stress. As the Modified Pippard
stresses are in general about 25% lower, this possibility could be eliminated if
a consistently conservative estimate of the masonry crushing strength is used in
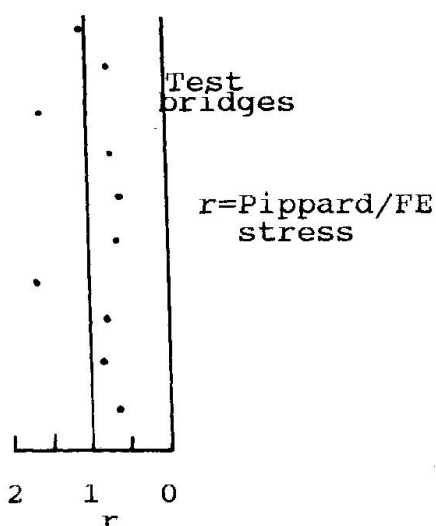the calculations.
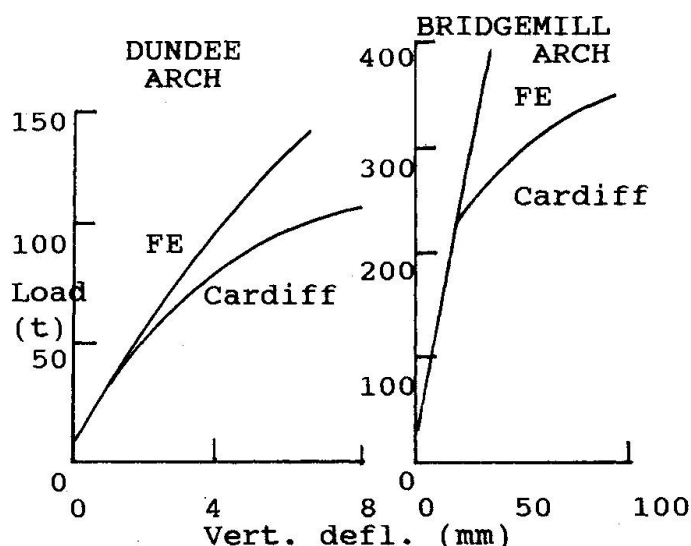
Fig.10 Stress comparison   Fig.11 FE-Cardiff comparisons

The finite element plane stress results show that, without a crushing strength
limit, and despite local passive yield of the fill, the load/deflection behaviour
remains almost linear.   This is shown in Fig.11 for two of the bridges.   This
figure also shows the load/deflection curves obtained from the Cardiff analyses
without deflection correction.   It should be remembered that the results from the
Cardiff analysis without deflection correction should be comparable to the finite
element plane stress analysis.

5. CONCLUSIONS

The finite element plane stress analysis results strongly indicate that fill
resistance increases proportionately with applied live loading and the behaviour
of a typical highway arch bridge is likely to be similar to that of Case B in 4.1.
As discussed earlier, both the Mechanism method and the Cardiff method are not
strictly applicable for the assessment of such situations although the simple
bending theory implicit in the Cardiff method seems to be confirmed by the

triangular stress distributions through the arch thickness given by the finite element plane stress analysis. A thinning method which eliminates the tensile areas of the cross-section and also able. to model crushing failure, would however be suitable. Furthermore, as shown in Fig.11, the Cardiff method produces failures in the arches without masonry crushing (the method does not consider this) which, according to the plane stress analysis, it should not. A possible reason for this may be that the horizontal soil spring idealisation used by the method does not adequately represent overall soil resistance. It has been observed from tests [11] that on the passive side of the arch, the vertical soil pressure also increases with load. The Cardiff method assumes this to be constant i.e, equal to the dead weight of the fill above per unit horizontal area. This could be the reason why the method gave poorer correlation for the flatter arches where vertical soil pressure might have greater influence.

The Modified Pippard method seems to predict realistic compressive stresses at the critical third hinge point, and hence may be used as a refinement of the empirical MEXE method.

ACKNOWLEDGEMENTS

REFERENCES

1. DTp Bridge Census and Sample Survey. Department of Transport, United Kingdom, 1987.

2. Departmental Advice Note BA 16/84 The Assessment of Highway Bridges and Structures. Department of Transport, United Kingdom, 1984.

3. Page J., Assessment of Masonry Arch Bridges. Proceedings of the Institution of Highways and Transportation National Workshop, Leamington Spa, 1990.

4. Pippard A J S., The Approximate Estimation of Safe Loads on Masonry Bridges, Civil Engineer in War. The Institution of Civil Engineers,London, 1948.

5. Heyman J.,The Masonry Arch. Ellis Horwood Limited, Chichester, United Kingdom, 1982.

6. Harvey W J., Application of the Mechanism Analysis to Masonry Arches. The Structural Engineer, Vol 66, No. 5, March 1988.

7. Bridle R J and Hughes T G., An Energy Method for Arch Brige Analysis. Proceedings of the Institution of Civil Engineers, London, Part 2, 1990.

8. Castigliano C A P., Theorie de l'Equilibre des Systems Elastiques et ses Applications. Augusto Federico Negro, Turin, 1897. Translated by Andrews E S., Elastic Stresses in Structures, Scot Greenwood and Son, 1919.

9. Choo B S et al., Finite Element Analysis of Masonry Arch Bridges Using Tapered Elements. Proceedings of the Institution of Civil Engineers, London, Part 2,1991.

10. Low A., Evaluation of Arch Bridge Analytical Techniques. Draft Contract Report, Transport Research Laboratory, Crowthorne, United Kingdom, 1992.

11. Melbourne C., Laboratory Tests on a 5m Span Brick Arch Bridge. Draft Report, Bolton Institute of Higher Education, Bolton, United Kingdom, 1992.

Rissbildung in gemauerten Kreuzgewölben

Crack Formation in Masonry Cross Vaults

Formation de fissures dans les voûtes en maçonnerie

Rainer BARTHEL
Dr. Ing.
Büro für Baukonstr.
Karlsruhe, Germany

R. Barthel, born 1955, received his Civil Eng. degree at the Techn. Univ. Karlsruhe and has been working in Karlsruhe and London on the structural design of new buildings and renovation of historical monuments.

ZUSAMMENFASSUNG

Aus Schadensaufnahmen werden typische Riss- und Schadensbilder in Abhängigkeit der Gewölbeform entwickelt. Die durchgeführten Finite-Element-Berechnungen berücksichtigen die Rissbildung infolge einer horizontalen Auflagerverschiebung. Bereits bei sehr kleinen Verschiebungen entstehen die als typisch erkannten Rissbilder. Durch Vergleich der errechneten Rissbilder mit den an Gewölben dokumentierten, lassen sich einerseits die Berechnungen kontrollieren, andererseits können die Rissbilder damit theoretisch erklärt werden. Ziel ist es, differenziertere Tragmodelle als bisher zu entwickeln, um daraus wirksamere und zurückhaltendere Instandsetzungsmassnahmen abzuleiten.

SUMMARY

Typical crack patterns depending on the various types of cross vaults are compiled and presented. The Finite Element Analysis simulates the crack formation due to horizontal displacements of the abutments. The typical crack patterns are created by very small displacements. The calculations can be checked by comparison of the simulated with the real crack patterns. On the other hand, the cracks can be explained theoretically by the analysis. The objective is to get a more detailed understanding of the statical behaviour of cross vaults in order to develop more effective and less drastic repair measures.

RÉSUMÉ

L'article présente un classement des modes typiques de fissuration en fonction de différents types de voûtes. La méthode par éléments finis permet de simuler la formation de la fissure résultant des déplacements horizontaux des culées. Les modes typiques de fissuration sont créés par de petits déplacements. Les calculs peuvent être contrôlés par comparaison de la simulation avec les fissures réelles. Il est aussi possible d'expliquer ces modes de fissuration de façon théorique par une analyse du développement des fissures. Le but de l'étude est d'obtenir une meilleure compréhension du comportement statique des voûtes afin de développer des mesures de réparation plus effectives et moins destructrices.

1. Einleitung

Bei der statischen Beurteilung von Kreuzgewölben treten in der Praxis immer wieder Unsicherheiten auf. Die Deutung von Schäden und die eindeutige Benennung ihrer Ursachen ist oft schwierig, da zu wenig über den Kraftfluß und dessen Abhängigkeiten von Form-, Konstruktions- und Materialparametern bekannt ist. Die Anwendung baustatischer Methoden der Berechnung wird erschwert durch die oft doppelt gekrümmte, dreidimensionale Form der Gewölbeflächen, den besonderen Materialeigenschaften des Mauerwerks sowie den Auflager- und Randbedingungen. So entscheidet man sich in der Praxis häufig zu Sicherungsmaßnahmen, die entweder nicht zum gewünschten Ziel führen oder allzu sehr auf der sicheren Seite liegen und damit aufwendiger und teurer als nötig sind.

In einem von der DFG geförderten Forschungsprogramm wurden Berechnungen mit der FE-Methode durchgeführt (1). Deren Ziel war es, für einige Grundtypen von Kreuzgewölben realistischere Tragmodelle als bisher zu entwickeln, um damit eine Grundlage für gezieltere und zurückhaltendere Sicherungsmaßnahmen zur Verfügung zu stellen.

2. Einige Grundformen der Kreuzgewölbe

Aus der nahezu unendlichen Vielfalt der existierenden Gewölbeformen werden vierteilige Kreuzgewölbe über rechteckigem oder quatratischen Grundriß für die näheren Betrachtungen ausgewählt. Für vergleichende Untersuchungen und eine numerische Erfassung werden vier geometrische Grundformen theoretisch definiert (Bild 1).

a) Kreiszylindrisches Kreuzgewölbe

b) Kreuzgewölbe mit geraden Scheiteln (halbkreisförmige Kreuzbögen, spitzbogige Gurt- und Schildbögen, gleiche Scheitelhöhen. Kappen sind leicht verwundene Flächen mit geraden Höhenlinien).

c) Kreuzgewölbe mit gebusten Kappen (Geometrie der Bögen wie bei b)

d) Kuppelartiges Kreuzgewölbe (Gurt- und Schildbogen mit niedrigeren Scheiteln)

Alle Gewölbe außer dem kreiszylindrischen sind über allen rechteckigen Grundrissen möglich. Der Vergleich der Höhenlinienverläufe zeigt, wie unterschiedlich die Gewölbeformen schon bei dieser engen Auswahl von Varianten ist.

3. Typische Schäden

Die für die jeweilige Gewölbeform typischen Schadensbilder werden zum einen mit Hilfe von Schadensdokumentationen realer Gewölbe und zum anderen aus den unten vorgestellten Ergebnissen der FE-Berechnungen ermittelt. Zahlreiche Schadensaufnahmen und Gutachten von Architektur- und Ingenieurbüros sowie selbst erstellte werden ausgewertet. Die Berechnungen helfen, die typischen Rißbilder zu erkennen und zunächst nicht erklärbare oder zufällig erscheinende Risse theoretisch nachzuvollziehen.

Die häufigste Ursache für Schäden und Risse ist das Nachgeben der Auflager infolge der horizontalen Gewölbekräfte. In einer Reihung von Gewölben, wie z.B. in einem Kirchenschiff, bedeutet dies die Vergrößerung der Spannweite bei gleichbleibender Gewölbebreite. Auf diesen Fall werden alle weiteren Betrachtungen konzentriert.
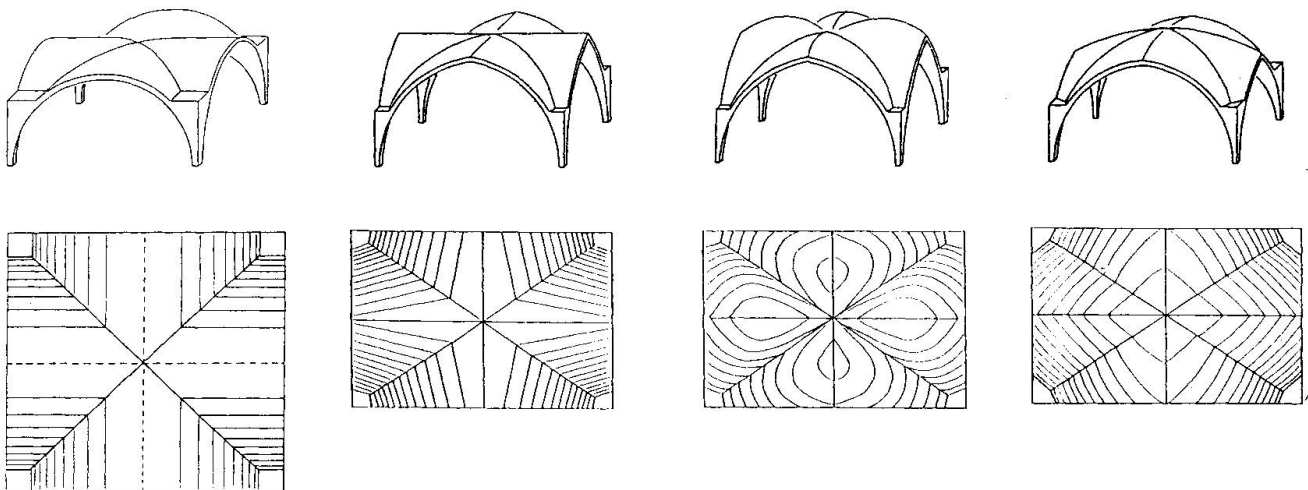
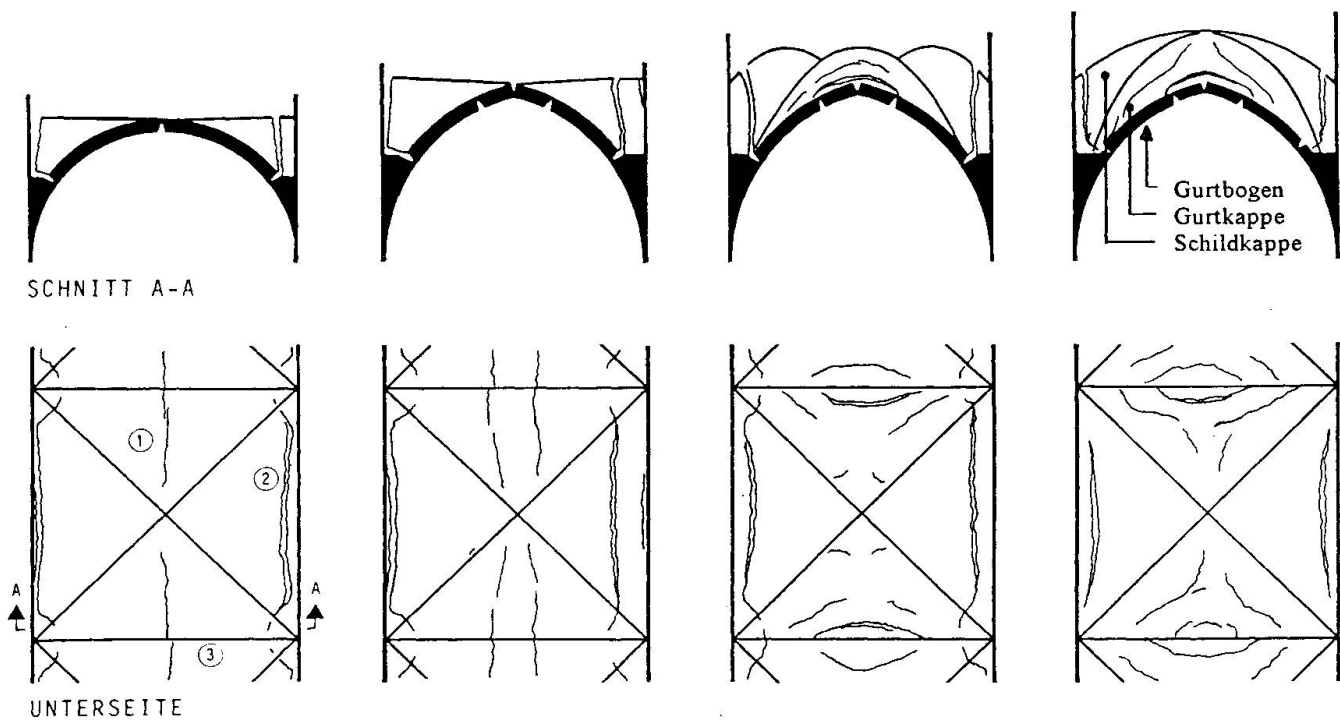Bild 1: Vier Grundformen der Kreuzgewölbe, Höhenlinien

SCHNITT A-A

Gurtbogen
Gurtkappe
Schildkappe

UNTERSEITE

Bild 2: Typische Rißbilder infolge einer horizontalen Auflagerverschiebung

3.1 Rißbilder

Aufgrund der fehlenden Zugfestigkeit des Mauerwerkes zergliedert sich das Kappenmauerwerk durch Abrisse und Gelenkbildungen in einzelne Teile. Es entsteht dabei ein Dreigelenkmechanismus, der als statisch bestimmtes System den Auflagerverschiebungen folgt und als Rißbild erkennbar ist.

Der einfachste Bewegungsmechanismus bildet sich am kreiszylindrischen Kreuzgewölbe. Es entstehen ein unten klaffender Biegeriß entlang den Gurtkappenscheiteln und oben klaffende Biegerisse in Auflagernähe. Außerdem reißen die Schildkappen von den Schildwänden ab. Da die Gewölbeteile an den Biegerissen relativ zueinander Rotationen erfahren, können diese Stellen als Gelenklinien bezeichnet werden. Damit entsteht wie in einem Tonnengewölbe ein Dreigelenksystem ohne innere Zwängungen (Bild 3).

In den doppelt gekrümmten Gurtkappen des gebusten und kuppelartigen Kreuzgewölbe bilden sich Abrisse von den Gurtbögen . Ein Gelenkmechanismus wie beim Tonnengewölbe oder wie am kreiszylindrischen Kreuzgewölbe mit geradlinigen und zueinander parallelen Gelenklinien kann sich hier wegen den gekrümmten Scheitellinien nicht einstellen. In Bild 4 ist ein möglicher Bewegungsmechanismus dargestellt, wie er sich aus den FE-Berechnungen herleiten läßt. Der niedrigere Kappenbereich entlang des Gurtbogens senkt sich bei einer Auflagerverschiebung mehr als der höhere Mittelteil und reißt von diesem ab. Jeder Kappenteil bildet ein eigenes Dreigelenksystem. Mit diesem Modell lassen sich die Rißbilder an kuppelartigen Gewölbe deuten.
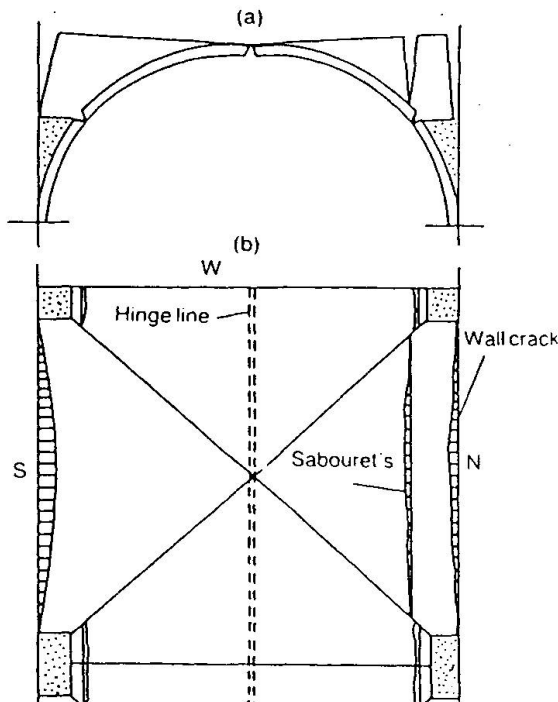
Bild 3: Bewegungsmechanismus am kreiszylindrischen Kreuzgewölbe infolge einer Auflagerverschiebung, aus (2)
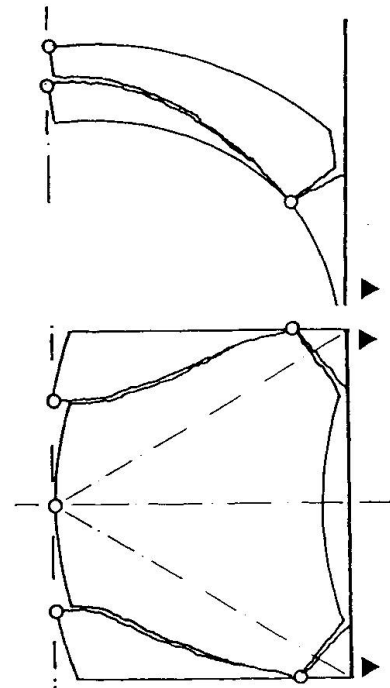
Bild 4: Bewegungsmechanismus am kuppelartigen Kreuzgewölbe

3.2 Schäden an den Rippen

Grundsätzlich sind Rippen mit schubsteifer Verbindung zu den Kappen von Rippen ohne schubsteife Verbindung zu den Kappen zu unterscheiden. Als schubsteife Verbindung kann gelten, wenn z.B. Rippenformsteine auch Teil des Kappenmauerwerkes sind und mit diesem im Verband gemauert sind.

Im Fall einer solchen schubsteifen Verbindung ergeben sich bei einer Auflagerverschiebung große Schäden am unteren Gelenk. Das Gelenk bildet sich nicht in der Kappe, sondern punktförmig an der Vorderkante der Kreuzrippe. Druck- und Querzugversagen der Rippensteine infolge hoher Kantenpressungen führen dann jedoch oft zu einer lokalen Zerstörung der Rippe und einer Zurückverlagerung des Gelenkes in die Kappen.

Im weitaus häufigeren Fall ohne starre Verbindung zu den Kappen, sind Risse zwischen Kappe und den Rippensteinen typisch. Oft sind Rippen, die zwar ins Kappenmauerwerk einbinden aber nicht verankert sind, deutlich herausgezogen. Schlußsteine sind häufig abgelöst. Abplatzungen der Rippenvorderkanten gibt es in Auflagernähe, im Bereich des Schlußsteines teilweise an der Oberseite der Rippensteine.

4. Berechnungen

4.1 Idealisierung und Annahmen

Mit der FE-Methode werden einige der Grundformen unter dem Lastfall Eigengewicht und dem Lastfall Eigengewicht plus Auflagerverschiebung berechnet. Verwendet wird das Programm ADINA. Das darin zur Verfügung stehende Materialgesetz für Beton wird an die Eigenschaften des Mauerwerks angepaßt. Folgende Randbedingungen und Annahmen werden getroffen:

Geometrie: Um die Ergebnisse vergleichen zu können, wird bei allen Berechnungen die Spannweite *s* auf 10m und die Gewölbedicke *d* auf 25cm festgelegt. Die kleine Spannweite bzw. die Jochbreite *b* wird variiert. Es werden die Grundrißverhältnisse *s/b* gleich 1/1, 3/2 und 2/1 berechnet.

Randbedingungen: Das Gewölbe ist, wie in einem Kirchenschiff, Glied einer Gewölbereihe mit den entsprechenden Symmetriebedingungen entlang den Gurtbögen. Die Höhe des rechnerischen Auflagers wird auf die halbe Scheitelhöhe festgelegt. Damit werden ca.95% der Gewölbefläche berücksichtigt, da der verbleibende, nicht berücksichtigte Zwickel sehr schmal ist.

Material: Vorgegeben wird eine nicht-lineare Spannungs-Dehnungsbeziehung im Druckbereich, ein Tangentenmodul von 3000 MN/m² und eine auf 60 kN/m² begrenzte Zugfestigkeit. Das spezifische Gewicht ist 20 kN/m³, die Querdehnzahl 0,25. Die Orthotropie wird nicht berücksichtigt. Berechnungen am kreiszylindrischen Kreuzgewölbe zeigen, daß er gering ist.

Elementmodell: Es werden Volumenelemente mit je 20 Knoten mit kubischem Ansatz in teilweise zweilagiger Schichtung übereinander verwendet. Damit können tief klaffende Biegerisse und Kantenpressungen simuliert werden.

4.2 Kreiszylindrisches Kreuzgewölbe

Die Spannungstrajektorien im Lastfall Eigengewicht zeigt Bild 5. Sie verlaufen nicht geradlinig zum Kreuzbogen, wie man es bei einer Stützlinienberechnung annehmen würde, sondern werden schon weit oben in Richtung Auflager abgelenkt. Nahezu die gesamte Kappe steht unter einem biaxialen Druckspannungszustand. Die Spannungen liegen überall weit unterhalb der Bruchspannung von Mauerwerk.

Das Gewölbe reagiert sehr stark auf Auflagerverschiebungen. Schon während des ersten Millimeters entstehen alle typischen Risse und die Auflagerkraft wird kleiner (Bild 6). Nach zwei Millimeter Verschiebung beträgt die resultierende Horizontalkraft nur noch knapp 75% der ursprünglichen. Bei weiteren Verschiebungen ändert sie sich nur noch wenig. Die Spannungstrajektorien zeigen gegenüber denen des Lastfalles Eigengewicht einen völlig veränderten Verlauf. Es entsteht im wesentlichen das Rißbild, welches dem Dreigelenkmechanismus in Bild 3 entspricht. Der Biegeriß am Scheitel ist bereits von unten her über zwei Drittel des Querschnittes aufgerissen. In diesem Zustand tritt entlang den als "Gelenklinien" bezeichneten Bereichen noch keine Plastifizierung ein. Es handelt sich somit eher um "elastische Gelenke" als um "plastische Gelenke".

Das Ergebnis für die resultierende Horizontalkraft läßt sich mit Ergebnissen anderer Berechnungsansätze vergleichen, die allerdings alle die Größe der Auflagerverschiebung nicht berücksichtigen (Bild 7): Für den Lastfall Eigengewicht stimmt das Ergebnis der FE-Berechnung sehr gut mit dem von Heyman (3) überein. Eine Stützlinienberechnung, ausgehend von Bögen entlang den Fallinien, ergibt wesentlich niedrigere Werte. Bei zunehmender Auflagerverschiebung nimmt die Horizontalkraft ab und nähert sich dem theoretischen Grenzwert, der sich bei Vorgabe von Gelenken mit einer Ausmitte von $d/2$ rechnerisch ermitteln läßt. Der Wert von Pieper (4), der von einer aus Erfahrung festgelegten Gelenklage ausgeht, liegt etwas höher als das Ergebnis der FE-Berechnung. Die Reduzierung der resultierenden Auflagerkraft infolge kleiner Auflagerverschiebungen ist für den Nachweis bestehender Gewölbe von Bedeutung.
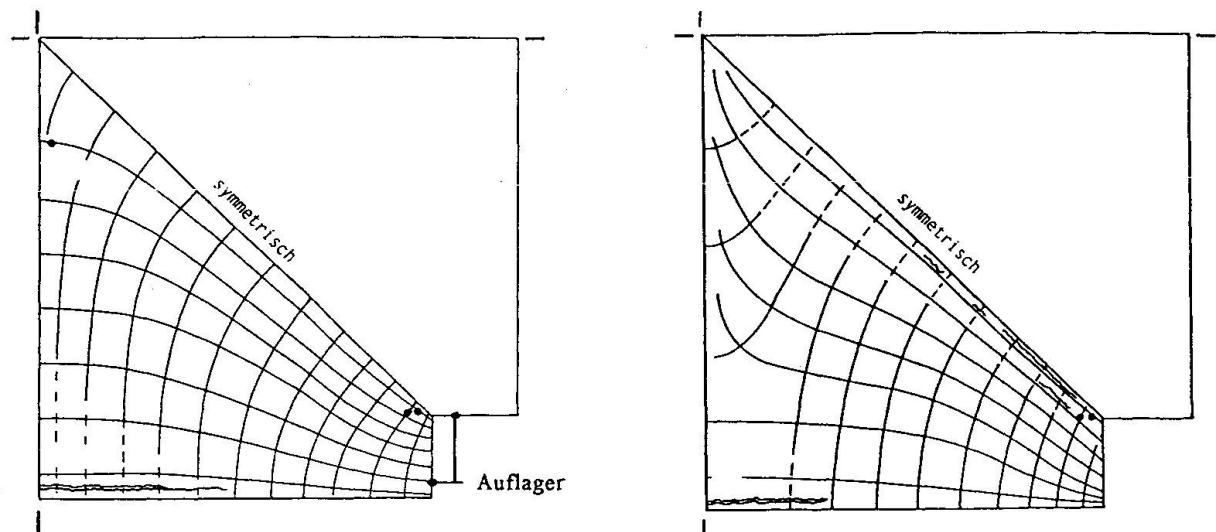
Bild 5: Spannungstrajektorien am kreiszylindrischen Kreuzgewölbe bei starren Auflagern
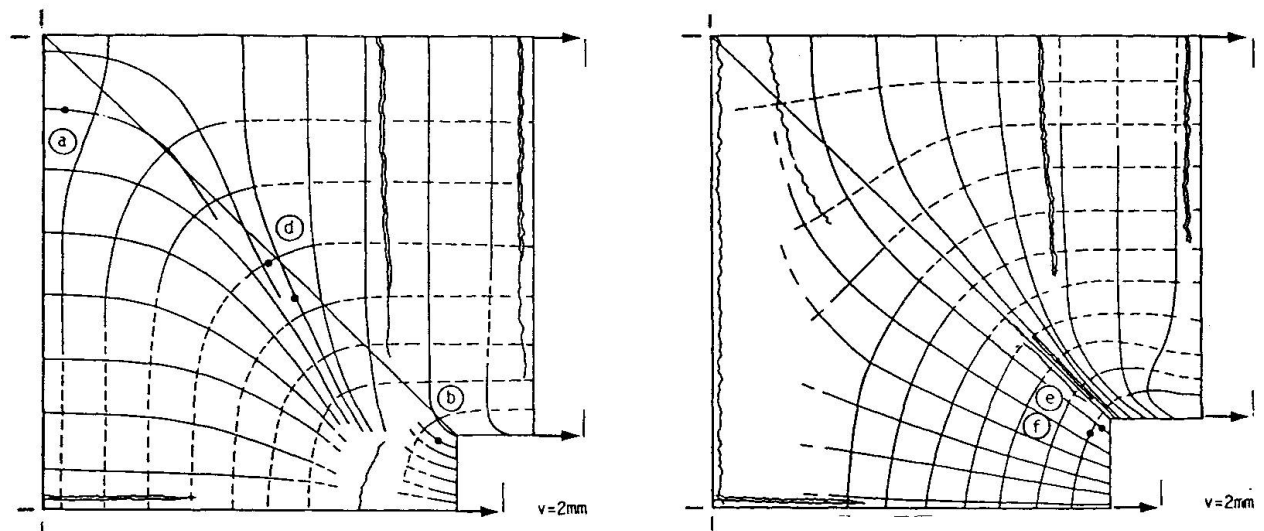a) Oberseite b) Unterseite

Bild 6: Spannungstrajektorien und Risse am kreiszylindrischen Kreuzgewölbe infolge einer Auflagerverschiebung a)Oberseite b) Unterseite
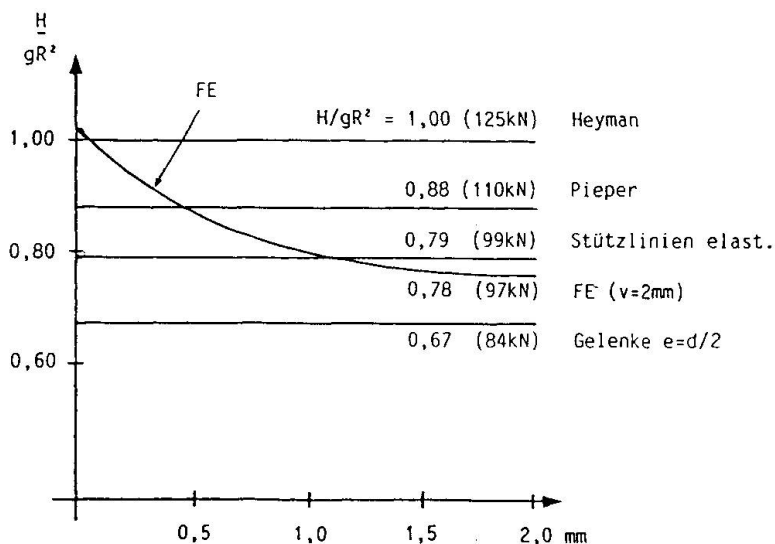

Bild 7: Resultierende Horizontalkraft H am kreiszylindrischen Kreuzgewölbe in Abhängigkeit der Auflagerverschiebung, Vergleich mit anderen Berechnungsergebnissen (g...Gewicht pro Flächeneinheit, R... Krümmungsradius der Kappen, Werte in Klammern für Gewölbedicke d=0,25m, R=5m, γ=20 kN/m²)

4.3 Kuppelartiges Kreuzgewölbe

Liegen die Scheitel der Gurtbögen nicht sehr viel tiefer als der Kreuzbogenscheitel, so ist der Kräftefluß im Lastfall Eigengewicht ähnlich dem des Kreuzgewölbes mit geraden Scheiteln. Erst bei einer Auflagerverschiebung wird ein wesentlicher Unterschied sichtbar. In der Gurtkappe entstehen Risse parallel zum Gurtbogen (Bild 8). Der höhere Teil trennt sich vom niedrigeren Teil der Gurtkappe. Desweiteren konzentrieren sich die Spannungstrajektorien sehr stark entlang dem unteren Teil des Gurtbogens. Es bildet sich der beschriebene Bewegungsmechanismus mit den typischen Rissen (Bild 4). Im gewählten FE-Modell läßt sich das untere Gelenk nicht vollständig simulieren.
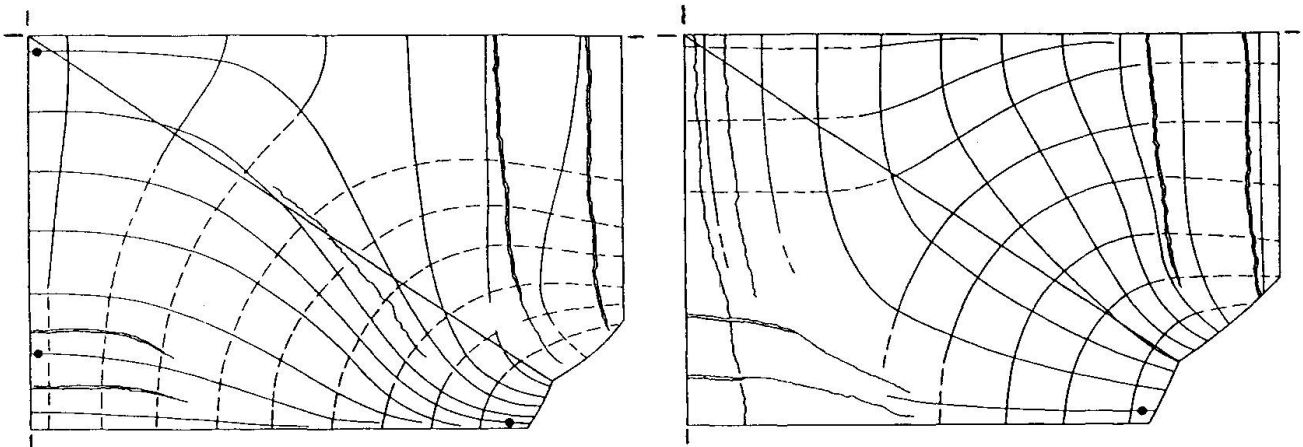

Bild 8: Spannungstrajektorien und Risse am kuppelartigen Kreuzgewölbe infolge einer Auflagerverschiebung a) Oberseite b) Unterseite

4.4 Gebustes Kreuzgewölbe

Der Spannungsverlauf steht in keinem direkten Zusammenhang mit dem Verlauf der Höhenlinien. Die Kräfte laufen über die Scheitellinien hinweg, ohne daß die Busung der Kappen an ihrem Verlauf direkt erkennbar wäre. Anders als bei den anderen Gewölben konzentrieren sich die Kräfte deutlich entlang dem Kreuzbogen.
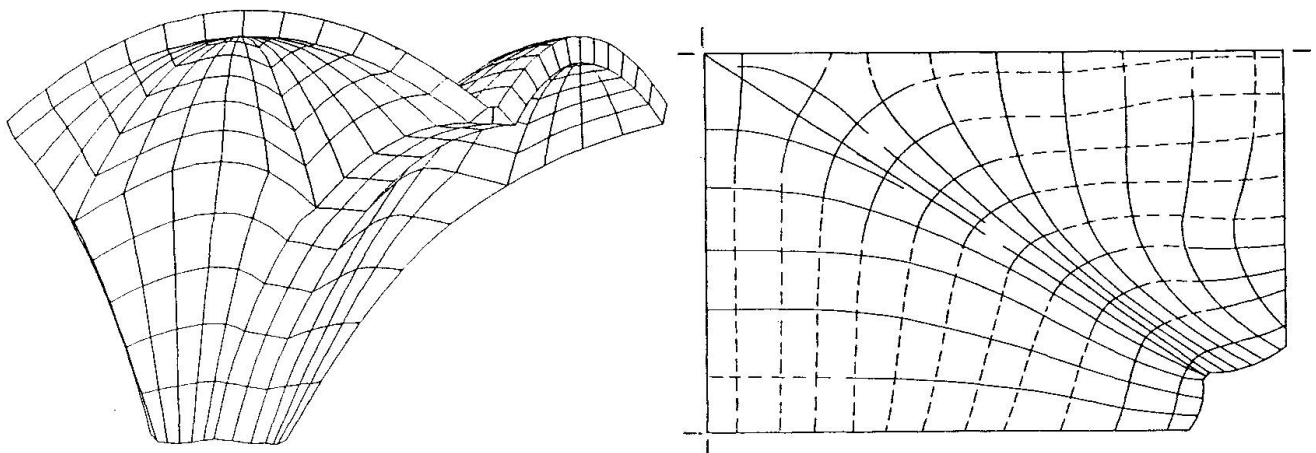

Bild 9: Kreuzgewölbe mit gebusten Kappen a) Elementnetz b) Spannungstrajektorien an der Oberseite

4.5 Tragwirkung der Rippen

Eine mit den Kappen schubsteif verbundene Rippe wird durch zusätzliche Balkenelemente entlang dem Kreuzbogen des kreiszylindrischen Kreuzgewölbes berücksichtigt. Erst bei einer unrealistisch

hohen Dehnsteifigkeit wird ihr Einfluß signifikant. So werden z.B. bei Annahme einer Sandsteinrippe mit einer Querschnittsfläche von A = 45x45cm und einem Elastizitätsmodul von E = 10000 MN/m² die Spannungstrajektorien zwar deutlich von der Rippe angezogen, aber sie verlaufen immer noch nicht geradlinig zu ihr hin, wie es bei einer Stützlinienberechnung angenommen wird.

Das Zusammenwirken einer nicht schubsteif mit den Kappen verbundenen Rippe wird an einem vereinfachten Ersatzsystem untersucht (Bild 10). Zwischen zwei parallelen, übereinanderliegenden Bögen wird eine Kontaktfläche definiert, welche zwar Druckkräfte, aber keine Zug- und Schubkräfte überträgt. Reibung wird zunächst nicht berücksichtigt. Bei einer Auflagerverschiebung entsteht in jedem Bogen für sich ein Dreigelenkmechanismus. Da sich der untere Bogen etwas mehr senkt als der obere, entsteht zwischen beiden ein dünner Spalt im oberen Bereich. Bedeutender sind aber die gegenseitige Verschiebungen der Bögen zueinander, die sich zwischen dem oberen und unteren Gelenk einstellen, und an wirklichen Gewölben in Form von Rissen zwischen Rippe und Kappe in Erscheinung treten.
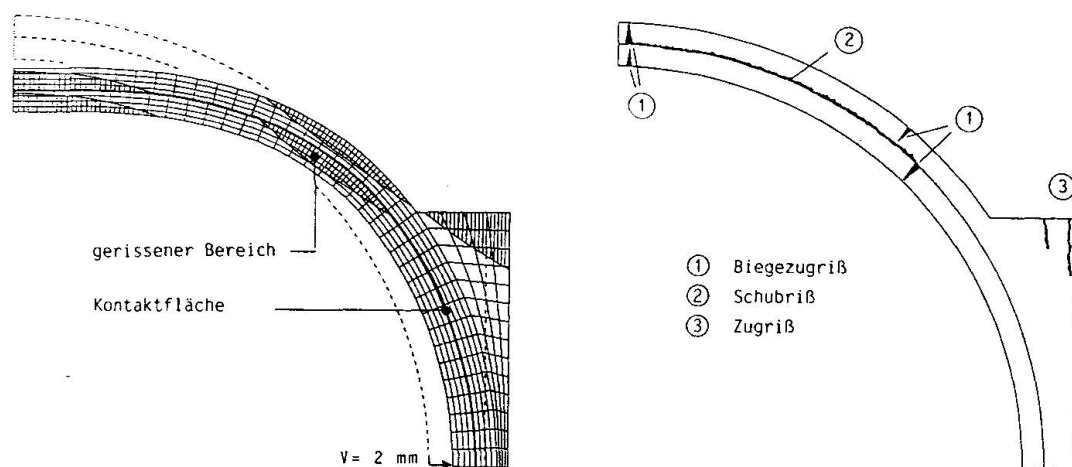

gerissener Bereich

Kontaktfläche

V = 2 mm

① Biegezugriß
② Schubriß
③ Zugriß

Bild 10: Zwei Bögen mit Kontaktfläche a) Elementnetz b) Rißverlauf

4.6 Standsicherheit

Alle in diesem Rahmen untersuchten Kreuzgewölbe sind standsicher. Die typischen Risse, wie sie bei den berücksichtigten Auflagerverschiebungen entstehen, stellen keine Beeinträchtigung der Standsicherheit des Gesamtgewölbes dar. Vielmehr ist der auf diese Art gerissene Zustand der eigentliche Gebrauchszustand der Gewölbe. Eine Gefährdung der Gesamtstabilität tritt erst bei wesentlich größeren Verschiebungen ein. Bei sich wiederholenden kleinen Auflagerverschiebungen können die beschriebenen Risse jedoch Ausgangspunkt für lokale Gefährdungen sein. Teile entlang den Rißufern können sich lockern und abstürzen. Größere Risse in den Schildkappen, die meist schon beim Ausrüsten entstanden, sind oft mit Steinen und Mörtel ausgestopft und sind gefährdet. Hohe Kantenpressungen an Rippensteinen können zum Versagen ganzer Steine führen. Rippen ohne Verbindung zu den Kappen können dadurch abstürzen. Derartige Schäden können mit lokal begrenzten Maßnahmen behoben werden. Mit Hilfe von differenzierten Tragmodellen lassen sich in vielen Fällen größere Sicherungsmaßnahmen, wie Zuganker im Kirchenschiff oder Spritzbetonschalen auf den Kappen, vermeiden.

Literaturverzeichnis

1.   Barthel R., Tragverhalten gemauerter Kreuzgewölbe. Aus Forschung und Lehre, Institut für Tragkonstruktionen, Universität Karlsruhe, 1993.
2.   Heyman J., Poleni's problem. Proc Instn Civ. Engrs, Aug 1988.
3.   Heyman J., The Stone Skeleton. Int.Journal of Solids Structures, Vol. 2 1966.
4.   Pieper K., Sicherung historischer Bauten, 1983.

Structural Assessment of the Leaning Tower of Pisa

Evaluation structurale de la Tour penchée de Pise

Einschätzung des Tragvermögens des Schiefen Turms von Pisa

Giorgio MACCHI
Professor
Univ. of Pavia
Pavia, Italy

G. Macchi has been Dir. of the Inst. of Construction, Fac. of Archit., Venice, from 1970 - 73, and became then Dean of the Fac. of Eng., Univ. of Pavia, where he is now Professor.

Marina EUSEBIO
Civil Engineer
ISMES
Bergamo, Italy

M. Eusebio, born 1961, received her degree at the Polytechnic of Milano. Her main interests are related to numerical analysis of civil structures.

Giovanni RUGGERI
Civil Engineer
ISMES
Bergamo, Italy

G. Ruggeri, born 1955, received his degree at the Polytechnic of Milano and is now Head of the Mathematical Modelling Dep. of ISMES.

Marco MONCECCHI
Civil Engineer
ISMES
Bergamo, Italy

M. Moncecchi, born 1965, received his degree at the Univ. of Pavia. His main interests are related to numerical analysis of civil structures.

SUMMARY

The safety of the Leaning Tower of Pisa requires preventive structural measures and their assessment on adequate models of the structure. Several models of analysis are compared and the inadequacy of the most simplified methods is proved, particularly in the interpretation of the role of the colonnade. The temporary prestressing at the first loggia is described and justified.

RÉSUMÉ

Le maintien de la sécurité de la Tour penchée de Pise nécessite des interventions au niveau structural par l'évaluation de modèles adéquats de la structure. Plusieurs modèles d'analyse sont comparés et l'inadéquation de méthodes les plus simples est démontrée, particulièrement dans l'interprétation du rôle de la colonnade. La précontrainte temporaire au niveau de la première loggia est décrite et justifiée.

ZUSAMMENFASSUNG

Die Sicherheit des Schiefen Turms in Pisa verlangt Eingriffe in die Gebäudestruktur und ihre Bewertung mittels geeigneter struktureller Modelle. Verschiedene Analysemodelle werden verglichen, und die Untauglichkeit der einfachsten Methoden wird dargestellt, insbesondere was die Funktionsbestimmung der Säulen betrifft. Die provisorische Vorspannung in der Ebene der ersten Loggia wird beschrieben und begründet.

1. INTRODUCTION

The increasing tilt of the Tower of Pisa* (the inclination is more than 5 degrees Southward) is causing a dangerous increase of the state of stress of the masonry in elevation.

The inclination, due to differential settlement of the subsoil, was already outstanding at the end of the construction, which took place from 1173 to 1370; the inclination was continuously growing in the following 600 years, and its rate, which was 3 seconds per annum in 1945, was estimated 6 seconds in 1990, and shows evidently a dangerous acceleration towards an overturning which apparently is not far. Moreover, as a consequence of the inclination, at the Northern edge of the cross section the vertical stress is near to zero, and the compression on the masonry is extremely high at the Southern edge.

The risk of a sudden compression failure of masonry (similar to the case of the Civic Tower in Pavia, 1989) is at least as high as the risk of overturning for a failure in the subsoil; and the state of stress is slightly increasing every day.

The cylindrical wall of the Tower is not homogeneous; between two marble linings of not constant thickness (between 250 and 400 mm) the core of the wall is made of rubble stones bonded with lime mortar (Fig.1).

The danger is particularly high at the level of the first *loggia*, where the section of the wall is substantially reduced by the helicoidal stairs and by local cavities. Moreover, the very stiff marble facing is pressing the underlying rubble masonry with a very high compressive stress (Fig.2). In the same zone, 2 long vertical cracks have been recently found on the external facing; they may be a sign of splitting under vertical compression. Finally, the presence of radial tensile stresses caused several circumferential cracks in the ceiling and on the steps of the stairs.

Such a complex state of stress had to be carefully analyzed in order to ascertain the present risk of structural collapse, and provide a sound basis for the temporary strengthening of the elevation (circular prestress, applied in 1992).

The analysis has been first performed on the critical zone, and then on the entire body of the Tower subject to self weight, wind, circular prestress, and on the structure affected by cracks and damages in the colonnade.
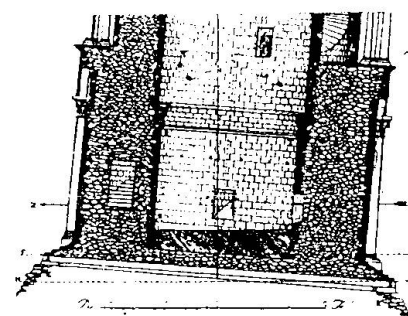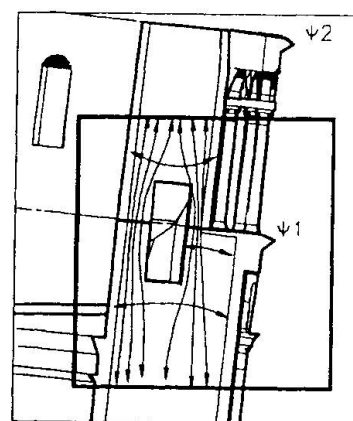

Fig.1 - Internal structure of the Tower

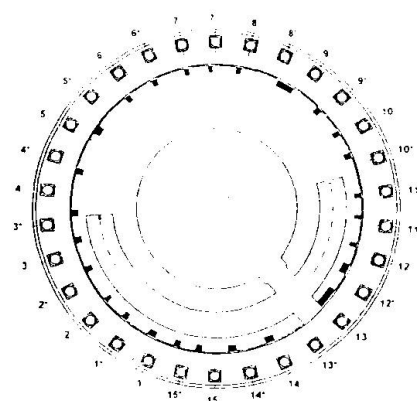Fig.2 - Critical zone of the Tower at the first loggia
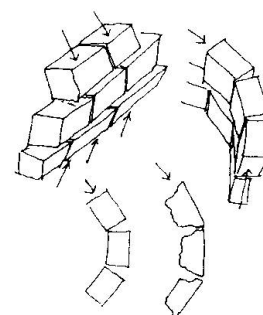

Fig.3 - Buche pontaie (recesses) at the first loggia

Fig.4 - Facing failure mechanisms

---

* The structural assessment of the Leaning Tower was carried out by the Consorzio Progetto Torre di Pisa (BONIFICA - ISMES - ITALSONDA - RODIO - TREVI).

The present report deals with the studies and interventions done by the International Committee installed in 1991 by the Italian Government for the safeguard of the Tower, after the closure which followed the collapse of the Civic Tower in Pavia. Frequent reference is made to investigations and computations published by previous Commissions, [1, 2, 3], since 1838. Very little consideration was previously given to the structural strength, even in the report 7 of 1988, where the previous Project Team described the stabilization project which was proposed at the time.

2. STATE OF STRESS AND STRENGTH AT THE FIRST LOGGIA

The recognition that a structural strengthening was urgently needed led the new Committee to conceive a reversible temporary prestress, dimensioned by preliminary analysis of state of stress; in the mean time, the refined 3D analysis was prepared.

The preliminary design was based on two simple approaches:
- a conventional linear elastic beam approach;
- a local bidimensional Finite Element analysis.

Both approaches were based on the existing knowledge 3 of the geometry and of the material densities of the Tower, as the refined survey could not by ready within the first year.

An evaluation of the ratio between the elastic moduli E of the marble facing and the rubble masonry was needed. The modulus of the facing was derived by previous tests done with double flat-jacks, and assumed to be E=50000 MPa. The modulus of the inner masonry was taken from dilatometer tests previously performed in some cores (direct tests on the cored material were not reliable) and was evaluated E=7000 MPa. Nevertheless the consideration of extreme values of the experimental results led to modular ratios ranging from 4.5 to 16.7, so that a sensitivity analysis was done; the possible error around the mean values of the stresses was estimated 25% in the facing and 35% in the inner masonry.

Corings operated by previous Commissions 3 proved that the internal masonry is interrupted by several cavities; nevertheless, coring in the critical zone was considered dangerous, so that a local evaluation of the quality of the masonry was only based on non-destructive tests (sonic tomography, radar measurement across the wall, thermography). The results were alarming, but could not provide any further precise information for a non-homogeneous modelling of the masonry.

However, a very important local deficiency as been well documented and was taken into account: a presence of 27 large recesses (the mean size was approximately 360x230x200 mm), the *buche pontaie*, left at the level of the first loggia during construction, for the accommodation of the scaffolding (Fig.3). Such recesses reduce by 18% the resisting horizontal section of the marble facing, and increase by 13% the edge stresses under permanent load.

The contribution of the colonnade has been neglected in this phase (if perfectly connected, with its high modulus of elasticity, it would considerably increase the moment of inertia of the critical section; its role will be discussed later on).

Taking into account the recesses (but not yet the internal cavities) the conventional linear elastic beam approach led to the following values of the vertical compression in the maximum lean plane:
- in the marble facing: σ_z max = 7.6 MPa
- in the rubble masonry: σ_z max = 1.1 MPa

Such values may not appear excessive for good marble stones and for good masonry. However, the situation is alarming. In fact:

- the marble stones of the facing have normally only a limited contact at the bedjoints; this may highly increase the local stresses or allow local buckling (Fig.4);
- the strength of the internal rubble masonry is highly dependent on the quality of the mortar, and very little on the strength of the undressed stones; its knowledge is insufficient at the time (it has been differently estimated by different Committees on the basis of few tests, but 4 MPa seems to be a reasonable conservative compressive strength; dilatometric tests showed cases of high permanent strain at 5 MPa);
- the uncertainty of the modular ratio may lead to values 35% higher than calculated; the cavities reduce the local strength;
- concentration of stresses near the openings may lead to premature failure (the collapse in Pavia occurred under a mean compression of 1.1 MPa, when the masonry mean strength was 2.8 [5]).

However, the main concern is due to the high pressure that the external marble facing applies on the underlying masonry, through a marble slab only 160 mm thick (Fig.2). Therefore, a more detailed study of the state of stress in that region has been carried out by Plane Strain Finite Element analysis (Fig.5).

Where the marble facing is pressing on the pavement of the loggia a vertical stress of 5.9 MPa was found, and under it, in the infil masonry, 3.0 MPa, value which is approaching the estimated strength. Radial tensions up to 0.3 MPa were found on the steps and roof of the helicoidal stairs, and may explain the existing circular cracks.

In order to provide an increased margin of safety of the elevation of the Tower during the envisaged intervention on the foundations, a temporary and reversible circumferential prestress of the critical zone has been studied in 1991 by Macchi and Leonhardt, and implemented by VSL/Preco in 1992 (Fig.6).

A circumferential prestress of 2100 KN is applied by 18 0.6" unbonded strands, specially anchored. The intervention creates a slight state of multiaxial compression, and so slightly increases the strength to vertical compression of the infil and of the facing; it counteracts and it provides also a passive strength preventing external local spalling or dilatation in critical zones.

3. GLOBAL ANALYSIS

A Finite Element 3D global analysis has then provided, in 1992, a comprehensive knowledge of the effects of permanent loads, wind, and circumferential prestress, which were only imperfectly known through the preliminary studies. Under the guidance of the Committee, ISMES first built a numerical
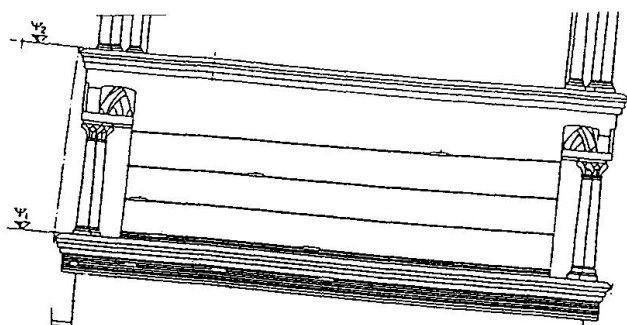
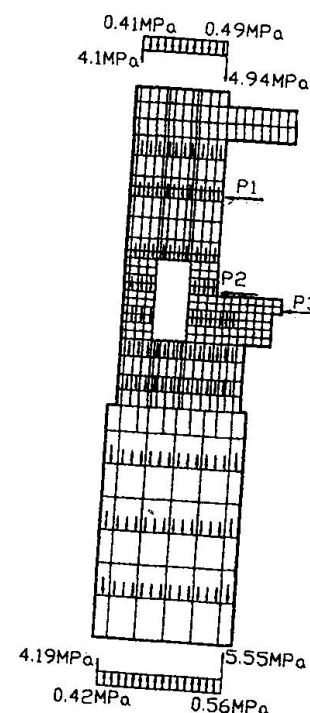*Fig.6 - Circumferential temporary prestress*

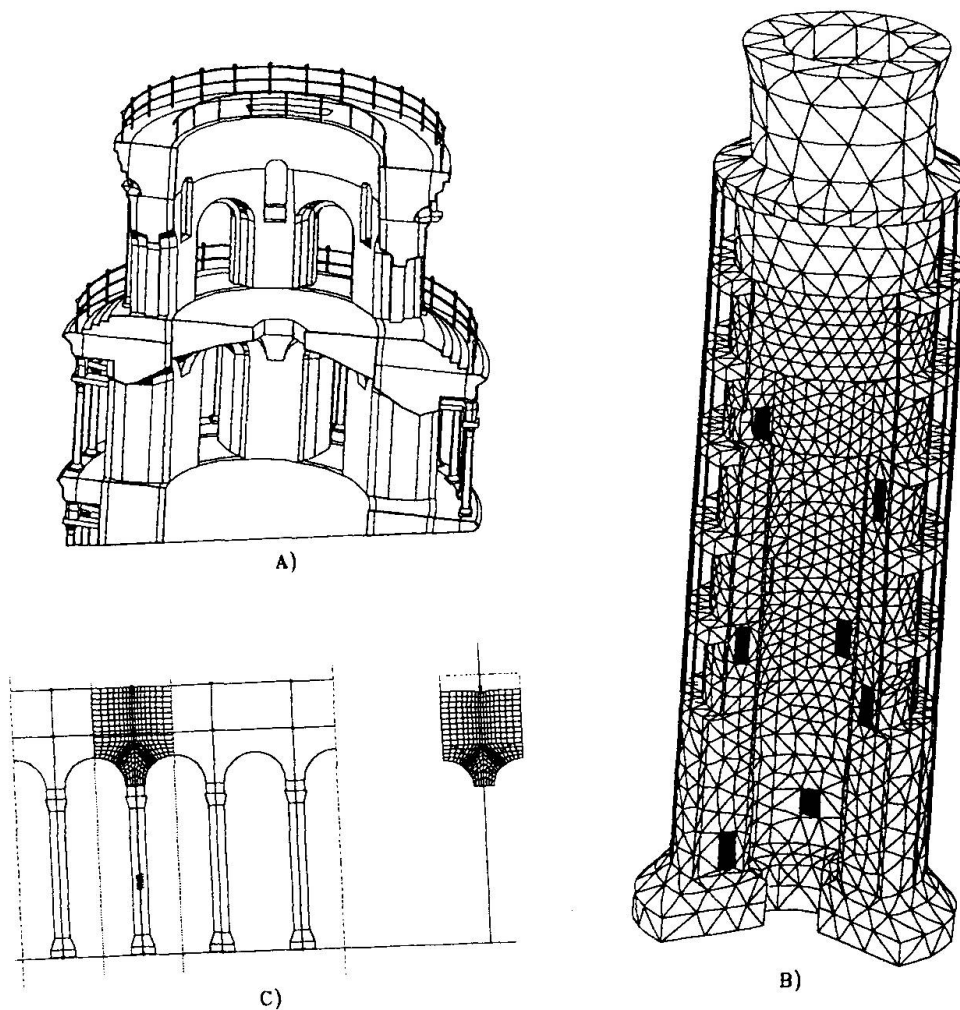*Fig.5 - Local bidimensional F.E. approach at the first loggia*

Fig.7 - Modelling of the Tower: numerical model (A), F.E.M. (B), substructuring of the colonnade system (C)

model of the Tower (Fig.7A), and then a Finite Element mesh (Fig.7B) of tetrahedral 10 nodes element (simulating the Tower and a block of linear elastic soil), for a total of 67000 degrees of freedom.

The model takes into account all the relevant openings and stairs, and 7 different densities for parts of the structure (from 18.2 to 2.7 KN/m^3). A reduced level of refinement of the mesh in the upper part allowed a considerable reduction of the complexity of the model; in the most critical zones (at South, for the lowest 4 sections) the refinement has been improved by increasing the order of polynomial shape function [6]. Nevertheless, the complexity would be excessive if the colonnade would be modelled in detail; therefore (Fig.7C) the elements of the external colonnade (columns and arches) are simulated by trusses of equivalent axial stiffness.

The analysis has been repeated with a second mesh taking into account the main cracks observed in the structure, and neglecting all columns ("3D global damaged" analysis).

The two 3D analyses were precious in providing information otherwise not available:

* the position of the zones of maximum stress (in Fig.8 the vertical stress contours show that the critical section at the first loggia is not in the plane of maximum lean, but at SW, at the edge of the door);
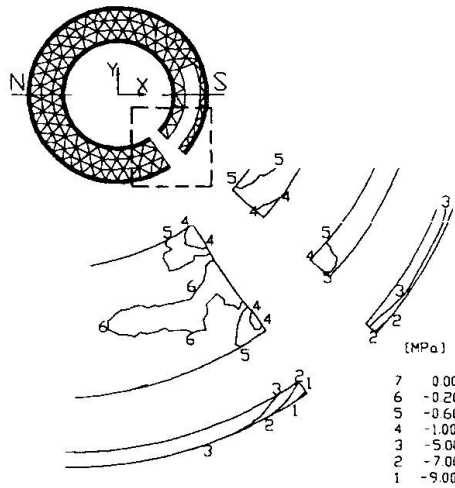
[MPa]

7	0.00
6	-0.20
5	-0.60
4	-1.00
3	-5.00
2	-7.00
1	-9.00

Fig.8 - Contours of the vertical stresses at the first loggia

X Normalized Displacements

·········· 3D global damaged

———— 3D global undamaged

———— Beam

— — — Beam with shear
deformability and 3D global
simmetric
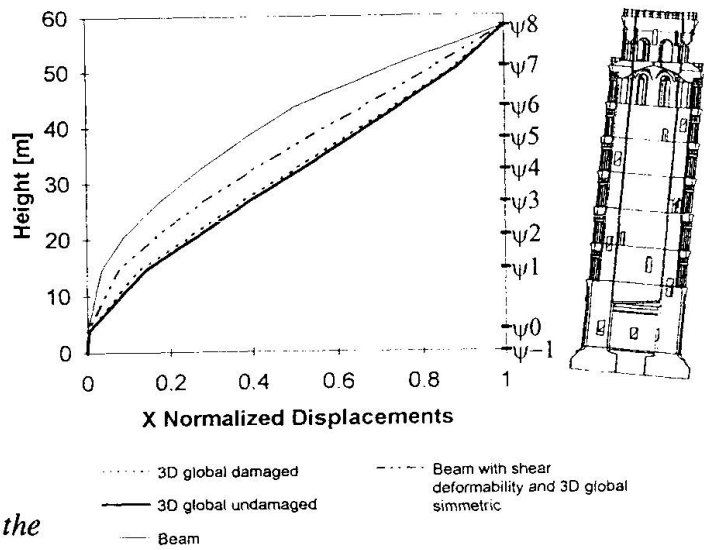
Fig.9 - Normalized horizontal displacements of the center line under permanent load

———— 3D global undamaged   ·········· 3D global damaged   ———— 3D global symmetric   ———— Beam
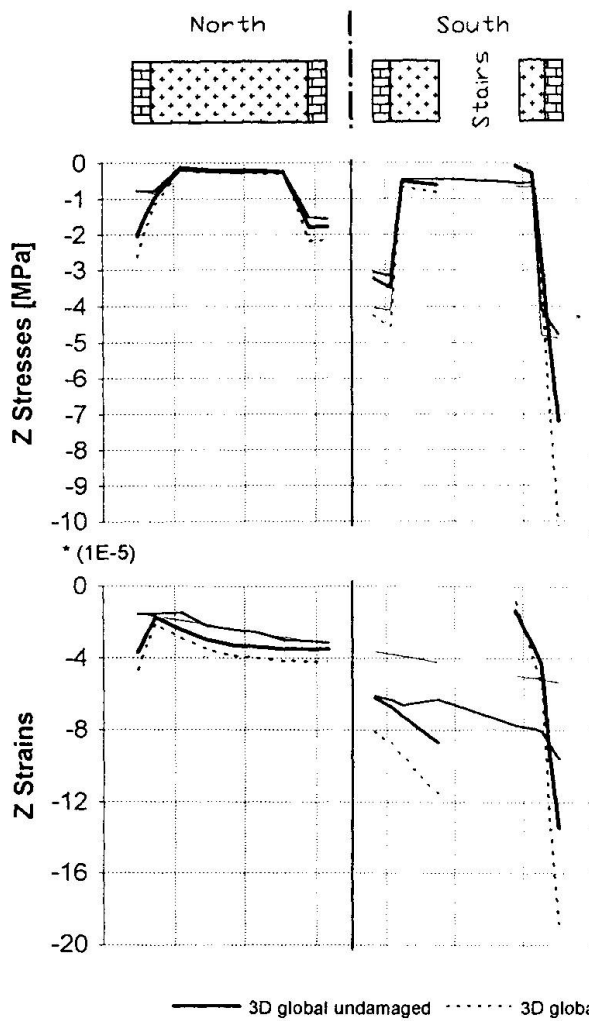
Fig.10 - Stresses and strains at the first loggia: comparison among different models
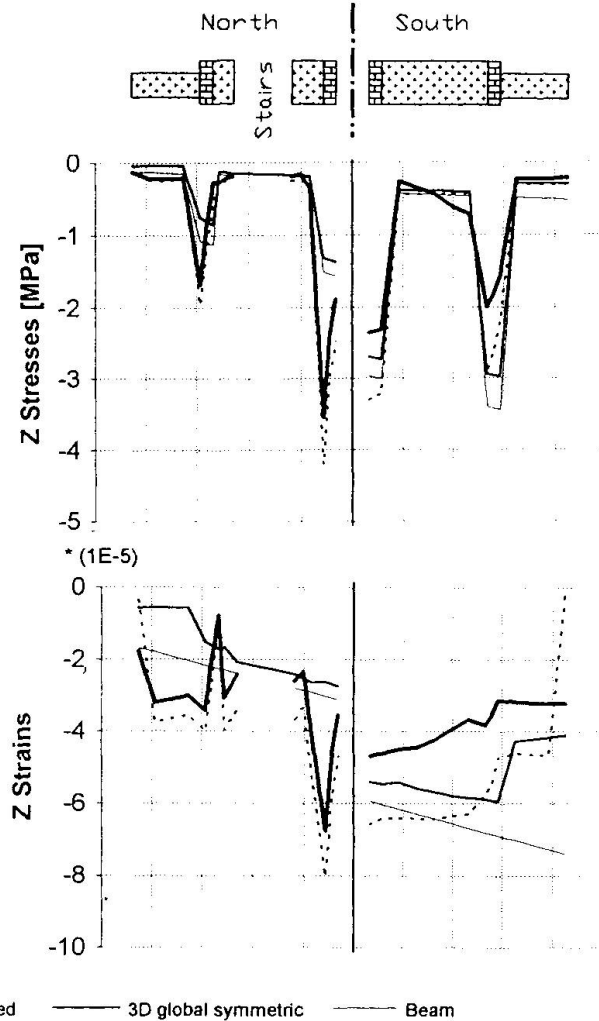
Fig.11 - Stresses and strains at the second loggia: comparison among different models

- the maximum of the stresses (10.0 MPa vertical compression under permanent load on the undamaged model, value which shall be increased to take account of the *buche pontaie*);
- the state of stress due to a 50 years wind (0.2 MPa only);
- the circumferential and radial stresses, and the extension of the beneficial effects of prestress;
- the effect of the existing damages, mainly of a possible lack of continuity of columns (this effect will be studied in the following Chapter 4).

4. DAMAGED MODEL AND SIMPLIFIED APPROACHES: COMPARISONS

The comparison of the "3D global damaged" analysis and the "3D undamaged" one had the aim of defining two boundaries between which the real state of stress should be, as a consequence of the existing cracks and of the fact that many columns have been substituted in recent times (and probably most of them in the past) so that their contribution to bearing the loads is doubtful. This is proved by the fact that the "3D global undamaged" analysis underestimates the compression at the South edge (meanly 1.8 MPa less) and overestimates the compression at the North edge (2.1 MPa more) in comparison of the values experimentally measured by means of flat-jacks.

The main results of the "damaged" analysis are the following:
- the existing cracks do not influence the global behaviour;
- a total absence of columns would lead to a considerable increase of the maximum vertical stress (the value of 10.0 MPa above mentioned at the edge of the door at the first loggia under permanent load is increased up to 13.5 MPa).

Therefore, it would be very important to state the (intermediate) real situation.

In general, the 3D model showed behaviours and states of stress which would be hardly found by simpler means which could not take into account the effects of the openings, of the non symmetric loading, and of the warping of the horizontal sections.

For this reason, in order to better understand a so complex structural behaviour, the Tower has also been analysed at lower levels of sophistication, so that a comparison has been made between the following analyses:
- 3D global undamaged;
- 3D global damaged;
- 3D global symmetric (without stairs and openings);
- Beam with shear deformability;
- Beam.

Figures 9, 10, 11, 12 show some of the most interesting results.

The inadequacy of the simple beam model is shown in Fig.9, where the deflection shapes are compared (under permanent load only): it gives flexural deflections only, when the "3D globals" act at the top as shear cantilevers, and show a peculiar contraflexure; intermediate is the behaviour of the simplified "3D symmetric", whose solid walls are less sensitive to shear; the latter may be well simulated by the beam with correction for shear deformability. The deflections are normalized to 1; in fact, "3D damaged" gives higher deflections than "3D undamaged".

Figures 10 and 11 compare the strain and stress distribution across the Tower, in the plane of maximum lean, at the first loggia $\psi 1$ and a second loggia $\psi 2$; the former has the stair at South, the latter at North. In both cases the stress distribution is far from the linear distribution of the plane section hypothesis ("beam" approach), and high vertical stress concentrations appear at the edges of the helicoidal stair opening. The "3D damaged" shows the higher stresses due to the absence of the columns.

Finally, Fig.12 compares the load in each column, at the different levels, according to the different assumptions; column 3* is at the Northern edge, column 11 at the Southern one.

Besides the clear proof of the large errors to which the plane section approach may lead, some interesting information arises:

- the loads on the columns are much more uniform than expected by the simplified methods of analysis;
- the columns at North are more efficient than foreseen by "beam";
- the helicoidal stairs have influence on the column load.

5. CONCLUSIONS

Refined Finite Element simulation, even if limited to linear elastic constitutive laws, may provide precious information on the behaviour of complex masonry structures and on their safety against brittle compression failures. The results may be a valid help in the study oh strengthening measures. Simplified approaches can only be useful for preliminary studies, and may lead to neglect important factors of the structural behaviour.

Fig.12 - Axial forces in the colonnade: comparison among different models

6. REFERENCES

1. GHERARDESCA, A., *Appendice alle considerazioni sulla pendenza del Campanile della Primaziale Pisana*. Miscellanee Artistiche, Pisa, Nistri, 1838.
2. *Relazioni compilate dalla Commissione Tecnica per lo studio delle condizioni presenti del Campanile di Pisa*, Firenze, Tip. Galileiana, 1913.
3. POLVANI, G. et al., *Ricerche e studi su la Torre Pendente di Pisa e i fenomeni connessi alle condizioni d'ambiente*, Firenze, Istituto Geografico Militare, 1971.
4. BARTELLETTI, R. et al., Stabilization of the Leaning Tower of Pisa, *Proceedings of the 13th IABSE Congress*, Helsinki, 1988.
5. MACCHI, G., Monitoring medieval structures in Pavia, *Structural Engineering International*, Vol. 3, n. 1, 1993.
6. ISMES, *FIESTA: software system for static analysis of solid structures based on the p-version of the finite element method*, Bergamo, 1992.
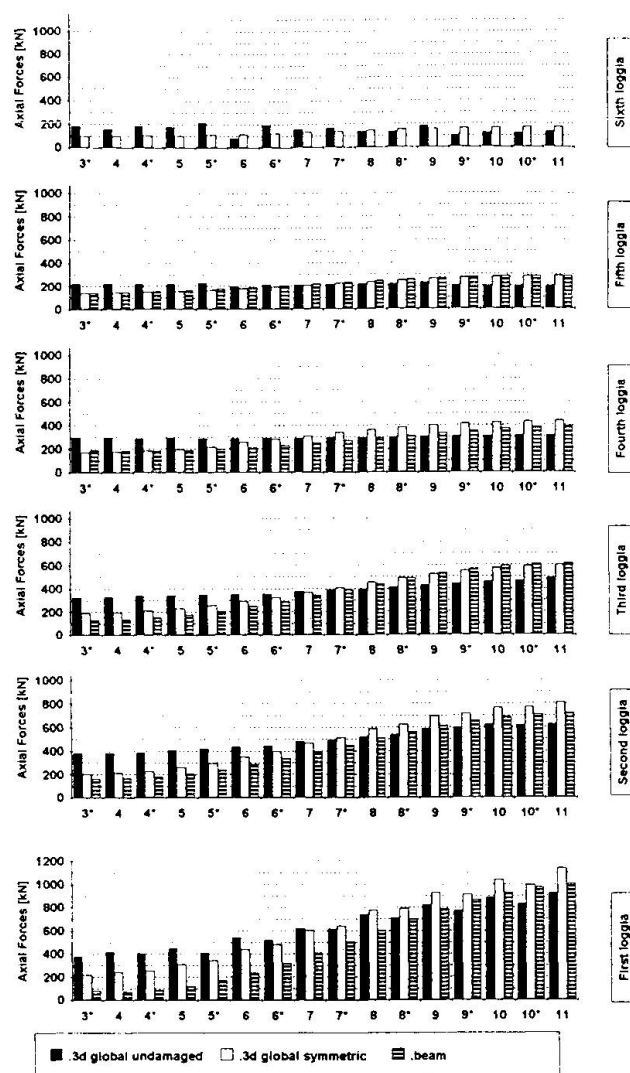
Studies for the Rehabilitation of the Mexico City Cathedral

Etude pour la réhabilitation de la Cathédrale de Mexico

Studie zur Instandsetzung der Kathedrale der Stadt Mexiko

Roberto MELI
Res. Professor
Inst. of Eng. UNAM
Mexico City, Mexico

R. Meli, got his PhD from the National Univ. of Mexico. He is a research prof. at the Inst. of Engineering and has been involved in research in structural engineering, particularly in earthquake engineering, since 1965. Presently, he is Research Dir. of the National Center for Disaster Prevention in Mexico.

A. Roberto SANCHEZ-RAMIREZ
Researcher
Inst. of Eng. UNAM
Mexico City, Mexico
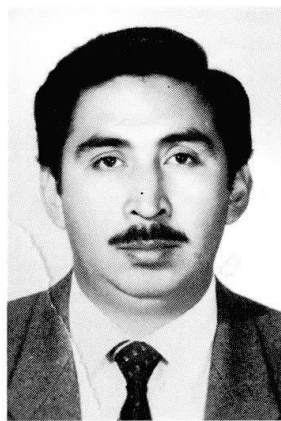
R. Sanchez, got is Civil Engineering degree from the National Univ. of Mexico. He has been involved in experimental research at the Inst. of Engineering in the last ten years, especially in static and dynamic testing of structures, and in situ measurements of structural properties of buildings.

SUMMARY

The Mexico City Cathedral is undergoing major rehabilitation work aiming at correcting its differential settlements, now reaching up to 2.4m. The most relevant structural investigations, performed to support decisions taken during the process, are briefly described; those related to assess the safety under vertical loads, the effects of the differential settlements and their corrections, and the seismic actions. Laboratory and in situ tests have been performed to determine the mechanical properties of the materials, the dynamic response and the state of stresses.

RÉSUMÉ

Des travaux considérables de réhabilitation sont entrepris sur la Cathédrale de Mexico afin de compenser des tassements différentiels qui atteignent 2,4m. Les études structurales les plus importantes, réalisées afin de contrôler les décisions prises durant les travaux, sont présentées; en particulier celles destinées à évaluer la sécurité, sous les charges verticales, des effets de tassements différentiels et leur correction ainsi que les actions sismiques. Des essais en laboratoire et sur place ont été réalisés afin de déterminer les propriétés mécaniques des matériaux, le comportement dynamique et l'état de contrainte.

ZUSAMMENFASSUNG

Grossangelegte Instanstellungsarbeiten werden an der Kathedrale von Mexiko ausgeführt, um den grössten Teil der beträchtlichen unterschiedlichen, bis zu 2.4m reichenden Senkungen zu korrigieren. Zahlreiche Konstruktionsnachweise dienten während der Ausführungsphase als Entscheidungsträger. Die wichtigsten werden kurz vorgestellt, jene betreffend den vertikalen Widerstand, das mechanische Verhalten, die Auswirkungen der Senkungen und deren Korrektur sowie das Verhalten bei seismischen Bewegungen. Tests im Labor und an Ort dienten der Bestimmung des dynamischen Verhaltens und des Druckwiderstands.

1. INTRODUCTION

The Mexico City Cathedral, probably the most important colonial monument in America, has been severely affected by differential settlements since the beginning of its construction in the 16th century. The monument is extremely heavy (127,000 ton) and is located on very soft clay deposits, which in some parts had been previously consolidated by Aztec temples and pyramids over whose remains the Cathedral was erected. In this century the intense pumping of the underground water has severely aggravated the subsidence.

During the protracted period of its construction (240 years) the severe differential settlements forced the builders to significant adjustments in the geometry of the monument. After its completion, the Cathedral has been sujected to an almost uninterrupted activity of repairing, especially in order to seal the cracks in the roof to avoid leaking.

Presently, the building has reached a condition of distortion seriously undermining its structural safety. The maximum differential settlement has reached 2.4m and it is increasing at a rate of 1.2 cm/year. Some of the main columns supporting the roof show an out-of-plumb exceeding 2%. Severe cracks in the roof, floor and walls evidentiate the effects of the differential settlements.

Considering that the regional subsidence of the area will not be eliminated in the near future because water needs to be pumped to satisfy the demand of the city, measures had to be taken to restitute the building to a stable and safe condition. A major rehabilitation project has been started in late 1991. The main structural aspects of the project will be described here, focussing on the experimental and analytical studies performed. A description of the geotechnical problemas and of the subexcavation technique can be found in Ref. 1.

2. DESCRIPTION OF THE BUILDING AND ITS PAST PERFORMANCE

The temple is constituted by five naves. The roof of the central nave is formed by a cilindral vault supported by arches and by 16 stone columns. The lateral naves have hemispherical vaults. A close array of robust masonry walls divides the extreme naves in small chapels. These walls along with the facades and some buttresses constitute a peripheral belt providing great lateral strength and stiffness to the monument. A large dome at the intersection of the central nave and the main transverse nave, constitutes the heaviest and most critical part of the roof. The main features of the construction can be appreciated in Figs. 1 and 2. The structure is supported by a grid of foundation beams (3.5 m deep) and by a foundation mat with a thickness of about 2m. Timber piles (with a diameter of 0.2m and a length of 2-3 m) are spaced every 0.6 m underneath the foundation mat.

The primary construction material is a kind of poor concrete constituted by volcanic stones, of different size and unit weight according to the structural member, agglutinated by a lime-sand mortar. The properties of this material will be discussed later. In arches and columns andesitic stone sills were used.

Large differential settlements started since the early stages of construction, as evidentiated by the many significant adjustments made to the dimensions and shape of the construction members. For instance, the length of the column varies according to the settlements experienced of their bases at the time when the arches and vaults were built. The maximum differences being 0.85 m. Several rows of sills with variable height were placed at the facade to correct the inclination
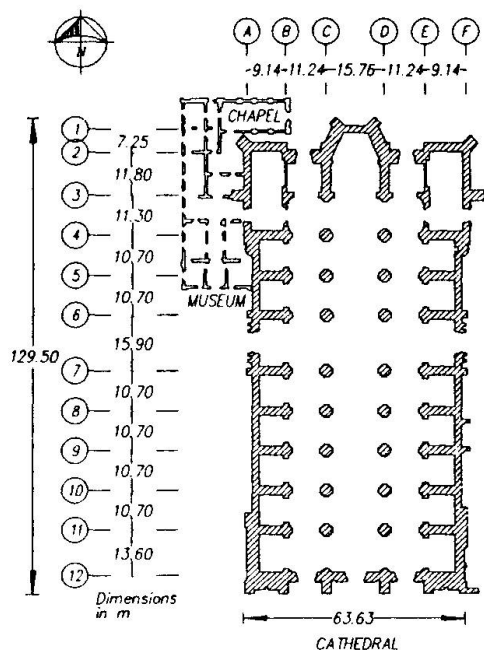
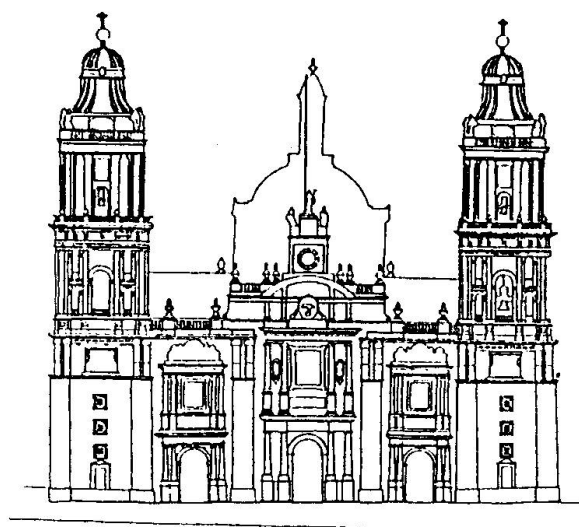Fig. 1 Plan view of the Cathedral

Fig. 2 Front view

at the time of the construction. The span and rise of the arches and vaults were varied in order to achieve an almost flat roof. After the completion of the roof, the structure adquired a greater stiffness thus the differential settlements increased at a lower rate. Nevertheless the large cracks and the inclination of the upper parts of the columns reflect the very large distortions suffered by the structure once it was completed.

Fig. 3 shows the pattern of differential settlements measured in the floor of the Cathedral some time before at the beginning of the rehabilitation work (late 1989). Another useful representation of the phenomenon is given by the curves of equal rate of differential settlements in the year before the commencement of the works (Fig. 4). Two major mechanisms of deformation can be appreciated. One is the sinking toward the Southwest corner, another is the "emergence" of the central nave in the Northern part.

The first mechanism has produced a pattern of transverse cracks in the roof and walls, especially near the central dome, and some separation of the Southern facade, with its very heavy towers, from the rest of the church.

The second mechanism produced the outward rotation of the columns and lateral walls, and the opening of the vaults and arches in the roof, originating a pattern of longitudinal cracks in the roof, floor and foundation. This second mechanism is the most critical from the structural point of view, because of the inclination of the columns receiving the greatest vertical loads, especially those supporting the central dome. As can be seen in Fig. 5, the present shape of the column shaft shows changes of direction due to corrections made during the construction. The total eccentricity between the upper and lower part of the column is, for this case, 0.6m representing 25% of the size of the column. Some vertical cracks at the upper part of the column are attributed to the compressive stresses generated by the eccentric compression.
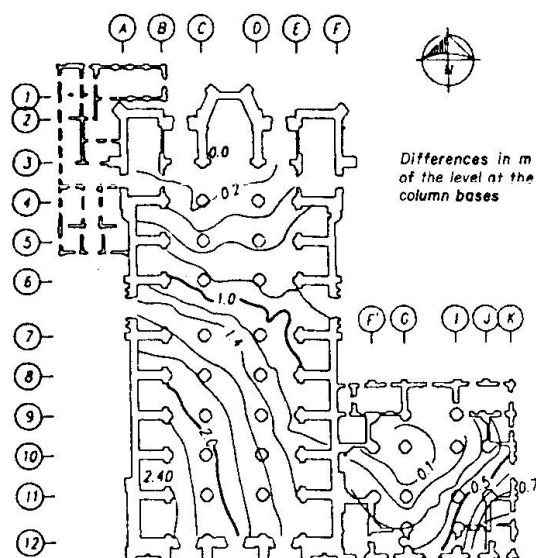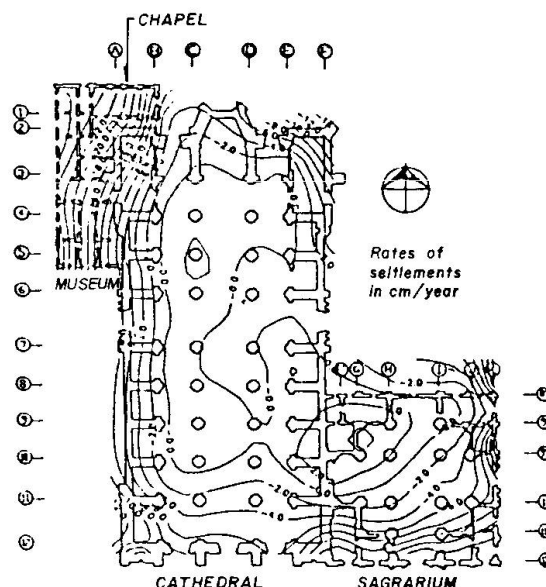
Fig. 3 Differential settlements (Dec. 1989)

Fig. 4 Annual rate of increase in differential settlements (1991)
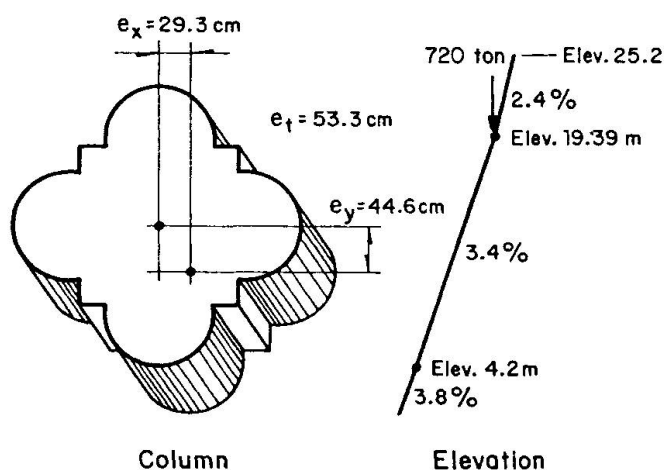

Column   Elevation

Fig. 5 Deformed shape of a central column and applied forces due to self-weight

3. ASSESSMENT OF THE STRUCTURAL SAFETY

The self-weight of the temple represents a very severe action on the foundation and on the soil. Its effect have been studied by a finite element analysis of a tridimensional linear model. The same model has been used to analyze the stresses induced by displacements of the supports, representing simplified patterns of the differential settlements suffered by the building, as well as of the motions to be induced by the correction process.

A thorough view of the state of stresses induced by the vertical loads in the central part of the monument is shown in Fig. 6. A move schematic representation of the flow of forces in members supporting the central dome is shown in Fig. 7. It can be appreciated that the weight is transmitted toward the foundation essentially by axial forces in the vaults, arches, columns and walls. The level of stresses in the members of the original structure disregarding the changes in their geometry due to settlements and adjustements, is well within the range of capacity of the materials.

The outward motion of the supports in the Northern part of the central vault has produced a mechanism of non linear
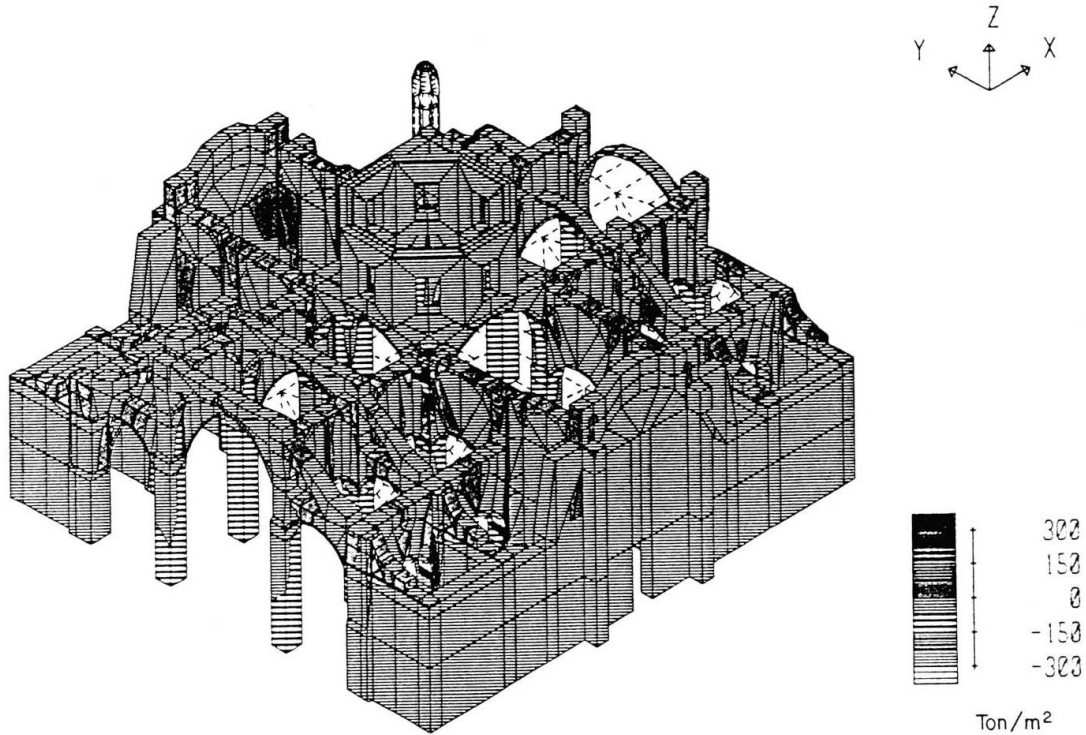
Fig. 6 State of stress due to gravity loading from a finite element analysis of the central portion of the Cathedral
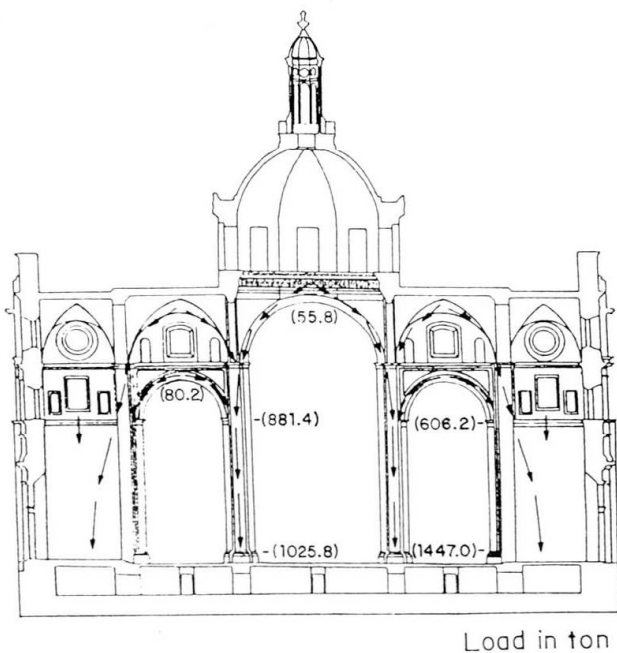

Load in ton

Fig. 7 Flow of self-weight loads in the zone under the central dome

stability of the central columns shows that bending moments induced by the eccentricity of the force produced by the weight of the roof, increase the maximum compressive stress 2.3 times above that computed for the undeflected shape of the column. In this fashion stresses are now very near to the maximum capacity of the stone.
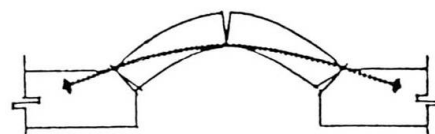
a) Shortening of the span

b) Opening of the span

Fig. 8 Mechanisms of inelastic deformations due to movements of the supports of the central vault

deformation as the one schematically shown in Fig. 8. The present deformed shape of the vault is still well within a stable configuration. On the contrary, the analysis of the

The seismic safety of monumental structures like the Cathedral cannot be assessed by the procedures prescribed by building codes for modern structures. It must be considered that the actual shaking induced in these very heavy and stiff structures founded on a very soft soil is much smaller than for ordinary buildings, because a significant part of the energy that the ground tries to impose to the structure in actually returned to the soil through radiation. Additionally, part of the seismic energy can be dissipated through opening and closing of cracks, through relative motions between parts of the structure and through uplifting. For these reasons monumental buildings have shown an outstanding capacity to withstand severe earthquakes in Mexico City, even when modern and apparently stronger structure have been badly damaged. Earthquake damage of monuments has been generally associated to cases of extreme degradation of the materials or to severe previous damage due to differential settlements.
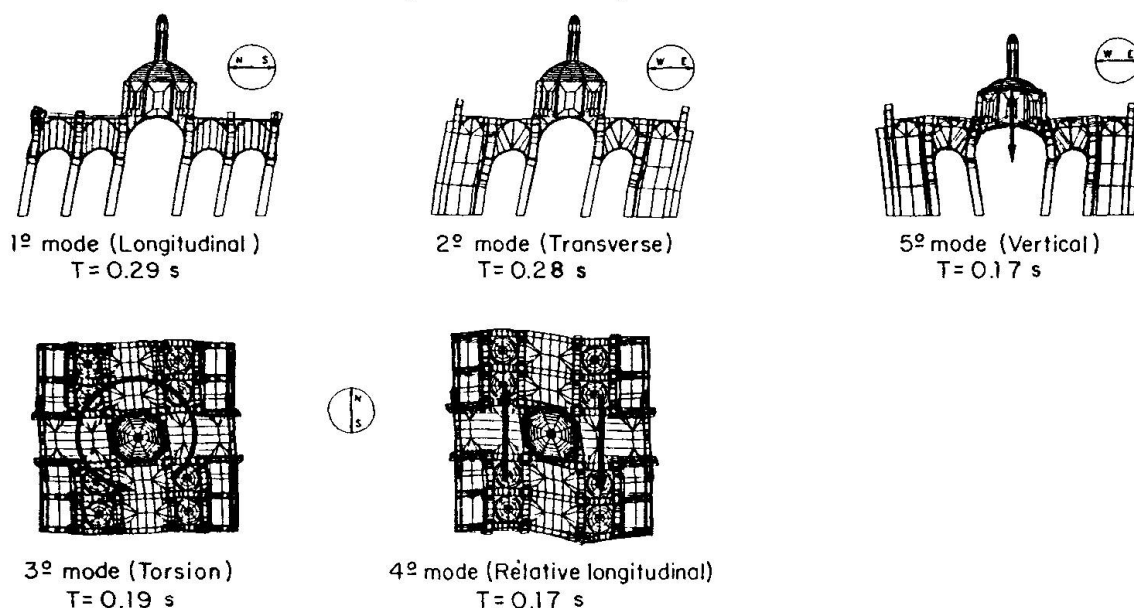

1º mode (Longitudinal)   2º mode (Transverse)   5º mode (Vertical)
T= 0.29 s   T= 0.28 s   T= 0.17 s

3º mode (Torsion)   4º mode (Relative longitudinal)
T= 0.19 s   T= 0.17 s

Fig. 9 Modal shapes of vibration from a finite element model of the central portion of the Cathedral

The previously described linear elastic tri-dimensional model was used for a dynamic analysis to compute the modal shapes and periods of vibration (Fig. 9). It was found that in plan deformations of the roof favoured torsional modes of vibration and that the large concentrated mass of the central dome produced significant vertical vibration. Computed periods were compared with those derived by measuring the vibration of the building in ambient conditions. Consistently, computed periods are smaller than those measured. This is attributed to the lack of fixity of the base of the structure where the foundation allows significant rotations of the walls and columns. Additionally, the extense cracking of the structure significantly reduces the stiffness, thus increasing the vibration period.

For the assessment of the seismic safety, a constant spectral ordinate of 0.2m was assumed. It was considered that, because of the existing cracking and of the small tensile strength of the materials, parts of the structure could vibrate independently from the rest. Therefore, the seismic safety of the most critical portions was assessed primarily by simplified methods. In general terms, it was concluded that the strong peripheral belt constituted by the facade walls and by the walls sorrounding the chapels provided a satisfactory overall safety. Nevertheless, the additional lateral displacements of the columns during their

seismic vibration could lend to their lateral instability and to a local collapse.

4. CORRECTION OF DIFFERENTIAL SETTLEMENTS AND ITS EFFECTS ON THE STRUCTURE

As shown in the previous section, in its present condition the Cathedral is structurally unsafe due mainly to the great inclination of the central columns, and the operation of the temple is greatly impaired due to the excessive slope of the floor and to the great cracking.

After evaluating several alternatives, a technique called "subexcavation" was adopted to correct parts of the settlements. Briefly, a controlled subsidence of the most elevated parts of the ground is produced by the extraction of soil from the deep strata of soft clay. As shown in Fig. 10, small diameter radial boreholes will be excavated from 23 shafts opened to a depth of about 20m. The closing of the holes due to the weight of the soil and structure produces a settlement at the surface. Through a careful programming of the amount and position of excavated soil a preselected configuration of ground settlements can be achieved with great precision.
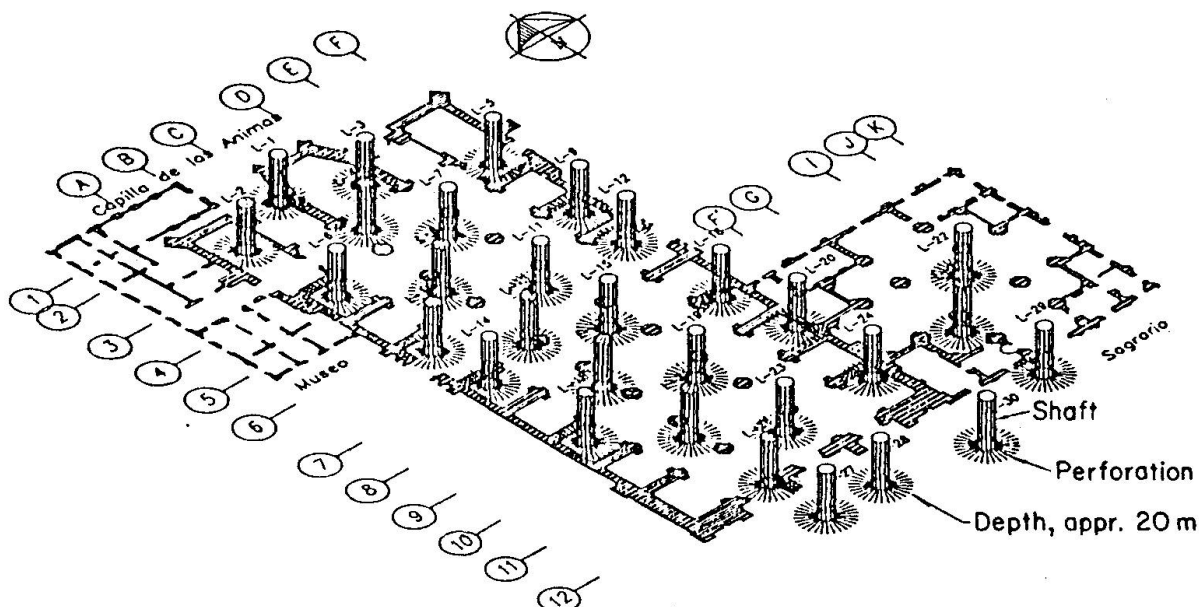

Fig. 10 Position of the main shafts and radial perforations for the correction of the differential settlements

The technique has been already applied to correct other modern and ancient buildings. At the time of writing this paper the 23 shafts beneath the Cathedral have been almost completed. In mid 1993 the subexcavation will be started to produce first a gradual settlement of the Northern part of the temple in order to correct the first mechanism of differential settlements which is quantitatively the largest, but structurally the less dangerous. Then, the second mechanism of differential settlements will be corrected, essentially by producing the inward rotation of the lateral naves in the Northwest part of the temple. The process will be carried out in several years in order to maintain a very slow settlement rate that will minimize the structural damage.

The effects of the corrections on the structure are being carefully analyzed. In general terms, it is expected that the correction of the first mechanism will produce a significant transverse cracking of the roof and walls. Provisions will

be taken to avoid the complete separation of the very heavy Southern facade from the rest of the structure. More critical is the correction of the second mechanism which will tend to close the span of the central nave and to upright the columns. Because the cracks formed when the arches opened, have already been repaired, the closing can only be reached through the formation of plastic hinges in the arches as schematically shown in (Fig. 8).

Undoubtedly, the structural damage will be significant, but, as the structure is thoroughly shored, no danger of collapse is foreseen. Nevertheless, the only way to prevent an undesirable behavior is by a close monitoring of the building response.

5. STRUCTURAL MONITORING AND TESTING

Several parallel measurement systems have been implemented to monitor the displacements of the structure. Bimonthly levelling of the position of several hundred points of the structure is performed through high accuracy surveying. Additionally, the inclination of the columns at different heights is being monitored through electronic inclinometers. The position and width of cracks in the main structural elements is checked every month. All the information is processed in a computer system providing maps and graphs of the deformations.

Additionally, some more sophisticated, special purpose measurements systems are being implemented. The loads taken by the shoring towers are determined by measuring the unit strain in the vertical pipes through 312 strain gages. 12 high sensitivity inclinometers provide a continous record of the motion of critical points of the roof, columns and floor, allowing the detection of sudden motions. They are also used as vibration transducers. An additional system providing continous record of the motion of the columns and of the changes in the span of some arches will be installed soon. Flat jacks are been placed in some columns and walls to monitor the state of stresses.

The mechanical properties of the main structural materials have been directly determined in the building. Samples have been extracted from columns and walls to determine unit weights, moduli of elasticity, and compressive and tensile strengths. Despite of a significant variability, the quality of the construction materials can be considered to be very good.

6. CONCLUSIONS

The rehabilitation technique adopted has never been used before for a building of this size, complexity and materials. Therefore, the detailed analysis of the effects and the close monitoring of the structural response are essential in order to select the most convenient and safe program of work. Up to this moment, the results have been completely satisfactory, nevertheless the most critical part of the process is still to come.

REFERENCES

1.   Tamez E., E. Santoyo and A. Cuevas, "The Metropolitan Cathedral in Mexico City, Correction of the Behavior of its Foundation", Mexican Society of Soil Mechanics, Mexico, aug 1992.

Damage and Repair of the St. Charles Basilica in Rome

Dommages et réparations à la Basilique de Saint Charles à Rome

Schäden und Eingriffsmöglichkeiten für die St.-Karls-Basilika in Rom

Francesco ZURLI
Superintendent
City Office for Architecture
Rome, Italy

F. Zurli, born 1935, received his degree in Archit. from the Univ. of Rome 'La Sapienza', in 1964. From 1966 onwards, he has been with the Ministry of Culture, directing restoration projects. 1976 he became Superintendent for Verona, 1981 for Ravenna and since 1991, directs the Superintendent of Architecture for Rome.

Raffaele M. VIOLA
Architect
Ministry for Culture
Rome, Italy

R. M. Viola, born 1950, received his degree in Archit. from the Univ. of Rome 'La Sapienza', in 1977. Since 1980, he has been working for the Ministry of Culture and for the Superintendents of Archit. in Abruzzo, Lazio, and Rome. He currently directs restoration works of the SS. Ambrogio e Carlo al Corso Basilica.

SUMMARY

The paper reports on studies of damage and solutions proposed for the restoration of the dome of the St. Charles Basilica in Rome. The study is based on the results of an indepth program of investigation on the soil conditions, the building materials and the analysis of the behaviour during this period. The data has been recorded by a computer connected to a monitoring system. The assessment of the safety levels was performed with the support of mathematical models, by studying historical information and a permanent analysis and comparison of theoretical results with reality.

RÉSUMÉ

L'article présente l'étude des problèmes structuraux et des propositions pour la restauration de la coupole de la Basilique de Saint Charles à Rome. L'étude a utilisé les résultats d'un programme de recherches sur les caractéristiques du sol et de la maçonnerie, et l'enregistrement de la variation de l'ouverture des fissures, grâce à un réseau d'instruments connectés à un ordinateur. L'estimation des niveaux de sécurité a été effectuée au moyen de différents modèles mathématiques, tenant compte des renseignements historiques et comparant les résultats théoriques avec la réalité.

ZUSAMMENFASSUNG

Der Bericht handelt von einer Studie über Schäden und Lösungsvorschläge für den Umbau der Kuppel der St.-Karls-Basilika. Die Studie gründet auf Ergebnissen eines Forschungsprogrammes über Bodenbedingungen, Baustoffe und Analyse des Verhaltens der Basilika, die von einem mit dem Computer verbundenen Beobachtungssystem während dieser Zeit aufgenommen wurden. Die Ermittlung des Sicherheitsfaktors erfolgte mit Hilfe von Computermodellen, dem Studium historischer Berichte und der Analyse und konstanten Vergleichen der theoretischen Ergebnisse mit der Wirklichkeit.

1. INTRODUCTION

The research and studies that will be discussed in the following paper, report on the results of an interdisciplinary operation between the Sovrintendenza of Rome and the consulting engineering of Prof. Ing. Giorgio Croci, with the cooperation of Ing. Giuseppe Carluccio. The construction works were carried out by Impresa Castelli Spa, the monitoring system and investigation were carried out by Società Tecnocontrolli Srl. This approach made it possible to investigate the globality of the problem with mutual exchange and enrichment of imformation from the historical survey, the archeological and geotechnical research, the architectural and artistic aspects (including statues, plasterwork, decoration, colour,....), the structural analysis, etc.

The interdisciplinary approach, which is appropriate for all restoration projects, allowed us to fully understand the problems and phenomena that have occurred and to identify a solution.

2. HISTORICAL SURVEY

The construction of the church began in 1612, after Pope Paul V canonised St. Charles Borromeo. It was finished in 1684 with the completion of the façade (fig. 1).

The builder and director of works was Onorio Longhi who must have also constructed the foundations, the basementwalls of the three naves, the presbitery and the tribune.

At the death of Onorio the project continued under the guidance of his son, Mario Longhi, with successive interuptions due to lack of funding, the most important being the interuption which occurred from 1625 to 1642, during which the central vault was absent; this probably lead to large deformations of the columns in the central nave that are now out of plumb by about 10cm (fig. 2).

Fig. 1

The drum and dome were built in 1668 and 1669 under the direction of Pietro Berrettini (known as "il Cortona") (fig. 3). By the time Rome was affected by the strong earthquake, which caused damage and failures in the Colosseum, in 1703, the building was completed.

An interesting collection of architects were consulted as problems emerged during construction, including Carlo Rainaldi, Giovanni De Rossi and Borromini himself.
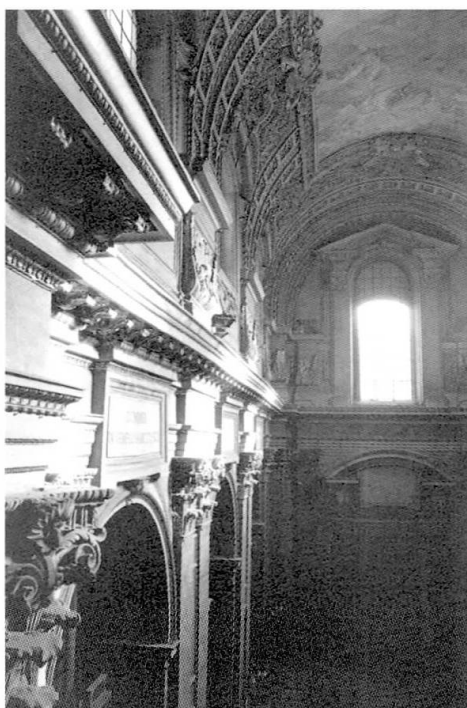

Fig.2

Fig. 3

3. CURRENT STATE AND INVESTIGATIONS

The church has suffered from large scale cracking present in the dome, the vaults of the lateral naves and the vaults of the preambulatory (in general they are diagonal and symmetrical about the longitudinal axis of the church), some cracks are also present in the walls, the crypt, the paving and in the floor above. The cracks in the dome are rather serious, being of the amplitude of a few centimeters (fig. 4); they follow the meridian curves and are concentrated around the ribs, where the architectural requirement of emphasing the ribs lead to a reduction of the dome section immediately next

Fig. 4

to them, they continue along the drum and also affect the fan arches connected to the drum.

In the apse area the crack pattern present at the vault level is repeated at the level of the vault of the crypt and at the upper levels; the cracks are almost symmetrical about the longitudinal axis of the church.

Longitudinal cracks are present along the lateral nave in the keys of the vaults, these are associated with a pronounced deformation of the columns along the central nave and a macroscopic deformation of the cornice (fig. 2).

In the course of the study, a series of tests and controls were carried out in order to ascertain the the structural characteristics of the basilica and to evaluate, as accurately as possible, the existing margins of safety.

An important part of this investigation was the monitoring system set up to automatically survey the opening and closing of the cracks over time, in relation to the variation of temperature and other phenomena (fig. 5).

During the control period, which took place, with interuptions, for over three years, no sign of evolutionary phenomena linked to the cracking was observed; however the longitudinal cracks showed a high sensibility to both the daily and seasonal temperature cycles, probably caused by the fact that these cracks represent a hinge which
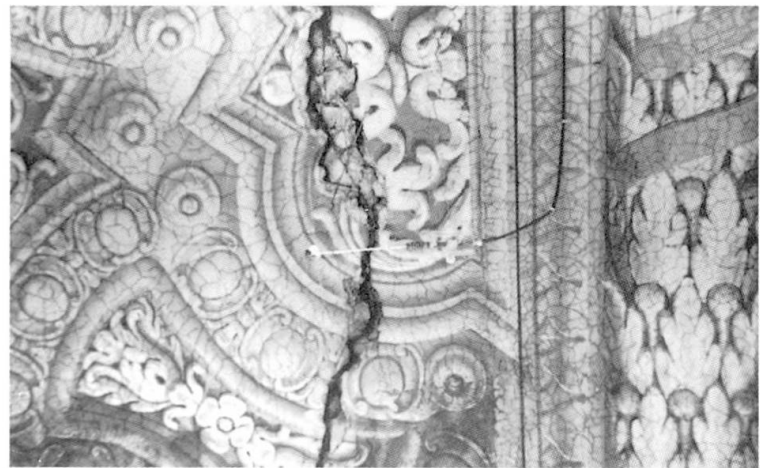

Fig. 5

runs along the centre of the basilica and along which the thermal deformations take place (fig. 6).

A series of tests were carried out in order to ascertain the nature of the stuctural constituents:
- traditional geognostic tests and inspection of the soil strata and foundations with a miniture telecamera;
- observation of the composition and condition of the masonry by means of an endoscope placed in small drilled holes, the presence of deep cracks or cavities could also be ascertained (fig. 7);
- sonic tests to determine the homogeneity and compaction of the masonry;
- in-situ flat-jack and pull-out tests, to determine both the strength and the existing stress levels of the masonry to a reasonable approximation (fig. 8);
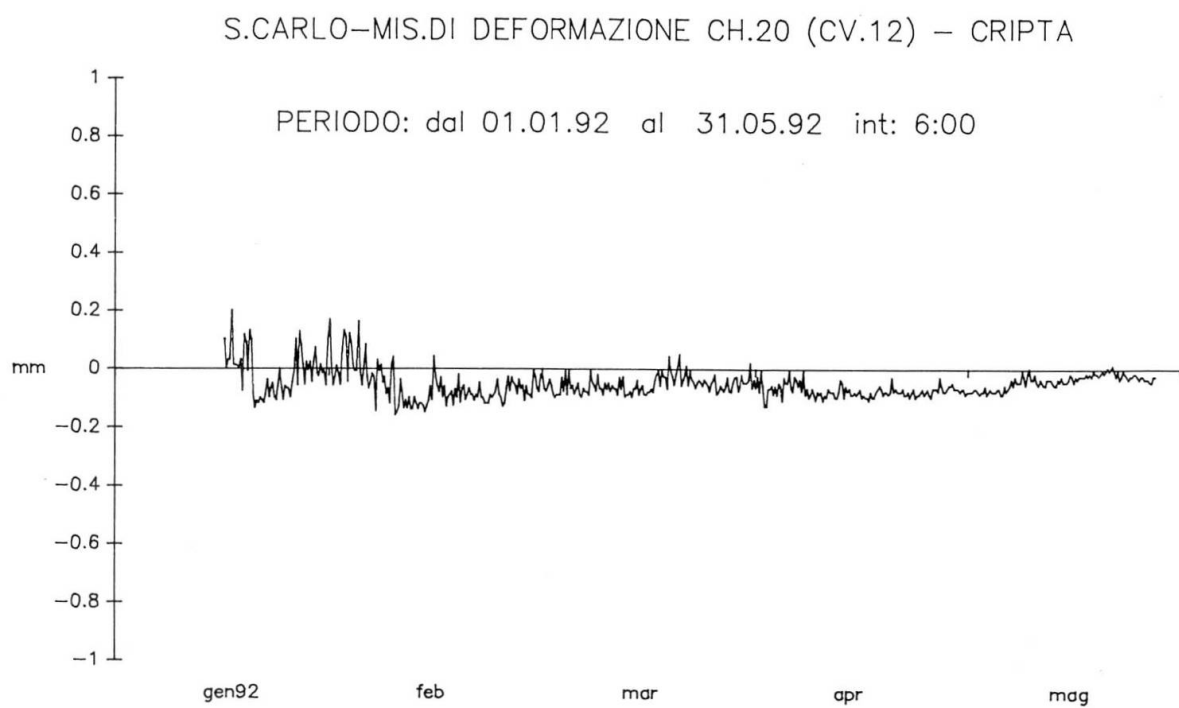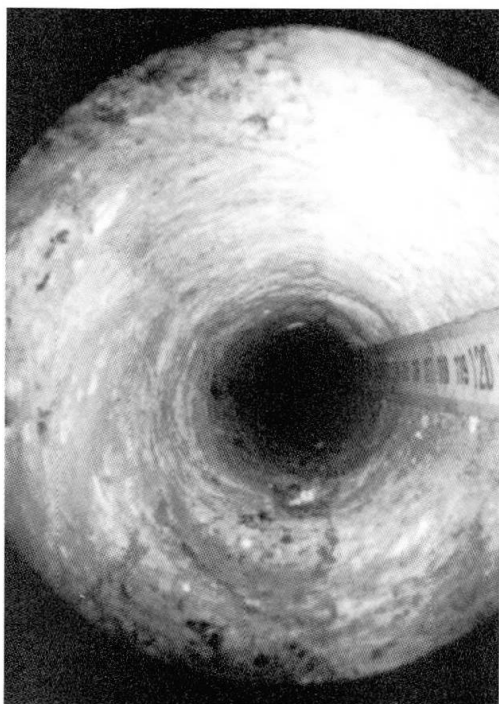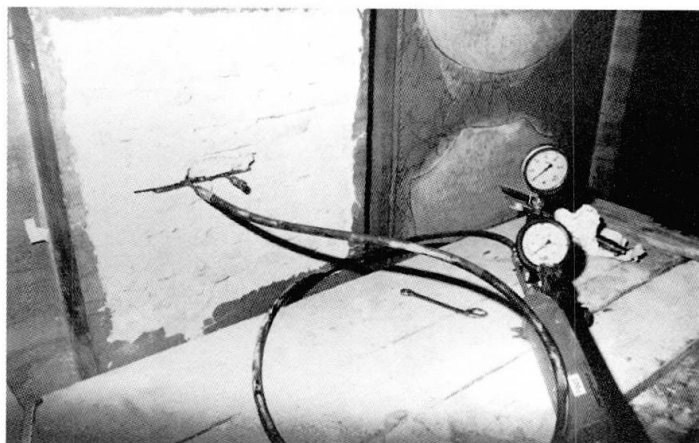- measurement of the verticality of the columns in the nave.

Fig. 6

Fig. 7

Fig. 8

4. ANALYSIS OF THE STRUCTURAL BEHAVIOUR

The theoretical analyses of the behaviour of the monument used the information obtained during the series of checks, and were carried out by means of different finite element mathematical models of the structure; the global model took into account the real three-dimensional distribution of the mass and rigidity of the basilica and of the adjacent buildings, closely connected to the walls of the lateral chapel (fig. 9).

Three different analyses were calculated by means of these models: the first considering the dead load only, the second taking account of seismic actions coresponding to the earthquake of 1703, the third considering the effects of temperature. In particular, the models took account

Fig. 9

of the entire form of the dome disregarding the presence of cracks in order to discover what caused them.

Regarding the central part of the basilica, the levels of tensile stress in the parallels of the dome were analized to find the correlation between them and the existing cracks. The maximum values obtained were:
- for dead load: $0.7t/m^2$
- dead load + seismic load: $0.8t/m^2$
- dead load + seasonal variation in temperature (summer to winter) + seismic action: $1.1t/m^2$.

The maximum tension was verified as being adjacent to the ribs of the dome, due to the reduction of the section at this point, corresponding perfectly to the existing crack pattern; however

Fig. 10

the low values of tensile stress do not justify the presence of cracks in otherwise strong masonry.

It thus appeared necessary to investigate other possible phenomena, and in particular the role of soil movements; a finite element model was then used to specifically study the interaction between structure and soil, and to evaluate the influence of soil movements on the formation of the cracks (fig. 10). This model took into account the mechanical characteristics of the soil gleaned from the series of tests carried out.

The analysis of the deformations caused by loads transmitted to the soil from the structure (fig. 11), showed a large settlement in the area of the crypt
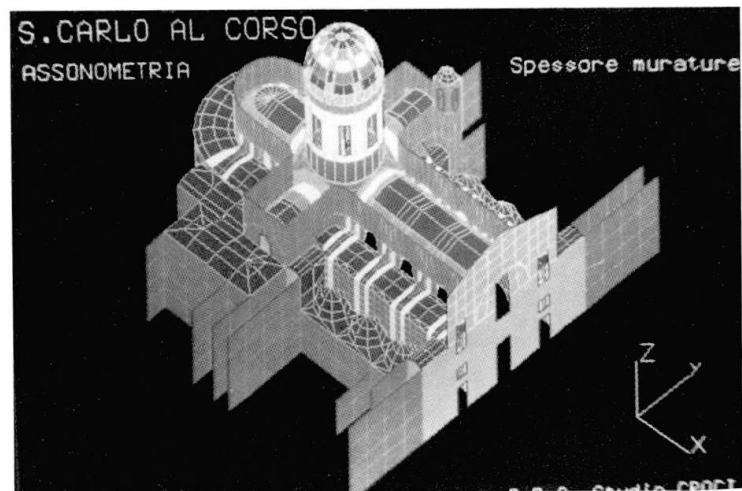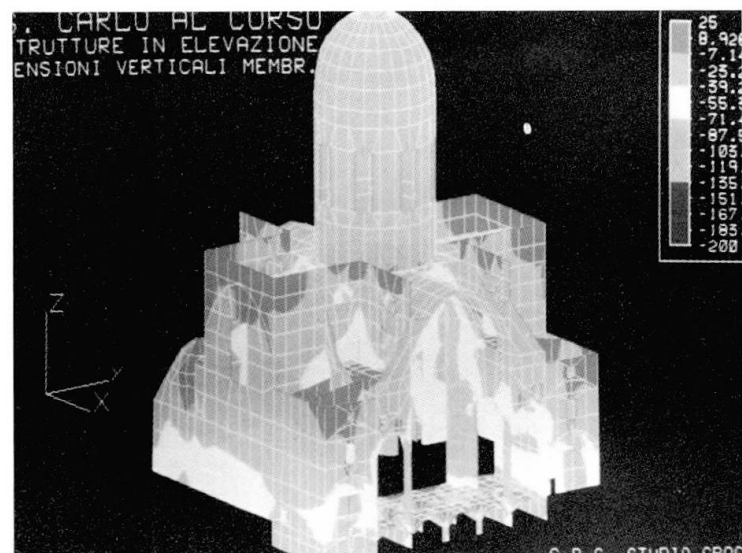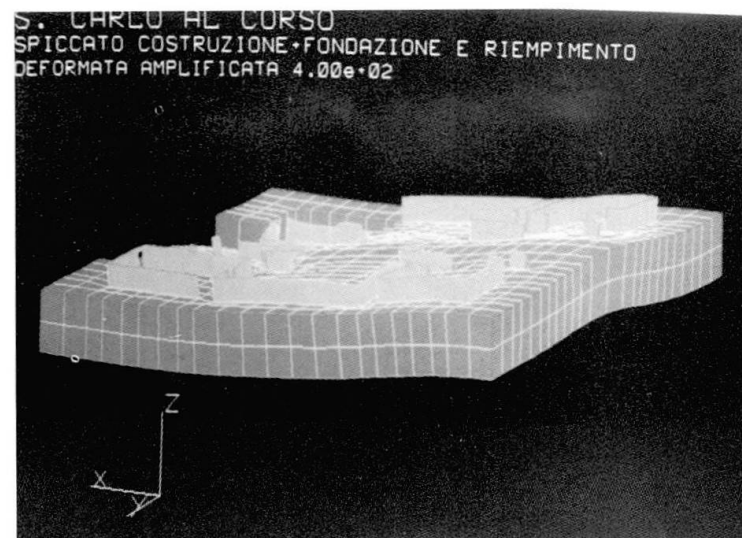

Fig. 11

and apse with respect to the lateral nave. The deformations of the transepts, with respect to the central part of the basilica, produce a rotation around the outer columns of the dome (fig. 12), and additional stresses in the rings of the drum and the dome itself.

As the drum is affected by four windows, which, for architectural motives of symmetry, occupy the principal axes of the basilica, the load of the dome is transmitted in the lower arches with an eccentricity in relation to the columns; this leads to a further increase in stress that is suoerimposed onto those generatedby load, temperature and seismic actions, overcoming the strength of the material thereby causing the distribution of cracks visible today (fig. 13).

The study of the soil - structure interaction also justified the lateral deformation of the columns in the nave and the curvature of the cornice, probably produced during construction due to the delay in the construction of the central nave which left the thrust from the vaults of the lateral naves unresisted for decades.
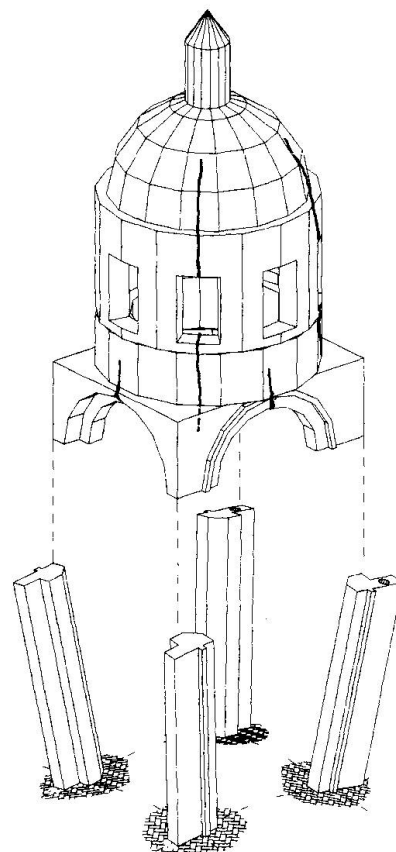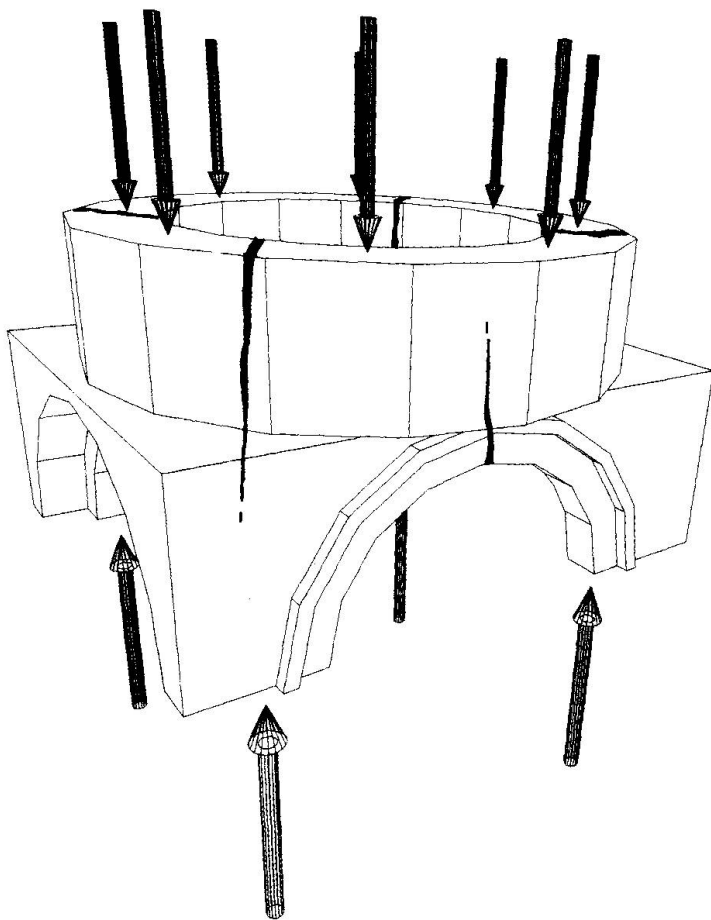

Fig. 12

Fig. 13

5. INTERVENTIONS

Thus having understood the origin of the cracks in the dome and the drum a new model has been made to verify the present safety level. The results show important bending moments in the "arches" created along the meridians by the cracks themselves (fig. 13). In order to eliminate this unfavourable situation a system of hoops, using metal cables placed at different levels on the outer surface of the dome, was proposed; the cables are not visible as they are placed beneath the lead sheeting which will be replaced and re-anchored.

The hooping cables, made of high strength stainless steel, (the type normally used for sailing boats) are lightly prestressed, in order to provide immediatly the optimum radial action and reestabilish a bidimensional "meridians-parallels" membrane behaviour. This solution incorporates economy, ease of construction, favourable structural behaviour anddurability.

To find the most appropriate positioning of the hoops, which consist of three separate pairs of cables, to determine the level of prestressing required in order to minimize the bending stresses in the meridians that developed as a result of the cracking and to assume appropriate safety levels, a final mathematical model was created (figg. 14 and 15).

Fig. 14

Fig. 15

This type of intervention is really a modern version of an ancient method for reinforcing domes, that used to involve chains built around the base of the dome. It is reversible and does not alter the architectural aspect of the dome; from the structural point of view moreover, notwithstanding the modest stresses directly applied to the masonry as shown by the mathematical model, it guarantees the survival of the monument even in the evet of future earthquakes.

REFERENCES

1. G. Croci, G. Carluccio, R. M. Viola, L. Bordi : "Restoration of the Basilica of s: Carlo in Rome" "Coloquio internacional : La conservaciòn del patrimonio Catedralicio" Madrid, noviembre 1990

2. G. Croci, G. Carluccio, R. M. Viola, L. Bordi : " Monitoring and structural analysis for the restoration of the Basilica of S. Charles in Roma " "Congreso Internacional Rehabilitacion del patrimonio arquitectonico y edificacion" Canarias, Julio 1992
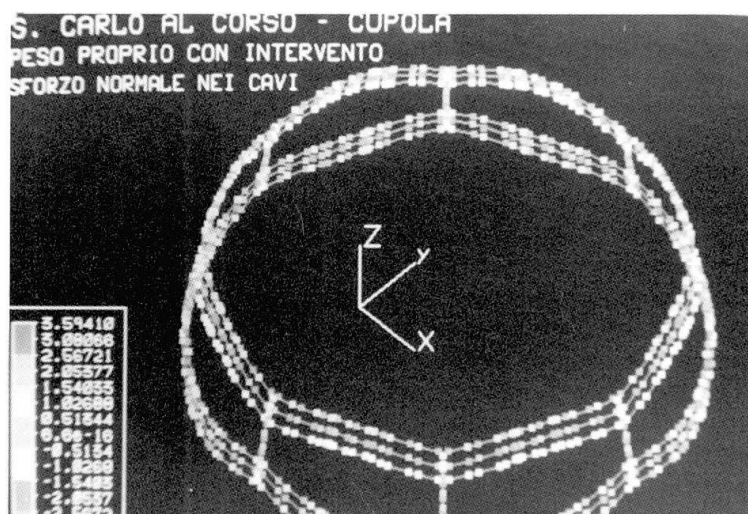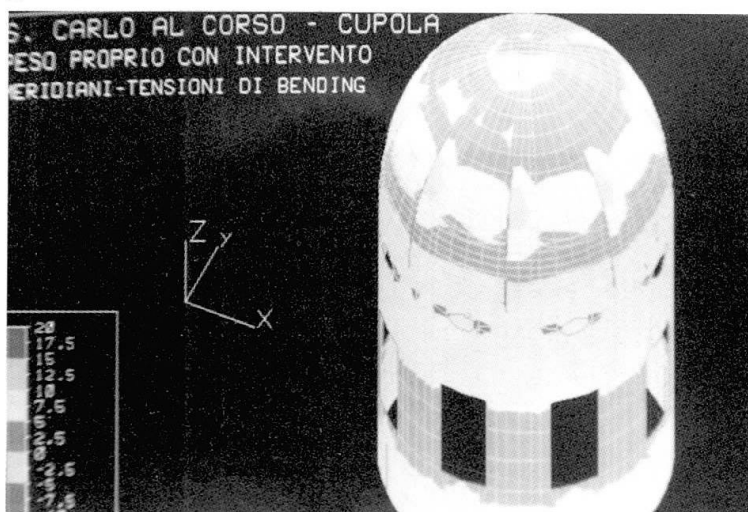
Leere Seite

Blank page

Page vide

Recent Developments in the Safety Assessment of the Colosseum

Études récentes de l'évaluation de la sécurité du Colisée

Entwicklungen in der Sicherheitsbeurteilung des Kolosseums

Giorgio CROCI
Full Professor
Univ. of Rome 'La Sapienza'
Rome, Italy

Dina D'AYALA
PhD Student
Univ. of Rome 'La Sapienza'
Rome, Italy

G. Croci, born 1936, has carried out research and project studies for the strengthening and restoration of historical buildings. Colosseum and Palace Senatorium in Rome, Ducale Palaces in Modena and Genova, Castle of Spoleto, Basilicas of S. Francis in Assisi and S. Ignatio de Loyola in Spain, are examples of his activity.

D. D'Ayala, born 1962, graduated in civ. eng. in 1988 with a thesis on historical and analytical investigation of structural behaviour of the Colosseum. Since then she has been involved in research and design of restoration techniques and is now working on a PhD on assessment of masonry dome safety levels.

SUMMARY

For ten years the Colosseum has been the object of interdiciplinary research aimed at assessing its overall and partial structural behaviour and safety level. Studies of the documentation, in situ observations and analytical modelling have allowed us to understand why the collapse has been asymmetric and why the failures, always originating from seismic actions, sometimes occurred decades or centuries after the recording of the earthquake. In this paper the results are discussed and the weakness of the monument with regard to earthquakes is outlined, the zones requiring strengthening and are outlined and the general theory underlying the interactive design is presented.

RÉSUMÉ

Au cours des dix dernières années, le Colisée a été l'objet de recherches pluridisciplinaires afin de comprendre le comportement structural partiel et global et d'évaluer les niveaux de sécurité. L'analyse des documents historiques, les observations in situ et la modélisation ont permis de comprendre les raisons de l'effondrement asymétrique et des affaissements, toujours causés par des actions séismiques, lesquels se sont produits parfois des décennies ou siècles après l'enregistrement de séismes. L'article décrit les résultats obtenus, la faible résistance du monument aux séismes, les zones nécessitant un renforcement ainsi que la théorie générale du projet d'intervention.

ZUSAMMENFASSUNG

Seit zehn Jahren war das Kolosseum Objekt pluridisziplinärer Forschung, um das teilweise oder gesamte Verhalten der Struktur zu verstehen und das Sicherheitsniveau zu bestimmen. Durch Studien der Dokumente, in-situ-Beobachtungen und analytische Modellierung wurde eruiert, warum der Kollaps asymmetrisch geschah und weshalb Kollapse, immer durch Erdbeben verursacht, manchmal Jahrzehnte oder Jahrhunderte nach dem Beben erfolgen. Dieses Dokument beschreibt die gewonnenen Erkenntnisse, die Schwächen des Monuments, was Erdbeben betrifft, die Zonen, die eine Verstärkung erfordern, und stellt die gesamte Theorie des Interventionsprojektes vor.

1. INTRODUCTION

This study was initiated for the double pourpose of discovering the actions that caused failures in the past and how the collapse mechanisms developed, and of assessing   the safety of the current configuration, this leading to the most convenient design of the repair and strengthening required against earthquakes.

The complexity of the structure and the various events that it underwent over the centuries oblige us to follow different approaches which take into account both subjective and objective aspects. Where the former are related to the interpretation of the history of the monument and the observation of the present state of the building, the latter concern in-situ survey, assessment of mechanical features and structural analysis through mathematical models. As it will be seen, it is actually only through a feed-back procedure of exchanging information between the two areas that the structural meaning of the historical notes can be correctly interpreted and the analytical models relate to the real situation [1].

2. THE HISTORICAL STRUCTURAL BEHAVIOUR

The construction of the Colosseum probably began in 72 a.D. and lasted almost ten years, the monument being dedicated under Titus reign in the 80 a. D.(fig. 1). One of the hypotheses that explains the rather fast realization of the monument is that the building-site was probably organised in four portions divided along the principal axes of symmetry of the plan. The connections between these portions can then be regarded as the weak points in the masonry. A second reason of amorphism is the building site, previously partially filled by the lake of the Domus Aurea, created by an alteration of the original hydrography settlement. The topography and the few available non-destructive drillings, it can be seen how the slopes on the two sides of the major axis have different gradients and soils: the mechanical behaviour of the ground beneath the structure is therefore not homogeneous and the foundation system presents variable depth and lay-out.

The first analitical model is a test of the structural original capacity of the monument under the dead load action. The f. e. model realised with 8 node-brick-elements, which best simulate the shear behaviour of the stone blocks, covers the three annular bands connected by the annular vaults, while the inner radial brick-masonry walls are neglected due to the high number of d.o.f involved. Under static conditions (fig. 2) the bearing capacity basically relies on the pillars whose average stresses vary from 23 KN/m^2, at the base of the first order, to 10 KN/m^2 at the base of the third order. A slightly flexural effect is also present due to the global circumpherential shape that does not completely absorb the thrust of the annular barrel vaults, causing a stress increment of 15% at the second order in the pillars close to the major axis of symmetry, where the radial component of the arches' thrust is maximum. The stress in arches and vaults is at least two order of magnitude lower than that in the columns and it can therefore be said that the monument is overdimensioned for static loading, even if we refer to the crowd load during the "spectacula", the failure stress of the travertino material being 500 KN/m^2, while the masonry limit stress, due to the roughness of the contact surfaces and the weakening due to the dressing of the stone, is definetely lower.

The natural events that followed the construction during the first centuries were not dangerous enough to compromise the safety of the monument even if fires, small earthquakes and floods certainly contributed in locally lowering the strength of the materials. Among others we only note here the fire of the 217 that destroyed the timber structure of the top roof. The first destructive event was the earthquake in 443, estimated of VIII-IX grade Mercalli Scale, with the epicentre in the roman region. The Colosseum suffered damages in the seating area, the arena, the podium and at the attic level. Some of the gigantic columns of the attic level fell down into the cavea and the damages were so serious that it took three consulates to be restored. Some of the works can still be seen at the top of the external wall, where a chaotic cyclopic masonry was set.

In order to identify the structural behaviour of the monument under seismic actions a second set of models of the original configuration has been analysed. The analyses are spectrum response dynamic elastic and, due to the dimensions of the overall mesh (46568 d.o.f.), the model has been divided in two halves along the principal axis and subjected to a seismic force acting along the dividing axis.

Two orders of problems arise; The first is related with the quantification of the seismic action that does not come straight from the M.S. information recorded. Examining the historical data regarding the seismic events recorded in the area it can be seen that an earthquake of VIII-IX grade has a return period of about 500 hundreds years. Giuffrè et al.[2] assessed that a Richter intensity of 6.68

can be attached to such period and therefore a ground acceleration of 0.05-0.06 g can be deduced. Evaluating the amplification of the masonry structure up to 2.5-3 times a design value of 0.15 g is obtained. It is worthwhile noting that the maximum seismic amplitude stated by the Italian Seismic Code for the III category areas is 0.16 g, Rome not being considered seismic area.

The second question is the interpretation of the results obtained with the hypothesis of elastic behaviour, while the structure over a certain stress level presents a strong dissipative behaviour due to friction between the blocks; on one hand, tensile stresses are feasible only in the case of a quite high compressive orthogonal stress level , on the other end the peaks produced by the elastic models are probably never attained due to the sliding and dissipation of energy that takes place at the contact surfaces. Nevertheless this type of analysis is still very valuable in defining the behaviour up to the elastic limit and in identifying the weaker and most stressed elements of the structures, and in evaluating the global collapse mechanisms. The stress and deformation values, given below, must be taken as indicative, referring to macro-elements that simulate extensive portions of the blockwork.

The cylindrical vertical surfaces (figg. 3-4) exerted a fundamental bidimensional behaviour which, as long as the friction limit is not overcome, lead to relatively low bending moments in the pillars: the maximum reaches 13.0 KN/m² that added to the dead load stress gives a top value of 36 KN/m² while the cross section is wholly compressed. On the other hand, in the upper part, due to the low vertical stress level and the lack of radial constraint, active in the lower part by means of the annular vaults, the friction limit is extensively overcome: tensile circumpherential stresses (σ_a) reach upto 4.53 KN/m², while the corresponding vertical stress (σ_v) is 6.6 KN/m² with a ratio 0.68 that is over the value of the dynamic friction coefficient $\mu = 0.433$, corresponding to the fact that the most severe damage occurred here.

The f.e. analysis further confirms that a single event of this magnitude cannot have taken the structure upto complete failure but can only have caused localised damages: distribution of stresses along the plan are not, infact, homogeneus and only arise to limit values on one or two radial alignments. Furthermore limit stresses do not take place on the same alignments for all the elements. This means that other causes and factors must be investigated in order to explain how the first vertical solution of continuity occurred and whether from there the collapses extended to a big portion of the structure. Again the analysis of the historical information may prove valuable for this purpose.

The next destructive earthquake recorded is in the year 801; it arrived after a period of almost 300 years during which, the monument was not only disused and abandoned (after 523) but also a few small earthquakes occurred, plant roots expanded existing cracks and formed new ones and finally, the structure underwent serious damage when the metal connections between blocks were removed. The earthquake probably had its epicentre in the Abbruzzese Appenino and caused damages up to the IX M. S. grade in the roman area. Extensive notes of the damages in the Colosseum are not available but it can be inferred that what was left of the cyclopic order at the attic level fell into the cavea causing huge damages in the inclined barrel-vaults of the arena, and other less striking structural cracks. It is likely that on this occasion the first important breach in the annular walls opened (fig. 5): if the location is deduced from later iconography (there being no remaining contemporary iconography), we can say that it occurred in the quarter overlooking the Constantinus Arch, this being common to all the available views. Whether it has occured at a point closest to the major or minor axis of symmetry can not be positively said, but our results indicate the portion close to the major curvature as the one with highest radial tensile stresses in the annular vaults (up to 3.25 KN/m² versus 2.66 KN/m² along the minor axis) and highest annular stresses in the attic wall, 5.6 KN/m² with a vertical compressive stress of 5.2 KN/m², that clearly exceed the frictional resistance. Once the sliding occurs there is a corresponding increase in the circumpherential length at the upper level leading to out of plumb and thus to relevant eccentricity of the normal force in the first order pillars, consequent reduction of the effective section, and finally an increase of stress level, which initiate instability.

In that occasion, with the extensive damages of the cavea's barrel-vaults, the radials connections also started weakening. As seen from the model, in the original state the annular vaults perform a fundamental role transmitting stress between inner and outer portions, in this way limiting flexural stress in the outer pillars. This bond was further released when during the X and XI centuries the noble families of the city started fighting for the possession of the Colosseum and eventually fortified it, destroying the original staircases (which may have been partially destroyed already) and opening holes in the annular vaults to put removable ladders between the floors. The medal of Ludwig The Bavarian, minted in 1328, depicts the monument with the upper ring closed, but the occasion of the representation, commemoration of the new emperor, and the small scale of the picture can explain

the lack of reliability. However this is the last known iconographic document before the destructive earthquake of 1349. Minor earthquakes of local origin had in the meanwhile occured in 1255, 1287, 1300, 1321 and in 1348, but none of them caused as much destruction as the one of September 1349, with epicentre in the Umbro-Abruzzese Appenino, which was very violent in l'Aquila, Montecassino and Perugia. Damages in Rome affected the S.Paolo and S.Giovanni basilicas, and caused the complete failure of the Torre dei Conti and Torre delle Milizie. This is thus remembered as the most destructive earthquake ever in Central Italy.

As for the Colosseum, all historical sources agree in recognising this as the event that produced the complete failure of the two external cylindrical walls on the Celio side. It has been said that the structural configuration had changed significantly since the origin and had, infact, become weaker, due to the relaxation of the block-work and the beginning of out of plumb phenomena, locally amplified by constructive defects (fig. 6). If this explains the more destructive effect of this earthquake compared with the previous ones, it still does not explain why the distribution of failures was not spatially homogeneus but concentrated on the Celio side. The reason may be found in the foundation system. More accurate studies will be required in order to assess the actual situation, the simulation of a different stiffnesses at the foundation level, by means of spring finite elements with variable stiffnesses, evaluated taking into account both the mechanical characteristics of the ground and the geometry of the foundations, helped to give a better understanding. The spectrum dynamic analysis produces smaller natural frequencies and higher amplification on the Celio side (fig. 7), the most important modes showing rotational symmetry. As for the stresses they reach a maximum in the inner pillars (with a maximum of 27.5 KN/m2) of the more flexible side, while the effect of different foundations decreases at the upper levels. If we add this value to the dead-load value we find that tensile stress is reached in a wide portion of the section, evntually causing crushing on the other edge. Even if we might initially assume that these actions were partially redistributed among the pillars and the inner brick walls, we have just seen how the historical events released radial collaboration, and while the inner pillars could benefit from it, the medium and outer ones definetely could not, their stress levels increasing upto collapse.

After this earthquake the Colosseum was abandoned apart for its use as a quarry for travertine blocks and loose bricks for use in furnaces. During the next three centuries, all sources agree in stating that most of the material that was taken for other building sites, apart from a few recorded exceptions, was not removed from the structure itself but from a large mound of rubble called "Coxa Colisei". Also in this period (beginning of the XVI century) the ruin of a wide portion of the inner ring on the Celio side around the minor axis is recorded. Other "spontaneous" failures took place in 1646 and 1689. These events, called "spontaneous" because they cannot be directly related with any seismic action, can be explained as consequences of the mechanism described above: the high compressive stress level, created cracks and microcracks sensitive to thermo-hygrometric conditions, provoking an increment of internal stress in the outer layers of the blocks, thus facilitating spalling. A deterioration process was therefore initiated, leading to a critical situation decades or centuries after the original action. This phenomenon, leading to near collapse, was observed by us in 1979, when following the removal of cladding blocks, a limit state situation was evident (fig. 8)

In 1703 another destructive earthquake occurred, again with its origin in the appenine region and the same energy characteristic as the one that occurred in 1349. Nevertheless damages were much less exstensive, only the ruin of an arch having been recorded. To understand the behaviour of the structure in this configuration, a new model has been prepared under the hypothesis that the most vulnerable part, the outer annular wall, had highly inefficient radial constraints. Results show a wave deformation of the attic level (fig. 9) both in the horizontal and vertical planes, and high vertical stresses in the pillars at the free edge of the surface, affected by an outward flexural action around the radial axis. The maximum flexural stress, $\sigma_v = 34.27$ KN/m^2, cannot be equilibrated by the dead-load stress. The annular horizontal stresses in the attic reach a maximum in the area of the minor axis ($\sigma_a = 12.1$ KN/m^2). As it can be seen the zones more stressed are the zones that a century later were affected by the large restoration works of Stern, Valadier, Salvi, and today the deformation provoked by the seismic action is still visible in part of the attic level (fig. 6).

According to the process outlined above, and to the frictional nature of the material, is likely that the high stress values resulting from the elastic analysis were not reached in the various elements in a istantaneus manner: more likely the damage phenomena slowly evolved toward the collapse, and their complete revelation was delayed up to forty years later, when, due to the spread state of ruin and incipient crash Benedetto XIV closed the monument and started its first restoration campaign.

3. ASSESSMENT OF THE CURRENT SAFETY LEVELS AND RESTORATION APPROACHS

As it has been seen in the previous paragraph the spatial distribution of structural alterations and the general state of conservation vary due to original oddities and are further accentuated by the train of events, so that today, in spite of the strenghtening works that took place in the last century, aimed at a global improvement of the structure performance, the safety levels also vary greatly.

Searching for the reasons why the three main interventions on the Colle Oppio side were realised, the Stern abutment (1807), the Valadier abutment (1825), Salvi's partial reconstruction of the third medium order and the system of radial tie-rods in the allignments around the imperial entrance, they appear to be attempts to stop an incipient collapse mechanism of the outer wall with characteristics very close to the f. e. model results. We have already seen how the outer edges of the surviving structure, where the constraints were lesser or inexistent, were the areas most under threat of collapse. The two abutments, with very different lay-outs and technologies involved, had the same aim of containing the annular thrust of the arches at the edge of the wall, limiting and preventing further development of vertical cracks and out of plumbs: both of them are connected to the original inner structure to recreate the collaboration along the radial directions. Their stiff and massive character highly modified the overall structural behaviour: having restrained its vertical edges, no longer allowed to move outward, deformations migrated to the area around the minor axis, whose bond between blocks had already been loosened. Outward movements, producing flexural stress in the lowest pillars, amplifying themselves because no tensile strength was available to counteract them, increased upto a point when Salvi's intervention was needed to prevent collapse.

These XVIII century restorations were all related to static stability, with no concern for dynamic actions. In fact, analysing their behaviour as part of the global structure under seismic actions, the abutments appear to be rather dangerous due to the difference in strength with regard to the original material, while also involving excitement of large masses. The worst result stems from actions orthogonally oriented to them; in the model analysed, connections in the radial direction are assumed to be active: the static situation is already quite different from the original one (fig. 10), the present configuration implying higher flexural stresses in the pillars of all orders (maximum eccentricity being up to 5 times higher than the original value); the seismic action, on a structure with fundamental natural frequencies 2 times smaller than the original one, greatly amplifies this phenomenon especially for the pillars of the third order where the stiffening contribution of the abutments is less and the connection with the inner rings are only partially realised (fig. 11). For those pillars flexural stresses produced by the earthquake are of the same order of magnitude as the static ones, therefore causing partialization of the cross sections (σ_v reaches 22 KN/m^2 versus -14.4 KN/m^2 of the dead load case). The attic portion has very low natural frequency these being caused by the low stiffness in the annular direction; stresses are of the same level as before but greater deformation and further sliding should be expected.

The study discussed above gives many indications of the criteria required to provide the monument with adequate safety levels and durability. The first task will be related to the deterioration process that affects many parts of the monument, for example the zone adjacent to the six pillars that were restored in 1979; it will be necessary to strengthen or replace some of the blocks. The second task is related to the vulnerability of the structure to seismic action: this inadequacy has increased throughout the centuries due to the loss of continuity, the separations formed between the elliptical walls, the out of plumb and the sliding of blocks. Consequently an improvement of the tensile resistance in both annular and vertical directions for the outer walls is required: this can be achieved by creating efficient circumpherential connections at the top of the wall and radial ties corresponding with the inner structure. In order to provide an efficient global behaviour, the region of interface between the original structure and the Stern and Valadier abutments also requires strengthening.

However, the historical value of the Colosseum obliges us to proceed with prudence in every intervention, and to avoid where possible further changes to the present form.

4.REFERENCES

1. CROCI G., D'AYALA D., I crolli e i dissesti del Colosseo: le ipotesi di effetti sismici. Notiziario ASS.I.R.C.CO, october 1989.

2.GIANNINI R., GIUFFRE' A., ORTOLANI F., PINTO P.E., VENEZIANO D., Dati storici e modello probabilistico della sismicità di Roma, Quaderni del Dip. di Ingegneria Strutturale e Geotecnica, Roma 1984

3. CROCI G., D'AYALA D., DI PAOLO A., Studi e ricerche sul Colosseo, Quaderni del Dip. di Ingegeria Strutturale e Geotecnica, Rome 1990.

4. CROCI G., D'AYALA D., CONFORTO M. L. Studies to evaluate the origin of cracks and failures in the history of Colosseum in Rome, I International Congress on Restoration of th Architectural Heritage and Building, Canarias July 1992.
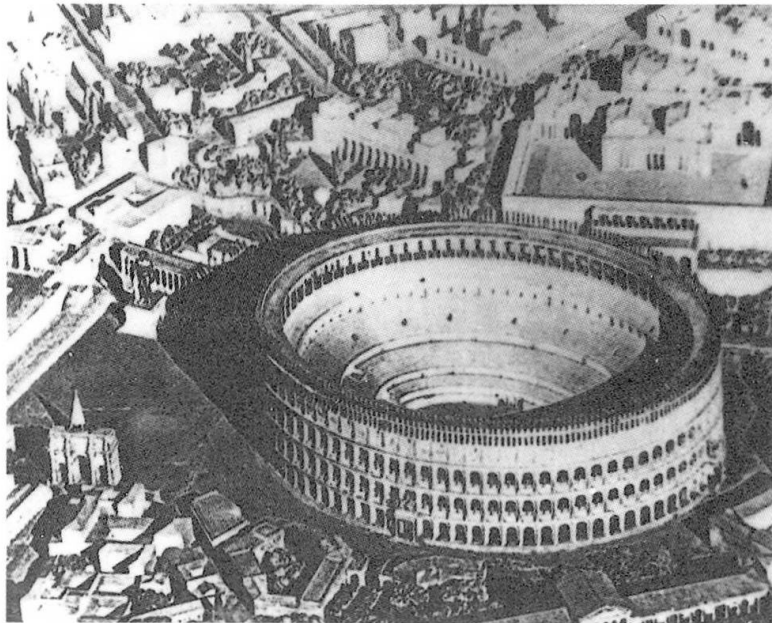
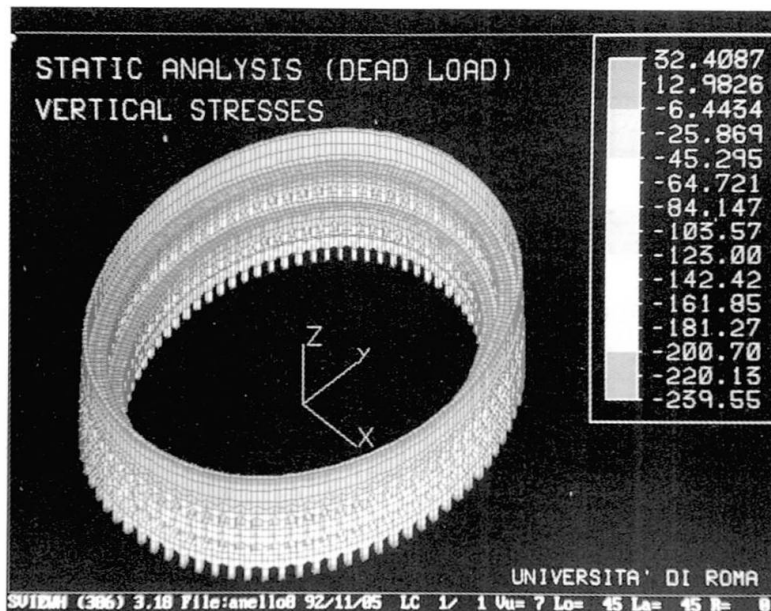fig. 1 - Model from the plastic of "Roma at the time of the Empire"

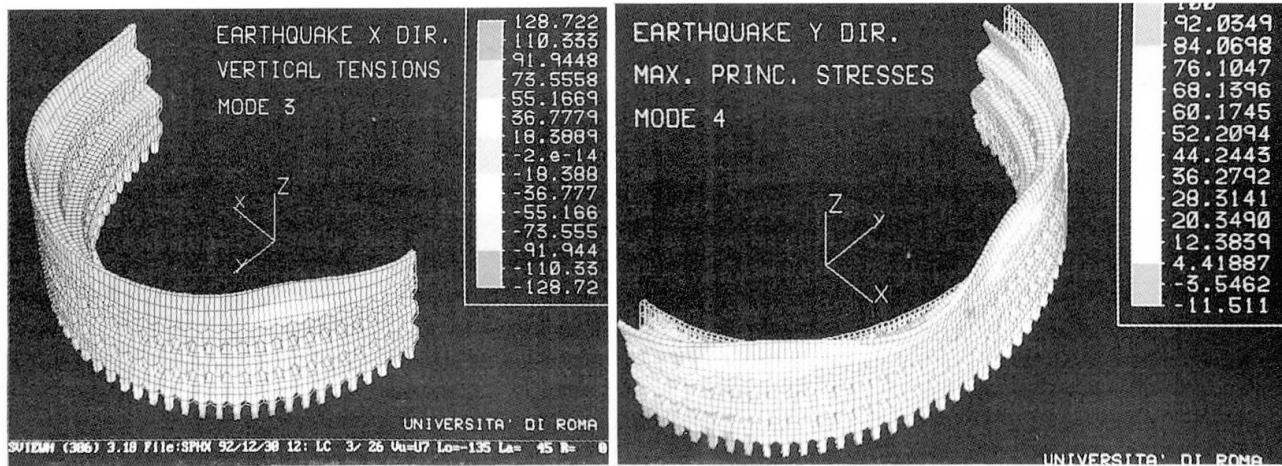fig. 2 - Analytical model for the original configuration

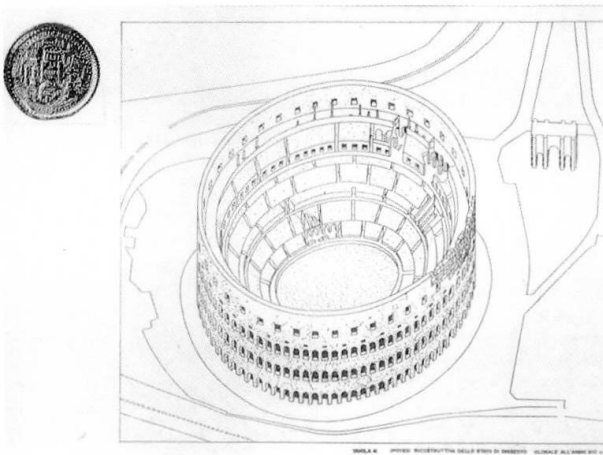fig. 3 - 4 Response spectrum dynamic analysis for the original shape

fig 5 Hypotethical state of conservation after year
801

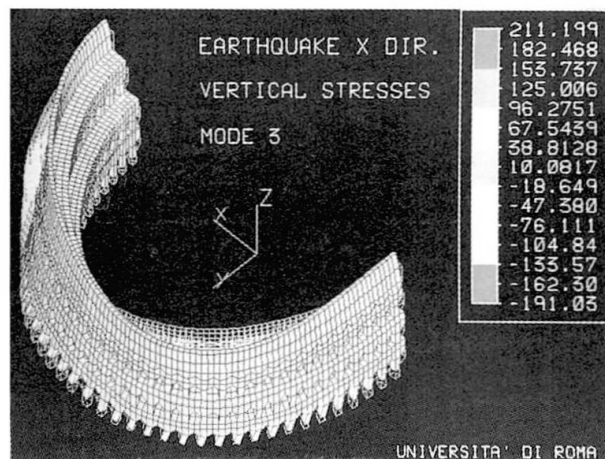fig.6 Synusoidal deformation of the parapet.

fig. 7 Spectrum response dynamic analysis
simulating differentiated foundations

fig.8 State of the pillars on the Stern abutment
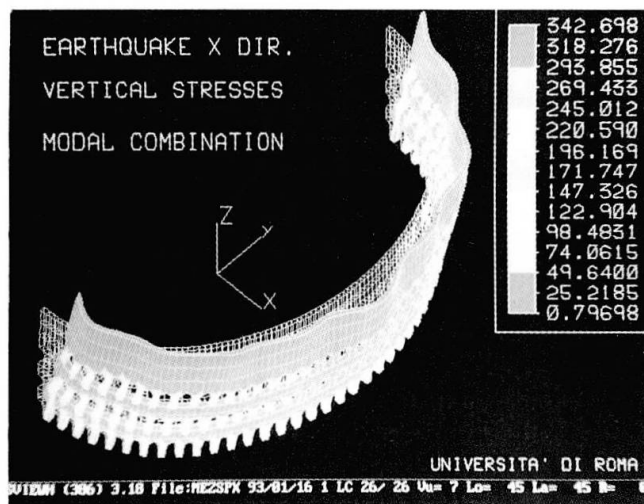side in 1979.

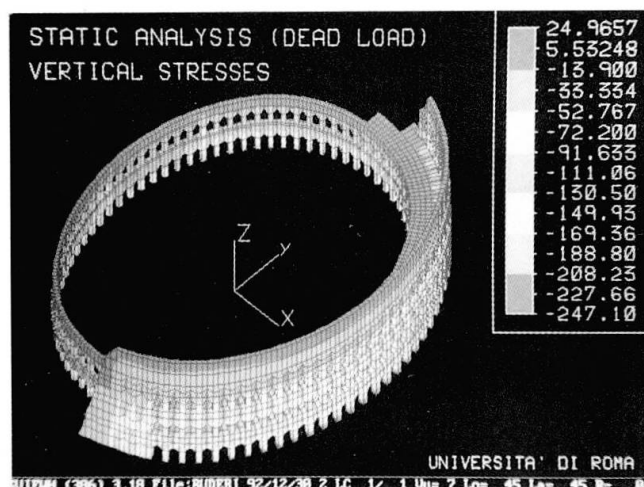fig. 9 Analytical model in the 1703 configuration

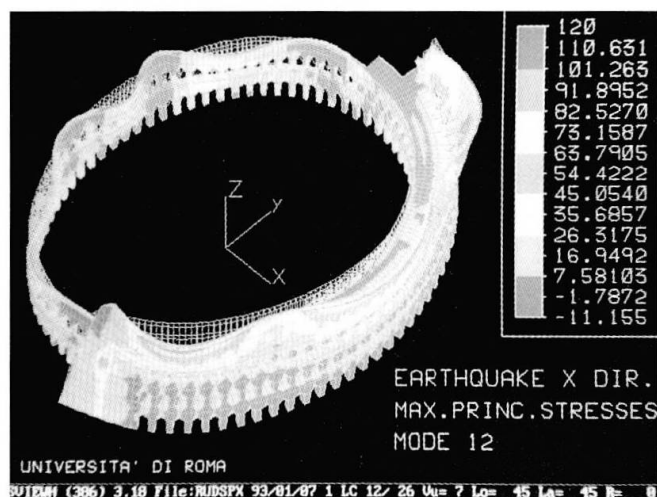fig. 10 - Analytical model of the today configuration

fig. 11 - Analytical model of the today configuration. Spectrum response dynamic analysis.

5. AKNOWLEDGEMENTS

Mechanical Characteristics of Ancient Roman Masonry

Propriétés mécaniques de la maçonnerie antique romaine
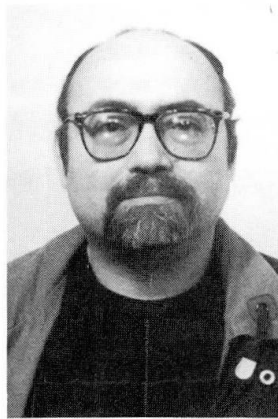
Mechanische Eigenschaften antiken römischen Mauerwerks

Christos IGNATAKIS
Dr. Eng.
Aristotle Univ.
Thessaloniki, Greece

E. STAVRAKAKIS
Dr. Eng.
Aristotle Univ.
Thessaloniki, Greece

George PENELIS
Dr. Eng.
Aristotle Univ.
Thessaloniki, Greece

SUMMARY

The procedure for the analytical evaluation of the mechanical characteristics of Roman masonry and the strength of the bearing structure of the Rotunda of Thessaloniki is presented. The mechanical properties and failure envelope of ancient Roman masonry were predicted using a specific finite element program for the non-linear analysis of masonry micromodels. Using the predicted properties of masonry, the structural system of the monument was analysed and proved to be cracked meridionally under dead loads. Finally the ultimate seismic capacity of the supporting piers has been calculated.

RÉSUMÉ

L'article présente une analyse des propriétés mécaniques de la maçonnerie romaine et de la résistance de la structure porteuse de la Rotonde à Thessalonique. Les propriétés mécaniques et la charge de rupture sont estimées à l'aide d'un programme d'éléments finis permettant l'analyse non-linéaire des micromodèles de la maçonnerie. Les propriétés estimées de la maçonnerie sont utilisées pour l'analyse du système de la structure du monument, lequel a montré des fissures méridiennes sous le poids propre. Finalement, la résistance ultime sismique des piliers qui portent le dôme est calculée.

ZUSAMMENFASSUNG

Im Aufsatz wird eine Vorgehensweise zur analytischen Bestimmung der mechanischen Eigenschaften des römischen Mauerwerks und der Festigkeit des Tragsystems der Rotunda von Thessaloniki dargestellt. Die mechanischen Eigenschaften und die Bruchlast des römischen Mauerwerks werden mit Hilfe eines speziellen Finite-Elemente-Programms bestimmt. Unter Verwendung der berechneten Eigenschaften wird das für die nichtlineare Berechnung von Mikromauerwerksmodellen statische System des Denkmals analysiert und gezeigt, dass es unter Eigenlast in Meridialrichtung gerissen ist. Abschliessend wird die seismische Grenztragfähigkeit der Mauerwerkstützen berechnet.

1. INTRODUCTION - ROTUNDA OF THESSALONIKI

The Rotunda of Thessaloniki, built in about 300 A.D., is the greater surviving monument of the late Roman Empire in the Balkan region. It is an imposing circular building, resembling the Pantheon in Rome, covered by a huge brick masonry dome 24.50m in diameter. The dome is supported by a, 20.00m in height and 6.25m in thickness, cylindrical drum divided into eight strong piers,by barrel vaulted niches and openings at two levels (Fig.1,5). The structure, already extensively cracked due to earthquakes during its life, suffered serious damage due to the earthquake of June 20, 1978 (epicenter 30km from Thessaloniki, magnitude 6.2 grades in Richter scale). The dome was radially cracked in its lower zone. The two southern piers P_2, P_3, weakened due to internal helical staircases (Fig.1), had wide shear-compression inclined cracks which have been reactivated.

Extensive emergency works were undertaken after the earthquake because of the critical structural condition of the monument. During the 1980 a team of specialists, supervised by Pr. Penelis, carried out a wide research project on the repair and strengthening of the monument including extensive in-situ investigations and laboratory tests. The greater part of structural analyses were carried out considering the masonry as homogeneous, isotropic and linearly elastic material [1].

Recently at the Reinforced Concrete Lab. of Aristotle University of Thessaloniki extensive research has been carried out for a better approach to the problem of evaluation of nonlinear mechanical properties of reinforced concrete and masonry structures by means of F.E.M. The following specific F.E. computer programs have been the fruits of these efforts:
"MAFEA": For the in-plane nonlinear analysis of unreinforced masonry under monotonic loading until failure. The program is capable of predicting cracking, crushing, or transverse splitting of bricks and mortars, as well as sliding or unstucking at the joints and simulating propagation of damage. It must be pointed out that the program calculates and takes rationally into account the transverse third principal stresses that developed in bricks and mortar joints under the in-plane loading of masonry·[2].
"AXICRACK": For the linear elastic analysis of isotropic or orthotropic axisymmetric structures. A nonlinear repeated process for the propagation or meridional cracking is included [3].
"RECOFIN": For the in-plane nonlinear analysis of reinforced or unreinforced concrete under monotonic loading until failure. The program is capable of predicting cracking or crushing of concrete as well as yielding or sliding of reinforcing bars and simulating propagation of damage [4].

In the following the three phases of limit analysis of the bearing structure of Rotunda in order to determine the ultimate strength of the monument under dead and seismic loading are presented. The mechanical properties and failure envelope of Roman masonry were predicted using the MAFEA program. The axisymmetric structural system of the monument was analysed using the AXICRACK program. Meridional cracks were predicted under dead loading at the upper ring which connects the piers. Finally the ultimate seismic capacity of the piers was calculated by the RECOFIN program using the previously predicted properties of masonry.

2. MECHANICAL CHARACTERISTICS OF MASONRY

The necessary input for the MAFEA program is the geometry of the masonry and the mechanical properties of bricks, mortar and joints. The most of them had been already determined by the in-situ and laboratory tests, as mentioned above, and are given in Table 1.

It is well known that in a structural member the dominant stress state under in-plane loading consists of a pair of compressive and tensile principal stresses ($\sigma_1 < 0$, $\sigma_2 > 0$) of various ratio. The stress state of masonry at the piers of

Materials	Dimensions	f_c(MPa)	f_t(MPa)	E_0(MPa)	v_0	ε_u(‰)
Bricks	30x40x5cm	f_{bc}=9.00	f_{bt}=1.20[2]	E_{bo}=10700	0.19[3]	2.50[3]
Mortar	t_{bed} ≈4cm	f_{mc}=1.20[1]	f_{mt}=0.40[2]	E_{mo}= 1350	0.19[3]	2.50[3]
Joints	t_{vert}≈3cm	Shear strength:f_{jso}=0.17,Tensile strength:f_{jt}=0.075MPa[3]				

(1) Prismatic strength from the strength of a short specimen: f^c_{mc}=1.80MPa

(2) Direct tensile strength from the flexural strength: f^{fl}_{bt}=2.25, f^{fl}_{mt}=0.65MPa

(3) From the literature according to relative measurements.

Table 1 Mechanical properties of masonry materials,input for the MAFEA program

Rotunda, under dead and radial seismic loading, consists mainly of normal stresses σ_n perpendicular to the bed joints and shear stresses τ in meridional level (Fig. 2a). The stress state (σ_n, τ) is equivalent to the principal stress state (σ_1<0, σ_2>0) mentioned above.

In order to determine the mechanical characteristics of Roman masonry, the micromodel shown in Fig.2a was analysed under various normal stresses σ_n increasing gradually to a defined value, followed by shear stresses τ increasing gradually until failure.

The model was analysed at first under uniaxial compression (σ_n, τ=0) and pure shear (σ_n=0, τ) in order to bound the (σ_n, τ) failure envelope and on the other hand in order to determine the following basic mechanical properties of masonry:
-Compressive strength perpendicular to bed joints: f^n_{wc}=3.111MPa
-Modulus of elasticity perpendicular to bed joints (initial value): E^n_{wo}=2667MPa
-Normal stress-strain curve (σ_n-ε_n): See Fig.2b
-Shear modulus (initial value): G^w_{wo}=1090MPa
-Strength under pure shear loading: f_{wso}=0.133MPa
-Shear stress-strain curve (τ-γ): Almost straight line.
The strong and early appeared nonlinear character of the stress-strain curve (σ_n-ε_n) must be attributed to the weakness of mortar which is almost the 50% of the masonry mass.

In order to define the failure envelope shown in Fig.2c, seven failure points (σ_n,τ_u) were determined for various predefined values of σ_n (points 2,3...8). It can be seen that the shear strength of masonry shows a serious reduction when the normal stress σ_n exceeds the 50% of the compressive strength of masonry. The corresponding failure envelope in principal stresses at the (-,+) region (σ_{1u}<0, σ_{2u}>0) is shown in Fig.2d. Finally in order to bound this curve at the tensile axis, the masonry micromodel was analysed for tenth time under uniaxial tensile loading (σ_1=0, σ_2) parallel to the bed joints until failure (f^p_{wt}=0.135MPa, see Fig.2d, point 10). The initial value of elasticity modulus under this loading found to be E^p_{wo}=5555MPa which is more than double in comparison with E^n_{wo}. The anisotropic character of the masonty is obvious.

In Fig.2c and 2d, are also shown in dashed line the corresponding failure envelopes of a "concrete like" material having a compressive strength equal to the masonry. These curves had been used as failure criteria at the strengthening project of Rotunda in the 1980. The compressive strength of masonry had been calculated according to the following formula:

$$f^n_{wc} = \sqrt{f_{bc}} \ \sqrt[3]{f^c_{mc}} = \sqrt{90.0} \ \sqrt[3]{18.0} \approx 25.0 kg/cm^2 \approx 2.50 MPa$$

It must be pointed out the great overestimation of strength if masonry considered as a homogeneous material ignoring the shear weakness of joints.

In the Fig.3a,b the families of failure envelopes of masonry under principal stresses at the (-,+) region for various orientations of principal axes to the bed joints, experimentally determined by Samarasinghe-Hendry[5] and Page[6] respectively, are shown. On these figures the failure curves corresponding to the $(\sigma_n, \tau) \rightarrow (\sigma_{1u} < 0, \sigma_{2u} > 0)$ loading has been drawn with dashed line. On each curve the points ① till ⑨, corresponding to the analytically determined failure points of the Fig.2d have been marked. Although on the masonry of Rotunda the bricks are much more flattened and the mortar joints are much more thick than those of the experimental programs mentioned above, the qualitative similarity of the analytically determined failure envelope of ancient Roman masonry with the relative experimentally determined curves is remarkable.

The propagation of damage, until failure of the models, predicted by the MAFEA program is very interesting. The gradual dominance of joint damage and the brittle character of failure are evident as the precompression decreases. In Fig.4a the damage pattern at failure of the model No 4 is shown. The most of header joints were unstucked during the phase of step by step application of uniaxial compression till the final value of $\sigma_n = 1.555$ MPa. Under the first steps of superadded shear loading, slidings and unstuckings of mortar elements at the bed-header joints crossings were occured. Finally failure occurs, under $\tau_u = 0.153$ MPa, due to successive inclined cracking of brick elements and sporadic cracking or crushing of mortar elements. In Fig.4b the damage pattern at failure of the model No 9, under pure shear loading, is shown. The failure has a strong brittle character. Ladder like slidings and unstuckings of mortar joints occured under $\tau_u = 0.133$ MPa, without any warning damage at the previous loading steps.

3. STRENGTH EVALUATION OF THE MONUMENT

3.1 Axisymmetric Structural System under Dead Loading

In Fig.5 the axisymmetric F.E. model of the structural system of Rotunda, analysed using the AXICRACK program, is shown. The masonry at the dome and the connecting rings is considered as linearly elastic isotropic material ($E_{wo} = 2667$MPa), because the compressive stresses developed in monumental structures under service loading are almost one order of magnitude smaller than the material strength. At the three zones of openings of the cylindrical drum, masonry is considered to be orthotropic with Modulus of Elasticity equal to zero at the circumferential direction. The excess of tensile strength of masonry ($f^p_{wt} = 0.135$MPa) has been used as failure criterion for the prediction and propagation of meridional cracks.

Under the thrust of the dome the upper connecting ring has been progressively cut after three successive analyses of the model (see Fig.5b). The lower ring and the lower zone of the dome are also under circumferential tension and it is expected that they will be cracked as well under the superadded action of a medium sized earthquake. So the piers must be considered to act as independent free standing cantilevers. Consequently the ultimate strength of the monument depends on the strength of the piers.

3.2 Strength of the Piers under Dead and Seismic Loading

Two piers were modeled, one without (P_1) and another with internal staircase (P_2) and were analysed, under dead and seismic loading, until failure using the RECOFIN program. The radial distribution of normal force N and horizontal thrust V of the dome at the top of a pier (see Fig.6) were determined by circumferential integration of the normal and shear stresses respectively, calculated using the AXICRACK program. The 2D F.E. models refer to the middle meridional level of the piers. In order to simulate the variable cross section of the piers, due to the openings, the masonry rings at the top, medium and foundation level and the staircase hole, the thickness of each element has been estimated appropriatelly.

The mechanical properties and the failure envelope of masonry under biaxial compression-tension (-, +), determined previously using the MAFEA program, are introduced into the RECOFIN program. In order to form the complete biaxial failure envelope required by the program, the failure curves for the (+, +) and (-, -) regions of an "equivalent concrete" are used. The dead loading was applied step by step in two successive phases corresponding to erection phases. At first the dead weight of the piers (W_{pier}: see Fig.6) was applied in four steps, afterwards the weight and the horizontal thrust of the dome (N_{dome}, V_{dome}: Fig.6) were added at the top of the pier in two steps. Finally the seismic loading was applied step by step up to failure.

In Fig.65 the cracking propagation of the two models until failure is shown. The models sustained the dead loading and the seismic loading up to a value of 10% and 8% for the seismic coefficient (c), for the pier P_1 and the perforated pier P_2 respectively, without any damage. The first horizontal crack at the model P_1 appeared at the inner part of the base for c_{cr}=11% and propagated till the core of the pier (Fig.6a). At the next loading step (c=12%) no further damage occured. Finally for c_u=13% inclined flexural cracks appeared at higher levels of the inner face of the pier propagating to the core and failure occurs due to vertical splitting at the outer face of the base. The model P_1 shows a flexural, rather ductile type of failure. On the contrary the model P_2 shows a shear-compression brittle type of failure. At a seismic coefficient of c_{dcr}=9% inclined cracking occured firstly at the very thinner elements of the core of the pier (see Fig.6b) and rapidly propagated diagonally up and down cutting the thin elements of the staircase hole till the base. The thicker elements along the inner and outer faces of the model remained intact with the exception of the lowest inner element at the base which was horizontally cracked. At the next loading step (c_u=10%) the horizontal crack propagates to the core of the base, the diagonal cracking propagates upwards cutting the inner face and finally failure occured due to vertical splitting at the outer face of the base. The cracking pattern of the model P_2 simulates successfully the existing active inclined sliding surface at the piers P_2 and P_3 of the monument (see Fig.5b, 6b). Furthermore the base shear resistance of both types of piers was found to be close to the results found during the 1980 research project [1].

4. CONCLUSIONS

The successful analytical simulation of the structural behavior of a huge masonry monument, starting from the material properties and ending to the strength evaluation and the failure patterns, is very encouraging and the procedure followed seems to have good prospects for further development. Of course several points and results should be justified through extensive parametric analyses, before this procedure would be considered as a useful tool for practical purposes. The authors are convinced that the analysis by means of F.E.M. with microelements of bricks and mortar is the most promissing one for the determination of the failure envelope and the constitutive law of old masonries as the only necessary inputs are the geometry of masonry and the mechanical properties of bricks, mortar and joints which can be rather easily experimentally determined.

REFERENCES

1. PENELIS G. et al., The Rotunda of Thessaloniki: Seismic Behavior of Roman and Byzantine Structure. Proc. of the Coll. of the Structure of Hagia Sophia from the Age of Justinian to the Present, Princeton Univ., USA, 1990.

2. IGNATAKIS C., STAVRAKAKIS E. and PENELIS G., Analytical Model for Masonry Using the Finite Element Method. Intern. Journal "Software for Engineering

Work Stations", April 1990.

3. IGNATAKIS C., STYLIANIDIS K. and STAVRAKAKIS E., A Special Finite Element
   Axisymmetric Model for the Analysis of Interventions in Domes Including Crack-
   ing Consideration. Proc. of the Intern.Techn.Conf. on Structural Conservation
   of Stone Masonry, Athens, Greece, 1989.

4. IGNATAKIS C., STAVRAKAKIS E. and PENELIS G., Parametric Analysis of Reinforced
   Concrete Columns under Axial and Shear Loading Using the F.E.M., A.C.I. Str.
   Journal, July-August 1989.

5. SAMARASINGHE W. and HENDRY A., The Strength of Brickwork under Axial Tensile
   and Compressive Stress. Proc.of the British Ceramic Society, No 30,Sept. 1982,
   pp. 129-139.

6. PAGE A., The Strength of Brick Masonry under Biaxial Tension-Compression. Int.
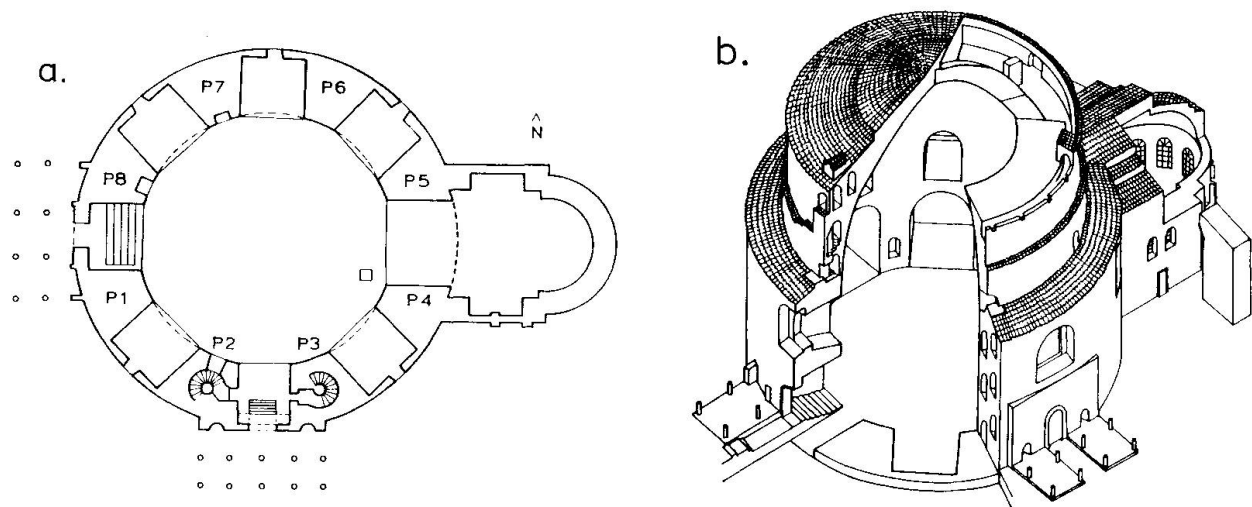   Journal of Masonry Construction, V. 3, 1983, pp. 26-31.

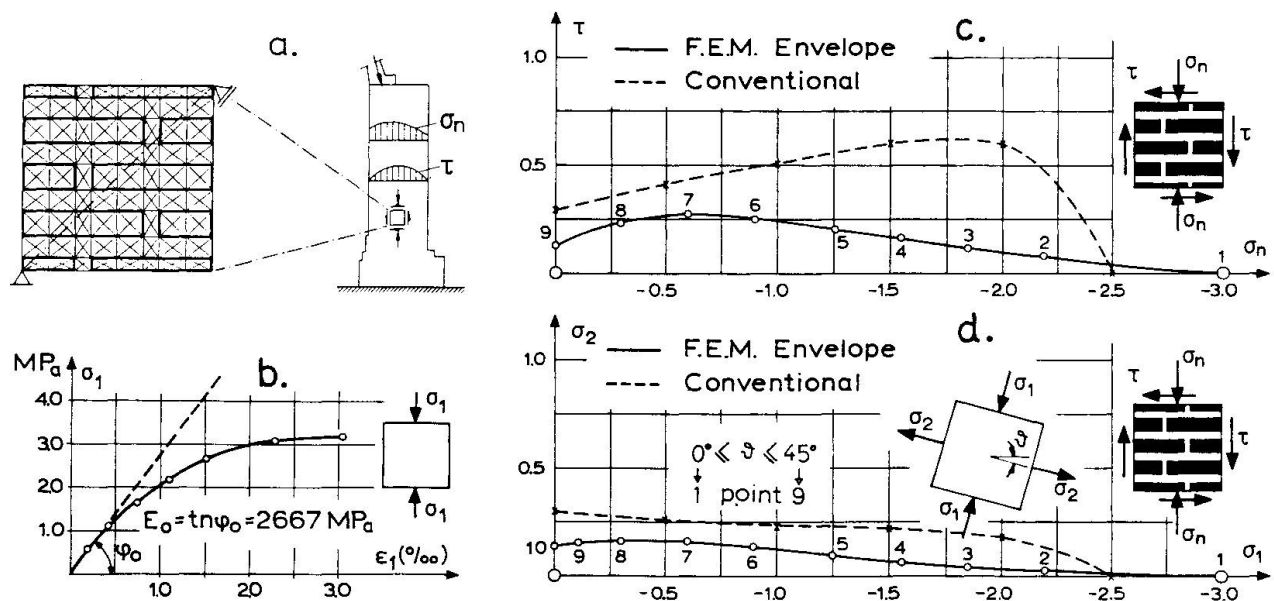**Fig.1** Rotunda of Thessaloniki: a.Plan at ground level, b.Isometric view

Fig.2 Analytical evaluation of masonry properties: a.Masonry micromodel,
b.Stress-strain curve (σ_n-ε_n), c.Failure envelope (σ_n,τ), d.Failure
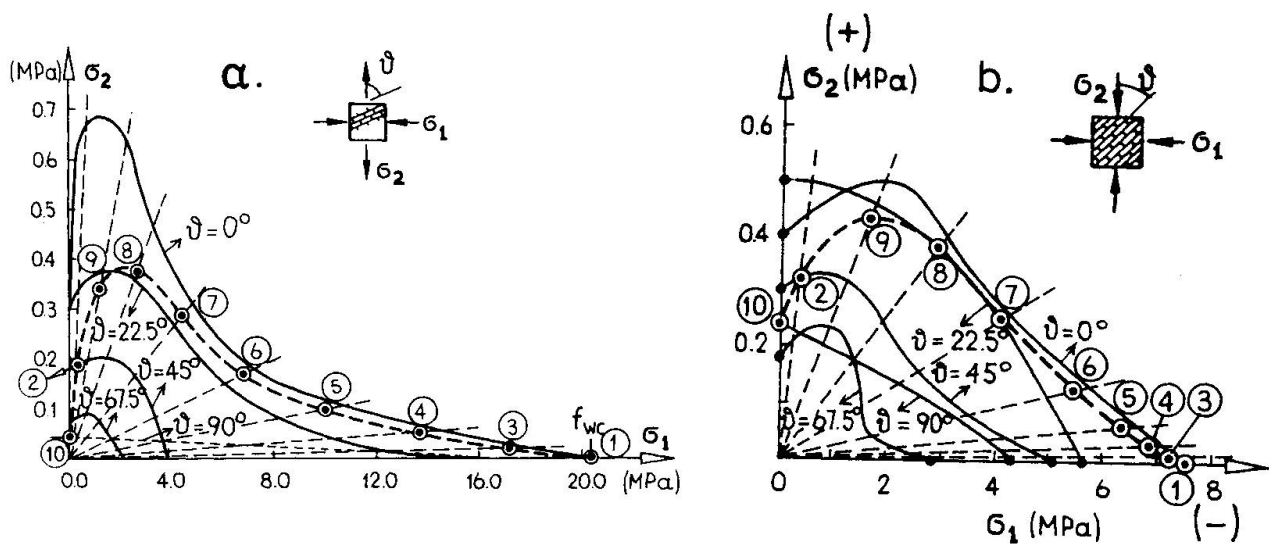envelope (σ_1,σ_2)

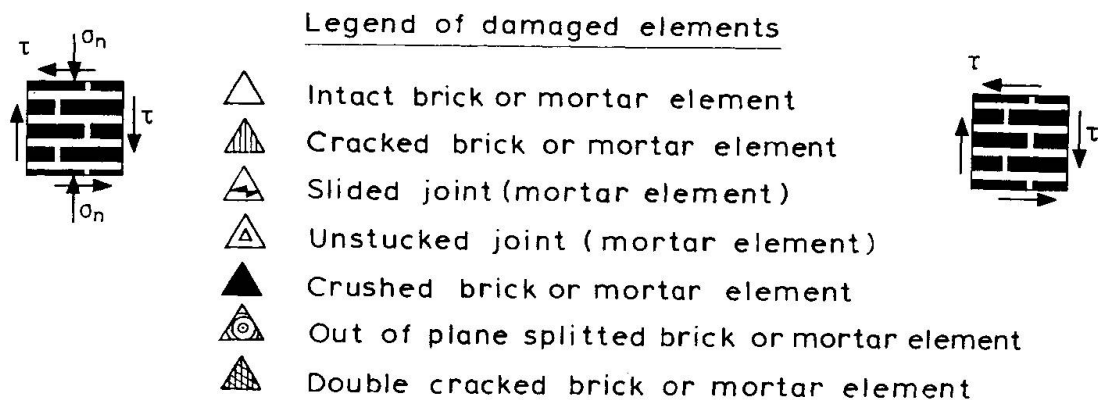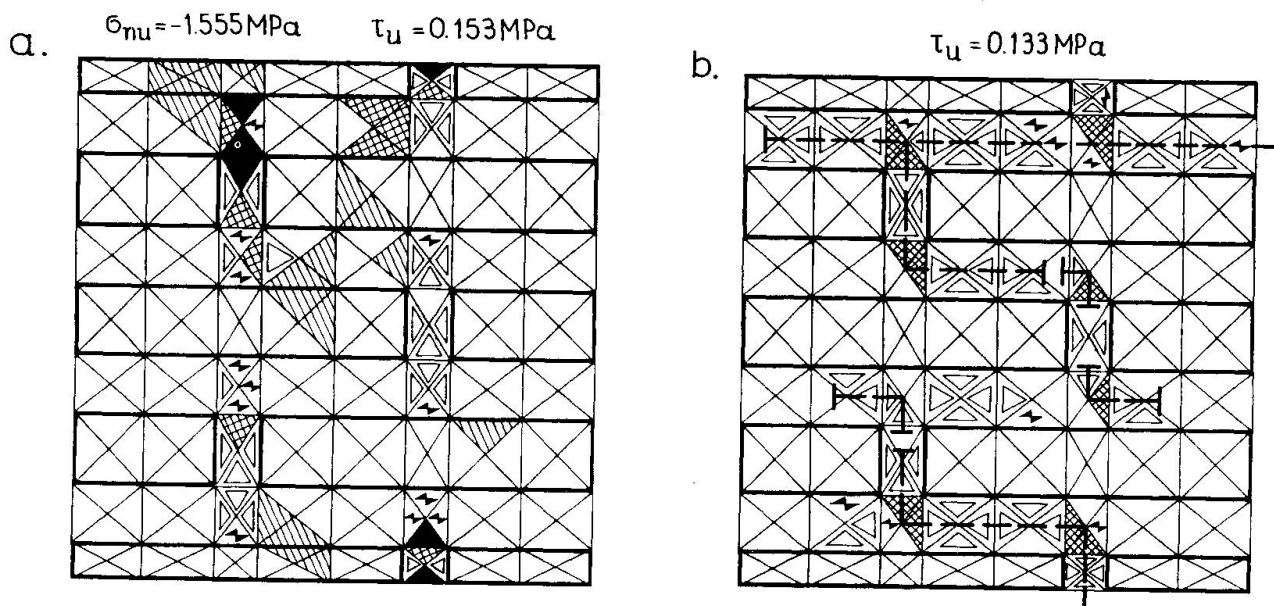Fig.3 Experimentally determined failure envelopes of masonry: a.Samarasinghe and Hendry[5], b.Page[6]

a. $\sigma_{nu} = -1.555\,MPa$ $\tau_u = 0.153\,MPa$

b. $\tau_u = 0.133\,MPa$

Legend of damaged elements

△ Intact brick or mortar element

◬ Cracked brick or mortar element

◮ Slided joint (mortar element)

◬ Unstucked joint (mortar element)

▲ Crushed brick or mortar element

◬ Out of plane splitted brick or mortar element

◬ Double cracked brick or mortar element

Fig.4 Failure patterns of masonry micromodels: a.Model No 4, b.Model No 9

Fig.5 Rotunda: a.Meridional cross section, b.Axisymmetric F.E. model, predicted cracking

Fig.6 Predicted cracking patterns of the piers P_1 and P_2 till failure: a.Massive pier (P_1), b.Pier with staircase (P_2)

Diagnosis and Strengthening of the Brunelleschi Dome

Diagnostic et renforcement de la Coupole de Brunelleschi

Diagnose und Verstärkung der Brunelleschi-Domkuppel

A. CHIARUGI
Professor
Univ. of Florence
Florence, Italy

M. FANELLI
Professor
ENEL-CRIS
Milano, Italy

G. GIUSEPPETTI
Engineer
ENEL-CRIS
Milano, Italy

SUMMARY

The paper begins by reviewing the historical information about the different studies carried out in past centuries in order to follow the evolution of the dome's state of damage. The diagnostic evaluation advanced in 1695 is confirmed in the light of modern studies. An intervention hypothesis is then illustrated, which could be assumed as the starting point for a consolidation strategy of the monument.

RÉSUMÉ

On reprend les renseignements historiques à propos des différentes études qui, à travers les siècles, ont suivi l'évolution de l'endommagement de la Coupole. On confirme ensuite le diagnostic de 1695, et enfin on examine les effets d'une intervention de renforcement que l'on pourrait prendre comme point de départ d'une stratégie de sauvegarde du monument.

ZUSAMMENFASSUNG

Der Bericht beginnt mit einem Rückblick auf die im Laufe von Jahrhunderten über die Beschädigung der Domkuppel gemachten Studien. Die 1695 vorweggenommene diagnostische Einschätzung wird angesichts neuerer Studien bestätigt. Die Auswirkungen möglicher Verstärkungsmassnahmen werden analysiert und als Ausgangspunkt für grundlegender Sanierungsarbeiten kritisch betrachtet.

INTRODUCTION

After 1434 (the year in which Filippo Brunelleschi achieved the construction of the Dome of Santa Maria del Fiore), and after the erection of the skylight, carried out after Brunelleschi's death, no direct information is available until 1600 about mechanical problems in the Dome. Successively, several investigation campaigns are mounted concerning the cracks observed on some of the dome's panels, especially on the sides directly above the absidal pylons, and in particular in the South-East corner, panel n° 4; see figgs. 1 and 2.

During the XVIIth century numerous studies are carried out, pointing to the conclusion - supported by reliable references - that the cracks must have been present since the beginning of XVIth century [1]. These studies are crowned by the report of a Commission, presided over by Vincenzo Viviani (a Galileo's pupil). Viviani, having carried out certain investigations, in 1695 illustrated the first diagnosis of the phenomenon, stating that the cause of damage is the dead weight of the construction, which produced a tensile-strength crisis in the masonry of some horizontal octagonal rings between the springing section of the dome and the drum apex. It is decided to proceed with a strengthening, consisting in laying down 4 iron belts, with rectangular cross-section of about 30 cm^2 each. Three of the belt should be placed externally between the springing section of the dome and the circular windows, while the fourth should be installed internally in the second walkway between the two shells.

This proposal arouses oppositions, explicit and not, as a consequence of which it is not put into effect. The diagnosis is disputed and it is requested that the number and size of the belts section be justified!

It is Father Leonardo Ximenes who resumes these contrary opinions in a study [2] published in 1757; in it we find the documentation of the cracks observed in the Dome, in the drum, in the pylons and in the rest of the Cathedral. The cause of the two main cracks (along the midline of panels 4 and 6), more or less vertical and involving the whole thickness, is attributed to an angular settlement of the pylon underlying side 4.

Only in 1937 a Commission, presided over by Pier Luigi Nervi, takes up again the problem. It is observed that the width of cracks presents also daily variations; as a consequence, a new diagnostic hypothesis is put forward, to the effect that thermal variations are the dominant damaging factor.

Last, in 1985 a new Ministerial Commission, on the basis of studies carried out by the Authors [3], concludes again that the geometry of the crack system is consistent with the expected dead-weight effect. One could almost say that three centuries were needlessly lost.

In the present work one recalls briefly the studies which led to the identification of the mechanical behaviour of the structure.

Then a possible reliabilitation scheme is considered. This is after the spirit of Freyssinet, i.e. the active consolidation by pre-stressing.

In this way the Authors evidence also the possibility of answering the question maliciously asked of Vincenzo Viviani, the Granduca's engineer.

Incidentally, it is to be remarked that the automatic on-line monitoring system existing since 5 years on the monument indicates for the time being a state of stationarity of the alteration phenomena.

2. THE GENERAL SCHEME OF CRACKS

Recent surveys evidence [4] a prevalent systems of cracks, formed by:
- "type A" cracks, subvertical, through the whole thickness. (panels with even numbering);
- "type B" cracks, subvertical, through the whole thickness, in the panels with odd numbering;
- "type C" cracks, penetrating only to a partial depth in the thickness, in the edges between adjoining panels;

- "type D" cracks, also penetrating only to a partial depth in the thickness, along the midline of the panels with odd numbering (see figgs. 1 and 2).

The time evolution of cracks is known too, insofar as in 1757 only "type A" cracks were observable, and then only on sides 4 and 6, whereas nowadays cracks are observable in all four sides above the pylons.

3. THE FIRST VIRTUAL MODEL

In the process of mechanical identification of the structure a first virtual numerical model was built up, formed only by the following members,: pylons, drum, dome. In this virtual F.E. model, 15 and 20 nodes isoparametric elements were used, with the same linear elastic constitutive law-throughout the structure. The first numerical analysis concerned the original (undamaged) virtual model under gravitational loads (deadweight).

A perusal of results clearly shows that the "parallels" just above the circular windows on the even-numbered panels undergo high levels of tensile stresses. Horizontal tensile stresses are found also in the drum, above the keystone of arches on the odd-numbered sides (see fig. 3 a, b, c, d).

4. THE "FIRST-IDENTIFICATION" MODEL

The results of the "continuous monitoring" yielded by the crack disposition allows to introduce cracks type A and B in the virtual model according to the dead-weight effects,. Thus the first-identification model is defined.

The results of the analysis carried out on this second model confirm the indications of the crack pattern, explaining in particular the origin of the cracks "type C and D". It is observed also that the external shell on the odd-numbered sides is subjected to vertical tensile stresses, whereas the highest level of vertical compressive stresses is found in the internal corners of cracks "type A".

This distribution of vertical stresses has been confirmed experimentally through another "continuous monitoring" operation using the flat jack technique (fig. 4 a, b, c, d; fig. 5 a, b, c).

5. ANALYSIS OF THE EFFECTS OF A STRENGTHENING HYPOTHESIS

By using the identified model one can simulate, starting from the present situation, the effects of the installation of horizontal belts.

The strengthening intervention could be effected through harmonic-steel cables placed at floor level in the first walking. The shape of these belts, pulled on at the midpoint of each side, would be octagonal; thus the interaction with the existing structure (apart from local effect) could be schematized by a system of radial forces, applied in the edges at the springing section of the dome.

Perusing the numerical simulation of this strengthening carried out on the "first-identification" model, one is surprised by the close- fitting antagonistic effect brought about by the intervention as against the dead-weight stress pattern (fig. 6 a, b, c, d).

One can remark that, according to the Betti theorem, the mutual work of the two force systems (dead-weight and prestressed belts) is obviously negative. However, one can moreover generally recognize that "almost everywhere" is negative also the local function which expressed the density of mutual work at every point of the structure.

It seems, thus, right to state that the intervention proposed in 1695 was a qualitatively correct therapy ensuing from a realistic evaluation of the main damaging factor.

Such an intervention, if carried out, would undoubtedly have produced positive effects, considering how far the phenomenon has advanced in the last 3 centuries.

These studies can also form the basis for the definition of a safety system to be put into action if the evolutionary phenomena should, for causes now not ascertainable, start to increase again.

Further studies are under development in order to define a "second-identification" virtual model, taking into account also the presence of the external chapels.

ACKNOWLEDGEMENTS

REFERENCES

1. BARBI L., DI TEODORO F., Le lesioni della Cupola di S. Maria del Fiore: una proposta di datazione. Bollettino degli Ingegneri 1983 n. 9.

2. XIMENES L., Del vecchio e nuovo gnomone fiorentino e delle osservazioni astronomiche, fisiche ed architettoniche fatte nel verificare la costruzione. Firenze, 1757, Nella Stamperia Imperiale Libro II°.

3. CHIARUGI A., FANELLI M., GIUSEPPETTI G., Analysis of Brunelleschi - Type Dome Including Thermal Loads. IABSE SYMPOSIUM, Venezia, 1983.

4. MINISTERO PER I BENI CULTURALI ED AMBIENTALI, Rapporto sulla situazione del complesso strutturale cupola-basamento della Cattedrale di S. Maria del Fiore in Firenze. Marzo 1985.
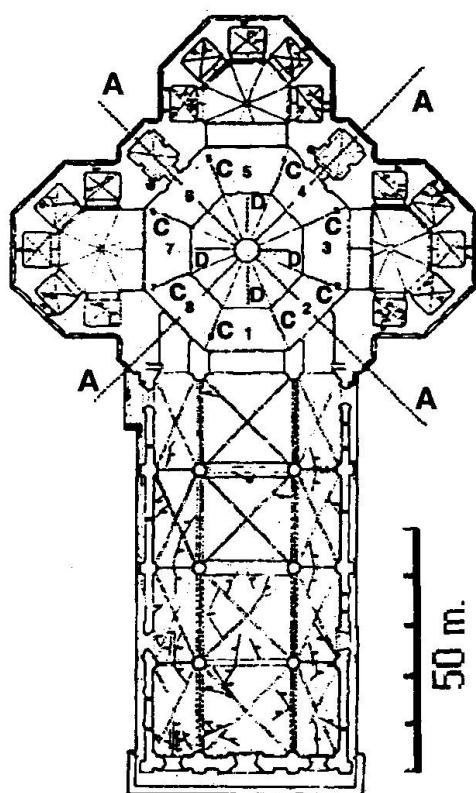
SETTORE 4

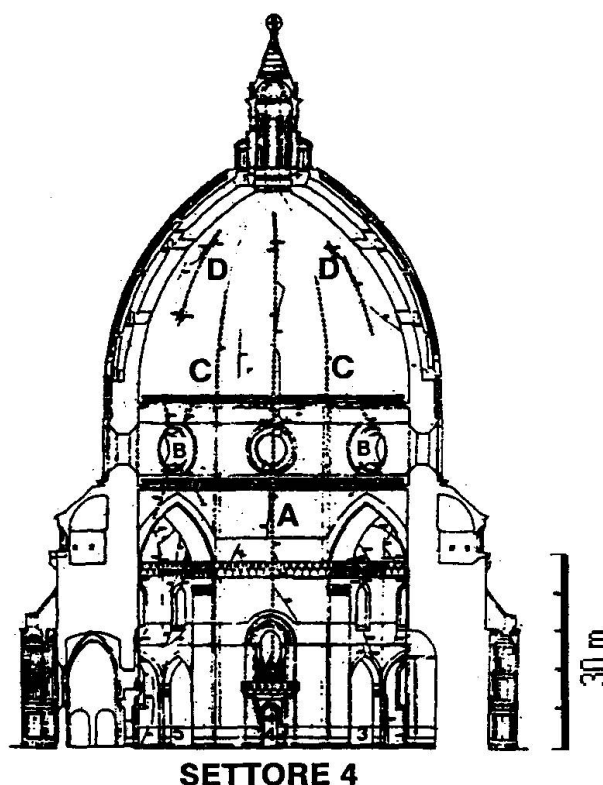Fig. 1 Sides numbering and planar position of type "A, B, C and D" cracks.

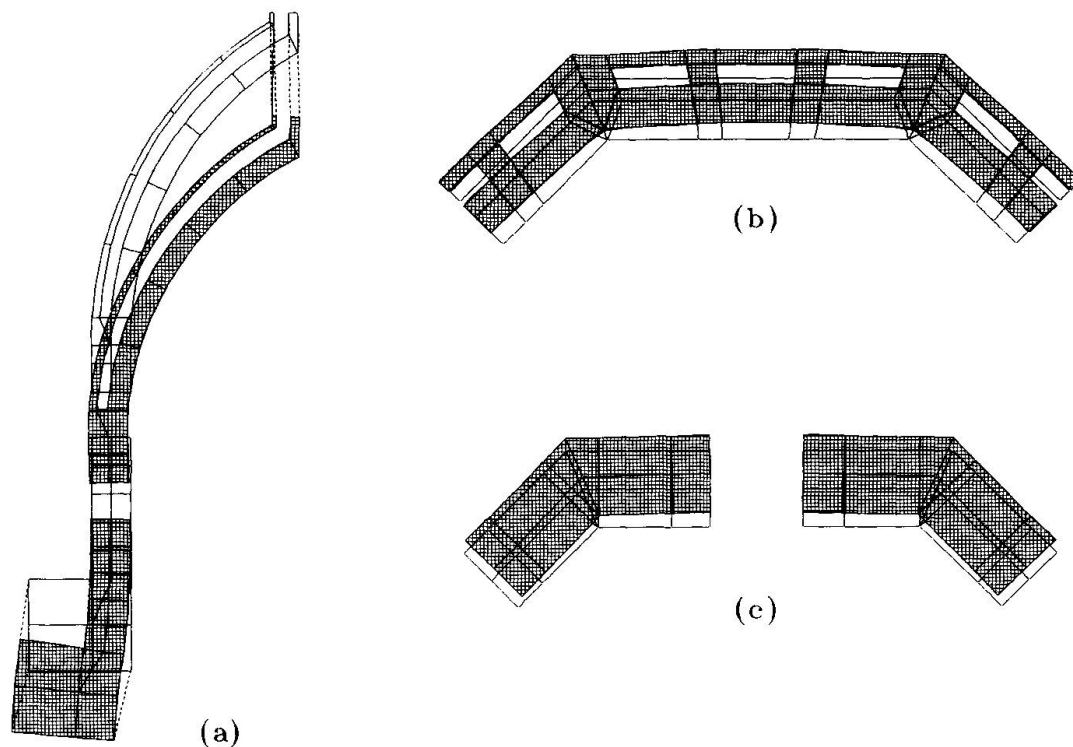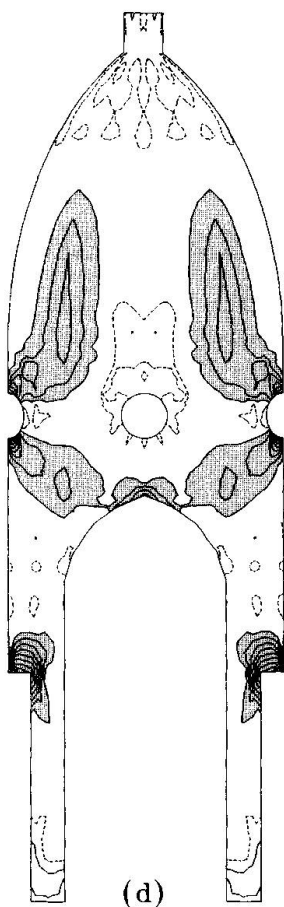Fig. 2 Crack description summary with type "A, B, C and D" cracks.

(b)

(c)

(a)

(d)

Fig. 3   "First virtual model" undamaged structure:

(a)   deformed line of vertical section in centerline on even-numbered panel;

(b)   deformed line of section 3-3 at 66 m level;

(c)   deformed line of horizontal section on circular centerline window (note ovalization of opening on even-numbered panel);

(d)   stress distribution σ horizontal on intrados face (note tension increase around the circular windows of even numbered panel and above the keystone of arch). Tension zone shaded.

-   "First virtual model" characteristic:
    n° nodes   3286
    n° elements   569
-   Elements characteristic:
    isoparametric hexahedrons with 20 nodes
    isoparametric pentahedrons with 15 nodes
-   Material characteristic:
    modulus of elasticity: $50000 \ \text{kg/cm}^2$
    Poisson's ratio   :   0.1
    Density   : $0.0018 \ \text{kg/cm}^3$
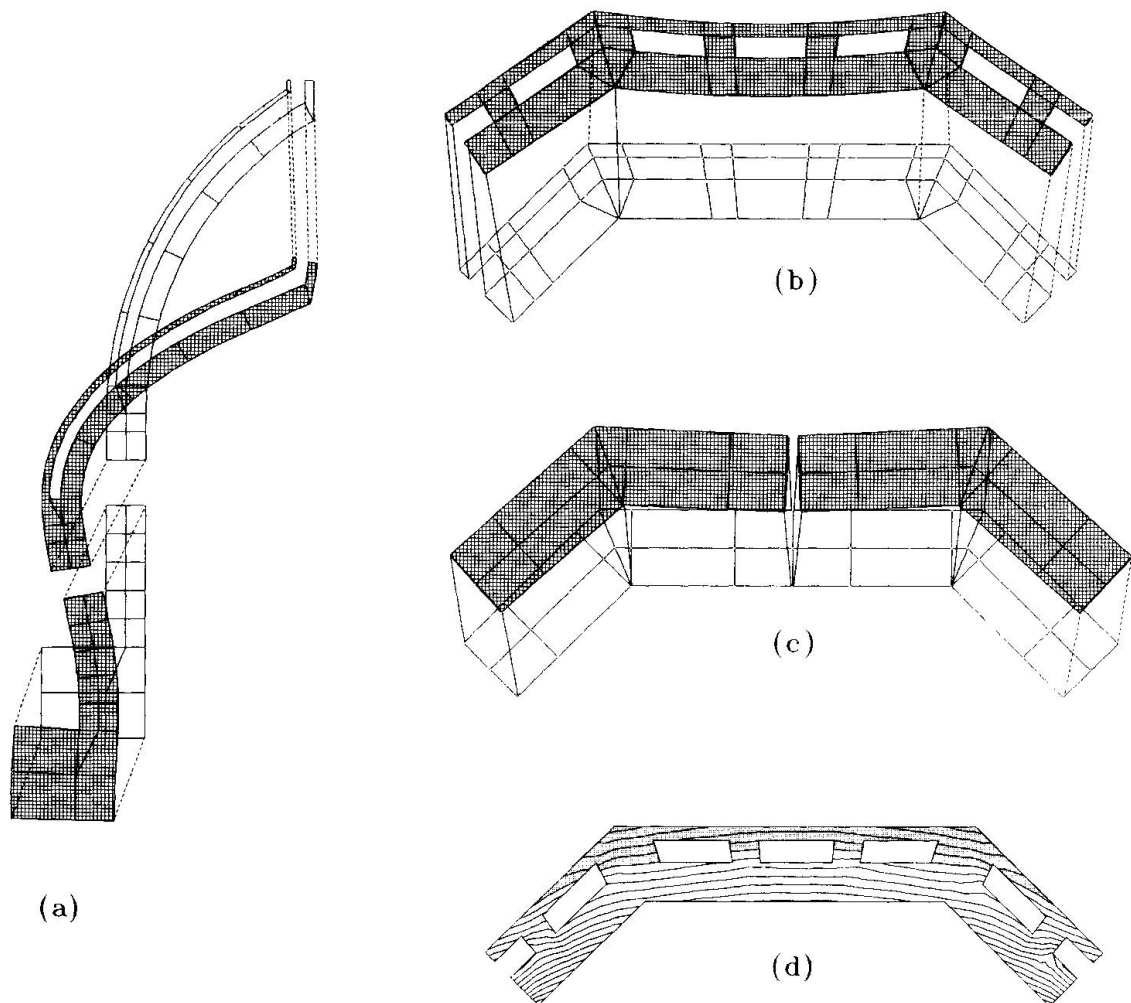
(b)

(c)

(d)

(a)

Fig. 4 "First identification model" with type A and B cracks:

(a)   deformed line of vertical section;

(b)   deformed line of section 3-3 at 66 m level
        (note inflexion on the section plane);

(c)   deformed line of section under circular window
        (note opening crack B);

(d)   stress distribution σ z vertical in section 3-3
        (note effects of bending with vertical tension
        localized in external panels with odd numbering).
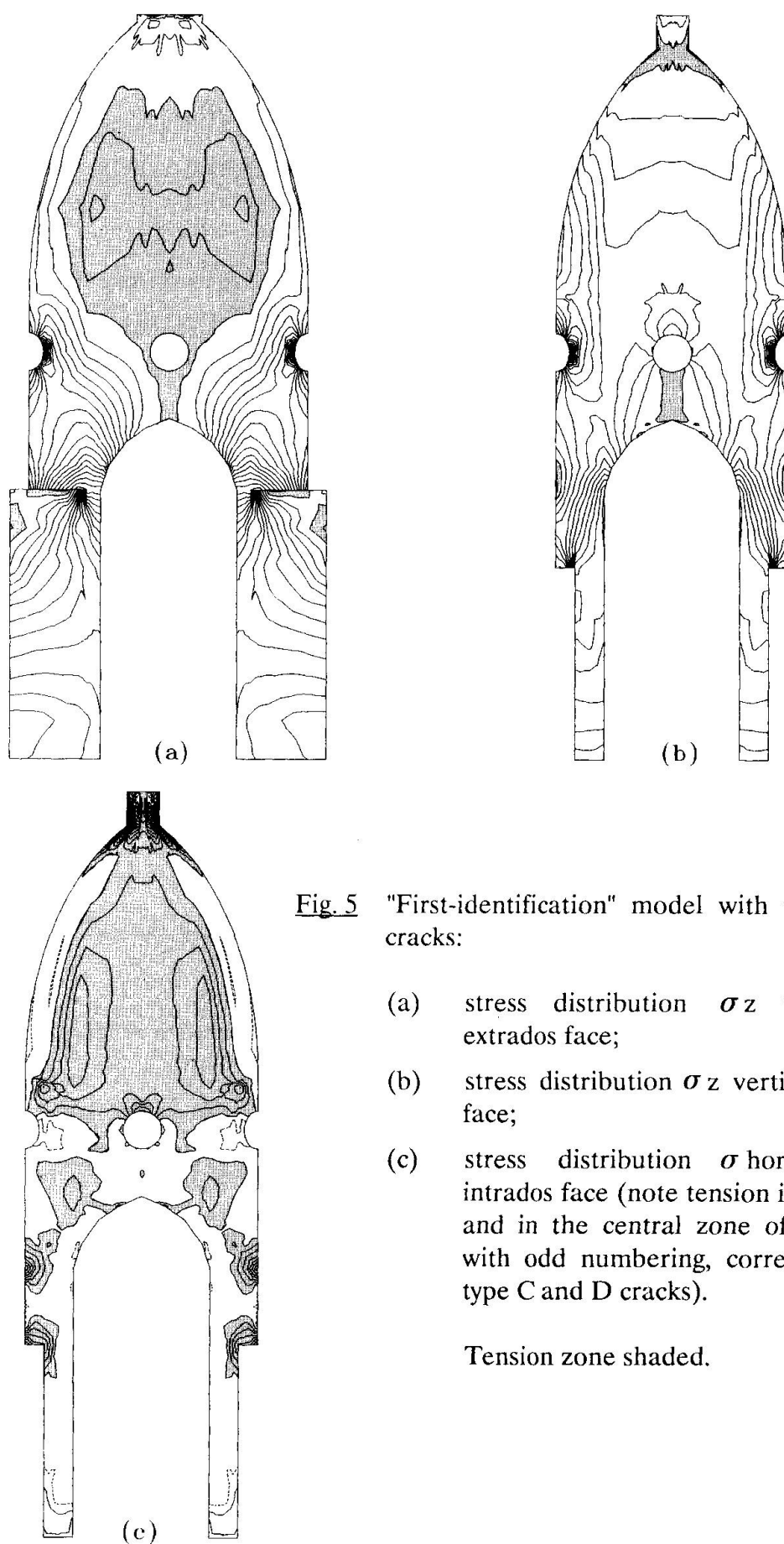   Tension zone shaded.

(a)

(b)

(c)

Fig. 5 "First-identification" model with type A and B cracks:

(a) stress distribution σz vertical on extrados face;

(b) stress distribution σz vertical intrados face;

(c) stress distribution σ horizontal on intrados face (note tension in the corner and in the central zone of the panels with odd numbering, corresponding at type C and D cracks).
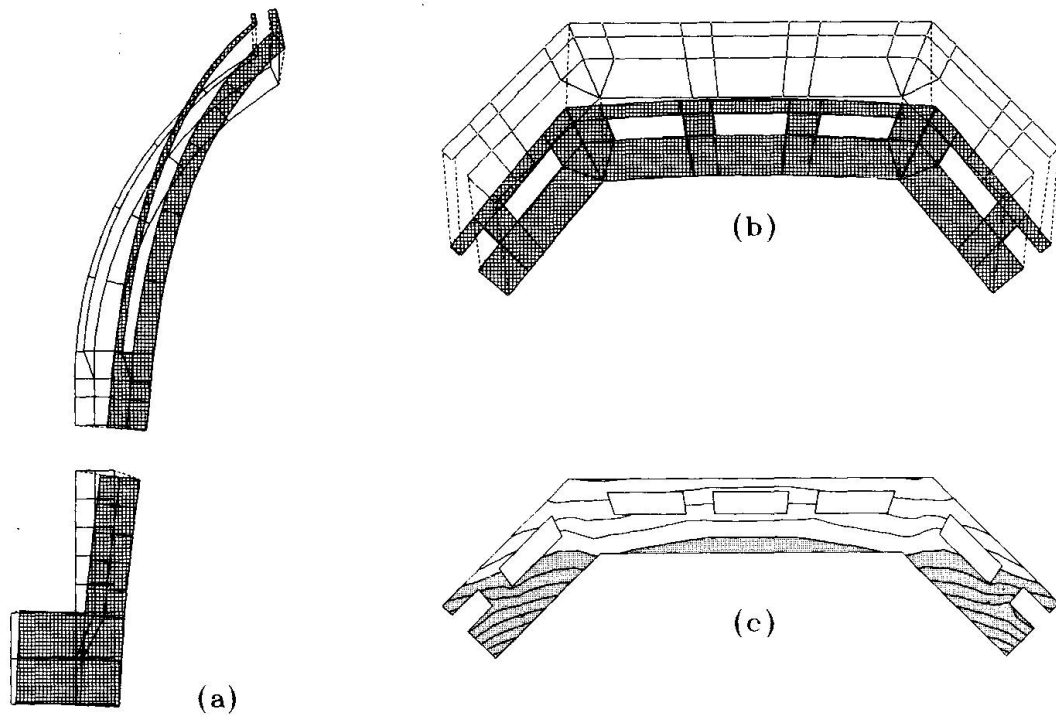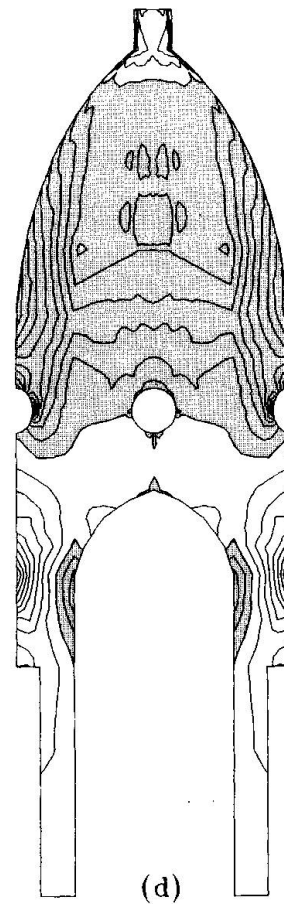
Tension zone shaded.

(b)

(c)

(a)

Fig. 6   "First identification model" under only strengthening effect:

(a)   deformed line of vertical section;

(b)   deformed line of section 3-3 at 66 m level;

(c)   stress distribution σz vertical in the section 3-3; with opponent distribution with espect to the dead-weight;

(d)   stress distribution σz vertical on intrados face;

Tension zone shaded.

(d)

Wind Induced Stresses in the Spire of Brussels Town Hall Tower

Contraintes dues au vent dans la flèche de la Tour de l'Hôtel de Ville de Bruxelles

Windinduzierte Spannungen im Turmhelm des Brüsseler Rathauses

B. ESPION
Dr. Eng.
Univ. of Brussels
Brussels, Belgium

S. ELINCK
Civil Eng.

Brussels, Belgium

P. HALLEUX
Prof. Dr.
Univ. of Brussels
Brussels, Belgium

SUMMARY

The tower of the Brussels Town Hall (1454) is a 96m high gothic structure presently undergoing a major restoration. The results of a finite element analysis of its spire are presented. Small tensile stresses appear under wind loading at the top of the spire and also in its skeletal part, where the ribs are subjected to bending. This preliminary study, which assumes a linear elastic behaviour, allows the assessment of restoration options. For instance, it shows that the corroded metallic reinforcement has no structural function.

RÉSUMÉ

La tour de l'hôtel de ville de Bruxelles (1454) est une construction gothique haute de 96m qui est à présent l'objet d'une restauration majeure. Les résultats d'une étude par éléments finis de la flèche sont présentés. Des contraintes de traction faibles apparaissent sous l'effet du vent au sommet de la flèche et dans sa partie ajourée où les côtes sont soumises à flexion. Cette étude, quoiqu'élastique, permet l'évaluation d'options de restauration. Par exemple, elle montre que les renforcements métalliques, corrodés, n'ont pas de fonction structurelle.

ZUSAMMENFASSUNG

Der 96m hohe, gotische Turm des Brüsseler Rathauses (1454) wird gegenwärtig gründlich restauriert. Es wird über die Ergebnisse einer Finiten-Elemente-Analyse des Turmhelms berichtet. Schwache Zugspannungen treten bei Wind an der Helmspitze und im Masswerk auf, wo die Rippen einer gewissen Biegung ausgesetzt sind. Aufgrund dieser vorläufigen Analyse, die nur ein linear-elastischen Verhalten annimmt, können Restaurationsmöglichkeiten bewertet werden. Sie zeigt beispielsweise, dass die korrodierten Metallverstärkungen für das Tragwerk ohne Bedeutung sind.

1. INTRODUCTION

The main tower of the Brussels town hall (Fig.1) is a masterpiece of Gothic architecture dating back to the middle of the 15th Century (1449-1454). The tower suffers now from severe disorders which may be attributed to sequels of the bombing by the armies of Louis XIV and to unwise previous restorations with unsuitable materials and reinforcements like iron rods that rust and induce fracturing of the stones. A major restoration is therefore needed and is presently taking place.

The most damaged part of the tower is its spire. The spire looks like a pyramid with octagonal cross section. The height of the spire is 20m. Its lower, or skeletal part (11m), consists of 8 slender inclined columns at the 8 edges of the pyramidal volume; the architects called these inclined columns ribs ("côtes"). The upper part (9m) is a solid (or assumed so) pyramidal shaped volume supporting a 3.1m height statue of archangel St Michael culminating at 96m above ground level.

The ribs are connected together at their mid height by a fine stone tracery ("remplage"); the initial function of this tracery was to provide an intermediate support for the ribs during their erection process. Since the ribs exhibit a slight inward curvature, it has sometimes been suggested that the stiffness of the tracery was too weak to provide an effective support of the ribs. The ribs are furthermore connected at five different levels by two hoops of metallic reinforcement. The inner series of hoop reinforcement may be original, but the outer series is probably a late addition.

Preliminary studies have shown that wind is the main action inducing bending and therefore possibly tensile stresses in such a high building. These tensile stresses, if they appear, would be localized in the spire, which justifies that we focus our detailed analysis on this part. From the structural point of view, the following questions have been raised :
(1) what is the actual structural safety against failure under exceptional wind action ?
(2) what is the role of the metallic reinforcement ? Do we have to replace all the non original iron rods by stainless ones or only some of them ?
(3) what is the structural effectiveness of the tracery in providing support for the ribs and wind bracing for the spire? It has been suggested, for instance, that a rigid connection between the ribs should be added under the form of a solid stone disk behind the tracery.

Mortar and lead joints cannot sustain tensile stresses and the existence of tensile zones implies nonlinear material behaviour. The precise answer to the previous questions requires therefore sophisticated numerical modeling. But the first step before proceeding with aerodynamic tunnel experiments and modeling the nonlinear material behaviour is to apply code provisions for wind effects with a linear elastic structural model. This paper presents and comments the results of this analysis.
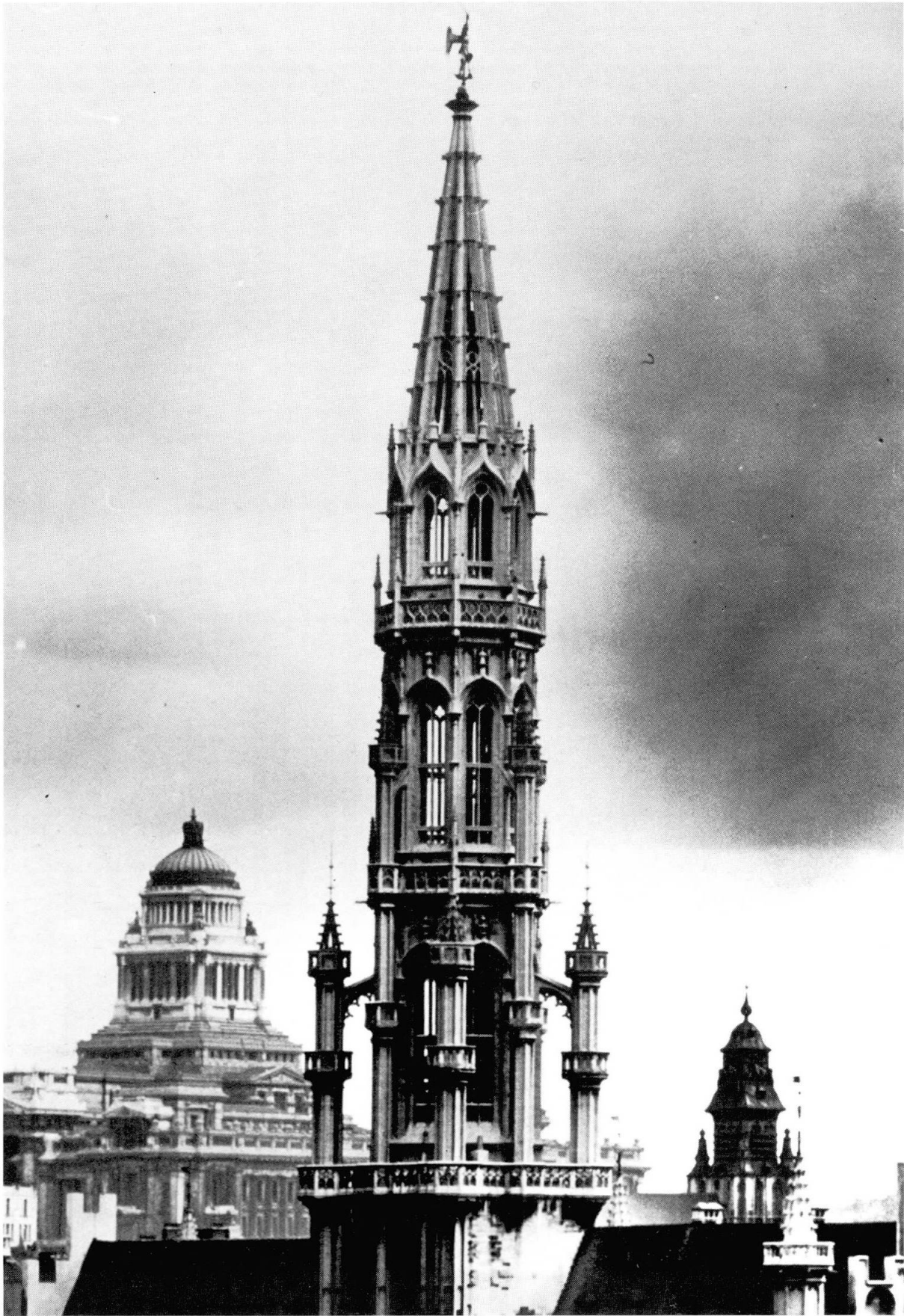
Fig. 1 The tower of the Brussels town hall (96m)

2. NUMERICAL MODEL

Thanks to symmetry, only one half of the spire needs to be considered. We built a very large three dimensional finite element model of the half spire : 4000 elements and 63000 degrees of freedom. All the geometrical dimensions are known from a recent survey. The mesh of the stone structure consists entirely of quadratic isoparametric volumic finite elements. Each rib is modeled by 37 layers of 10 elements. The area of the cross section of one rib is 3300 cm^2. We assumed for the stone a Poisson's ratio equal to 0.15 and Young's modulus equal to 50 GPa, which is the mean value for the "Gobertange" stone used during the 19th Century restoration and predominantly visible today. But we tested the sensitivity of the results to the value of the Young's modulus for the stone by introducing in one of the analyses a lower value (20GPa) corresponding to the original sandstone, which may still be present to a certain extent inside the structure. The total computed weight (with a specific weight equal to 24 kN/m^3) of the half spire is 569 kN. The cross section of the reinforcing rods varies between 9 and 25 cm^2, depending on their location in the spire. Four different structural models were considered : (1) present state, with hoop reinforcement; (2) without hoop reinforcement; (3) without hoop reinforcement, but with addition of a solid stone disk behind the tracery; (4) without hoop reinforcement and without tracery.

The wind forces and pressures were computed with the Belgian code on wind actions NBN B03-002-1 (1988), which is in agreement with the latest international recommendations in the field. At the mean level of the spire, the characteristic value of the peak wind speed is 154 km/h for a period of return of 10 years and 196 km/h for a period of return of 500 years. The corresponding dynamic pressures are 1,12 kN/m^2 and 1,84 kN/m^2 respectively. In fact, we subdivided the spire in five levels, and assumed for each zone a uniform value for the dynamic pressure, equal to its value at the mean height of the zone. The wind pressure acting on the surface of the model is then computed as the product of the dynamic pressure by a pressure coefficient c_p. The value of the pressure coefficients in each zone depends on the form of the cross section of the spire at the mean level of the zone, and of the orientation of the element of surface under consideration with respect to the wind direction. The value of the external pressure coefficients varies between -0,5 (suction) and 1 (pressure); the order of magnitude of the internal pressure coefficients (for the surface of the ribs inside the hollow part of the spire) is 0,1. Finally, wind forces are applied to all finite element sides belonging to the surface of the spire; the computed value of the wind resultant on the half spire is 62 kN for a period of return of 500 years. The wind force acting on the statue (9.9kN) contributes significantly to the wind action on the spire.

3. NUMERICAL RESULTS

The slenderness of the spire allows us to concentrate ourselves on the vertical component of the stress tensor referred to as "stress" below. Fig. 2 is a schematic section in a plane of symmetry representing the distribution of vertical stresses under self weight in the model without hoop reinforcement. There are

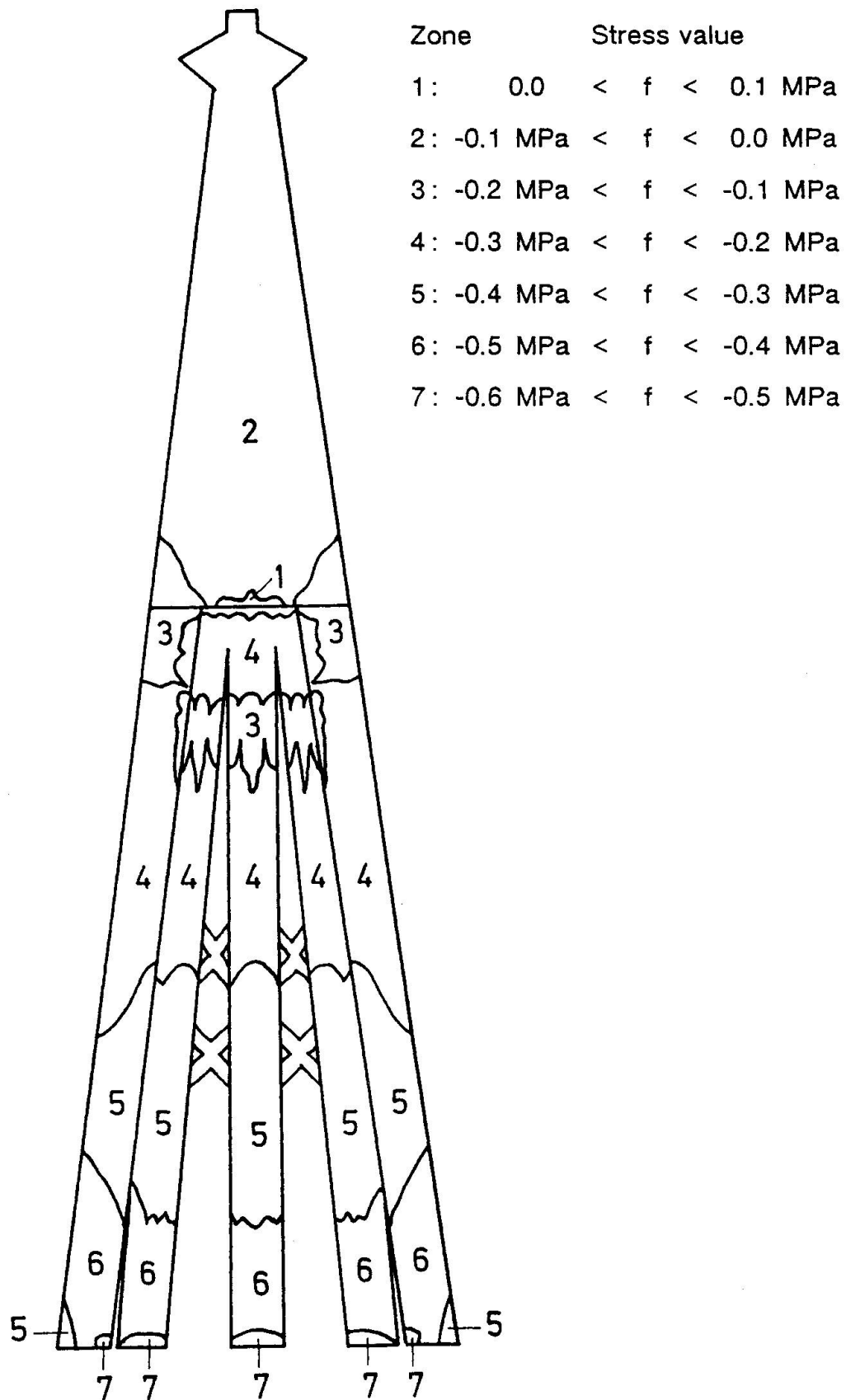| Zone	Stress value
1 :	0.0 < f < 0.1 MPa
2 :	-0.1 MPa < f < 0.0 MPa
3 :	-0.2 MPa < f < -0.1 MPa
4 :	-0.3 MPa < f < -0.2 MPa
5 :	-0.4 MPa < f < -0.3 MPa
6 :	-0.5 MPa < f < -0.4 MPa
7 :	-0.6 MPa < f < -0.5 MPa

Fig. 2 Vertical stress distribution in the spire under self weight

practically no differences in this distribution when hoop reinforcement is added. Fig.2 exhibits a very limited zone of small tensile stresses (< 0.1 MPa) along the axis of symmetry at the connection between the ribs and the solid part of the spire, and compressive stresses elsewhere. The ribs are mainly subjected to normal force. The slope of the ribs with respect to the axis of gravity is small (8.5°), but nevertheless sufficient to induce a slight bending behaviour of the ribs which may be seen as columns built in at both ends and supported at mid-height by the tracery. If the tracery is omitted, the span of the ribs doubles and the bending behaviour is fairly more noticeable with tensile stresses (≈ 0.2 MPa) appearing on the outer arrises at both ends of the ribs. The introduction of a solid stone disk behind the tracery has no influence on the stress distribution above the tracery and induces a slightly less favorable bending behaviour of the ribs between their springing and the tracery. We may therefore conclude that the tracery provides an effective support and that the introduction of a stiffer support behind the tracery seems neither necessary nor desirable.

Fig.3 represents the distribution of vertical stresses under combined action of self weight and a wind with a period of return of 500 years. The section shown lies in the direction of the wind and the windward side is on the left. Once again, we hardly notice any difference when the hoop reinforcement is added: some rods are in tension, other in compression, and the largest computed force in one rod is 1.8 kN when E = 50 GPa for the stone. The stress distribution in the masonry remains practically unchanged when E = 20 GPa for the stone, while the mean force increase in the rods is 33%. The upper, solid part of the spire behaves like a tapered short column and is typically submitted to bending combined with compressive normal force. Nearly all the windward side exhibits tensile behaviour, with values around 1 MPa in a 2m height below the statue and 0.1 MPa at the base of the solid part of the spire. These values are roughly halved for a wind with a period of return of 10 years. In the skeletal part of the spire, the windward rib exhibits a definite bending behaviour with relatively large tensile zones and a peak tensile stress of ≈ 0.6 MPa at the springing of the windward arris. The largest compressive stress (≈ -1.2 MPa) is observed at the springing of the outer arris of the leeward rib and remains a very low working stress for this kind of masonry.

4. DISCUSSION OF NUMERICAL RESULTS

The fact that nearly all the windward side of the upper part of the spire is submitted to tensile stresses is not astonishing and may be shown by application of elementary concepts of strength of materials. Heyman [1] furthermore recalls that the top of a solid slender spire is always subject to instability under wind. Heyman compares the overturning (wind) and stabilizing (self weight) moments computed with respect to the leeward arris. If we add the stabilizing effect of the weight of the statue (≈ 4kN) and the overturning effect of the action of the wind on the statue to the application of Heyman's analysis of equilibrium, we find that the upper half of the solid part of the spire is subject to overturn by wind. It has never been reported for this spire, and we must therefore infer that the anchorage of the statue (whose state is unknown and which has not been accounted for in the finite element analysis) contributes to the bending resistance of the upper

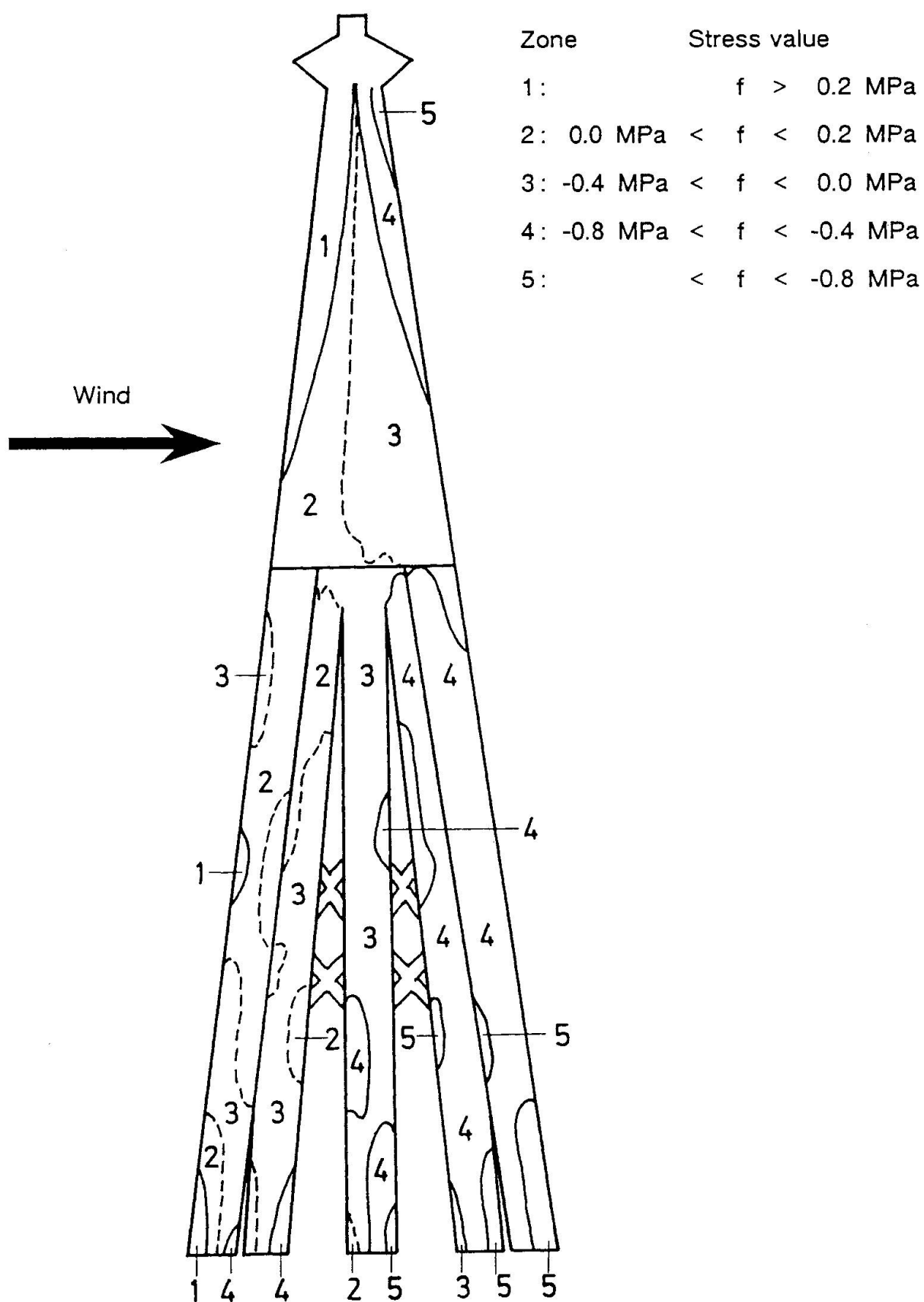| Zone	Stress value
1 :	f > 0.2 MPa
2 :	0.0 MPa < f < 0.2 MPa
3 :	-0.4 MPa < f < 0.0 MPa
4 :	-0.8 MPa < f < -0.4 MPa
5 :	< f < -0.8 MPa

Fig. 3 Vertical stress distribution in the spire under self weight and wind loading

part of the spire. This favorable element could easily be estimated during the restoration and the theoretical existence of tensile stresses in the solid part of the spire is not worrying. More concerning is the magnitude of the tensile stresses at the springing of a windward rib. We cannot conclude from the present elastic analysis that such stresses are high enough to jeopardize the stability of a rib, or even the durability of joints which would open under strong wind and remain close under self weight and moderate wind. The answer to this question justifies further studies -more precise evaluation of wind action in an aerodynamic tunnel and modeling the nonlinear behaviour of a unilateral material like masonry- which are presently under progress.

5. CONCLUSIONS

The present study is therefore only one step in the process of determination of the restoration options, but it helped us to understand finely the structural behaviour of the spire and to reach some practical results:
1) the structural role of the metallic reinforcement, which could not have been tackled by simple analysis based on equilibrium concepts, appears very limited and not essential to stability. We may now propose to simply remove them or, if the archaeologists want to keep them, to treat the rods against further corrosion and disconnect them structurally from the stone. Their expensive replacement by stainless reinforcement is not structurally justified.
2) the tracery provides enough stiffness to sustain the ribs and there is no need for additional bracing at this level.
3) the anchorage of the statue should be unveiled during the restoration and carefully assessed because it probably plays an essential role in the stability of the upper part of the solid part of the spire.
4) further studies are necessary to determine whether the springing of the ribs needs strengthening to be able to withstand the tensile stresses occurring, if any, under the most severe wind loading.

ACKNOWLEDGEMENTS

REFERENCES

[1] HEYMAN, J., "Hemingbrough Spire", Proc. of the 2nd Int. Conf. Structural Repair and Maintenance of Historical Buildings, ed. by C.A. BREBBIA et al., Vol. 1, pp.13-22, Computational Mechanics Publications, 1991.

Studies of Gaudi's 'Cripta de la Colonia Güell'

Etudes de la 'Cripta de la Colonia Güell' de Gaudi

Studien zu Gaudi's 'Cripta de la Colonia Güell'

Antoni GONZALEZ
Architect
Gov. Archit.Heritage Services
Barcelona, Spain

Albert CASALS
Dr. Archit.
Catalunya Politechnical Univ.
Barcelona, Spain

Pere ROCA
Assoc. Prof., Dr.
Catalunya Politechnical Univ.
Barcelona, Spain

José Luís GONZALEZ
Prof., Dr.
Catalunya Politechnical Univ.
Barcelona, Spain

SUMMARY

The Crypt of the Colonia Güell is the only part actually built of a construction envisaged by Gaudí and erected during the period 1908 to 1915. To assess the design of its unique structural system, Gaudí developed a tridimensional funicular model in which strings were used to represent actual brick masonry arches and oblique brick or stone columns. This paper describes a numerical analysis which was performed to study in detail the actual resisting mechanism under gravity loads for the built part of the structure, aiming to measure the alteration of the funicular equilibrium and relate it to the observed damage.

RÉSUMÉ

La Crypte de la Colonia Güell est en fait la seule partie existante d'une construction imaginée par Gaudí et construite entre de 1908 à 1915. Pour concevoir cette structure unique, Gaudí avait développé un modèle tridimensionnel des forces dans lequel des cordes étaient utilisés pour représenter les voûtes réelles en maçonnerie de briques et les colonnes obliques en briques ou en pierres. Cet article décrit une analyse numérique qui a été réalisée pour étudier en détail l'état actuel du mécanisme résistant sous les charges gravitaires de la partie construite de la structure, dans le but de mesurer le déséquilibre des forces et d'en tirer une relation avec les dommages observés.

ZUSAMMENFASSUNG

Die Krypta der Kolonie Güell ist der einzige wirklich errichtete Teil einer von Gaudí projektierten Kirche. 1908 begonnen, wurde ihr Bau 1915 eingestellt. Um ihr einzigartiges Tragsystem zu konzipieren, hatte Gaudí ein dreidimensionales Seilpolygon-Modell entwickelt, in dem Schnüre zur Darstellung des Kraftflusses in den Mauerwerksbögen und schiefen Ziegel- und Steinpfeilern verwendet wurden. Der Beitrag beschreibt eine numerische Analyse des tatsächlichen Lastabtrags des Eigengewichts im unvollendeten Bau, mit der die Abweichungen der Stützlinien bestimmt und mit beobachteten Schäden verglichen werden sollen.

1. THE CRYPT OF GAUDÍ

1.1 Description of the building

The crypt of the Colonia Güell is the only part actually built of what was to have been the parish church of the model village founded by Eusebi Güell in 1890. Gaudí was commissioned to design the parish church in 1894, when he was also working on the Casa Calvet, Bellesguard and the Expiatory Temple of the Sagrada Familia. The foundation stone of the church was laid in 1908, fourteen years after the commission, ten of which were spent on the preparation of the project. Gaudí abandoned the work in 1914, leaving the crypt and the portico finished.

The general form of the floor plan is oval, with a star-shaped outline, and it measures 26 m by 63 m. On the south facade there is a portico which signals the entrance to the crypt, and was intended as the access, via two flights of steps, to the church, located on the floor above. The external walls of the crypt itself reveal elevations with different inclinations in such a way that the base of these configures the star-shaped perimeter; the upper part of the walls are pierced by rhomboidal windows.

The interior of the crypt is in two parts, clearly differentiated as far as their structural conception is concerned; the rear part, containing the choir and the service areas, is covered by brickwork vaults which rest on metal T-section beams. The other part is the presbytery and chapel. The roof consists of bricks board (in Catalan 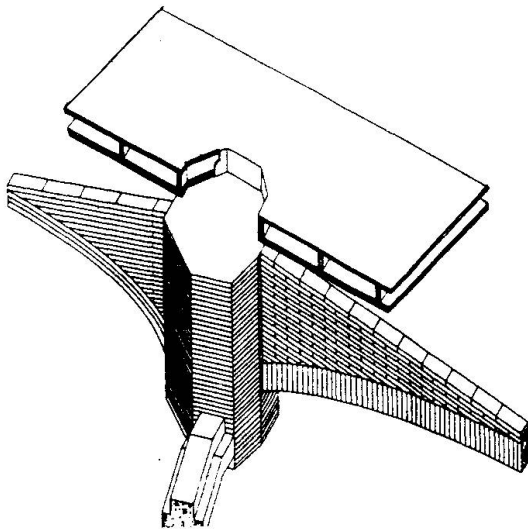and in the Catalan variety of Castillian, this type of slab is known as a *solera*), supported on brickwork ribs (a rib-shaped structural element formed of a flattened arch supporting a wall of the same thickness which fills in the void) supported by rowlock arches or resting directly on the supports whose longitudinal axis is inclined to a greater or lesser extent, with an inclination dictated by the funicular model which generates the shape of the building. (Fig. 1) Our study is limited to this latter space.

Fig. 1

The central nucleus is delimited by four basalt columns and the arches which separate it from the choir, all of them angled in towards the centre of the nucleus, and two peripheral aisles forming a double ambulatory, made up of ten columns arranged in a double semi-circle around the nucleus. Columns and pillars support the main brick rowlock arches, from which the ribs spring. These are also of brick, and have been treated in two different ways; those which converge on the two circular bosses – linked by a practically flat brick arch – consist of a brick rowlock arch 15 cm thick, supporting a wall of the same thickness. The remaining ribs are walls 12 cm thick, but these are raised over brickwork arches three courses thick. The reticulum formed by the meeting of the ribs is flush at the same level and supports the *solera* mentioned above. It consists of a first triple layer of facing brick, with a suspended floor over this, formed by brick partitions, supporting the final double layer; presumably the paving of the church was to have been laid over this.

The whole arrangement of columns, arches and ribs is the realisation of the funicular model which Gaudí built and studied over the ten years before work started on the building. More details in regard to historic or construction aspects may be found in[1].

1.2 The stereo-funicular model

It is known that the method used by Gaudí to approach the planning of the shape of the church was based on the properties of funicular polygons. The use of funicular lines as a system of determining intrinsically stable shapes had already been known for some time. Nonetheless, no major building had been erected on this principle; there is no doubt that the crypt is the first, with the peculiarity of being a set of funicular lines interwoven in the three spatial dimensions. The limitations of the graphical or numerical methods available to him obliged Gaudí to work out his stereo-funicular structure using a physical scale model.

But these are forms which, by virtue of the funicular device, reveal in their essential form the optimisation of the mechanics of their construction, with which Gaudí created shapes of overwhelming plastic expressiveness backed by a deep knowledge of the laws that govern the behaviour of the built fabric.

The only surviving documentation of the original model is a few photographs, most of them of the part which was not built. However, this lack may be in part made up for thanks to the initiative of a group of Dutch and German admirers of Gaudí's work who carried out the huge task of reconstructing the hanging model which, together with the publication which describes the lengthy and complex experience of its creation, is a very valuable contribution[2]. The correlation demonstrated by comparing photographs of the new model and that by Gaudí permits reasonable speculation about new images of the unbuilt church.

Examination of the model supplies data which greatly contribute to better understanding and knowledge of the existing building, such as, for example, the following point which has never been brought out and is doubtless of some importance. While the columns and the perimeter wall owe their inclination to the general funicular lines of the building as a whole, the same is not true of the two basalt columns close to the altar. The columns of the floor above were to have been essentially vertical. (Fig. 2) The inclination of those in the crypt was imposed by Gaudí for compositional reasons, and it has been achieved thanks to the thrust generated by the arches or ribs which would support the floor of the church and which were to divert the vertical loads towards the axes of the inclined columns. At all events, all this gives rise to a doubt: if the structure is in equilibrium at the moment, with lines apparently distant from the funicular model, would it be in equilibrium once it was finished?
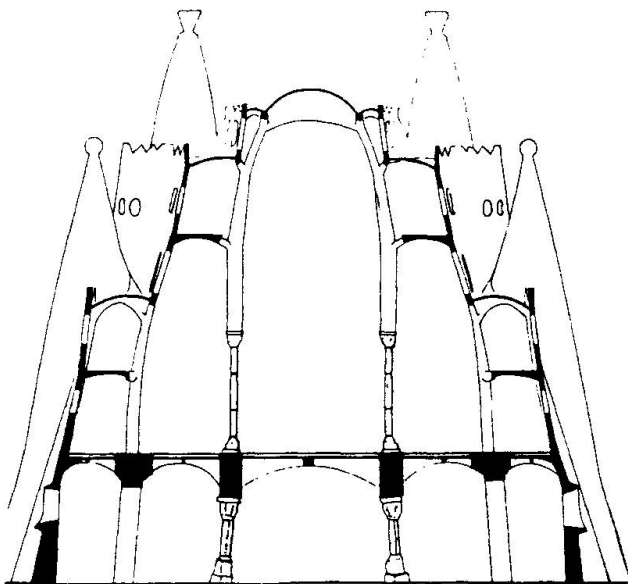

Fig. 2

We have here precisely the great paradox of the crypt. It is a building which was conceived to be stable once it was finished, but nonetheless it is stable now, in its unfinished state. Graphic statics does not help us to analyse this problem.

However, one may still think that the structure behaves according to the funicular model, albeit only partially. This may be deduced from an indicator which has generally been

overlooked but is of considerable importance when it comes to checking the possible hypotheses about the behaviour of the building: the intricate pattern of cracks in the facing brick ceiling or *solera* which covers the central nave of the crypt, and those which affect several of the ribs and some of the arches.
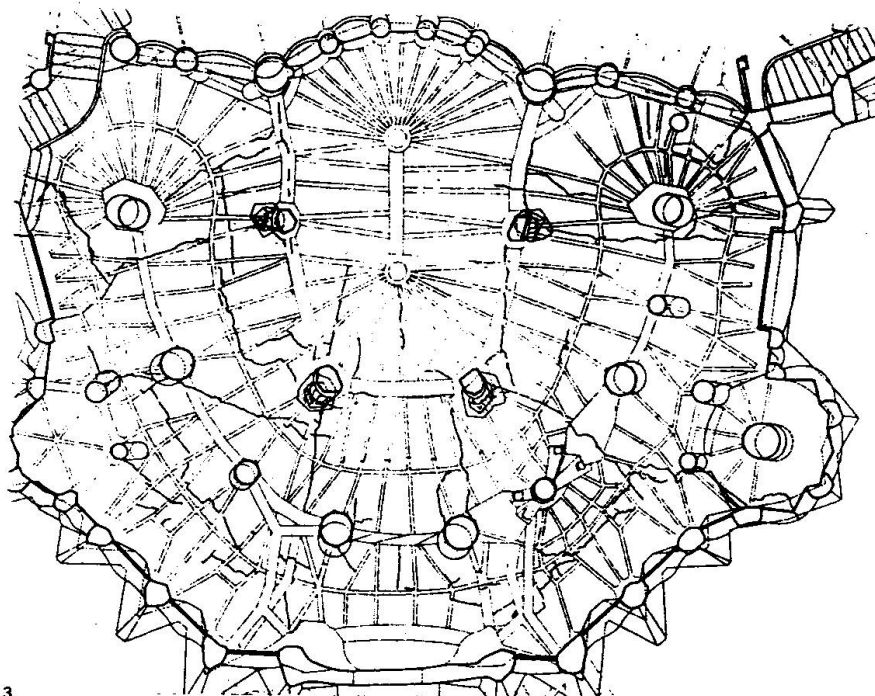
Detailed analysis through direct observation and an exhaustive photographic survey of over 1 000 images has enabled us to determine the pattern of cracks we reproduce here, which is only an overall view amongst all those that were detected. (Fig. 3)

In fact, while the building has not collapsed, neither can we say it is undamaged; that is to say, structural damage has occurred which implies a distribution of forces other than that which was planned.

Fig. 3

2. STUDIES

2.1 Numerical analyses performed

In order to reach a better understanding of the present state of equilibrium of the structure, a detailed numerical model was developed, in which the geometric complexity of the structure was accounted for by means of finite linear elements with curved centroidal axes, as well as arbitrary cross-sections, which made it possible to model the arches, ribs, diaphragms and columns incorporated into the existing structure. In addition, solid undeformable elements were introduced to simulate the massive capitals where columns, arches and ribs connect. The formulation adopted for the linear elements makes it possible to reproduce states of stress caused by combined axial, shear, bending and torsion forces, and thus to simulate possible modes of global equilibrium more complex than that of a funicular model, also taking into account the influence of the distribution of rigidity between structural elements. The used method of analysis was based on a Generalised Matrix Formulation [3].

2.2 Development of a detailed model

Using the technique described above, a detailed model of the structure was constructed from the information provided by the elevation, the *in situ* measurements and the photographic report. The available funicular model was also taken into account for a better understanding of the structuring of some hidden parts where ribs were connected to the perimeter wall. The
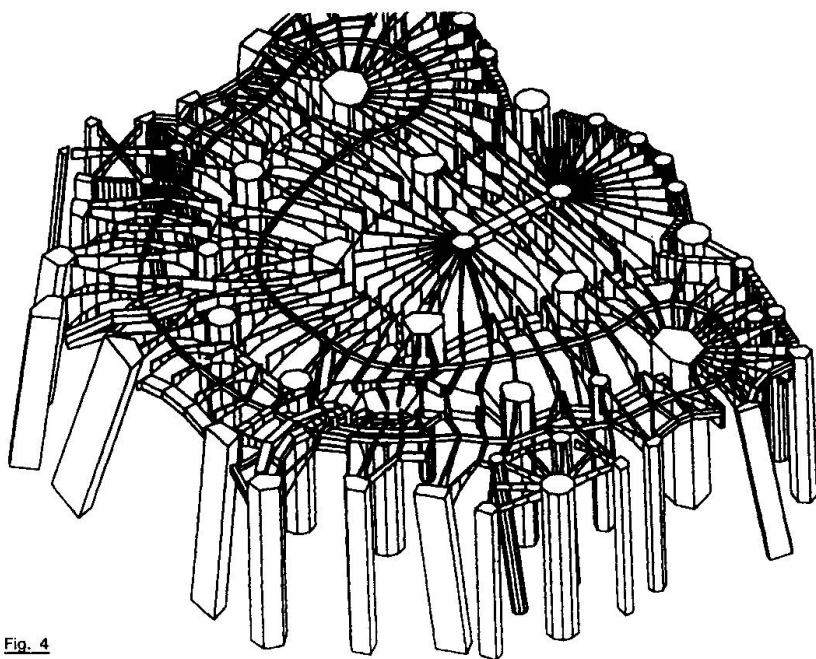
result was the computer model represented in Fig. 4 and some preliminary analyses were carried out to discover its performance. The lead joints on the central columns at their junction with the pedestal and the capital were treated alternatively as completely fixed or rotationally free hinges.

Fig. 4

2.3 Assessment of the present state of the structure

The first analysis consisted of a study of the existing part of the structure subjected to the vertical load produced by the weight of the skeletal system of ribs, arches and columns, as well as the weight of the upper slab, which rests on the first.

The following conclusions were drawn:

A correlation was found between the zones where tensional stresses were concentrated and the cracks observed in the structure. All these cracks match the analytical prediction, which nevertheless showed many other potentially cracked zones which were apparently intact. These are interpreted as parts which, although cracked, do not show an evident structural damage or which, although intact, are subject to a high level of stress and might be easily damaged by overloading or altering the present geometry of the structure.
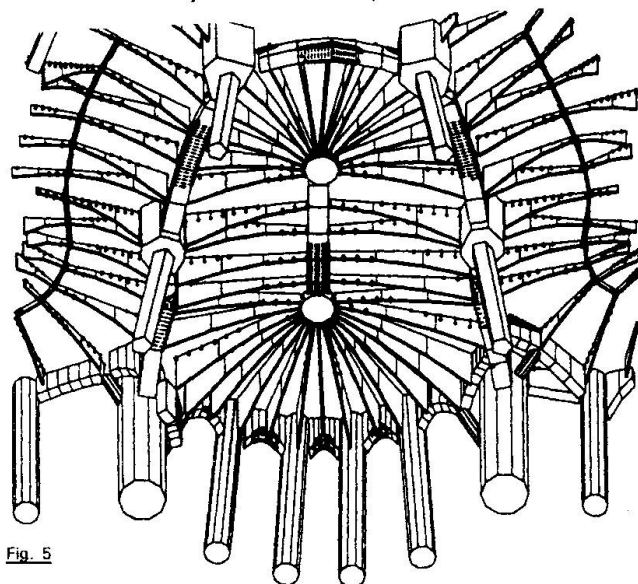
Fig. 5

According to the behaviour obtained, horizontal movements remain very small, showing the stability of the existing structure. The tensional stresses obtained in the different elements (Fig. 5) are mainly caused by their behaviour under vertical load and are hardly influenced by interacting forces due to global equilibrium. Thus, higher tension zones appear at the joints between ribs and capitals or arches and lower tension zones at the middle of the span of the ribs. Both types of tension zones have been correlated with existing cracks.

2.4 The rheological actions

But there are very significant radial cracks which cannot be explained by mechanical forces. Having discounted other causes, the only probable one is hydraulic shrinkage.

The values which are habitually handled to dimension the movement due to hydraulic shrinkage in masonry structures lie between 1 and 7 to 8 tenths of a millimetre for each linear

metre of wall. No values have been found which refer to sheer brickwork elements, since this is a constructional procedure which is not ordinarily used, and on which tests have not generally been carried out. However, the values could not be lower in view of the larger relative proportion of mortar in the section.

We now have to consider a point of considerable importance: the usual way of constructing these vaults is to treat the first skin, the *senzillat* in Catalan, with plaster, hence avoiding the need to use any auxiliary means of support, while its expansion compensates in part for the contraction of the other layers of limestone mortar. However, examination of the exposed layers of this material leads us to doubt that it is plaster. Diafractometric analysis revealed something unusual: the first skin is Portland cement.

The slow setting speed of this mortar made it necessary to locate battens, as can be seen from the marks left in the surface, to support the bricks while construction proceeded. The same tests showed that the two intermediate layers of mortar are also of Portland cement, although it was not possible to determine the proportions since a large enough sample was not available. The reason for this decision may lie in the desire to achieve greater strength in the structural element which was to support the congregation, and also so that the *solera* would be resistant to the elements until the whole complex construction which was to cover it had been finished.

If we take the longer dimension of 23 metres and consider that, although hard to determine precisely, the total of the cracks in this direction amounts to 3 millimetres, this leads us to believe that there has been a contraction of 2 or 3 tenths of a millimetre per metre, which in view of the mortars used is the least that could be expected.
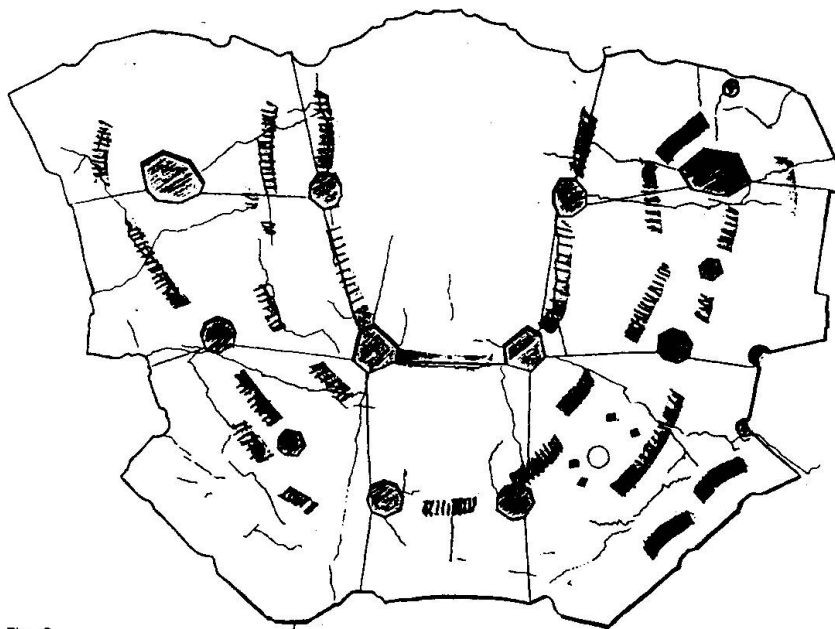

Fig. 6

The figure 6 is a plan of the *solera* which shows the gaps provided to leave room for the columns of the church above, which no doubt is relevant to the matter of shrinkage. On this plan, if we observe the numerical forecasts and the present evaluations which recommend the provision of walls with expansion joints every eight metres, and if we look for the areas where, because of their smaller cross-section and a geometry which might provoke cracking, assuming a uniform grid, we reach the conclusion that it was to be expected that tensions would occur along these lines.

To all this should be added the plan showing the areas where, according to the computer model, the upper part of the ribs is under tension. If we suppose complete adherence between the ribs and the *solera*, we may suppose that this tension is transmitted to the latter. Hence, in addition to the tension due to hydraulic contraction we must consider the tension due to mechanical behaviour. There is a fairly considerable correlation between

hypothesis and reality, and hence it seems we must inevitably conclude that the radial cracks are all due to contraction, while the cracks between the heads of the columns, the capitals, are due to a combination of contraction and the tension phenomena of the rib arches.

Hence we can draw a further conclusion: contraction is the process which makes visible many cracks of gravitational origin, or contributes to their appearance when it is added to the mechanical tensions in the cases where tension in the ribs and foreseeable lines of fracture in the *solera* coincide.

The computer model together with hydraulic contraction theory allow us to define a model which adequately represents the real structure and supports the following conclusions.

3. CONCLUSIONS

3.1 The actual state

The building is stable under its own weight and the permanent loads at present affecting it. This is so in spite of the fact that the present loads were the cause, at some time, of the existing damage to the structure. While the combined effect of the tensions of mechanical and rheological origin – as well as possible compressions greater than the permissible level on some of the crushed bricks – have caused failures in the structure, namely the cracks in the *solera*, some ribs and some arches, the overall stability is more than assured, thanks to the inertia of the interior columns and the perimeter walls. That is, the horizontal structure has given way somewhat to the forces bearing on it, while the vertical structure has plenty of strength and stability in hand in spite of certain structural peculiarities or trangresions which might counter this.

The change to public use of the terrace above would mean an increase in the load supported by the ribs, and hence an intensification of the effects which can be observed or detected by computerised study: the generation of tensions in the key (lesser), the springer (to a greater extent) and the possible appearance of cracks.

Evidently it is dangerous to place further loads on the ribs which are visibly damaged, since their present state of equilibrium may be precarious, although there is the possibility of carrying out some sort of repair which would restore their ability to function as arches. The probability that there are imperceptible or potential cracks in itself makes it inadvisable to apply variable loads which would submit the structure to cycles of load and unload, since this would have the effect of creating new cracks and opening the existing ones.

Hence we can state that any hypothetical use of the terrace would have to avoid the direct application of loads on the *solera*. At all events, in view of their robustness, the columns will allow far higher load levels than those to which they are at present subjected, so that they could be used as the support of a new load-bearing structure. It must be borne in mind that the central columns, as discussed below, can only be loaded up to some 20 tonnes without producing desequilibrium in the opposite direction.

When lead joints are treated as perfect hinges, a significant movement of the central columns and upper capitals is obtained (Fig. 7) and produces balancing axial and flexural forces in the adjacent ribs. Some real effects observed in these zones may also be correlated to such a movement of the capitals, such as a more extended cracking in the ribs and the existence of diagonal cracks in the upper slab.
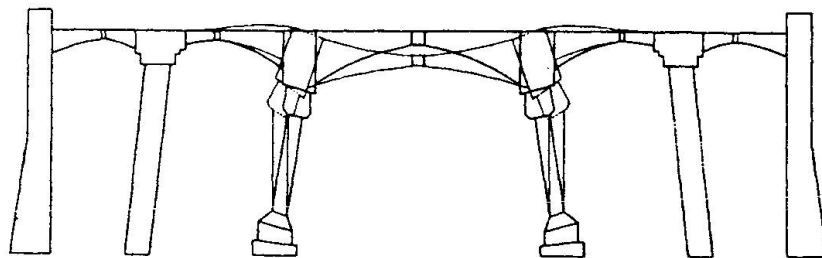
Fig. 7

Except in the zone close to the moving capitals, the distribution of forces obtained at the level of the arches and ribs remains similar to that of a funicular type of equilibrium, although the geometry does not correspond to that of the model. It may be seen that, owing to their much larger sectional dimensions, the deformations of columns and the perimeter wall are very small in any case, so that the equilibrium of arches and ribs is not affected by the fact that the devised overall structural system is not completed.

3.2 Analysis of the hypothetical complete structure

The unbuilt part of the structure was simulated by the hypothetical forces that it would have exercised on the existing part, and on the model. These forces were known from labels which can be seen in extant photographs of the original model.
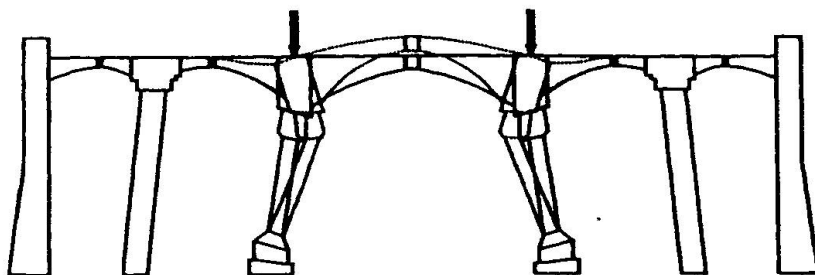

Fig. 8

It was established that absolute funicular equilibrium would not have been obtained for the finished building either. In particular, with the introduction of hinges and lead joints, the capitals tend to move in the opposite direction to that produced by the vertical load of the crypt level itself (Fig. 8). This suggests that the theoretical state of funicular equilibrium is only reached at an intermediate stage of the construction of the building.

REFERENCES

(1) CASALS, A., GONZALEZ-MORENO J. L., Gaudí and the mystery of the encarnation (the mysteries of the Crypt of the Colonia Güell). Rev. Informes de la Construcción, Vol.92, no. 408, July 1990 (written in Spanish).

(2) TOMLOW, J., The hanging model of Gaudí and its reconstruction. New information for the design of the Church of the Güell Colony. Institut für leichte Flächentragwerke, Universitat Stuttgard, 1989.

(3) MARI, A. R., Unidimensional models for the long-term nonlinear analysis of reinforced and prestressed structures. Departament d'Enginyeria de la Construcció, Universitat Politècnica de Catalunya. November 1987 (writen in spanish).
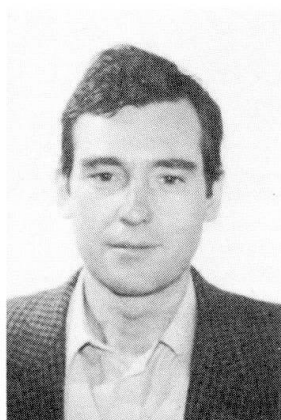
Ultrasonic Methods for Damage Evaluation in Limestone Columns

Méthodes par ultrasons pour l'estimation des dommages dans des colonnes en calcaire

Ultraschallmethoden für die Schadensermittlung in Kalksteinpfeilern

Andrea BENEDETTI
Assoc. Professor
Univ. of Basilicata
Potenza, Italy

A. Benedetti, born 1954, got his enginering degree at Bologna Univ. where he worked as Researcher. Since 1992 he is Assoc. Prof. at the Univ. of Basilicata. He focuses on non-linear structural analysis and probabilistic methods and takes part in large experimental programs, involving ancient Italian buildings.

Marco BARBONI
Civil Engineer
Studi d'Ing. Strutturale
Bologna, Italy

M. Barboni, born 1960, got his civil Engineering degree at Bologna Univ. He then spent several years in the design of prestressed and precast concrete elements. Now, with Studio d'Ingegneria Strutturale, he has completed a number of monitoring and strengthening projects for large monuments and industrial buildings.

SUMMARY

The paper examines the possibility of assessing the damage level evaluation of sandstone and limestone columns from non-destructive testing carried out by means of ultrasonic probes, with a view to finding out relations able to relate material parameters before and after strengthening operations. The discussion of an experimental program regarding the columns of a monastery in Bologna allows for a practical application of the proposed damage indicators.

RÉSUMÉ

L'article examine la possibilité d'évaluation des dommages de colonnes en calcaire et en molasse à partir d'essais non-destructifs conduits à l'aide de moyens ultrasoniques, afin de déterminer des relations entre les paramètres du matériau avant et après des actions de renforcement. La présentation d'un programme expérimental sur des colonnes dans un couvent à Bologne montre une application pratique d'indicateurs de dommages proposés.

ZUSAMMENFASSUNG

Der Bericht prüft verschiedene Möglichkeiten zur Ermittlung des Schädigungsgrads von Kalk- und Sandsteinsäulen auf der Basis einer zerstörungsfreien Prüfmethode mittels Ultraschall. Ziel ist die Ermittlung der Beziehungen zwischen Werkstoffparametern vor und nach Verstärkungsmassnahmen. Ein experimentelles Programm für die Säulen eines Klosters in Bologna wird vorgestellt und die praktische Anwendungsmöglichkeit der Schadensermittlungsfaktoren diskutiert.

1. INTRODUCTION

Ultrasonic pulse velocity attenuation measurements are non destructive monitoring methods well suited for the evaluation of the damage level or the effect of strengthening in structural materials such as concrete, wrought or cast iron or, hard stones which are homogeneous at the macro level [1,2,3].

As a matter of facts several signal properties and transducer arrangements are available in order to assess the damage or strengthening indicators of structural slender elements such as sandstone or limestone columns [4].

More precisely pulse velocity, amplitude dacay, or spectral content can be measured; following the relative position and the form of transducers, direct or indirect (side) layouts alongwith planar or punctual probes can be used.

Thus, it is important to point out that a careful selection of the testing features is not only necessary in order to obtain useful informations, but is a complicated task too, which must take into account even non mechanical factors such as uman and environmental ones.

In the paper direct and indirect testing methlogies are reviewed pointing out some simple analytical treatments which allows for a preliminary evaluation of damage or strengthening indicators as a relative measure to a selected specimen assumed the reference state.

Then, some results of an experimental program carried out on the sandstone columns of the cloister of the Archeological Museum in Bologna are discussed.

Finally, the evaluation of the parameters from the test measurements is worked out in order to show the effectiveness of the proposed relations.

2. ULTRASONIC SCANNING FOR DAMAGE EVALUATION

The preservation of isolated uncoated structural elements such columns and vaults is strongly withstood by the combined attack of loading and environmental agencies; in this respect, it is well known that the presence of ambiental vibrations, diffusion of wet air pollutant and a high sustained load can often lead to a premature failure of the structural element.

With relation to the metric of the microstructure, we can have concetrated or geeralised damage; in the first case, which is typical of fine grain materials (marble, granite and brittle metals), it arrives finally at a well defined crack pattern or even to a material spalling [5,6].

In the latter case, which is proper of large grain or composite materials (metamorphic stones or concrete), the damage involves an overall net of microcracks at microscopic level; these last sometimes can coalesce to a macrocrack but anyhow they change the structural properties of the material [7,8]. As a consequence, a proper testing method must take into account the nature of the investigated phenomena in order to select procedures able to quantify the damage and suggest the repair techniques.

More precisely, in presence of rough localised cracks, ultrasonic scanning can be used in a way similar to tomography, by means of several intersecting travelling paths, which enable to draw information on the geometry of cracks [9] (fig.1).

Alternately, when we are dealing with sandstone or limestone and no macrolevel cracks are present, we can analyse the ultrasonic velocity and amplitude decay data in order to evaluate the site properties of the material [1,3,8].

Moreover, the comparison of these data with those obtained from a reference specimen (which often can be found enclosed in foundations, walls or other undamaged sites of the construction), leads in a nearly straightforward way to an accurate damage definition. In lack of a reference specimen, the material data of an active quarry or even given from Literature can be used, but anyway with fuzzier results.

2.1 Damage Indicators

Referring now to the case of generalised damage, we look for a link between the ultrasonic test results and the damage index; as a matter of fact this last can be conveniently defined making use of a mechanical property and a suitable metric scale [5,10]. By example, selecting the ultrasonic velocity itself and a linear scale with respect to a reference velocity v_o, we pose:

$$D_E = 1 - \frac{v_{us}}{v_o} . \tag{1}$$

On the other hand, following the direct relationship between the ultrasonic velocity and the dynamic modulus of the material, a very common definition of the damage indicator is:

$$v_{us} = \sqrt{\frac{n\ E_d}{\rho}} , \qquad n = \frac{1-\nu}{(1-2\nu)(1+\nu)} , \qquad D_E = 1 - \frac{v_{us}^2}{v_o^2} . \tag{2}$$
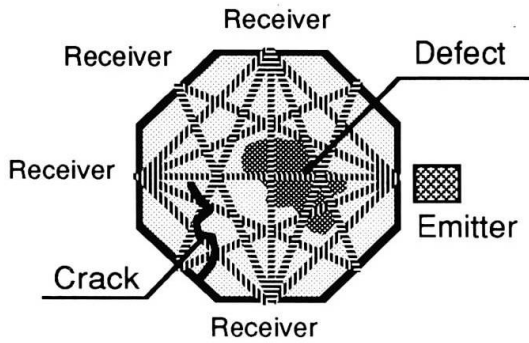
Fig. 1 : Multi path scanning for
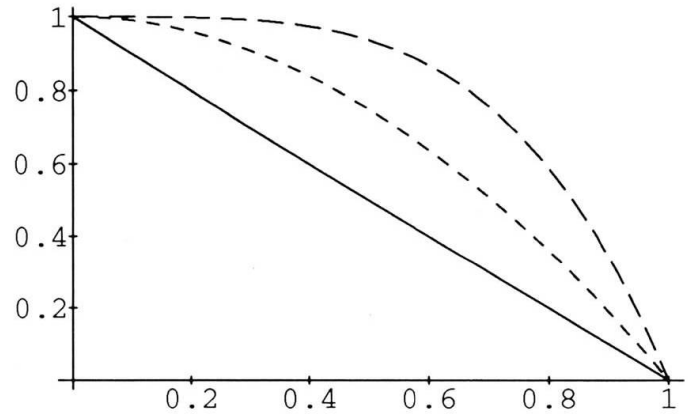defect positioning

Fig. 2 : Damage index as a function of
the proposed velocity relations

As a further step, we can suppose that the damage may be interpreted as a strength reduction; again, making use of a linear index, and expressing the strength as a function of the dynamic modulus at the origin [11,13], we obtain:

$$D_f = 1 - \frac{f_{kus}}{f_{ko}} , \qquad E = \frac{E_{ref}}{k_d} \sqrt{\left(\frac{w}{w_{ref}}\right)^3 \frac{f}{f_{ref}}} , \qquad (3.a)$$

hence:

$$f = \alpha \, v_{us}^4 , \qquad D_f = 1 - \frac{v_{us}^4}{v_o^4} . \qquad (3.b)$$

As a matter of fact, the relation (3.a) encompasses nearly all formulas proposed in the Literature, once adjusted the reference strength f_{ref}, the reference weight density w_{ref}, and the static-dynamic ratio k_d; in particular, referring us to natural sedimentary stones and including some results for low strength concretes [1] it arrives at:

$$E = 1800 \sqrt{f} , \ (E \text{ and } f \text{ in MPa}). \qquad (4)$$

In fig. 2 the results of the presented damage laws are compared; As is clearly apparent, the different order of the exponent gives rise to a divergence of the indices; on the other hand, each definition is tailored on a different parameter and this should be taken into account when a damage measure has to be kept.

As a first comment, we recall that for cementitious materials there is a treshold under which the material behaves as elastic linear neglecting initial defects; moreover, despite damage starts at relatively low stress level [11-13], it begins to be significant near the collapse [3,6,8].

On the other hand, describing the uniaxial constitutive relation with by example the Sargin or the Hognestad formula [13], the derivative of the stress is continuosly varying from the zero strain up; so, neglecting a treshold parameter will result in a damage function null only for virgin materials.

But, as is well understood, the evolution of the volumetric strain is a clear map of the damage rise; in fact, the void increase caused by microcracking turns into materials dilatancy, which appears in a change of sign of the volumetric strain derivative.

In this respect, Cervenka [12] has shown that a suitable interpolation of the stress - volumetric strain relation can accurately reproduce the damage evolution; more precisely, introducing a polynomial interpolation we have:

$$\frac{\varepsilon_c - \varepsilon_{vc}}{\varepsilon_{vc}} = D_{vc} = \begin{cases} 0 \ , \ \sigma < \sigma_{vc} \\ \alpha \left(\dfrac{\sigma - \sigma_{vc}}{f_k - \sigma_{vc}} \right)^m , \ \sigma > \sigma_{vc} \end{cases} \tag{5}$$

Obviously, assuming σ_{vc} null will lead to a continuous damage index; in this case, in order to fit rel. (5) the exponent m must be doubled or so.

If we mean to link the measured ultrasonic velocities with the dilatancy based damage index, it is necessary to select a suitable constitutive relation and set up the relation between the stress and its derivative; in this preliminary study we assume the Hognestad formula:

$$\sigma = f_k \frac{k \, \eta - \eta^2}{1 + (k-2)\eta} \ , \qquad k = \frac{E \, \varepsilon_u}{f_k} \ , \qquad \eta = \frac{\varepsilon}{\varepsilon_u} \ , \tag{6.a}$$

$$E = \frac{1}{\varepsilon_u} \frac{d\sigma}{d\eta} \tag{6.b}$$

where we signed with (ε_u, f_k) the limit point of the stress strain relation.

Once obtained an ultrasonic velocity measure and upon assuming a reference strength, we can invert rel. (2) and use the computed mean dynamic tangent modulus to determine a mean stress level; finally this allows for the evaluation of the damage index.

Alternately, assuming known the stress level in the column (peraphs, from a numeric analysis), we can solve the nonlinear system 6.a-6.b looking for the actual strain ε and the strength σ_u.

A drawback of rel. (5) is the need of the value of σ_{vc} which is of difficult definition indeed. However, contrary to the linear damage law, this type of representation involves a filtering (due to the exponent m), which runs finally to a step damage function; in fig.3 the results for m=2 and m=4 (solid lines) are compared with the case $\sigma_{vc}=0$, showing a relative insensitivity to the choice of the various constants.
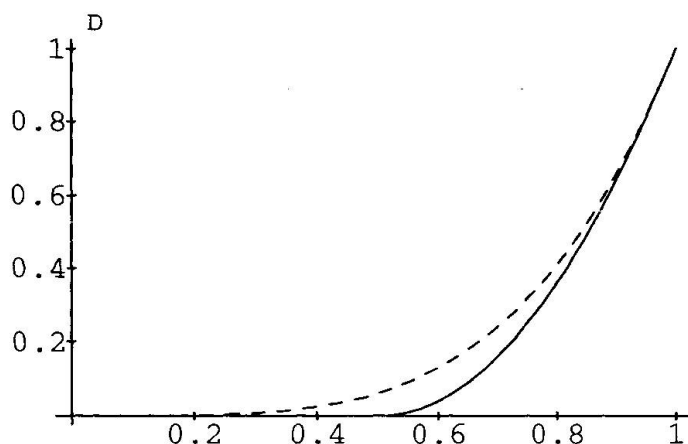
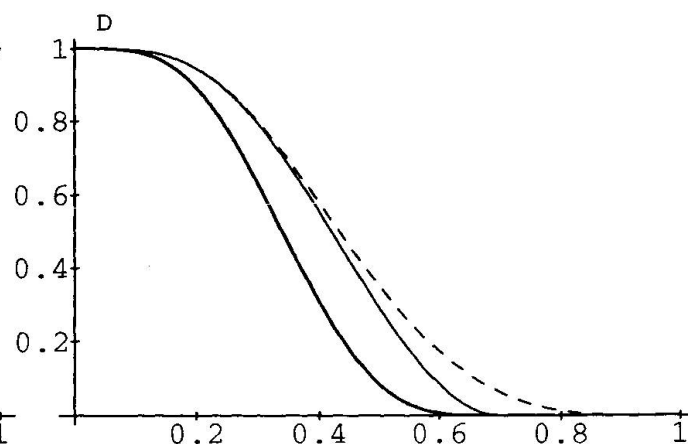**Fig. 3.a** : Damage evolution as a function of stress level σ/f_k, as predicted by dilatancy

Fig. 3.b : Damage evolution as a function of the ultrasonic velocity ratio v_{us}/v_0

Section	Path	Initial	Repaired
1	a	-	2767
	b	-	3131
	c	1758	2344
	d	-	2103
2	a	-	1994
	b	1875	1857
	c	1825	1867
	d	-	1923
3	a	1740	2255
	b	1955	2056 .
	c	2157	1891
	d	1864	2062
4	a	1907	2272
	b	2161	1975
	c	2262	1852
	d	2036	2076
5	a	2037	2850
	b	2211	2461
	c	2408	2222
	d	2183	2091
		m/s	m/s

Table I
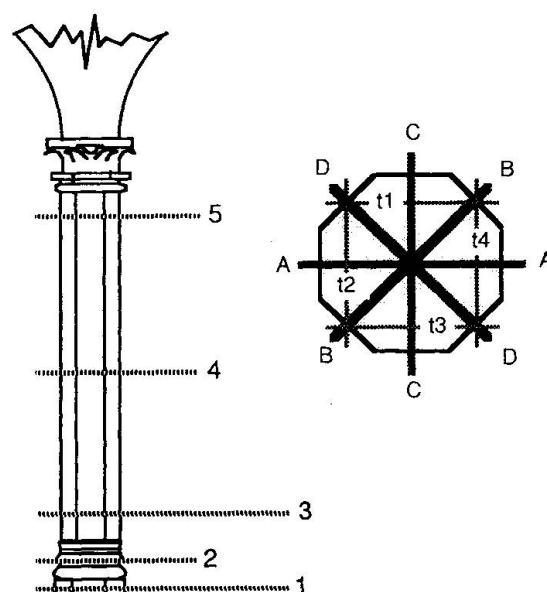
Fig. 4 : Representation of the measure paths

3. THE CLOISTER OF ARCHAEOLOGICAL MUSEUM IN BOLOGNA

The internal cloister of the Archaeological Museum in Bologna contain 16 limestone column of octagonal shape whose material cames from a local quarry which today is thoroghly exhausted. The yellow limestone appears sufficiently uniform but, due to the low strength and the environmental attack several

microcracks are present resulting in the ultrasonic velocities reported in fig.4.

In order to achieve a target load increase necessary for architectural purposes, a restoration test was carried out on the selected column; more precisely it was grouted at low pressure with a low viscosity epoxy resin. Following compatibility consideration we selected a resin with an elastic modulus of nearly the value of the virgin limestone.

In the table of fig. 4 the values of the ultrasonic velocities measured after the filling operation are shown; as is apparent, the major change involves the sections what initially were not transparent.

In fig.s 5 and 6 the computed damage indices are compared for both conditions, before and after repair. As we said before, the various statements differ dramatically and is difficult to extract the correct one.
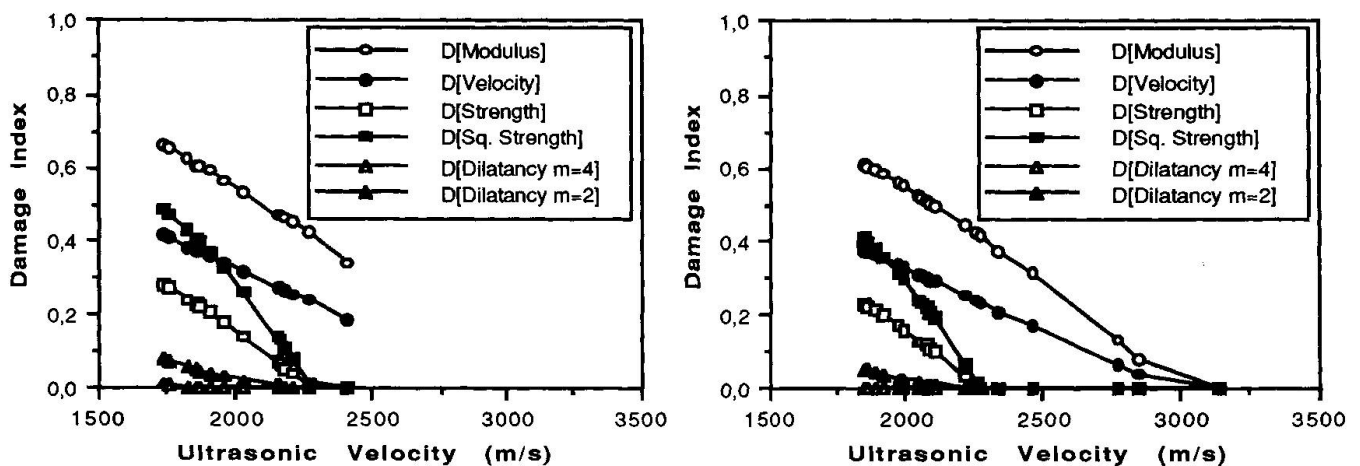
Fig. 5 & 6 : Damage indices resulting from the various formulations for the damaged and restored column
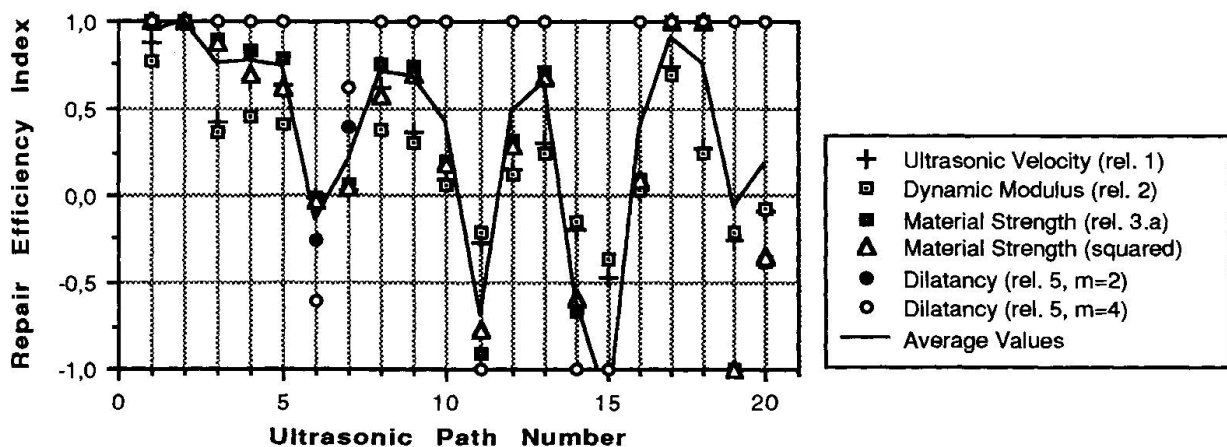

Fig. 7 : Repair Efficiency as computed from the ratio of damage indices, before and after the strengthening

On the contrary, expressing the efficiency of the strengthening by means of the ratio of the relevant damage indices we can observe a significant agreement of the introduced indices. In fig. 7 the efficiency ratios for the various measurement paths are compared.

4.   BIBLIOGRAFIA

1.   TOMSETT H.N., The practical use of ultrasonic pulse velocity measurements in the assessment of concrete quality. Mag. of Conc. Res., vol.32, p.7-16, 1980.

2.   LESHCHINSKY A., LESHCHINSKY M., GONCHAROVA A., Whitin test variability of some non-destructive methods for concrete strength determination. Mag. of Conc. Res., vol.42, p.245-248, 1990.

3.   SUARIS W., FERNANDO V., Ultrasonic pulse attenuation as a measure of damage growth during cyclic loading of concrete. ACI Mat. Jour., vol.20, p.185-193, 1987.

4.   BRITISH STANDARDS INSTITUTION, Recommendations for Non-Destructive Methods of Test for Concrete. BS4408-5, 1974.

5.   LEMAITRE J., CHABOCHE J., Mechanics of Solids Materials, Cambridge University Press, 1990.

6.   FRANTZISKONIS G., DESAI C., TANG F., DANIEWICZ D., Degradation Mechanisms in Brittle Materials Investigated by Ultrasonic Scanning. Engnrg Frac. Mech., vol.42, no.2, p.347-369, 1992.

7.   TASSIOS T.P., Physical and Mathematical Models for Re-Design of Damaged Structures. IABSE Symp. on Strengthening of Building Strucures, p.29-77, Venezia, 1983.

8. DAPONTE P., MACERI F., OLIVITO R., Frequency Domain Analysis of Ultrasonic Pulses for the Measure of Damage Growth in Structural Materials. Proc. of the Ultrasonics Symposium, p.1113-1118, 1990.

9.   DI TOMMASO A., PASCALE G., CIANFRONE F., Analisi dello stato fessurativo interno di elementi strutturali lapidei in edifici storici. Giornale delle Prove non Distruttive, no.3, pp.81-90, 1988.

10.   KRAJCINOVIC D., DA SILVA M., Statistical Aspects of the Continuous Damage Theory. Int. Jour. Solids Struct., vol.18, no.7, pp.551-562, 1982.

11.   CHEN W.F., Plasticity in Reinforced Concrete. Mc Graw-Hill, New York 1982.

12.   CERVENKA V., Behaviour of Concrete under Low Cycle Repeated Loadings. Proc. of the V WCEE, vol.4, pp.15-20, Rome 1974.

13. DEI POLI S., Microfessurazione, leggi costitutive e condizioni di rottura del calcestruzzo in stati di tensione mono e pluriassiali. Costruzioni in Cemento Armato, Studi e Rendiconti, vol.15, Politecnico di Milano, 1978.

Numerical Analysis of the Moisture Behaviour of Building Elements

Analyse numérique de l'état hygrométrique des éléments de construction

Numerische Berechnungen zum Feuchteverhalten von Bauteilen

Haral GARRECHT
Civil engineer
Univ. of Karlsruhe
Karlsruhe, Germany

H. Garrecht, born 1957, obtained his diploma of civil engineering at the Univ. of Karlsruhe in 1985 and his doctoral degree in 1992. He is concerned with research in field of conservation and restoration of historic buildings. His special interest lies in experimental and numerical research on moisture behaviour of materials and masonry structures as well as on moisture protection methods.

SUMMARY

The effectiveness of moisture protection measures may be substantially improved if these are supported by numerically modelling the moisture behaviour of a given building element. For this, the known fundamental laws of moisture transport in porous materials have to be applied to real masonry structures. Then calculations of the moisture distribution may be used to analyze the influence of changing boundary conditions as well as the effectiveness of possible protection methods.

RÉSUMÉ

L'efficacité d'une mesure d'assèchement peut être améliorée considérablement à l'aide des calculs numériques sur l'état hygrométrique d'un élément de construction. Pour cela, il faut appliquer les lois fondamentales des mécaniques du transport d'humidité dans des matériaux poreux aux constructions réelles. De cette manière, il est possible de démontrer la cause d'une charge hygrométrique élevée aussi bien que l'influence des mesures d'assèchement sur l'état hygrométrique.

ZUSAMMENFASSUNG

Die Planung wirksamer Trockenlegungsmassnahmen kann mit Hilfe numerischer Berechnungen zum Feuchteverhalten unterstützt werden. Hierzu ist die für poröse Baustoffe gültige Feuchtebilanzgleichung auf Mauerwerk zu übertragen. Damit können Berechnungen zur Feuchteverteilung durchgeführt werden, die die Ursache der hohen Feuchtebelastung ebenso aufzeigen, wie den Einfluss zeitlich veränderlicher Feuchtebeanspruchungen am Bauwerk. Vor allem kann die Wirkungsweise möglicher Trockenlegungskonzepte nachvollzogen werden.

1. INTRODUCTION

In the repair and conservation of historical structures the pro-
tection of building elements against moisture is of importance
because most types of degradation of natural stones, clay bricks,
mortars and plasters occur in the presence of moisture.
Aside from rain and condensation of water vapor in many cases ex-
cess moisture is absorbed by the foundations of the building due
to capillary rise of water.
In the past, numerous attempts to install or reinstall protection
against moisture in outer walls failed, and occasionally even ac-
celerated the degradation processes. These failures were mainly
caused by a lack of knowledge of moisture behaviour and moisture
movement in porous materials.
The selection of an effective moisture protection method, there-
fore, should be based on a careful analysis of the structure and
its materials, the exposure conditions, and the mechanisms of
moisture ingress, moisture movement and drying of the element.
With the help of the necessary material parameters the moisture
balance of a structural element then may be modelled numerically
for the prevailing boundary conditions. Also different protection
techniques may be simulated by introducing locally modified mate-
rial properties in a cross-section or by modified boundary condi-
tions of a structural element. Based on these case studies effec-
tive moisture protection methods can be chosen.

2. MOISTURE BALANCE IN A STRUCTURAL ELEMENT

2.1 Moisture behaviour of porous materials

In an exterior wall moisture transport takes place through the po-
rous material by diffusion of water vapor or at higher moisture
concentrations by capillary flow in the liquid phase. Moreover,
moisture flow may also be caused by a temperature gradient or by a
hydrostatic pressure acting on the structural element. Assuming
isothermal and isobaric conditions, the moisture balance of a po-
rous material is described by eq. (1) [1,2]:

$$\frac{\partial \theta}{\partial t} = \nabla \left(\frac{D_v}{R_D T} \nabla p_v \right) + \nabla \left(D_{\theta l} \nabla \theta + K \nabla z \right) \tag{1}$$

In eq. (1), the material parameter D_v characterizes the flow of wa
ter vapor by diffusion due to a gra-
dient of water vapor pressure ∇p_v.
The last two terms in eq. 1 repre-
sent the moisture transport due to
capillary effects in a porous materi-
al. Here, the gravity term character-
ized by the product of the capillary
conductivity K and the height of the
moisture front counteracts the dri-
ving force due to capillary pres-
sure. The capillary rise of moisture
can be expressed by the product of
moisture diffusivity $D_{\theta l}$ and the gra-
dient of the local moisture concen-
tration $\nabla \theta$ [2]. All the material pa-
rameters are strongly influenced by
the local moisture concentration θ
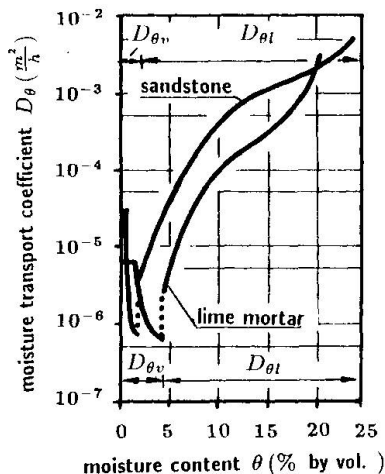and the ambient temperature T and

Fig. 1 Transport coefficient

they have to be determined experimentally. With the help of sorption isotherms the diffusion coefficient of water vapor D_v can be expressed for isothermal conditions as a function of the moisture concentration $D_{\theta v}=f(\theta,T)$.

Experimental and theoretical results showed, that due to their fine pore system for most building materials gravitational effects are negligible [1]. Then the gradient of moisture concentration $\nabla\theta$ is the driving force both for water vapor diffusivity and for capillary flow given in eq. 2:

$$\frac{\partial\theta}{\partial t} = \nabla\big((D_{\theta v} + D_{\theta l})\nabla\theta\big) \qquad (2)$$

Although the mechanisms of capillarity and diffusion are effective in different ranges of moisture concentrations, the transport characteristics $D_{\theta v}$ and $D_{\theta l}$ may be superimposed as shown in Fig. 1 for two different materials, i.e. a sandstone and a mortar. As can be seen the shape of the curve is determined by the diffusion in the range of low moisture content and by the capillary flow for higher concentrations.

2.2 Moisture behaviour of masonry structures

Masonry exhibits an heterogeneous structure because it is composed of at least two very different materials, i.e. the masonry units either artificially made such as clay bricks or natural stone and a joining material such as hydraulic or lime mortar. In most cases the moisture behavior of these individual components of masonry differ considerably beceause of differences in their pore structure. In equilibrium with the relative humidity of the ambient air, the moisture concentration of a building material is determined by the adsorption of water vapor at the interior surfaces of the pores for an initially dry material or by desorption processes for wet materials. At higher relative humidities capillary condensation in very fine pores with radii of $r < 10^{-8}$ m may occur [1]. For a given equilibrium condition materials with a very fine pore structure and a large specific surface area, therefore, have a higher moisture content than materials with a coarse pore size distribution. If two materials with different porosity characteristics are in contact to one another as it is the case for masonry units and the mortar joint, the moisture distribution should exhibit a discontinuity across the interfacial zone.
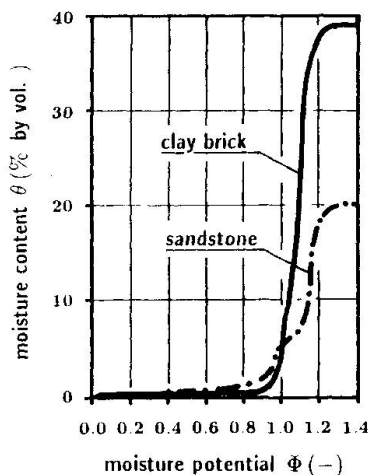

0.0 0.2 0.4 0.6 0.8 1.0 1.2 1.4

moisture potential Φ (−)

Therefore, eq. (2) is not applicable to describe the moisture balance of the inhomogeneous masonry structure Kießl [4] has introduced a moisture potential Φ to formulate the moisture transport through the pore system of different materials. Each building material is characterized by a specific curve as shown in Fig. 2, which relates the moisture content θ to the moisture potential Φ. In Fig. 2 these correlations are presented for a sandstone and a clay brick. For low moisture concentrations this relation is given by the sorption isotherm. Here, the moisture potential Φ increases with the relative humidity h from $0 < h < 100$ % r.h. to $0 < \Phi < 1$.

Fig. 2 Moisture potential

If the porous material is in contact with liquid water, capillary flow occurs in larger pores with radii in the range of 10^{-7} m < r < 10^{-3} m. Therefore, the moisture potential at a higher moisture content of the material can be described by the pore structure. For a corresponding analysis the cumulative pore volume and the pore size distribution is used, which was measured with the help of mercury intrusion porosimetry [1]. In Fig. 2 the shape of the cumulative pore volume characterizes the moisture potential for higher moisture concentrations of the material. Here, the moisture potential Φ rises from Φ =1.0 for pores with a radius of 10^{-7} m to Φ =1.4 for pores with a radius of 10^{-3} m according to eq. (3):

$$\Phi = 1.7 + 0.1 \log r \tag{3}$$

The upper value of the moisture potential Φ =1.4 does not represent a limit. Instead, this value is a result of the low volume of pores with a radius r > 10^{-3} m and the effect of gravitational forces which counteract capillary suction in larger pores.
With the help of this correlation between the moisture content θ and the moisture potential Φ shown in Fig. 2 the transport characteristics for diffusion and capillarity are expressed as a function of the moisture potential Φ. Then, the moisture balance of a masonry structure may be expressed by eq. (4):

$$\frac{\partial \Phi}{\partial t} = \nabla\big((D_{\Phi v} + D_{\Phi l})\nabla\Phi\big) \tag{4}$$

In Fig. 3 the superimposed transport characteristics $D_{\Phi v}$ and $D_{\Phi l}$ are given for a sandstone and a mortar. They demonstrate the extreme nonlinearity of this coefficient.
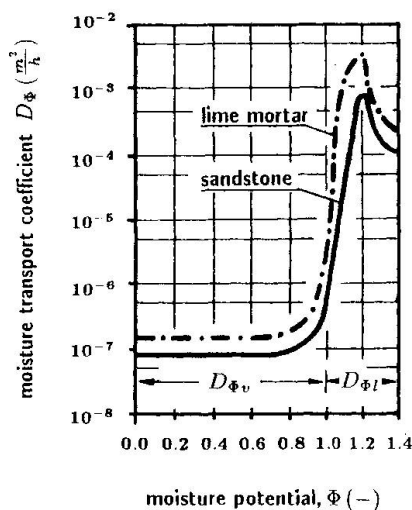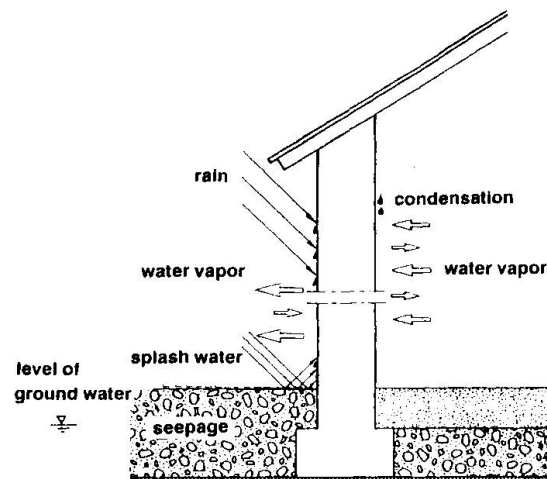

Fig. 3 Transport coefficients   Fig. 4 Boundary conditions

3. NUMERICAL SIMULATION

The wetting and drying behaviour of structural elements is determined by the moisture transport and storage capacity in the materials of the structure as well as by the boundary conditions prevailing on the site. Water in the liquid phase will be absorbed by capillary suction. At the evaporation zone the desorption of water is also governed by the boundary conditions. The higher the tempe-

rature and the lower the relative humidity of the climate in the ambient atmosphere the better the drying conditions of a moist masonry structure. For known climatic conditions to which the structural element is exposed the moisture behaviour can be analyzed with the help of eq. (4). The transient field problem is solved with a finite element model.

3.1 Boundary conditions

Fig. 4 shows the analyzed system which represents the cross-section of an exterior wall with a height of 5 meters and a thickness of 0.8 meters. With the foundation immersed in ground water and the lower portion of the external wall in contact with wet soil, water will be taken up by capillary activity. In the upper section, the wall surface is exposed to the atmosphere. The relative humidity of the atmosphere and the exposure of the wall to liquid water may vary with time. At the interior surface of the wall evaporation may take place, e.g. at 55% rel. humidity in the ground floor and 90% in the basement, respectively. Fig. 4 also shows possible boundary conditions, such as driving rain, splash water, condensation of water vapor etc..

To simulate the moisture behaviour of real building elements, the cross-section of the external wall was divided in up to 7000 elements. This element arrangement allows to consider different types of building materials used in the structural element. Aside from natural stones, bricks and mortars also plasters inside and outside of the external wall as well coatings may be taken into account. Most important is the possibility to evaluate the effectiveness of moisture protection methods. These methods may alter the hygric behaviour of the building elements, e.g. due to chemical injection or other moisture barriers.

3.2 Results of numerical modelling

In the left part of Fig. 5 the distribution of the moisture potential within a wall, which is exposed to ground water, wet soil and surrounding air with a relative humidity of 55, 80, and 90 percent respectively, is shown. The moisture potential profiles represent the state of equilibrium starting from saturation at the bottom, where the wall is immersed in ground water. This equilibrium condition is equivalent to a moisture potential of $\Phi = 1.4$. At the upper part the distribution of the moisture potential is determined by the outer moisture condition at the evaporation zone. The difference between two adjacent profiles amounts to $\Phi = 0.05$. The numerical results demonstrate that at a level of 1 meter above the ground level the moisture potential indicates a high moisture content. In the left part of Fig. 5 also the quantity of up-take and loss of moisture is shown.

With the relation between the moisture potential and moisture concentration given in Fig. 2 the moisture distribution in the masonry structure can be calculated. For the presentation of the results, the degree of saturation of the material is represented by the scale in Fig. 5. Here the color shade changes from a light grey for dry materials to a dark grey for water saturated materials.

As shown by the distribution of the moisture potential this figure demonstrates the high moisture content in the masonry structure, even 1 meter above the ground level. It can be seen also, that the surface of the wall at the evaporation zone will be wet up to a height of half a meter above the ground level.

Fig. 5 Equilibrium moisture distribution
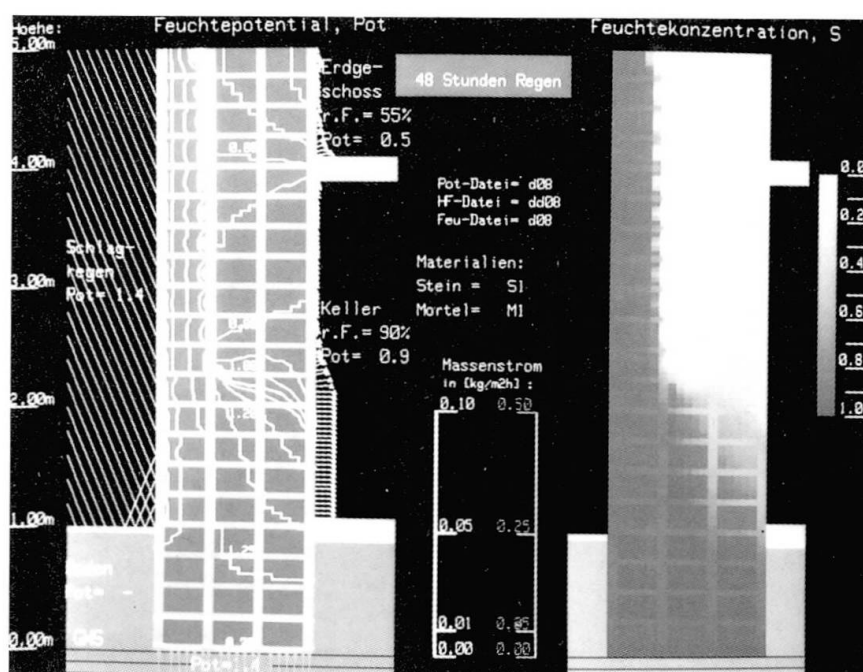
Further calculations of the equilibrium moisture distribution inside the structural element can demonstrate the effect of changing boundary conditions such as changing evaporation conditions as well as the effect of higher relative humidities inside and outside the building. Also the geometric situation of the structure can be varied. As an example, Fig.6 shows the effect of driving rain over a period of 4 days. The distribution of moisture concentration demonstrates how the moisture front moves into the interior sections of the wall. The ingress of moisture is faster in the mortar joints than it is in the sandstone units. Therefore, the wetting of the sandstone units does not only take place in a horizontal direction but also from the mortar joints.

The numerical simulation of subsequent drying of the element shows the well known fact, that drying processes are much slower than the wetting of building structures.

Fig. 6 Effect of 4 days of driving rain

Only in rare cases a wall will be exposed to 4 days of continuous driving rain. However, dirty facades of historic buildings are often cleaned by sprinkling of water on their surfaces for periods of several days. This may cause a moisture distribution similar to that shown in Fig. 6. If the masonry is effectly injected at the socle zone a further moisture transport from the soil into the structure is prevented and the
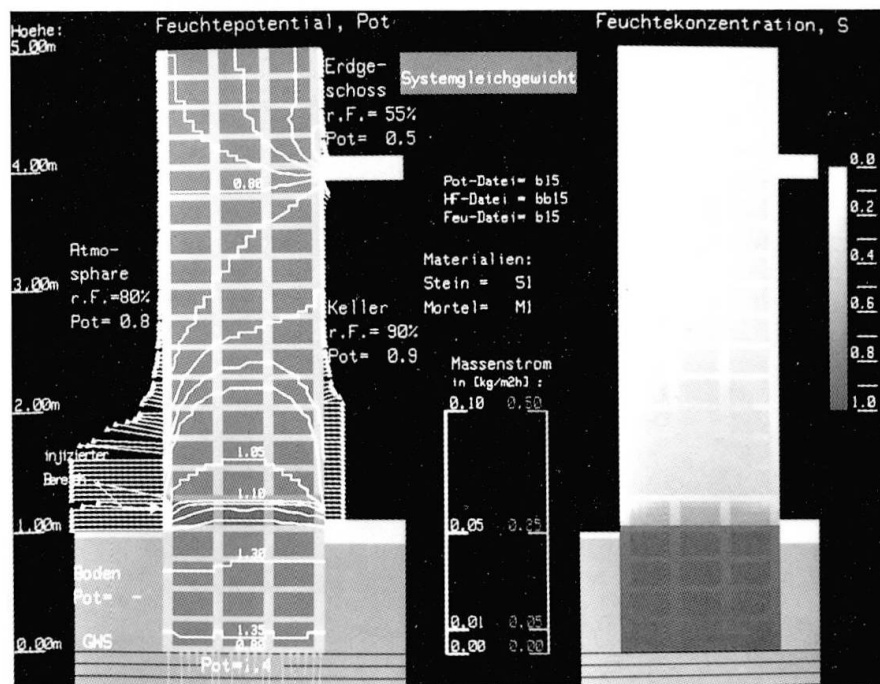
Fig. 7 Effect of an injection with reduced effectiveness

cross-section above the injected masonry section will dry. Most of the excess moisture is lost after a drying period of 3 months.
In many cases it is difficult to carry out a complete injection, particularly when the moisture content in the pores of the building materials exceeds 50 percent of the saturation moisture content. Fig. 7 shows the moisture distribution after treatment of the socle zone with an injection which only fills the larger pores of the materials with a radius of $r > 10^{-6}$ m.
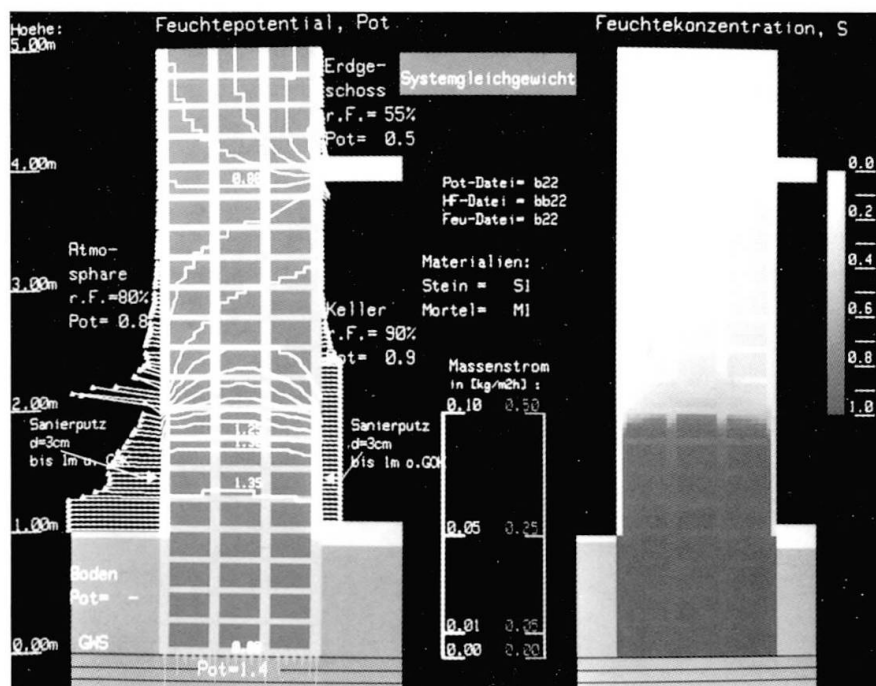
Fig. 8 Effect of an water repellent plaster

Of course, this method can also be used to simulate the effectiveness of other protection measures or a combination of several methods.
Although it is well known that water repellent plasters with very good drying behaviour cannot stop the capillary suction of the protected wall sections they are frequently used against rising dampness. As a result of the hydrophobic behaviour of such plasters, the moisture front remains inside the masonry structure behind the plaster. Hence, the surface of the plaster appears to be dry but numerical results shown in Fig. 8 proof that the moisture front inside the structure will rise drastically. The evaporation rate of the masonry is controlled by diffusion through the plaster. Therefore, the thicker the plaster and the lower the evaporation rate the higher the moisture front will rise inside the structure. These numerical results are also supported by field observations.

4. CONCLUSIONS

The wetting and drying behaviour of structural elements can be simulated with the help of numerical methods. These calculations require detailed information on materials properties such as sorption isotherms and various transport coefficients for the flow of water in the liquid and in the vapor phase. The calculations demonstrated that high moisture concentrations in building materials can arise from soustained contact with liquid water, e.g. due to driving rain or ground water. However, the equilibrium condition between capillary rise and evaporation limits the level of the moisture front. To model the moisture transport in masonry structures, the differences in moisture content of mortar and stone materials subjected to the same hygric conditions makes it necessary to define a common moisture potential as proposed by Kießl. The numerical simulation then allows to perform case studies of possible protection methods, thereby introducing locally modified material properties or partially modified boundary conditions. Different methods then may be compared with regard to effectiveness, effort and required drying time.
In this paper the infuence of temperature as well as the influence of salts often found in historic structures was negleted. These additional effects are presently incorporated into the numerical model.

REFERENCES

1. GARRECHT H., Porenstrukturmodelle für den Feuchtehaushalt von Baustoffen mit und ohne Salzbefrachtung und rechnerische Anwendung auf Mauerwerk. Dissertation Universität Karlsruhe, 1992.

2. DE VRIES D.A., The theory of heat and moisture transport in porous media revisited, Int. J. o. Heat a. Mass Transfer, 30, 1987.

3. GERTIS K., WERNER H., Die Problematik der Porenanalyse von Baustoffen - Kritische Ansätze zur Interpretation des Porengefüges. Deutscher Ausschuß für Stahlbeton, Heft 258, 1976.

4. KIESSL K., Kapillarer und dampfförmiger Feuchtetransport in mehrschichtigen Bauteilen - Rechnerische Erfassung und bauphyiskalische Anwendung. Dissertation Universität Essen, 1983.

Posters - Session 3

Leere Seite

Blank page

Page vide

Simulation of the Design Schemes for Architectural Monuments

Simulation de projets d'études pour des monuments architecturaux

Simulation von Entwurfsmodellen für architektonische Bauten

Gennady L. SEMENETS
Civil Eng.
Kharkov Inst. of Railway Eng.
Kharkov, Ukraine

Marina A. KIRICHENKO
Civil Eng.
Kharkov Inst. of Railway Eng.
Kharkov, Ukraine

The purpose of this paper is to propose of the general ideas on simulation of the historical architectural constructions (destroyed buildings as well) design schemes, also recommendations on their analysis and a more precise definition.

The simulation of the design schemes allows to obtain an obvious situation of the construction stress and deformation state both nowadays and originally. Besides it allows to reveal the reasons of the destruction and to forecast durability and reliability with a definite degree of approximation.

The simulation is implemented in such a sequence:
1. according to the remained part of the construction a space rod design scheme is created as being the most visual one;
2. the geometrical characteristics of the conventional rods are specified so as to bring the work of this design scheme to the work of the real construction as near as possible;
3. the massive parts of the construction are simulated by volume finite elements.

The finite element method and the superelement method are used for the analysis of constructions. It is recommended to use separate parts of the construction as superelements. These parts can be separated out of the construction according to the definite sign and calculated by any method indepedently.

It is proposed to consider the following kinds of superelements:
1. base superelements - the parts of the structure having sufficient strength and degree of stability;
2. unstable superelements - the parts of the structure working under unfavourable conditions, having heavy damages and increased value of the flexibility;
3. cantilivers - various parts of the structure, being in breakdown state, partly destroyed, having different cross sections, representing themselves as handing down parts of structure at different angles. They may be destroyed parts of archs, frames, plates and continuous beams, separately standing columns and other elements.

The cantilivers may be classified and reduced into several types for which research work can be done and recommendations can be

made to determine their carrying capacity.

The analysis of constructions may be performed in two directions:
by carring out strength verification of construction parts and by
finding out possible reasons of its destruction. While realizing
the first direction of analysis besides static calculations great
attention is paid to dynamic and seismic calculations. It acquires
especial significance if calculated constructions are located in
seismic dangerous region such as Mediterranean, Transcaucasus,
Middle Asia and other regions.

In the second case analysis is made by defining the possible vari-
ants of the foundation settling or by the strength factors appli-
cation. According to these data theoretical situation of destruc-
tion is defined and these results are compared with real situati-
on.

The paper presents analysis of continuous beams, frames and canti-
livers with axis in the form of a broken space line,taking into
account that geometrical characteristics are changed according to
arbitrary law. Stiffness matrixis are determined for these cases.

Geometrical Shape of Stone Arches

Forme géometrique des arcs en maçonnerie

Geometrische Form von Mauerbögen

Aldo RAITHEL
Professor
Univ. of Naples Federico II
Naples, Italy

Paolo CLEMENTE
Researcher
ENEA
Casaccia, Italy

Antonio OCCHIUZZI
PhD Student
Univ. of Naples Federico II
Naples, Italy

Despite it could appear obvious, the effective structure of an arch made by stone voussoirs seldom fits its geometrical shape. In this paper it is shown that, in particular cases such as the round arches, structural stability almost always requires static collaboration of the backfill. As it is known, successful design of a masonry arch depends more on its geometrical shape than on the characteristics of the materials. Indeed, in order to state the stability of this kind of structures, a thrust line of acting loads lying wholly within the arch profile needs to be found (if it exists); in particular, the closer the thrust line fits the arch centreline, the better is the shape designed.

This kind of circumstance can never be verified dealing with round arches under gravitational loads, considering that the affinity between the thrust line of the loads and the respective bending moment diagram of a simply supported beam having the same span excludes vertical tangents at the ends. With reference to figure 1, let us consider the subsequent arches, featuring cross-section of uniform dimensions, obtained by increasing the angle α and leaving unchanged the bending radius R and the depth s. At the beginning, being α small, it is always possible to find a thrust line of the applied loads (self-weight, backfill and overload) lying wholly the arch outline; this is true, in general, up to a certain value α^*. The problem can be faced defining the minimum thickness needed to contain the thrust line, once fixed R and per each value of α.

The minimum depth can be defined as follows: let us suppose that depth is exactly equal to the minimum one, then just one line of thrust lying wholly within the masonry can be found. This line touches the arch profile in a finite number of cross-sections. Being α small, one can observe that the thrust line touching the arch profile intrados at the crown and at the springing is wholly above the intrados. This consideration suggests the way to find the minimum thickness: if the depth is equal to the minimum one, the thrust line touches the arch profile intrados at the crown and at the springing, as well as the extrados at the haunches. If the thrust line touches the arch outline in these points, the structure turns into a mechanism. Being α greater than a certain value α_1, the collapse mechanism concerns only a part of the structure, defined just by α_1, as, in general, the thrust line is included in the arch profile up to an angle value $\alpha_2 < \pi$; therefore the minimum thickness found for $\alpha=\alpha_1$ keeps unchanged up to this limit (figure 2). In order to determine the minimum thickness beyond this threshold (α_2), one should refer to the condition that the thrust line be within the arch outline near the springing, as there is no more question of mechanism type failure.

To the purposes of the present paper, a numerical code for the automatic research of the minimum thickness has been written, solving the problem both in the case of mechanism type criterion and in the case of thrust line exceeding the arch profile near the springing [3,4]. A comprehensive numerical investigation has been carried out to show the influence of each parameter concerning the problem, whose major results are shown in figures 3 and 4. In the first one (fig. 3) the lines corresponding to the values of s_{min}/R (minimum thickness over bending radius) obtained varying α are plotted for

different values of the ratio γ between the stone self-weight and the backfill weight; in this figure the overload height h is equal to 0. Figure 4 shows the same lines plotted for different values of h, representing an uniform load over the arch, being $\gamma=0.5$. As estimated, the curves show three ranges of α. In the first one s_{min}/R increases with α up to a certain value, say s_1, corresponding to α_1. Being α in the range defined by α_1 and α_2, s_{min}/R keeps unchanged to s_1. When α increases beyond α_2, and up to the maximum value π, s_{min}/R fast climbs to exaggerated values. As in general stone arches do not feature such large values of the thickness, one can state that, in these circumstances, just the static collaboration of the backfill assures the structural stability.

The threshold values α_1 and α_2 can be considered not very variable; they can be assumed to be equal respectively to $2\pi/3$ and to $\pi/1.1$.

The diagram showed can be used to assess the stability of an arch, once known its bending radius and the loads. The ratio between the actual depth and the minimum one provides a measure of the safety degree of the structure. Should the actual thickness be smaller than the minimum one, the structural stability can be thought entrusted to the static collaboration of the backfill near the springing. One has to stress the role played by the backfill in defining the acting loads as well as in participating to the effective structure of stone arches.
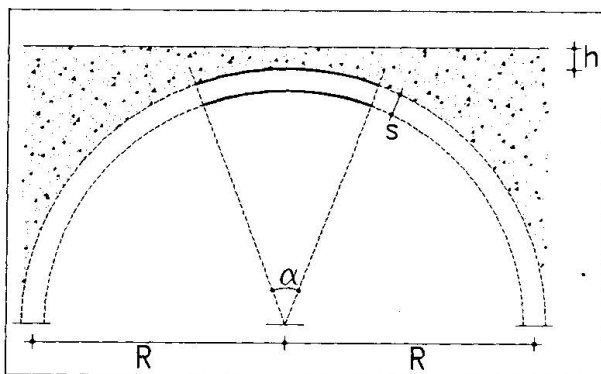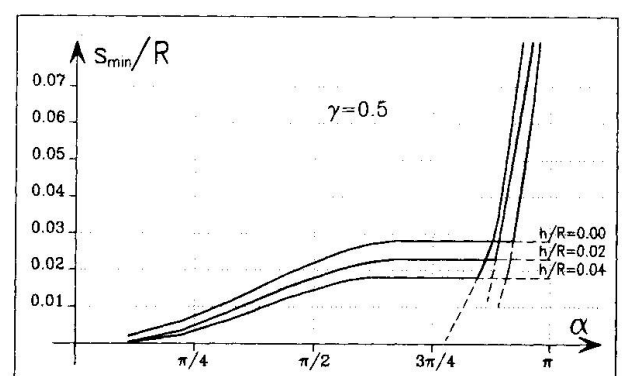

Fig. 1
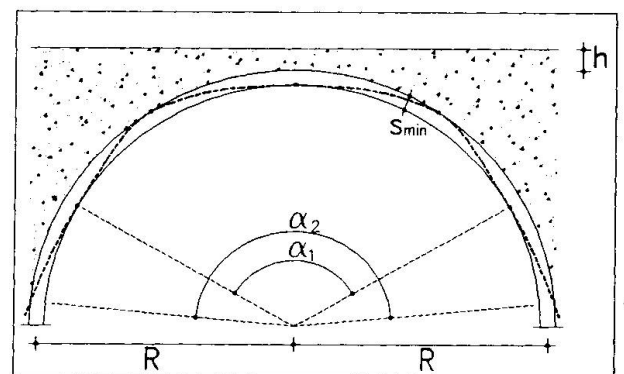
Fig. 2
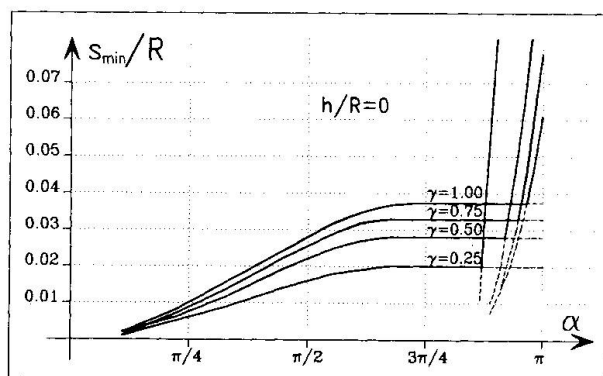
Fig. 3

Fig. 4

REFERENCES

[1] HEYMAN J., The Stone Skeleton, Int. J. Solids Structures, vol. 2, 1966

[2] CLEMENTE P., OCCHIUZZI A., Il Minimo Moltiplicatore di Rottura degli Archi Murari, Atti dell'Istituto di Costruzioni di Ponti - Univ. di Napoli "Federico II", n. 129, (6th Italian Workshop on Computational Mechanics, AIMETA, Brescia 1991)

[3] OCCHIUZZI A., CLEMENTE P., Meccanismi di rottura e sicurezza degli archi murari, IV Convegno Nazionale ASS.I.R.C.CO., Prato 1992

[4] RAITHEL A., CLEMENTE P., OCCHIUZZI A., The limit behaviour of stone arch bridges, To be published.

Dynamic Analysis of Church Masonry

Analyse dynamique d'une église en maçonnerie

Dynamische Berechnung von Mauerwerkskirchen

Carlo GAVARINI
Prof. of Structural Mech.
University 'La Sapienza'
Rome, Italy

Fabrizio MOLLAIOLI
Civil Eng.
CNR-GNDT
Rome, Italy

Gianfranco VALENTE
Ass. Prof. of Struct. Eng.
L'Aquila University
L'Aquila, Italy

1. INTRODUCTION

For the acient masonry wall, we neglect the tensile strength and fracture energy, due to the time damaging. Tensile failure occurs when one tensile principal stress tends to become positive. In this case a plane of failure develops at right angle to the previous principal direction and is conserved its orientation at onset of cracking for the whole loading process. Subsequent failure planes could be only orthogonal to the first and between them. After tensile failure, the normal coefficient in local stiffness matrix is abolished and shear coefficient is multiplied by a constant retention factor less than unity. The nonlinear uniaxial compressive behavior is defined by initial Young's modulus E_0, crushing point $C(\varepsilon_c, \sigma_c)$, ultimate point $U(\varepsilon_u, \sigma_u)$. In multiaxial compressive state compression, the crushing and the ultimate points of uniaxial test may be enhanced relating to the projection on the triaxial failure envelope. Unloading from a compressive state is parallel to the initial Young's modulus. Isoparametric plane elements with a maximum of eight nodes and four integration points in each direction are used. The tangent stiffness matrix is referred to:
- principal stress direction before tensile failure;
- failure coordinate system (axes parallel and transverse to the crack planes after tensile failure.

Various acient buildings are taken into account. Different accelerograms are used, a few real, other obtained by power spectra according to current rules. The Newmark's integration method is used obtaining: stress and strain fields, crack patterns, displacements velocities and accelerations in each node. In conclusion, a method apt to analyse dinamically any masonry building with great accurancy is proposed.

2. PROBLEM DESCRIPTION.

ADINA Code is used. A church masonry is taken into account, having span and height 10.20m, depth 3.90m. The vertical walls are stone made and in the upper arch and over there are bricks. The materials mean features are: E_o=1000. N/mmq, σ_c=-3. N/mmq, ε_c=-.01, at crushing and tension cut-off. The Model and F.E. mesh are represented in Fig.1. Accelerations are applied as in Fig.2, having maximum value 0.2g. The Newmark's integration method is used obtaining the nodal results as in Figs. 3-5.

Node 76

Node 57

Fig. 1a)Model.

Fig. 1b)F.E.Mesh.

0.2g
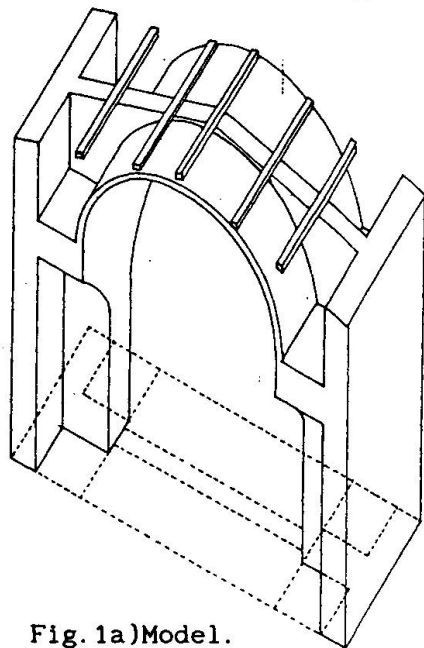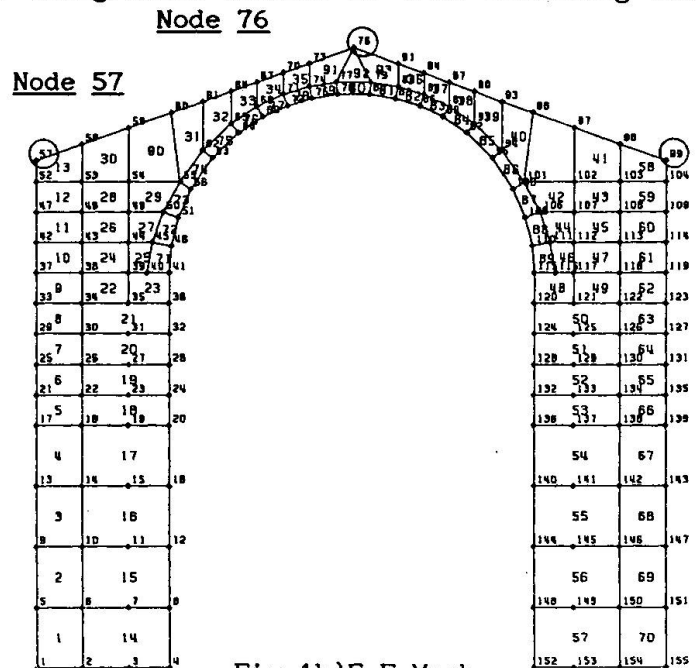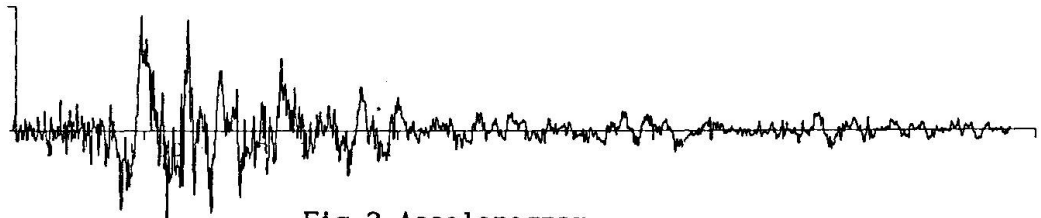
Fig. 2-Accelerogram.
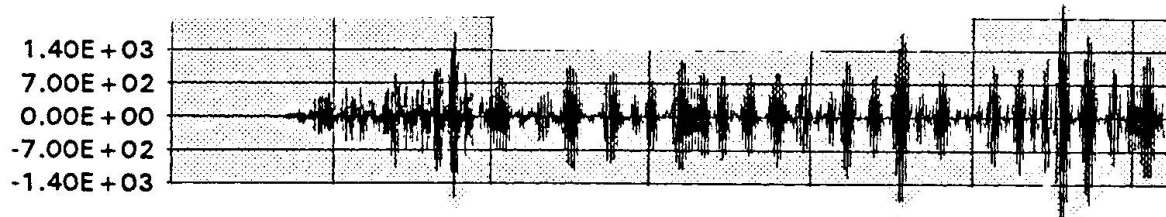
Fig. 3-Accelerations Node 76, [cm/sec^2].
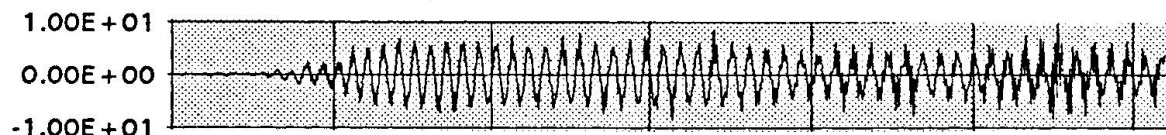
Fig. 4-Velocities Node 76, [cm/sec].

0.0   5.0   10.0   15.0   20.0   25.0   30.0[sec]
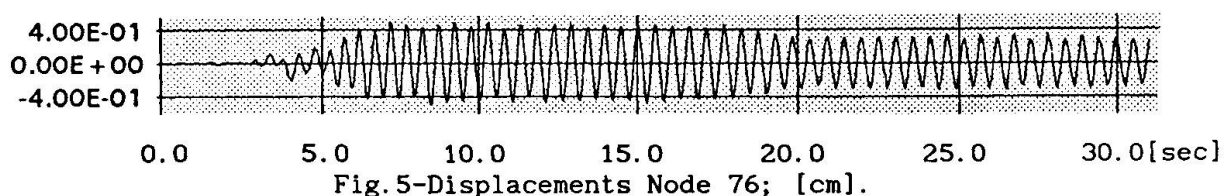
Fig. 5-Displacements Node 76; [cm].

Structural Analysis of the Damage at the Cathedral of Sibenik

Calcul statique des dégâts de la cathédrale de Sibenik

Statische Berechnung der Schäden an der Kathedrale von Sibenik

M. SIMUNIC BURSIC
M. Arch.
University
Zagreb, Croatia

Adrijana BJELANOVIC
Structural Eng.
University
Zagreb, Croatia

Zvonimir ZAGAR
Professor
University
Zagreb, Croatia

Structural analysis of the octagonaly shaped ribbed dome of cathedral of Šibenik, a masterpiece of the Croatian Quattrocento architecture, damaged by a bomb-shell in 1991. contains a condensed review of its structure, a brief art-historical analysis and the analysis of the mechanical characteristics as well as behavior of its structural mechanism. Special emphasis is placed on the spatial, formal and structural significance of its vaults erected with the peculiar technique, unique in its kind. The barrel vaults with the thin one-layer plates, shells, which also create the roof of the church, are constructed by mounting the large thin stone slabs on the relatively slender semi-circular stone arches tightened with iron ties. It is clearly a prefabricated structure. This structure, which seems formally Renaissance, but is structurally Gothic, for its plain skeleton, its clear distinction and hierarchy of primary and secondary structural elements, is used even for the dome structure. The dome, generally a spatial structure par exellance, here is carried out as a system of planar arches, converging into one point, and the envelope, acting as a covering, consists of stone slabs, like that one of the barrel vaults.

The main objective of this research was the FE computer modeling and analysis of the dome, demaged by a bomb- projectile explosion. The modeling and the static FE analysis was carried out using the COSMOS/M FE program. As we have suspected, the demage, a circular hole in the upper part of the stone slab-shell dome system has not much consequences on the carrying capacity of the dome. Luckily that it is on the part of the dome where the stresses are low, and the deformations extremely small. Fortunately, it is not a structurally dangerous injury which could jeopardize the stability of the Chatedral because only a secondary element was damaged. This could be seen on the presented screens. Only by chance the projectile has missed the rib: there could be done a devastating effect to the dome stability, if the rib has been hit and demaged.

We have had another objective before the 1991. and the well known aggression on Croatia: to build up a comprehensive FE model of the whole Cathedral. But with the war going on, and the drastically reduced foundings, as well as the damage done to the dome, the attention was shifted to the macroelement modeling of the damaged dome only.

Because of the peculiarity of the problem (nonhomogeneous masonry structure, nonresistant to tensile stresses), different variations of modeling have been made and examined, to approximate as close as possible the real behavior of the stone structure. Some of the most comprehensive classical approach to the stability and force-stress distributions was done by M. Šimunić in her M.Sc. thesis (in 1990.), and was accompanied by some limited FE model simulations of the dome's stone slabs (shell) behavior (using IBM v. ICES STRUDL2 and COSMOS/M). The structural role of some elements of the fabric is examined

in particular, creating alternative models of the structure by changing and eliminating those elements. The preliminary structural analysis of the whole structure have proved that the structure is very logical and purposeful and that every element, even the decorative ones, has a precisely determined structural function.

The further work on a more comprehensive analysis is still going on. Displayed are some of the obtained CAD/COSMOS/M screens of the work in progress.
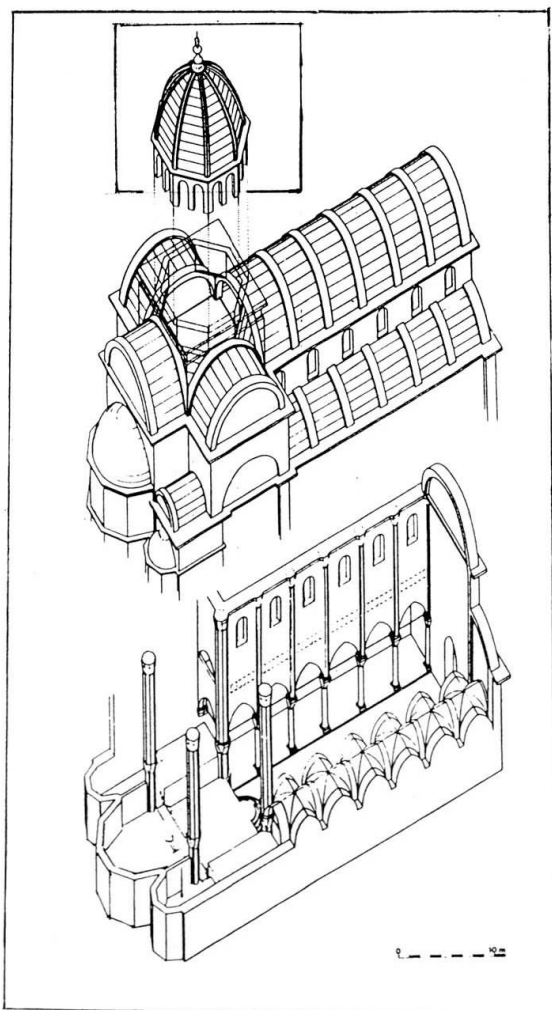

Fig. 1. Vaults of the Cathedral of Šibenik and the substructures.
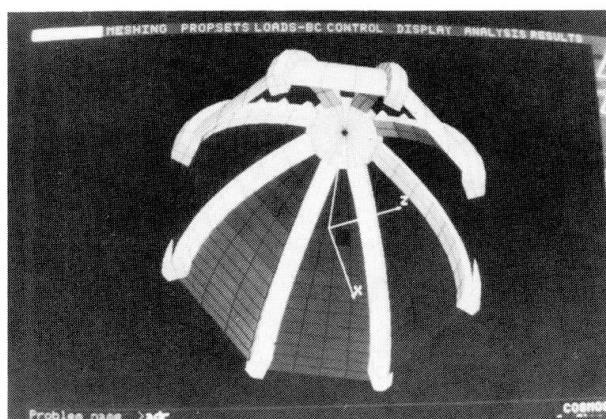
Fig. 2. The FE mesh of the dome-macroelement. The damaged part (a hole) is clearly visible.
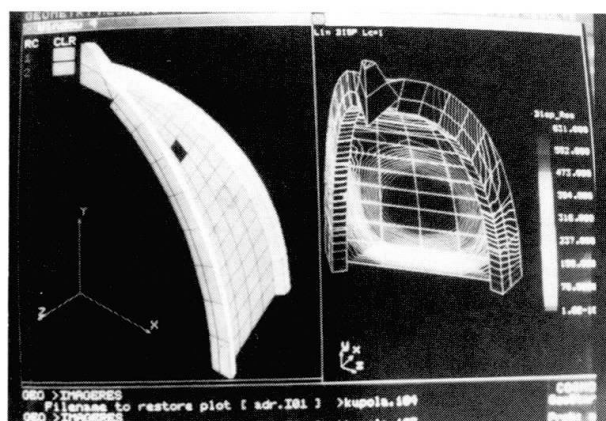
Fig. 3. The deflection lines of the substructure due to the selfeight.

Soil - Structure Interaction in the Leaning Tower of Pisa

Interaction du sol et de la structure de la Tour Penchée de Pise

Wechselwirkung Baugrund - Konstruktion beim schiefen Turm in Pisa

Paolo NAPOLI
Assoc. Prof.
Politecnico di Torino
Torino, Italy

The main aspects of the time-dependent behaviour of the leaning tower of Pisa are: creep and the non-linear response of the soil; second order effects due to the increase in leaning; the progressive reduction in the loaded area.

The model shown in Fig. 1 has been developed to take all these aspects adequately into account, by making the following assumptions: a) the structure of the tower is a rigid body; b) the foundation area is subdivided into 19 strips, arranged perpendicularly to the leaning plane; c) the soil under each strip is a Maxwell element, consisting of a non-linear spring and a non-linear dash-pot, applied to the strip's centre of gravity.

The response of the elements of the chain (for a unit of area) is illustrated in Figs. 2a and 2b (for non linear springs and non-linear dash-pots, respectively).

The displacement of a point of the foundation can then be expressed as:

$$y_i (t_K) = a (t_K) + b (t_K) \cdot x_i$$

where $a(t_K)$ and $b(t_K)$ denote the displacement of the foundation centre and the rotation at time t_K, respectively.

The equilibrium equations during the time step $\Delta t_K = t_K - t_{K-1}$ are:

$$\Delta a(t_K)\sum_{i=1}^{19} K_i A_i + \Delta b(t_K)\sum_{i=1}^{19} K_i A_i x_i - \sum_{i=1}^{19} \Delta y_i^c(t_K)K_i A_i = \Delta N(t_K),$$

$$\Delta a(t_K)\sum_{i=1}^{19} K_i A_i x_i + \Delta b(t_K)\sum_{i=1}^{19} K_i A_i x_i^2 - \sum_{i=1}^{19} \Delta y_i^c(t_K)K_i A_i x_i = \Delta M(t_K).$$

(1)

where

$$\Delta y_i^c(t_K) = \sigma_i(t_{K-1})\beta_i\left[\log t_K - \log(t_{K-1})\right],$$

is the increase in displacement produced by the dash-pot.

The stiffness of the non-linear springs has been continuously updated according to the stress level, as shown in Fig. 2a, cutting off the elements in tension. Similarly, the external moment $\Delta M(t_K)$ on the right-hand side of eqs. (1) increases with increasing tilt (second order effect), while both the axial load and the external moment could vary if some stabilising measures were applied. Convergence has been reached, at each time step, through an iterative procedure.

The range of non-linear spring and dash-pot parameters has been deduced from the extensive geotechnical tests performed on the soil near the tower [1]; final calibration has been obtained by comparing the slope history provided by the model and the measurements taken on the tower since 1550 [2].

In Fig. 3, the tilt vs. time diagram obtained from the model is compared with the available measurements. Agreement seems to be very satisfactory; in particular the simultaneous effects of the reduction in the loaded area and second order effects produces a strong increase in the tilt rate, in keeping with the observations made since 1970.

The model makes it possible to predict the future behaviour of the tower and to assess its response to external actions. If no stabilising measures are taken, the tower will collapse between 2030 and 2040, due to divergence of equilibrium.

A simulation of a very soft stabilising intervention, consisting in the application of a vertical force of 2123 kN at a distance of + 6.83 m from the centroid of the foundation, is presented in Fig. 4. This would achieve a very small instantaneous reduction in tilt, but its delayed effect would be considerable, as a number of springs and dash-pots would return from the plastic to the elastic field, leading to a substantial stabilisation of the tower.

REFERENCES.

[1] LANCELLOTTA R., PEPE M. C., "'Mechanical behaviour of Pisa clay", Rapporto di ricerca n. 2.2, Laboratorio Geotecnico, Dipartimento di Ingegneria Strutturale, Politecnico di Torino, (11.1990).

[2] LANCELLOTTA R., PEPE M. C., "A Report on the movements of the Tower and the Surrounding Square", Rapporto di ricerca n. 4, Politecnico di Torino, (1.1991).

[3] NAPOLI P., Tower of Pisa: numerical modelling of the soil-structure interaction (in Italian), Politecnico di Torino, Atti del Dipartimento di Ingegneria Strutturale, No. 39, October 1992.
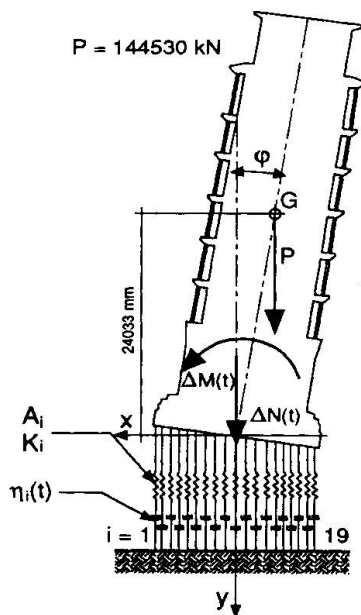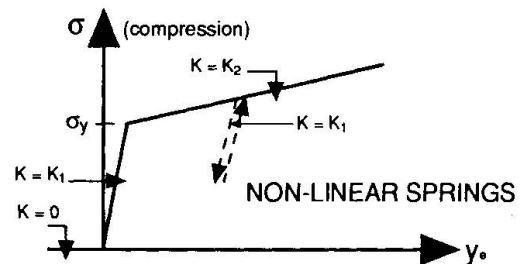

Fig. 1 - Soil-structure model.

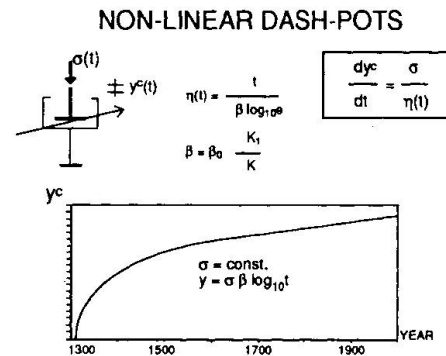Fig. 2a - Stress/displacement relationship in non linear springs.

Fig. 2b - Stress/time/displacement relationship in non-linear dash-pots.
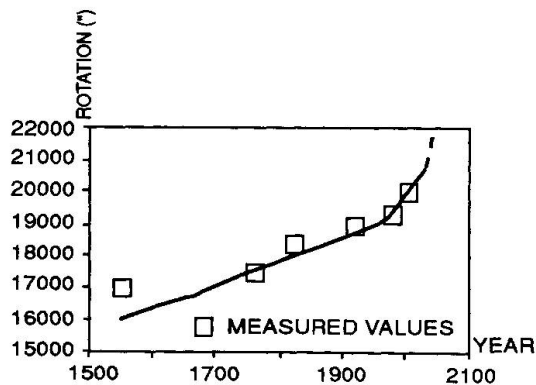

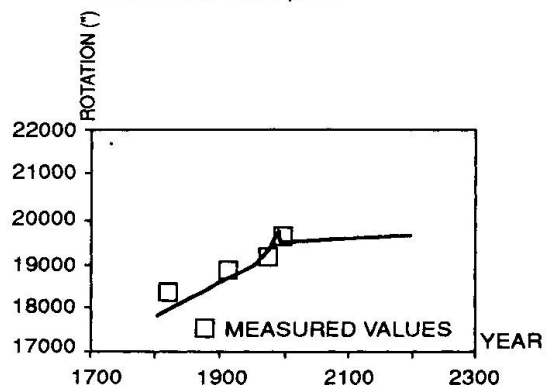Fig. 3 - Rotation/time diagram and comparison with measured values.

Fig. 4 - Instantaneous and delayed effects of the stabilisation measures.